BEHAVIOR OF REINFORCED MASONRY COLUMNS UNDER SUSTAINED LOAD

BY

HAMZA A. BEN-OMRAN

A Thesis

Submitted to the Faculty of Graduate Studies

in Partial Fulfilment of the Requirements

for the Degree of

Doctor of Philosophy

Department of Civil Engineering

University of Manitoba

Winnipeg, Manitoba

ISBN 0-315-78038-X

BEHAVIOR OF REINFORCED MASONRY COLUMNS UNDER SUSTAINED LOAD

BY

HAMZA A. BEN-OMRAN

A Thesis submitted to the Faculty of Graduate Studies of the University of Manitoba in partial fulfillment of the requirements for the degree of

DOCTOR OF PHILOSOPHY

This thesis
is dedicated to
the memory of my father in-law

ABSTRACT

Most research into the structural response of masonry has considered the effect of loading of short duration, and this is true of experimental investigations. Since the bulk of masonry structures actually sustain a large portion of their load throughout their service life, greater consideration should be given to the effect that sustained load has on structural response. This thesis describes an investigation that considered the effect of the time-dependent phenomenon of shrinkage and creep.

The research has led to the development of a one-dimensional analytical model that predicts the response of reinforced masonry to axial load, taking into account stress redistribution resulting from sustained load. The development of a three-dimensional analytical model supports the validity of the simpler one-dimensional model.

An experimental investigation comparing the response of pairs of preloaded and non-preloaded reinforced masonry columns, along with the attendant material tests, was also undertaken. These tests involved percentages of reinforcement ranging from 0.37% to 1.83%.

Although the efficacy of the simpler one-dimensional analytical model is borne out by comparison with the three-dimensional analytical model, the experimental investigation, while in general supporting the theory, points to the sensitivity of the structural behaviour to the actual material properties. More thorough experimental work is required to generate more reliable data for the analytical model.

ACKNOWLEDGEMENTS

The author would like to gratefully acknowledge the invaluable guidance and advice offered by Professor J.I. Glanville throughout all stages of this investigation. The friendship we have had over the years is the most appreciated.

The author also wishes to thank Dr. M.A. Hatzinikolas for his insightful help as the research developed, and Dr. A.B. Thornton-Trump and Dr. A.M. Lansdown for their suggestions and constructive comments during the revision of this work.

Thanks is extended to Tallcrete for the donation of materials, and the staff of the Civil Engineering Structures Laboratory at the University of Manitoba for their assistance during the experimental stage of the research. The assistance of many friends, particularly J.W. Glanville and L. Lamari is gratefully appreciated.

The financial assistance provided by the University of Garyounis, Benghazi, Libya in the form of scholarship and the financial assistance provided by the Natural Sciences and Engineering Research Council are gratefully acknowledged.

The author would like to thank his family and especially his wife Thanaa Hamouda for their interest and support throughout the years of his graduate study.

Last, but not least, the author is grateful to his daughter Eeman, and sons, Almabrouk and Yacine for making life more pleasant.

TABLE OF CONTENTS

LIST OF TABLES

LIST OF FIGURES

CHAPTER I
INTRODUCTION

1.1 Introduction

Although masonry has been in use as a major construction material for millennia, not a great deal is known about its fundamental response to loading. The main reason is that with the development of the theory of elasticity, and what were seen as exciting and more versatile materials, namely, structural steel, reinforced and prestressed concrete, masonry was seen as a more cumbersome material to be used only in monumental public buildings or as brick veneer. As a consequence, masonry fell into disuse for the majority of buildings.

Although Marc Brunel used steel bars to reinforce 50 foot diameter brick shafts for the Thames River Tunnel project in 1825, the value of reinforced masonry was not realized until a century later when engineers in India and Japan incorporated steel into their structures to provide resistance to earthquake loading.

With more innovative developments, such as the hollow concrete block, which could be reinforced and grouted, multi-story buildings were constructed with walls only several inches thick, rather than several feet. However, this very significant reduction in the thickness was accompanied by a corresponding increase in stress and the need for stronger materials, the use of reinforcement to resist compression and tension, and the need for theories to accurately predict behavior under load and margins of safety.

Masonry structures sustain a substantial permanent dead load, whereas live loads are for the most part transitory. A thorough investigation of the behavior of such structures should include a consideration of the effect of sustained load in collaboration with the phenomenon of creep and shrinkage. Research to date into the fundamental behavior of reinforced masonry has dealt only with short-term loading. In order to understand better the behavior of masonry under sustained load, the problem investigated

in this research is the response of reinforced masonry columns under axial load including the time-dependent effects of creep and shrinkage.

Reinforced masonry is a multi-component structural material. It consists of mortar, grout fill and reinforcing steel in addition to the masonry unit themselves. During the period of sustained load these constituent materials, with the exception of the reinforcing steel, experience time-dependent deformations in the form of creep and shrinkage. The existence of such deformations may result in a transfer of load to the reinforcement and may have a significant effect on the manner in which reinforced masonry columns resist the applied load.

1.2 Objective and Scope

The main objective of this research investigation is to understand the fundamental response of reinforced masonry to load. Based on this objective the following goals guided this investigation:

- Determine the effect of sustained load on the ultimate strength of reinforced masonry columns.
- Study the effect of shrinkage and creep on the distribution of stress between the constituent materials in reinforced masonry columns.
- Examine the effects of the percentage and size of vertical reinforcement steel on the behavior of reinforced masonry columns.
- Develop a theoretical analysis to explain the effect of the time-dependent deformation and to predict the ultimate strength of masonry columns under long-term loading.

1.3 Organization of the Thesis

Chapter II reviews previous work on the behavior of load bearing masonry

members and creep and shrinkage as related to the topic of this investigation. Chapter III discusses the experimental program, describing the apparatus used for preloading and sustaining the load, and detailing the construction methods, the test specimens and testing procedures. The properties of the constituent materials are examined and summarized in Chapter IV. Chapter V discusses the test results for columns both during the sustained load period and during testing to failure. The preloaded columns behavior was compared with that of a companion non-preloaded control specimen. The theoretical part of this investigation is outlined in Chapter VI, the behavior of the masonry columns being presented in a three-dimensional consideration and as a simplified one-dimensional model more suited to practical analysis. Application of both models to the experimental results of the masonry columns is discussed in Chapter VII. Finally, the summary, conclusions and recommendations compiled from this investigation are provided in Chapter VIII.

CHAPTER II
LITERATURE REVIEW

2.1 Introduction

Masonry structures in many countries, including Canada, are designed by the working stress design method and empirical rules that are considered quite conservative. Much research is needed to develop more rational design methods, similar to those used for other conventional materials such as, reinforced concrete, structural steel and timber, thereby improving the efficiency and economy of masonry construction. Although a limit states design version of the *Canadian Standard Association* standard *CAN3-S304.1-Masonry Design for Building* is under development, a clear understanding of the fundamental response of masonry to load, whether short-term or sustained, has yet to be attained.

This chapter provides a review of previous studies related to the behavior of columns under concentric axial load and including the time-dependent effect of creep and shrinkage. In addition, relationships used in the theoretical part of this investigation describing the behavior of the constituent materials are also reviewed.

2.2 Review of Previous Investigations

Investigations into the behavior of reinforced masonry columns have been limited. The majority of these investigations were primarily concerned with the deformation under short-term loading and generally do not fully represent the effect of actual loading conditions in buildings. Since reinforced masonry columns are similar to reinforced concrete columns, some of the previous investigations into the behavior of the latter are also reviewed.

2.2.1 Reinforced Masonry Columns

The first study of the behavior of reinforced concrete block masonry columns was conducted by Feeg[1] in 1979 at the University of Alberta. Feeg tested short concentrically loaded columns in an investigation designed specifically to determine the effects of reinforcement detailing on the strength and behavior of these columns under compressive load. Of the thirty-seven columns Feeg tested, thirty-four were constructed with 200 x 200 x 400 mm., lightweight concrete masonry block laid in running bond. The remaining three columns employed 400 x 400 mm single core, lightweight, autoclaved pilaster units laid in stack bond. The columns were constructed with type S mortar and face shell bedding. The variables investigated in this study were tie diameter and location, size and percentage of vertical reinforcement and grade of the vertical reinforcement. All of these columns are reported to have exhibited elastic behavior or a straight-line relationship up to about 75% of their ultimate strength. It was also found that the column strength decreases with an increase in reinforcement bar diameter for a given reinforcement percentage. Feeg also observed that the use of high slump grout in the columns that were constructed with pilaster units led to excessive shrinkage and cracking at the block-to-grout interface.

In a 1978 study of masonry walls at the University of Alberta, Hatzinikolas[2] tested as part of an experimental program nine reinforced and seven plain specimens under compression in an attempt to establish the contribution of vertical reinforcement and grout in sustaining axial loads. The specimens were reinforced with 3-#3, 3-#6 and 3-#9 bars. The bar sizes noted are imperial. The percentage utilization of steel (that is the percentage of the yield stress attained at failure) in the three groups of specimens with vertical reinforcement was 77%, 64.1% and 46% respectively. It was concluded therefore that the efficiency of vertical reinforcement decreases with increasing bar size and that the vertical reinforcement was not fully developed at ultimate load, that is the

steel did not yield. Hatzinikolas also found that the presence of joint reinforcement in the reinforced specimens had no significant effect on the capacity of the section.

Sturgeon[3] 1980 at the University of Alberta, investigated the behavior of reinforced concrete masonry columns subjected to axial compression and to combined bending and axial compression. In this experimental investigation, a total of forty-three columns were tested under axial compression. The columns employed 400 x 400 mm single core, lightweight, autoclaved pilaster units laid in stack bond. The columns were constructed with type S mortar and full bedding. Variables considered in this program include the percentage and grade of vertical reinforcement, grout compressive strength and slump, lateral tie details and eccentricity of load. Based on this study, empirical equations for the prediction of masonry columns strength were suggested. Similar to the previous study, Sturgeon found that the vertical reinforcement in these columns did not reach the yield stress at failure. However, both Hatzinikolas and Sturgeon, in their respective investigations, did not measure reinforcement strain, reaching their conclusions instead from a load comparison between reinforced and un-reinforced columns tests. This research also shows that the effectiveness of the masonry shell in resisting load decreases as the contribution of the vertical reinforcement in resisting axial load increases. Therefore, it was concluded that the principal of superposition used to predict the strength of reinforced concrete columns could not be applied to masonry.

The foregoing investigations into the behavior of reinforced masonry have been primarily concerned with the deformation under short-term loading. A consideration of the effects of the time-dependent deformations caused by creep and shrinkage was excluded from these research works. The subject of time-dependent deformation in masonry was not investigated for reinforced masonry until a pilot study was undertaken at the University of Manitoba in 1986. Roy[4], conducted a comparative pilot study to investigate the behavior and ultimate strength of reinforced concrete masonry columns

under sustained loading. Normal-weight two-core concrete masonry blocks of 200 x 200 x 400 mm nominal size , and type S mortar with face shell bedding were used in constructing ten pairs of reinforced masonry columns. The program was designed originally to subject one of each pair of the columns to sustained loading for a period of time, while the remaining column was used to monitor the shrinkage effect and for comparison purpose. All columns were to be tested to failure under concentric compression at a later stage. Due to an underestimation of column ultimate strength and the limitation imposed by the capacity of the testing machine, most of the specimens were tested to failure under eccentric load, only four pairs of columns being tested to failure under concentric load. The remainder of the columns were tested to failure under an eccentricity of 55 mm top and bottom except for column pair 5 which was loaded with 65 mm eccentricity at the top only. A qualitative analysis of the test results concluded that the effects of the creep and shrinkage are greatest in the early stages and over 90% of the total deformation due to sustained load occurred within the first sixty days. The time-dependent deformations cause a transfer of load to the vertical reinforcement, increasing its efficiency in resisting the load over the preload period, the increase being greater for the larger bars. Roy attributed this to the greater bond strength between those bars and the surrounding grout. The preloaded columns failed at an average ultimate strength about 8% greater than the non-preloaded columns. This was attributed to the increase in steel efficiency due to transfer of load resulting from creep. The reinforcement in the preloaded columns nearly yielded, reaching about 95% efficiency, at ultimate strength. Roy recommended that his results should be viewed with caution until they can be supported by further research and also indicated that most of his conclusions and recommendations are for the most part speculative.

2.2.2 Reinforced Concrete Columns

In contrast to reinforced masonry columns, a comparatively large number of studies have been directed toward establishing the effect of the time-dependent deformations on the ultimate strength and behavior of reinforced concrete columns under sustained load. Selected investigations are reviewed in this section to present the information available on the effect of sustained load on reinforced concrete columns to assist in understanding the behavior of reinforced masonry columns under sustained load.

In a comprehensive investigation of creep and drying shrinkage of concrete that extended over a period of nearly thirty years, Troxell, Raphael and Davis[5] 1958,tested thirty-six round-spirally reinforced concrete columns to determine the progressive change in length and stresses due to both shrinkage and creep of concrete. All columns were reinforced with six evenly spaced longitudinal bars with either 1.9% or 5% steel. All specimens were cured for three weeks, and loaded at an age of 28 days. The test results shows that load is transferred from concrete to steel until in a few cases the concrete was actually in tension while the steel reached its yield point in compression. In general, 25% of the twenty years creep took place in the first two to three months and about 75% in the first year. The test results indicated that the older the specimens at first load application the less the creep. As for deformations due to shrinkage, the test results suggested that between 14% to 34% of the total shrinkage deformation during the twenty years of observation occurred in the first two weeks of drying and 66% to 85% within one year. The test results also indicate that the moisture conditions of the storage had a great effect on both creep and shrinkage.

In 1966, Holm and Pistrang[6] observed a structural-size, reinforced, lightweight concrete column under sustained load for one year while parallel physical property tests were being conducted on plain concrete cylinders. The primary objective of this investigation was to verify a modified analytical method for the determination of the

time-dependent transfer of load from concrete to reinforcing steel. A subsidiary purpose was to emphasize the importance of understanding the time-dependent behavior of reinforced concrete structures that was being eroded by an excessive preoccupation with the behavior at ultimate load. The results of the experimental investigation were used to modify the classical equation demonstrated by Peabody[7] for the predictions of the load transfer from concrete to the reinforcing steel. The revised equation resulted in improved prediction of the actual behavior. However, it was admittedly an empirical relation based on this set of experimental data.

In 1969, at the Portland Cement Association, Pfeifer[8] investigated the time-dependent shortening of various reinforced concrete columns containing lightweight and normal-weight aggregate. Both concrete types were of comparable compressive strength. These columns were observed for the instantaneous strain under loading, time-dependent deformation due to creep and drying shrinkage, and eventually for the ultimate strength and strain behavior during short-time tests to failure. He concluded that the instantaneous strain of the lightweight concrete columns was greater than that of the normal-weight concrete columns due to the lower modulus of elasticity of lightweight concrete. The difference in the time-dependent deformations between the lightweight concrete columns and the normal-weight concrete columns are minimized for the larger percentage of reinforcement, creep and shrinkage of concrete resulting in a transfer of load to the vertical reinforcement, this transfer being greatly affected by the percentage of reinforcement. In some cases the load was carried entirely by reinforcement and it was in excess of the applied column load, leaving the concrete under small tensile forces due to shrinkage. Finally, he concluded that both types of columns have closely similar ultimate strain capacity when they are reinforced.

In 1982, Balaguru and Nawy[9] presented a method to calculate the stress redistribution due to the time-dependent deformation and total strains for both

concentrically and eccentrically loaded reinforced concrete columns. In this method the time-dependent behavior of both plain and reinforced concrete were examined through a visco-elastic model. Shrinkage and creep strains were modeled to occur concurrently. The time-dependent creep strain of concrete is given by the following expression[9]:

$$\epsilon_{cc}(t) = \frac{\sigma_o}{E_{ci}} \left[1 + K\left(1 - e^{-0.08753t}\right) \right] \qquad (2.1)$$

where

$\epsilon_{cc}(t)$ = time-dependent creep strain of concrete

σ_o = concrete stress - constant

E_{ci} = instantaneous modulus of elasticity of concrete

t = time under load expressed as the square root of the actual time in days.

K = $k_b\ k_c\ k_d\ k_e$, which are coefficients that depend on variables such as composition of concrete mix, relative humidity of storage, age at loading and thickness of member respectively.

The coefficients k_b, k_c, k_d, and k_e are quantities that can be obtained using graphs provided by *COMITE EUROPEAN DU BETON - FEDERATION INTERNATIONALE DE LA PRECONTRAINTE* (**CEB-FIB**)[10].

The time-dependent shrinkage strain of concrete is given by the following expression[9]:

$$\epsilon_{sh}(t) = \epsilon_{shu}\left(1 - e^{-0.067t}\right) \qquad (2.2)$$

where

$\epsilon_{sh}(t)$ = time dependent shrinkage strain

ϵ_{shu} = ultimate shrinkage strain

t = age of concrete expressed as the square root of the actual time in days.

The total time-dependent concrete strain for a stress σ_o can be obtained using the creep

strain of equation 2.1 and the shrinkage strain of equation 2.2 as follows[9]:

$$\epsilon_c(t) = \epsilon_{shu}\left(1 - e^{-0.067t}\right) + \frac{\sigma_o}{E_{ci}}\left[1 + K\left(1 - e^{-0.08753t}\right)\right] \qquad (2.3)$$

The time-dependent behavior of reinforced concrete columns is also modeled using the same principle as that for plain concrete. When the column is subjected to an applied load **P** and assuming that the load carried by vertical reinforcement and concrete is $\mathbf{P}_1$ and $\mathbf{P}_2$ respectively, then by imposing the equilibrium conditions[9]:

$$P = P_1 + P_2 \qquad (2.4)$$

From the compatibility conditions, the total strain in the column $\epsilon(t)$ is written as follows[9]:

$$\epsilon(t) = \frac{P_1}{E_s A_s} = \frac{P_2}{A_c E_{ci}}\left[1 + K\left(1 + e^{-0.08753t}\right)\right] + \epsilon_{shu}\left(1 - e^{-0.067t}\right) \qquad (2.5)$$

Using equations 2.4 and 2.5, the load taken by concrete $\mathbf{P}_2$ is first obtained and then the load taken by steel $\mathbf{P}_1$ and the resultant strain in the column $\epsilon(t)$ can be obtained.

This method of analysis was checked using the experimental results reported by Pfeifer[8] and the results predicted by this method were in reasonable agreement with the experimental results. This method of calculating the time-dependent reinforcement strain in concrete columns was compared with other methods of analysis proposed by Pfeifer[8] and Jordaan et al[11]. It was found that this method accounts for the different variation of creep and shrinkage with time, and it provides an explicit expression for calculating strain in concrete. The method proposed by Balaguru and Nawy[9] also considered eccentrically loaded reinforced concrete . However, eccentrically loaded columns are beyond the scope of this thesis.

The theoretical part of this thesis discussed in Chapter VI uses the creep and shrinkage expressions of equations 2.1 and 2.2 to estimate the creep and shrinkage strains of the constituent materials in reinforced masonry columns. The analysis also follows the basic principal outlined in the model proposed by Balaguru and Nawy[9].

CHAPTER III
EXPERIMENTAL PROGRAM

3.1 Materials

In an investigation leading to an understanding of the performance of masonry structures, the physical testing of representative structural components is essential to confirming the development of theoretical models for the design process. The components tested should be relevant not only to the theory, but also, if possible, to contemporary construction practice. In the experimental program described in this thesis, all materials used in the construction of the test specimens are representative of those used locally in the Winnipeg area for masonry building construction.

3.1.1 Concrete Masonry Units

All columns and prisms were constructed using standard 150 mm normal-weight hollow concrete block. These units were marketed as 15 MPa strength at 28 days. The unit dimensions are shown in Fig. 3.1. The physical properties of the unit are listed in Table 3.1.

3.1.2 Mortar

Type S mortar was used throughout the experimental program. The mortar was mixed in accordance with the *Canadian Standard Association* standard *CSA-A179M-1976 Mortar and Grout for Unit Masonry*. In order to develop higher early strength, type 30 cement was used instead of the type 10 recommended by the standard. Material mass densities required to convert mortar proportions by volume to proportions by mass were assumed to be those supplied by *CSA* standard *A179M-1976*. Mortar mix proportions are given in Table 3.2.

The mortar was initially mixed in an electrically driven mixer and then by hand. Retempering of mortar was permitted to obtain the desired consistency to complete construction of the specimens. Mortar samples from each initial and retempered mix were cast and cured in accordance with *Canadian Standard Association* standard *CAN3-A5-M83 Portland Cement.*

3.1.3 Grout

A mixture of normal weight aggregate (10 mm. maximum particle size), concrete sand and type 30 cement was used to grout the masonry prisms and the reinforced columns. The materials were proportioned to produce a mixture of about 30 MPa compressive strength and a 150 to 200 mm slump. Table 3.3 gives the grout mix proportions. Each batch of grout permitted the filling of one pair of columns, with enough material remaining for specimens for control testing. From every batch, grout prisms were cast in accordance with CSA standard A179M-1976.

3.1.4 Reinforcing Steel

Four different sizes (10M,15M,20M and 25M) of deformed bars of Grade 300 were used for vertical reinforcement. The bars were cut into lengths of 1.95 m to provide 25 mm clearance at each end of the column. Two pieces were cut from each 6 m length of bar and one piece used in each pair of columns. The columns were reinforced in the horizontal direction with #9 gauge wire reinforcement placed in the mortar joints. The joint reinforcement was of a ladder type and consisted of two parallel longitudinal wires welded to a perpendicular wire, as shown in Fig. 3.2.

3.2 Test Specimens

Twenty reinforced masonry columns were built in pairs, one of each pair for preloading, the other being the non-preloaded control specimen. All columns were ten blocks in height and one block wide, built in stack bond configuration. Each column was reinforced with two or four bars, one or two in each core. The specimen details are given in Table 3.4.

3.2.1 Construction

All columns were constructed by an experienced mason, thereby ensuring good and consistent workmanship. Preceding the construction of the masonry columns, the bottom crossheads for the preloaded and non-preloaded columns were levelled on the laboratory floor. All bottom blocks of the columns had clean-out holes cut in one face using a rotary concrete saw blade. Any block with flaws, such as large chips or cracks, was rejected. The first block of each column was laid on a mortar bed in a steel crosshead to provide a flat surface, as shown in Fig. 3.3.

Joint reinforcement was placed on the previously laid block. Mortar was then placed around the perimeter of the block, as shown in Fig 3.4. The next block was then placed, centred, levelled and the mortar joint thickness checked. After five courses of block had been laid for each column, the core reinforcement was placed with the strain gauge leads extending from the end face of the column, as shown in Fig. 3.5.

Mortar was retempered as required and mixed by hand to retain the desired consistency to complete construction of the columns. Mortar samples were taken for each initial and retempered mix and placed in the moist curing room.

Following construction of each column the mortar joints were tooled and excess mortar inside the column was removed through the clean-out holes. The columns were

covered with wet burlap and vapour barrier to provide moist curing for the mortar. The columns were then allowed to cure for 7 days before grouting commenced.

At the end of the curing period the columns were prepared for grouting. The reinforcing bars were centred in the core and seated to provide 25 mm clearance at each end. The clean-out holes were closed by clamping oiled plywood against the column. Each column pair was grouted at the same time and from the same batch of grout. The columns were filled one quarter at a time to permit thorough vibration. Grout samples were taken from each batch.

The columns were again covered with wet burlap and vapour barrier and left to cure for another 14 days. Depending on its condition, the burlap was rewetted while still on the column. The grout samples were cured in the moist room for the same period of time.

3.2.2 Instrumentation

Since masonry column strains were to be measured using a 200 mm demec gauge, demec buttons were attached with epoxy to the face shells of the columns using a 200 mm spacing bar, as shown in Fig. 3.6. The demec strain gauge was calibrated and a gauge factor of 8.04×10^2 obtained.

The strains in the vertical reinforcement were measured by means of 5 mm electrical resistance strain gauges. Two strain gauges were attached to opposite sides and located at the mid-height of each bar. A rubber coating was applied to the gauges, wires and the immediate area to protect the gauges from moisture and abrasion during the grouting process.

3.3 Test Procedure

One of each of the pairs of columns was preloaded for a period of ten months to study the effect of creep while the other was left unloaded and used as a control specimen to monitor the effect of shrinkage. At the end of the preload period all columns were tested to failure. Standard procedures were followed during the preloading and the ultimate testing of the masonry columns.

3.3.1 Preloading

A steel frame was used to subject the masonry columns to long term loading. The frame was designed such that the preload was not removed prior to testing to failure. Therefore, the frame was required to sustain not only the preload but also the failure load without damage, thereby permitting its re-use.

The frame was designed as a three-piece assembly connected by four Dywidag bars. The assembly consisted of two upper crossheads and a lower crosshead between which the column was seated, as shown in Fig. 3.7. The Dywidag bars tied the system together and transferred the preload to the column. Three demec buttons were attached with epoxy to the opposing faces of the Dywidag bars and located at mid-length. The strains in the Dywidag bars were measured using a 200 mm strain gauge. These strain measurements together with the load vs. strain characteristic of the Dywidag bars (*EA* value) were used to monitor the column load during the sustained loading period.

A polyurethane rubber compound was used as the load sustaining material in preference to springs which would be damaged during ultimate testing. Two holes were cut in the polyurethane to allow easier flow of the material under compression, thereby increasing the total deflection. Two pieces of polyurethane were used in each frame. A 12 x 175 x 350 mm steel plate was placed on each side of the polyurethane to provide a plane, rigid surface. Two pieces of 20 x 175 x 350 mm plywood were used as fillers

between the primary upper crosshead and the polyurethane. The polyurethane and the plywood were load-cycled and left overnight at the preload to reduce future creep deformations.

The plywood, polyurethane and the steel plates were arranged and centred on top of the secondary upper crosshead, as shown in Fig. 3.8 The primary upper crosshead was then lowered on top and the two upper crossheads tied together. The upper crossheads, together with the Dywidag bars, were placed on the column to be preloaded, as shown in Fig. 3.9. A bag of plaster of paris was placed between the secondary upper crosshead and the column to provide a uniform load transfer. The crossheads were then centred and levelled and nuts attached to each end of the Dywidag bars. A set of initial strain readings were taken on each column in the pair and on the Dywidag bars. The strains in the vertical reinforcement were also recorded. These readings form a reference data base for subsequent readings.

After placement of the frame, the column was placed on a plaster bed, centred and levelled in the 600 kip testing machine. Once the plaster had set (one to two hours) load was applied slowly to the column. Once reached, a load of 800 kN was maintained for a period of half an hour before tightening the Dywidag nuts.

Two hydraulic jacks connected to a pressure pump were mounted on each side of the top crosshead, as shown in Fig. 3.10, to help in tightening the nuts. The Dywidag bar was held stationary, as shown in Fig. 3.11, and the nuts were tightened gradually in a specific order to keep the space between the two upper crossheads relatively equal all around. Tightening the nuts continued until the testing machine displayed 100 kN. The goal of this procedure was to transfer 700 kN of preload to the column. This load represents about 45% of the compressive strength of a grouted masonry prism.

Strain measurements were taken immediately after the application of the load. All columns were stored in a relatively constant temperature environment and strain

readings were taken throughout the sustained loading period for both the preloaded and the non-preloaded columns.

3.3.2 Ultimate Testing

Upon expiry of the preloading period each column pair was tested to failure, a bottom assembly providing a hinged base that was bolted into the testing machine, as shown in Fig. 3.12. The column was aligned concentrically in the testing machine, and bags of plaster of paris were placed on the top and bottom of the column to assist in levelling and in distributing the load uniformly. The top and bottom courses of the column were confined using four steel plates tied together and acting against the crossheads as shown in Fig. 3.13. The reason for the confinement of the top and bottom course was to prevent local end failure due to stress concentration.

A linear variable differential transducer (LVDT), attached to the mid height of the column, as shown in Fig. 3.14, was used to measure lateral deflection of the column and, consequently, to check for concentricity of the load.

The electrical resistance strain gauges, the LVDT and the testing machine load cell were connected to the IBM data acquisition system shown in Fig. 3.15. The data acquisition system monitoring all channels continuously was set to record readings at every 50 kN increment of load.

The preloaded column was tested first. A set of demec and strain gauges readings were taken before load application. The load was applied first up to the level of the remaining sustained load, at which time all the Dywidag nuts were loosened to remove all load from the Dywidag bars. The testing machine now displayed the true load on the column and a set of demec gauge readings were taken. Loading continued with another set of readings being taken every 100 kN up to 1500 kN. At this stage the two upper crossheads were bolted together to prevent the release of the strain energy stored in the

load sustaining materials, and plywood sheets were placed around the column for safety. Loading continued to failure with only reinforcement strain and load being recorded. Details of the mode of failure were recorded and photographs taken.

Following the testing of a preloaded column, the corresponding non-preloaded column was prepared for testing. The two upper crossheads were placed on the non-preloaded column to replicate the height of the preloaded column. The upper crossheads were welded together and used in testing all the non-preloaded columns. To model the confining behavior of the bottom crosshead on the preloaded column a steel confining assembly was prepared for the bottom of the non-preloaded column. The top and bottom courses were confined in a similar fashion to the preloaded column, as shown in Fig. 3.16. Other preparations for testing were identical to those used in the preloaded columns.

An initial set of demec readings was taken before the loading began. The column was then loaded at a constant rate with demec readings being taken every 100 kN up to 1500 kN. Testing of the column continued following the same procedure used for the preloaded column.

TABLE 3.1 Dimension and Physical Properties of Concrete Block Unit

Actual width (mm)	140
Actual Height (mm)	190
Actual length (mm)	390
Minimum face shell thickness (mm)	26
Minimum web thickness (mm)	26
Gross area (mm^2)	54,600
Net area (mm^2)	31,700
Percentage solid (%)	58
Minimum compressive strength -Based on net area- (MPa)	15

TABLE 3.2 Mortar Mix Proportions

Material	Mass(kg)
Type 30 high early cement	13.6
Hydrated lime	2.9
Mortar sand	56.0
Water (to start)	13.2

TABLE 3.3 Grout Mix Proportions

Material	Mass (kg)
Cement	15.1
Sand	81.6
Aggregate (10 mm)	71.4
Water	16.3
W/C	1.08

TABLE 3.4 Column Details

Column Number	Bar Size	Steel Area (mm^2)	Steel Ratio ($p\%$)	Loading	
				Preloaded	Non-Preloaded
CP1U	2M10	200	0.37		X
CP1L	2M10	200	0.37	X	
CP2U	2M10	200	0.37		X
CP2L	2M10	200	0.37	X	
CP3U	2M15	400	0.73		X
CP3L	2M15	400	0.73	X	
CP4U	4M10	400	0.73		X
CP4L	4M10	400	0.73	X	
CP5U	2M20	600	1.10		X
CP5L	2M20	600	1.10	X	
CP6U	2M20	600	1.10		X
CP6L	2M20	600	1.10	X	
CP7U	2M10 & 2M15	600	1.10		X
CP7L	2M10 & 2M15	600	1.10	X	
CP8U	4M15	800	1.47		X
CP8L	4M15	800	1.47	X	
CP9U	2M25	1000	1.83		X
CP9L	2M25	1000	1.83	X	
CP10U	2M20 & 2M15	1000	1.83		X
CP10L	2M20 & 2M15	1000	1.83	X	

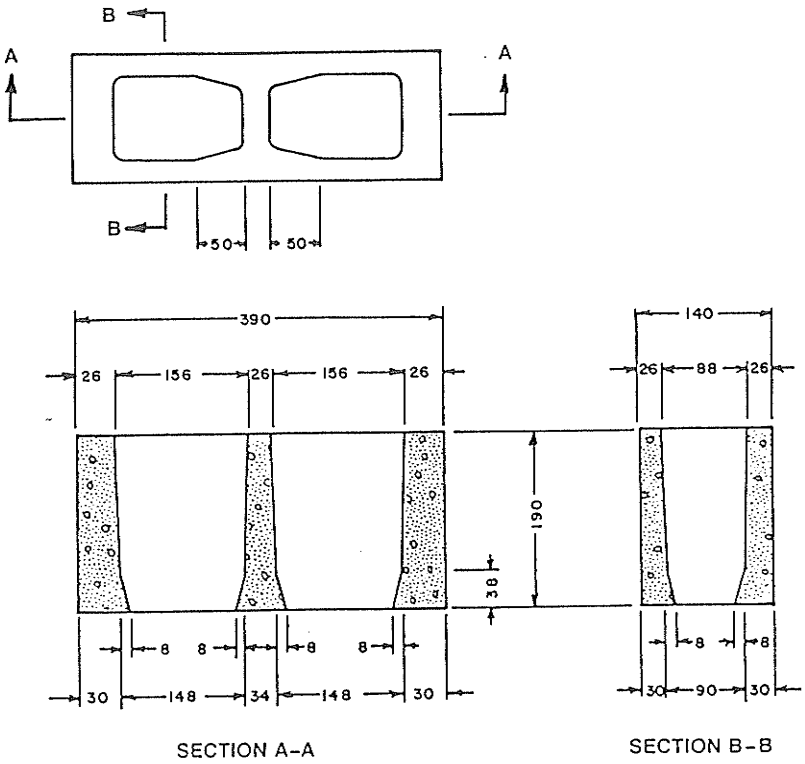

Figure 3.1. Physical properties of the masonry unit

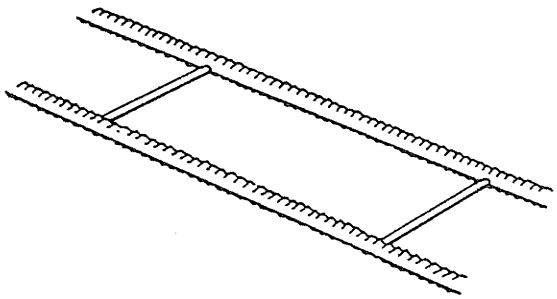

Figure 3.2. Ladder type joint reinforcement

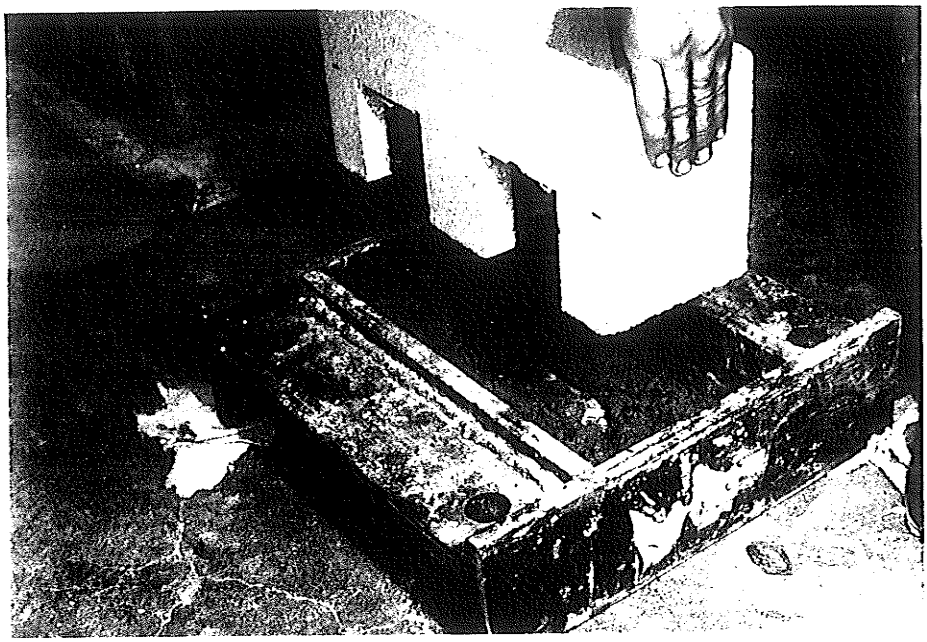

Figure 3.3. First stage of column construction

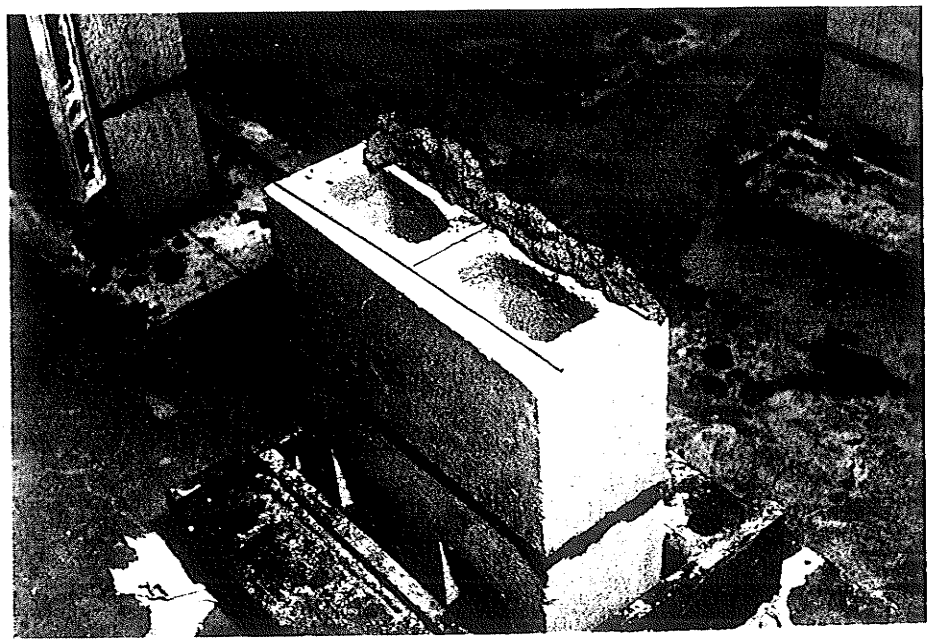

Figure 3.4. Placement of joint reinforcement

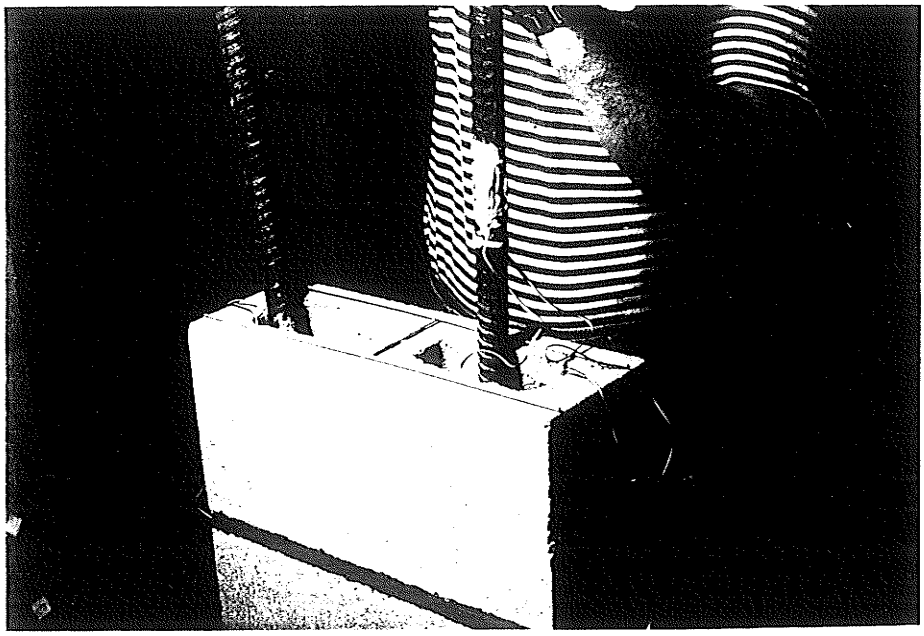

Figure 3.5. Placement of core reinforcement

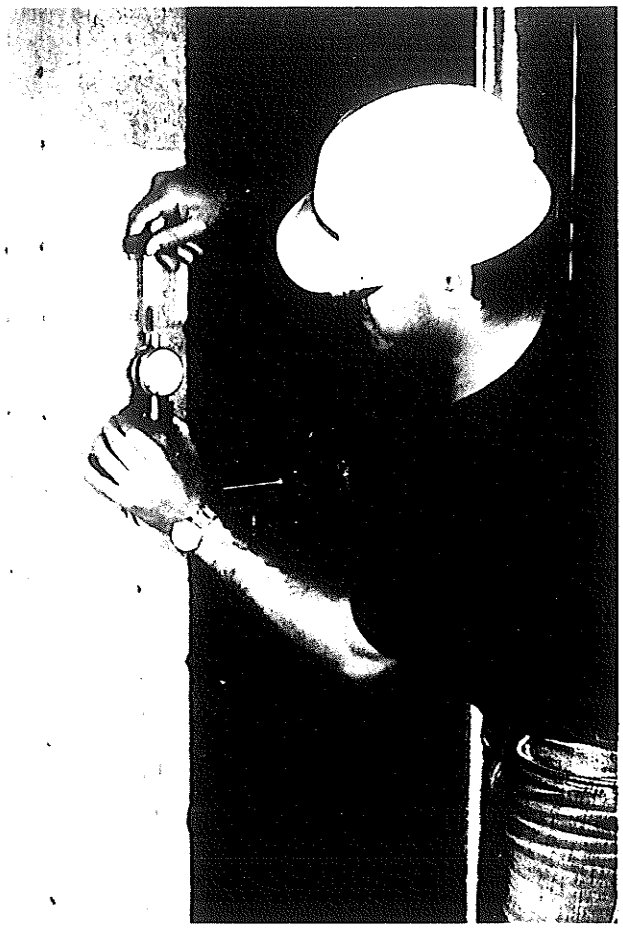

Figure 3.6. Demec button placement on test column

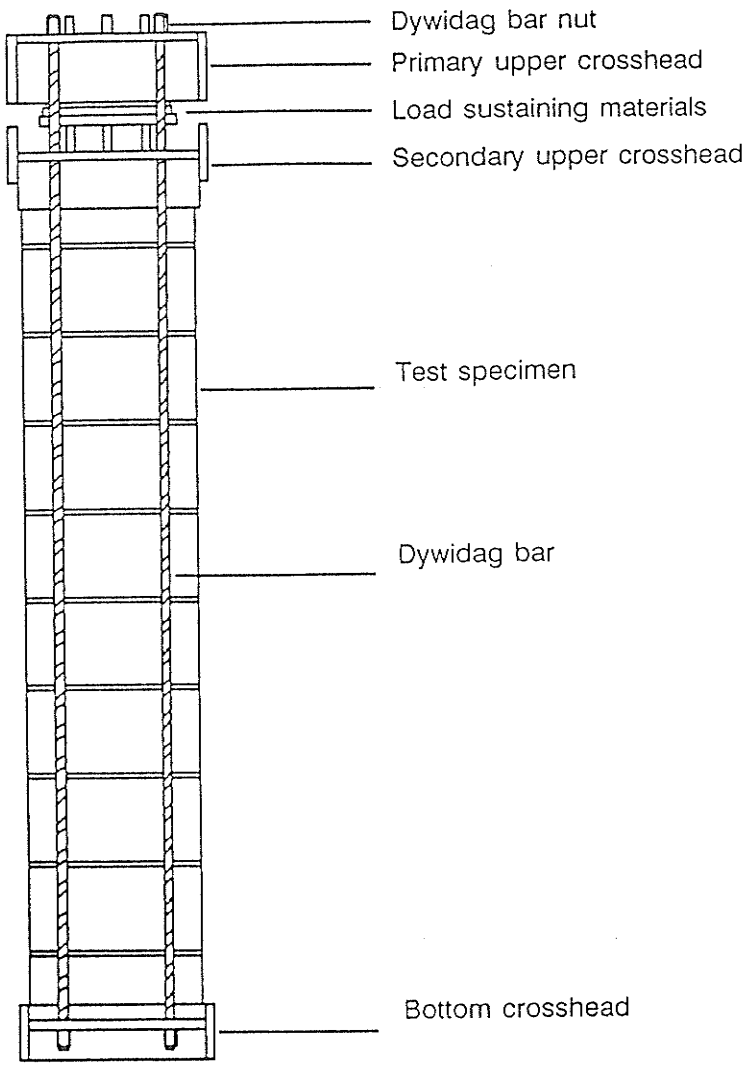

Figure 3.7. Typical pre-loaded column

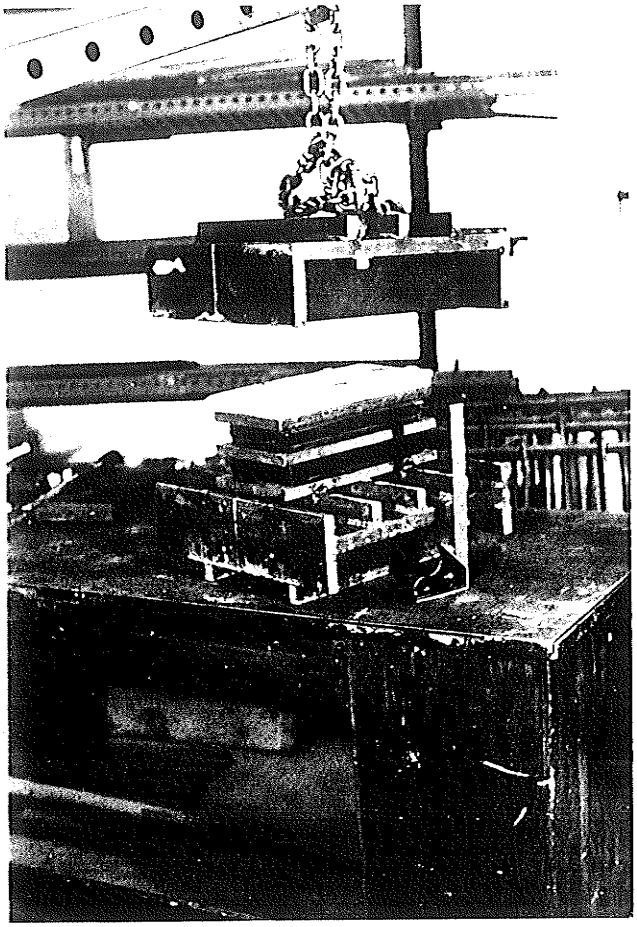

Figure 3.8. Placement of the load sustaining materials

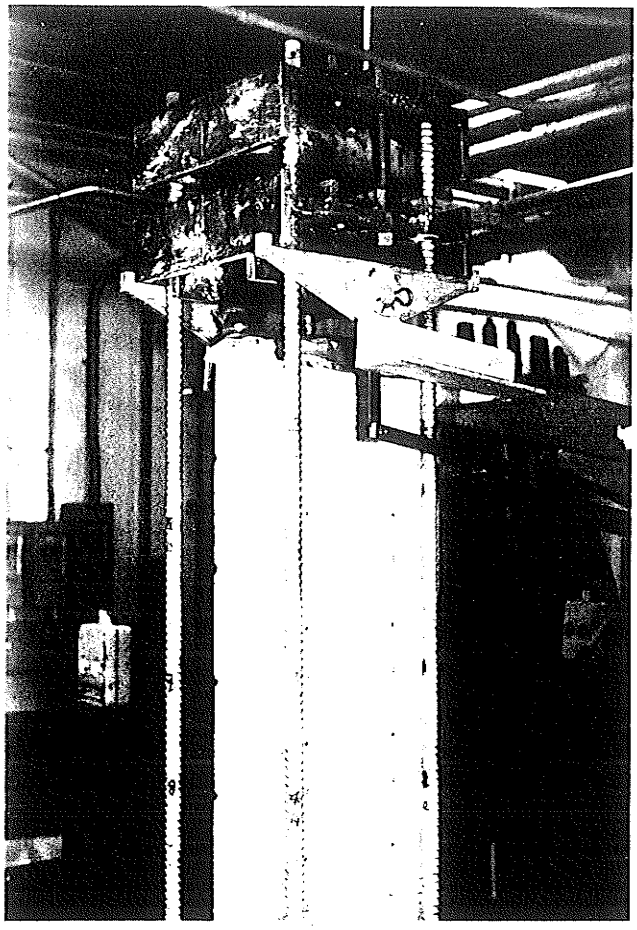

Figure 3.9. Placement of the upper crosshead

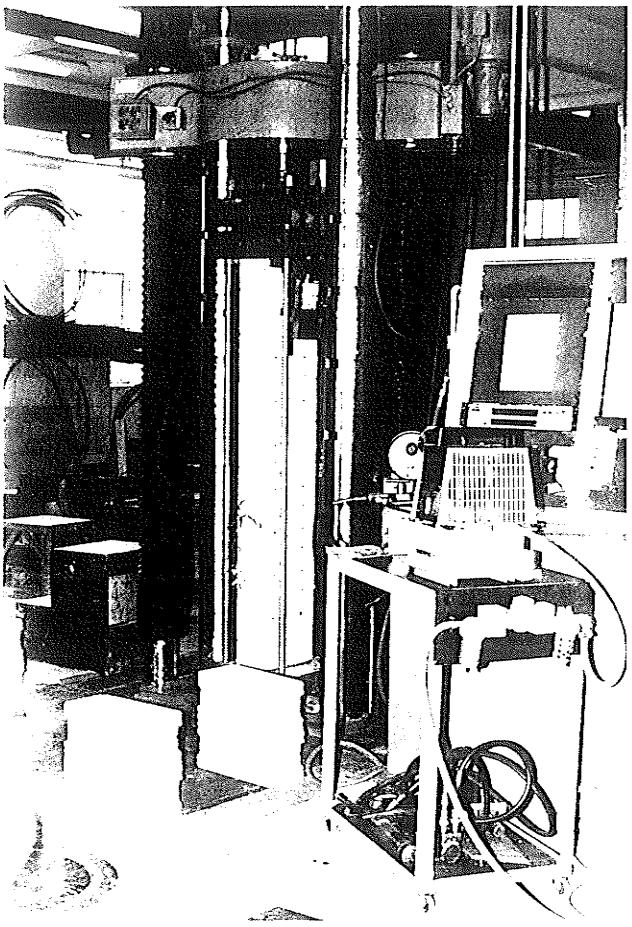

Figure 3.10. Tightening Dywidag bar nuts

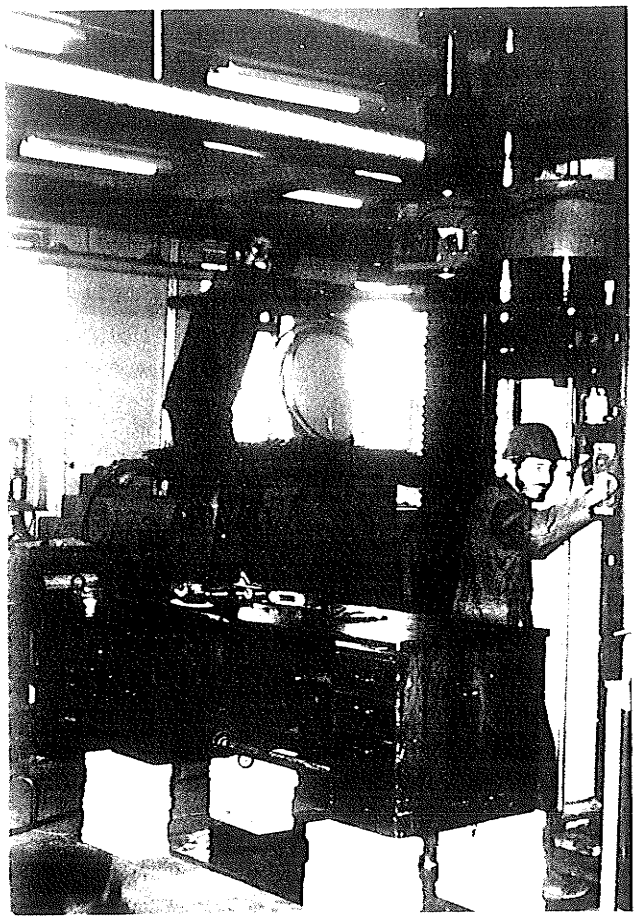

Figure 3.11. Pre-loading the test column

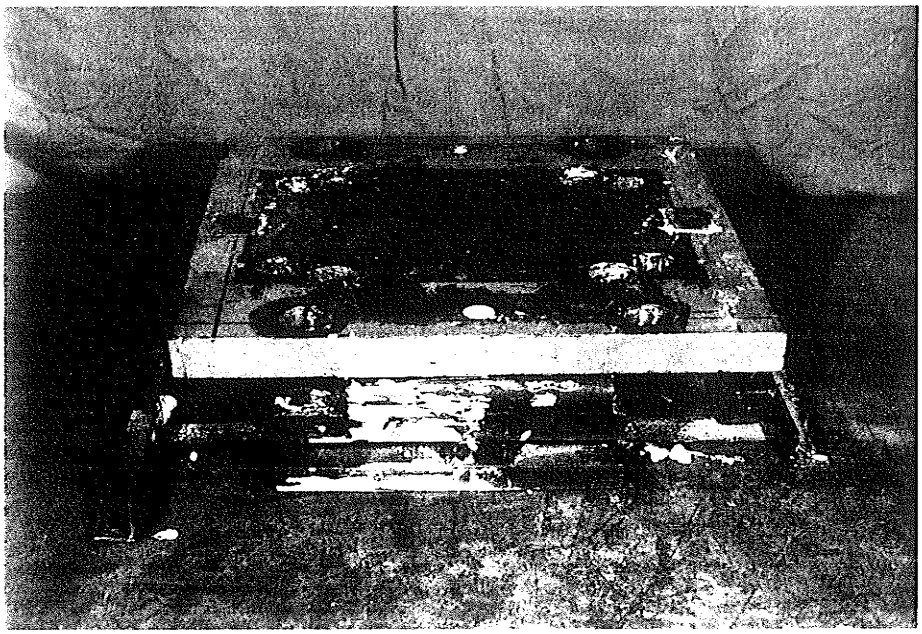

Figure 3.12. Bottom connection assembly

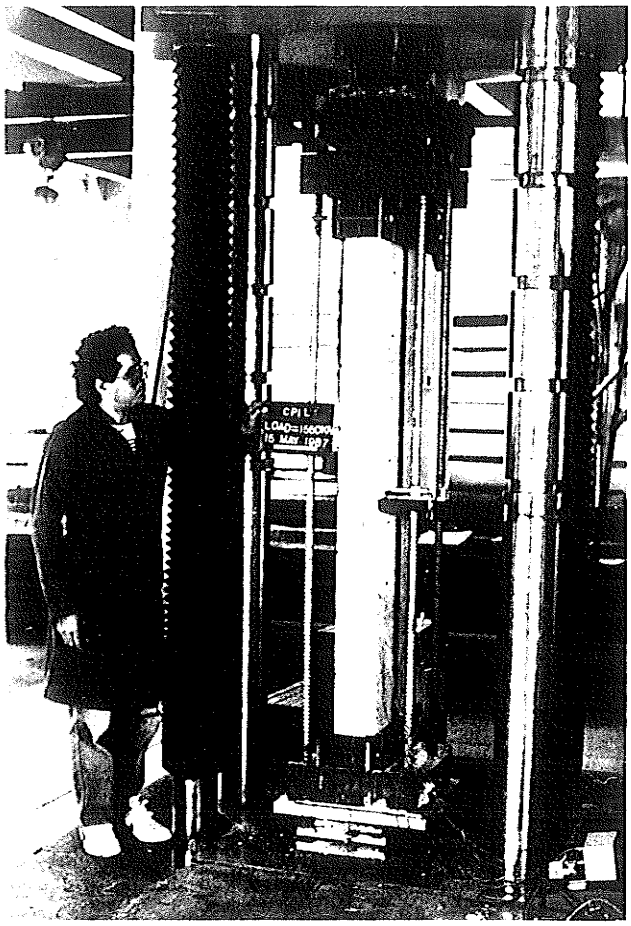

Figure 3.13. Typical column testing arrangement

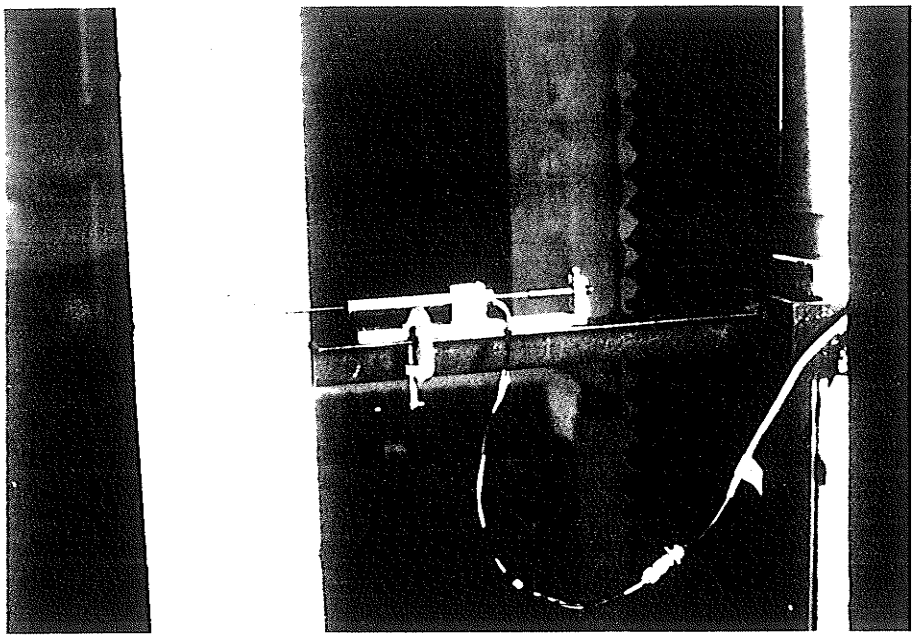

Figure 3.14. Column instrumentation

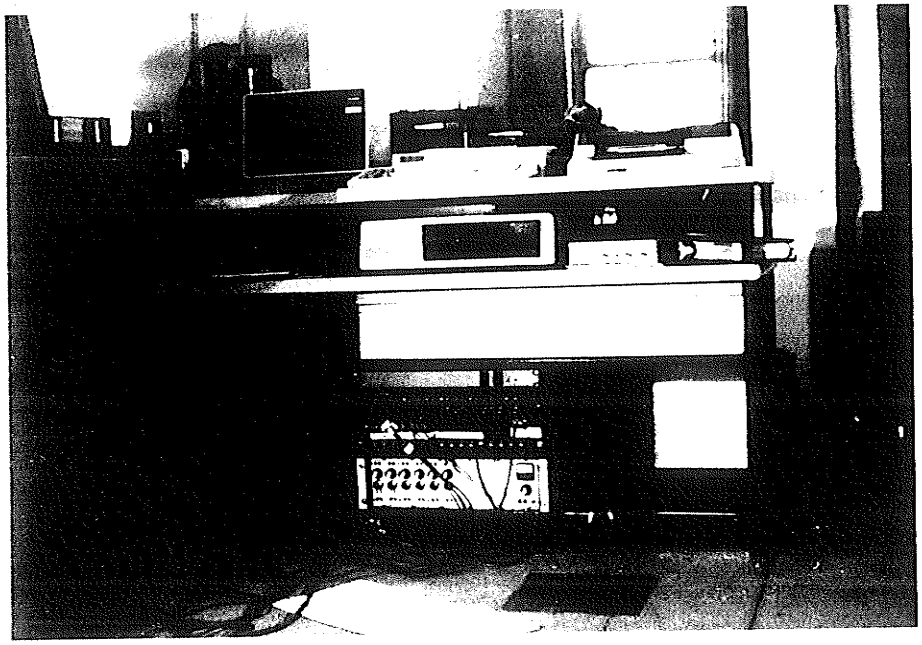

Figure 3.15. Data acquisition system

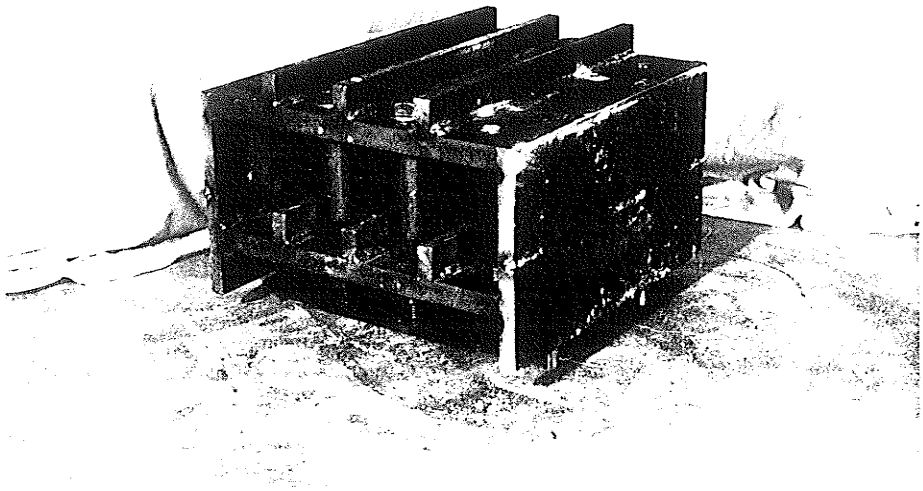

Figure 3.16. Upper crossheads welded together

CHAPTER IV
MATERIAL PROPERTIES

4.1 Introduction

Essential to the analysis of the test results for the columns described in Chapter III is a knowledge of the properties of the materials used in the construction of these structural elements; as well, the material specimens should be subjected to representative curing and testing conditions. In this chapter the experimental program to determine the properties of the constituent materials of the reinforced masonry column is discussed. In order to evaluate representative column material properties, the mortar and grout specimens were subjected to similar curing conditions and tested at the same time as their corresponding columns. The properties of masonry prisms constructed with these materials were examined and used to assist in determining the value of the sustained load. The load-strain characteristics of the Dywidag bars used in the preloading steel frame were examined and used to monitor the preload.

4.2 Properties of Masonry Units

4.2.1 Compressive Strength

The standard compressive strength test for masonry units consists of capping the ends of a single masonry unit and applying an axial load. Compressive strength values of masonry units obtained from such tests are influenced by a number of factors such as dimensions, testing procedure, and support conditions.

Masonry units are normally tested between steel platens which are much stiffer than the units and tend to restrict the lateral expansion at the unit ends. Due to this restraining effect, masonry units of different dimensions, particularly of different height-to-width ratios, yield different compressive strength values for a given material. The capping material between the masonry unit and the steel plate can also affect the strength

by either increasing or decreasing the frictional restraint of the steel plates. Other factors which affect the masonry unit strength are curing conditions and moisture content in the units, age at testing, loading rates, and load control at failure. The effect of these factors on the strength of masonry are discussed in detail by Maurenbrecher[14, 15].

In addition, the state of stress developed in a standard compression test of a masonry unit differs from the stress state in a masonry assembly. In a masonry assembly, the masonry unit is normally laid with mortar on the face-shells but not on the web (face-shell bedding) while the capping of a single unit is full mortar bedding . Experimental results indicate, predictably, that masonry with face-shell bedding fails at a lower strength than do those of full mortar bedding. In addition to stresses in the direction of applied load, the masonry unit in an assembly is subjected to tensile stresses in the lateral direction resulting from differences in the strength and deformation characteristics between the unit and the mortar. The uniaxial compressive strength and the modulus of elasticity of the mortar are considerably lower, and Poisson's ratio comparable to or higher than the corresponding values of the masonry unit. Consequently, the mortar tends to expand laterally more than the units. However, since the mortar and the masonry unit are bonded together, the mortar is confined laterally by the unit. As a result, tensile stresses are introduced into the block and tensile failure can occur before the unit compressive strength is reached. For these reasons, researchers have some difficulty relating the strength of masonry to that of the unit.

In this study, the compressive strength of the masonry units was determined by testing ten randomly chosen masonry blocks. These are the same masonry units whose physical properties were reported in Table 3.1. All units were capped with a thin layer of plaster and tested in accordance with *American Society for Testing and Materials* Standard *ASTM C140 Sampling and Testing Concrete Masonry Unit*. For samples B1 to B4, the maximum and minimum observed net area failure stresses were 31.1 MPa and

23.5 MPa, respectively, with a mean value of 28.9 MPa and a coefficient of variation of 12.47%. These four samples were tested shortly after delivery, and used to assist in the determination of the level of the sustained load. Masonry unit samples B5 to B10, were tested about one year later at the same time as the column specimens. The maximum and minimum observed net area failure stresses for these samples were 34.0 MPa and 25.4 MPa, respectively, with a mean value of 28.8 MPa and coefficient of variation of 10.42%. The strength of all samples tested are recorded in Table 4.1. Comparison of the compressive strength of both sets of samples indicated that the strength was fully developed at the time these units were being delivered.

4.2.2 Creep

Fifteen randomly chosen masonry units were prepared for testing to investigate their creep properties. Each unit was capped with plaster. After the plaster had set, demec buttons were attached with epoxy to the face shell of the masonry unit on both sides using a 50 mm spacing bar. The specimens were placed under sustained load in the steel frame shown in Fig. 4.1. Three frames each containing five masonry units in series, were used. The frame consisted of three steel plates connected together by four Dywidag bars. The load was applied to the specimens in the following manner.

A load of 400 kN, representing about 45% of the unit strength, was applied to the specimens through a hydraulic jack, and maintained through a self-adjusting, air pressure control system.

An initial set of demec readings were taken before the load was applied. Included in this set of readings are before and after control readings on a standard bar. These readings provide a reference data base and a correction factor. Once the load was applied and the pressure in the supply line reached the value corresponding to the desired

load, another set of demec readings were taken. Demec readings continued throughout the testing period.

Using initial readings as a data base, the measurements taken on the loaded masonry unit specimens during the sustained load period were reduced into time after loading and average masonry unit strain. These results are presented graphically in Figs. 4.2 to 4.4 where the data for each graph represents the average measurements for the three specimens in series for each test. Applying equation 2.1 for the time-dependent strain and a factor of *KB* of 0.98, as obtained in section 7.1, the predicted strain-time relationship plotted in Figs. 4.2 to 4.4 is in good agreement with the measured data.

4.3 Properties of Grout

4.3.1 Compressive Strength

Prior to grouting the columns, two trial mixes were prepared and tested to select the grout mix that yielded the desired compressive strength and workability. However, the workability of the grout used in this investigation was considerably less than that used in masonry construction. Mix design for the grout was presented earlier in Table 3.3. Because of the large number of columns tested and the size of the concrete mixer, one batch of grout was used for each set of two columns. All the grout ingredients were drawn from identical stock piles to ensure consistency. Grout prism specimens were taken from each batch for testing.

Grout prism sampling was done in accordance with *CSA* Standard *A179M-1976*. Fig. 4.5 shows the details of a typical mould used for casting grout specimens. The grout specimens were subjected to curing conditions similar to and tested at the same time as their corresponding columns. The specimen ends were capped with sulphur to get plane and parallel bearing faces. The mean compressive strength was 35.4 MPa,

with a standard deviation of 3.5 MPa, and a coefficient of variation of 9.9%. Table 4.2 presents the compression test results for grout specimens.

4.3.2 Creep

Six grout prisms, representative of the different grout batches used in grouting the masonry columns, were selected for testing to investigate the grout creep properties. The specimens were capped with sulphur to get plane and parallel bearing faces. After the sulphur had set, two demec buttons were attached to opposing faces of the grout prism using a 50 mm spacing bar. The specimens were placed under sustained load using a concrete creep testing frame, as shown in Fig. 4.6. The frame was used to load six specimens at one time (in series). The load was applied to the specimens in the following manner.

A load of 72 kN, representing the same stress level as that of column specimen, was applied to the specimens through a hand pump connected to the hydraulic ram placed in the top portion of the creep frame. The load was then maintained through heavy springs placed in the lower portion of the frame.

An initial set of demec readings were taken before and after the application of the load. Demec readings continued throughout the testing period.

Using initial readings as a data base, the measurements taken on the loaded grout specimens during the sustained load period were reduced into time after loading and average strain. These results are presented graphically in Fig. 4.7. The data presented in this graph represents the average measurements for the six specimens in series for each test. Applying equation 2.1 for the time-dependent strain and a factor of KG of 1.06, as obtained in section 7.1, the predicted strain-time relationship plotted in Fig. 4.7 is in good agreement with the measured data.

4.4 Properties of Mortar

4.4.1 Compressive Strength

The purpose of mortar is to bond the masonry units together to form a weatherproof composite material capable of safely resisting the applied load. Mortar workability is essential for bonding and ease in laying masonry. Re-tempering (i.e. re-wetting and mixing) of mortar was permitted once to obtain the desired consistency to complete construction of the columns specimens. Although no tests were conducted to check the consistency of the mortar, the mason was advised to maintain a consistent level of workability. Mix proportions of type *S* mortar used throughout the experimental program are those reported earlier in Table 3.2.

Mortar sampling was carried out in accordance with *CSA* Standard *CAN3-A5-M83*. The standard requires that the compressive strength of mortar be determined from 50 mm cubes which have been placed in the moist room for 20 to 24 hours before de-moulding and curing in lime-saturated water until testing. Understandably, these preparation and curing conditions seldom reflects actual construction practice. Since mortar in the masonry assembly is placed in 10 mm thicknesses and loses water due to suction into the units reducing the mortar water/cement ratio and potentially increasing its strength[16, 17]. For this reason the compressive strength of mortar indicated by the cube test may not represent the strength of the mortar in the masonry assembly. However, the results obtained by the cube testing can be used as an indication of mortar consistency.

Brass moulds were used to prepare three test specimens, 50 mm cubes, from each initial and re-tempered mortar mix. The mortar cubes were moist cured for 21 days , with the cubes being demolded after 24 hours. All mortar cubes were tested at the same time as their corresponding column specimens except for four specimens which were tested earlier to assist in the determination of the sustained load. A summary of the

ultimate strength results is given in Table 4.3. The mean compressive strength of the initial mix cubes was 29.4 MPa with a coefficient of variation of 2.28%, and for the retempered mix cubes, 29.4 MPa with a coefficient of variation of 5.24%.

4.4.2 Creep

Twelve mortar cubes, representative of the different initial and retempered mortar, were selected for testing to investigate the mortar creep properties. A demec button was attached with epoxy at the middle of the opposing faces of each mortar cube using a 50 mm spacing bar. The specimens were placed under sustained load in the steel frame shown in Fig. 4.8. Three frames were used, each of which was used to load four mortar cubes in series at one time.

Once the specimens were in place, the frame was transferred to the testing machine and a set of initial demec readings taken. A load of 33 kN, representing the same stress level as that of column specimen, was then applied slowly to the specimens. The load was kept constant for a period of about 30 minutes before the nuts were slowly tightened in order to transfer the load to the frame. Immediately following the loading, the frame was removed from the testing machine and a set of demec readings taken. Strain measurement continued throughout the testing period at a decreasing frequency.

The data collected on the mortar prisms during the period of sustained load were reduced into time after loading and average mortar strain. These results are presented graphically in Figs. 4.9 to 4.11 where the data for each graphs represents the average measurements for the four mortar specimens in series for each test. Applying equation 2.1 for the time-dependent strain and a factor *KM* of 1.17, as obtained in section 7.1 of Chapter VII, the predicted strain-time relationship plotted in Figs. 4.9 to 4.11 is in good agreement with the measured data.

4.5 Masonry Prism Strength

According to *Canadian Standard Association* Standard *CAN3-S304-M84 Masonry Design for Buildings*, the compressive strength of masonry is established by the strength of prisms having a height-to-thickness ratio of 2.70. Such prisms consist of two concrete blocks, stack bonded by mortar to form the two-course construction shown in Fig. 4.12. Both hollow and grouted prisms were tested to determine the compressive strength of the masonry, f'_m, to assist in determining the value of the sustained load.

A total of eleven prisms were constructed from 150 x 200 x 400 mm, two-core, hollow concrete blocks manufactured from normal weight aggregates. The blocks were chosen at random from a lot containing more than 200 blocks used for the construction of the column specimens. The prisms were constructed by the same professional mason who built the column specimens. Mortar type S, with the mix proportions reported earlier in Table 3.2, was used in all specimens. Joint reinforcement, while customarily provided in the mortar bed joints, is not employed in the prism specimens. Five of these prisms were grouted with the same concrete mix used to grout the column specimens. The properties of the concrete mix are reported earlier in Table 3.3. Both grouted and ungrouted prisms were subjected to the same curing conditions as the column specimens.

All prisms were capped with a thin layer of plaster before being tested. The prisms were tested in the 600-kip capacity universal testing machine. Five prisms, three ungrouted and two grouted, were tested at the age of 28 days and used to assist in the determination of the sustained load. The remaining prisms were tested at the end of the sustained load period. Table 4.4 summarizes the results of the prism tests.

4.6 Properties of Steel

Dywidag bars were used to transfer the load to the preloaded masonry columns. In order to monitor the sustained load throughout the testing period, strain readings from

the Dywidag bars were used. The load on the masonry columns at any time was obtained from the stiffness, *EA*, of the Dywidag bars. Therefore it was necessary to evaluate experimentally the properties of the Dywidag bars.

Reinforcement steel bars of grade 300 and various sizes were used to reinforce the masonry columns. The yield point of these bars is significant in the analysis of the strain measurements taken during testing of the reinforced masonry columns. The properties of the different sizes of the reinforcement bars were evaluated in this program.

4.6.1 Dywidag Bar Properties

A total of 10 Dywidag bar specimens were tested for material properties. Mechanical, electrical and demec strain gauges were used in the instrumentation of these specimens. Four specimens were instrumented with a mechanical strain gauge. Six specimens were instrumented with electrical resistance strain gauges. Of these six specimens, two were also instrumented with demec buttons for use with a demec strain gauge. Testing of the specimens was carried out in accordance with *Canadian Standard Association* Standard *G30.12-M1977 Billet-Steel Bars for Concrete Reinforcement.*

A typical load-versus-strain behavior of the Dywidag bars, determined from tension tests, is shown in Fig. 4.13. The test results indicate a linear behavior and a distinct yield point. The yield load and *EA* results are summarized in Table 4.5. The average yield load for the Dywidag bars was 285.5 kN with a coefficient of variation of 3.46% and the average *EA* value was 131.03 MN with a coefficient of variation of 2.08%.

4.6.2 Reinforcing Bar Properties

60 mm long tension specimens were taken from each full length of reinforcement bar used in the experimental program. From each full length, three specimens, one of

which is instrumented with two electrical strain gauges, were tested to evaluate the characteristics of reinforcing bars.

All bars exhibit a well-defined yield point and a linear behavior up to the yield point. Table 4.6. summarizes the yield and ultimate strength results of the different sizes of reinforcement bars used in the experimental program.

TABLE 4.1 Compressive Strength of Concrete Block

Block Number	Failure Load (kN)	Ultimate Strength (MPa)
B1	986.1	31.1
B2	745.6	23.5
B3	972.8	30.7
B4	961.8	30.3
Average	916.6	28.9
C.V.		12.47%
B5	935.3	29.5
B6	1078.4	34.0
B7	804.3	25.4
B8	837.5	26.4
B9	909.1	28.7
B10	914.6	28.9
Average	913.2	28.8
C.V.		10.42%

TABLE 4.2 Compressive Strength of Grout

Batch Number	Failure Load (kN	Ultimate Strength (MPa)
1	202.4	37.0
2	193.5	37.5
3	169.0	34.0
4	146.8	28.5
5	204.6	36.4
6	184.6	34.0
7	244.7	43.5
8	180.2	33.2
9	175.7	34.0
10	191.3	35.6
11	200.2	36.4
12	195.7	34.8
Average	190.7	35.4
C.V.		9.9%

TABLE 4.3 Compressive Strength of the Mortar

50 x 50 x 50 mm. Cubes

Mix	Identification	Failure Load (kN)	Compressive Strength (MPa)
Initial	M1	75.82	29.38
	M2	73.96	28.66
	M3	75.07	29.09
	M4	78.79	30.53
	M5	80.15	29.30
Average			29.39
S.D.			0.67
C.V.			2.28%
Retempered	M1	73.29	28.40
	M2	71.74	27.80
	M3	80.0	31.0
	M4	74.06	28.70
	M5	80.26	31.10
Average			29.40
S.D.			1.54
C.V.			5.24%

TABLE 4.4 Compressive Strength of Masonry Prisms

Hollow Prisms			Grouted Prisms		
Prism Number	Failure Load (kN)	Compressive Strength (f'_m)	Prism Number	Failure Load (kN)	Compressive Strength (f'_m)
HP1	932.92	29.43	GP1	1554.56	28.47
HP2	876.70	27.66	GP2	1572.17	28.79
HP3	1008.36	31.81			
Average		29.36			28.63
S.D.		2.08			.23
C.V.		7.03%			.79%
HP4	1043.20	32.91	GP3	1810.30	33.16
HP5	765.60	24.15	GP4	1752.90	32.10
HP6	1044.70	32.96	GP5	1779.0	32.58
Average		30.01			32.61
S.D.		5.07			.53
C.V.		16.9%			1.63%

TABLE 4.5 Properties of Dywidag Bars

Bar Number	Yield Load (kN)	*EA* (MN)
1	281.56	127.083
2	270.17	137.283
3	296.37	130.442
4	276.80	130.060
5	299.90	132.231
6	293.00	131.839
7	295.00	132.450, 129.712
8	278.00	131.148, 127.666
9	182.78	132.068
10	281.48	128.800
Average	285.50	131.03
S.D.	9.877	2.723
C.V.	3.46%	2.08%

TABLE 4.6 Mechanical Properties of Steel Reinforcement

Bar Size	Bar No.	Yield Strength f_y (MPa)	Ultimate Strength f_u (MPa)	Elastic Modulus E (MPa)	Yield Strain ε_y
10M	1	351.41	551.58	205,109	1640×10^{-6}
	2	359.19	552.69		
	3	362.53	553.80		
	4	395.89	637.20		
	5	391.44	630.50	190,583	2032×10^{-6}
15M	1	351.97	544.90	170,907	2117×10^{-6}
	2	350.86	537.12		
	3	350.30	538.24		
	4	349.19	549.63		
	5	355.02	544.91		
20M	1	373.65	587.54	180,292	2100×10^{-6}
	2	364.76	576.05	179,813	2022×10^{-6}
	3	356.97	580.50		
25M	1	349.53	555.20		
	2	349.60	547.40	179,277	1983×10^{-6}

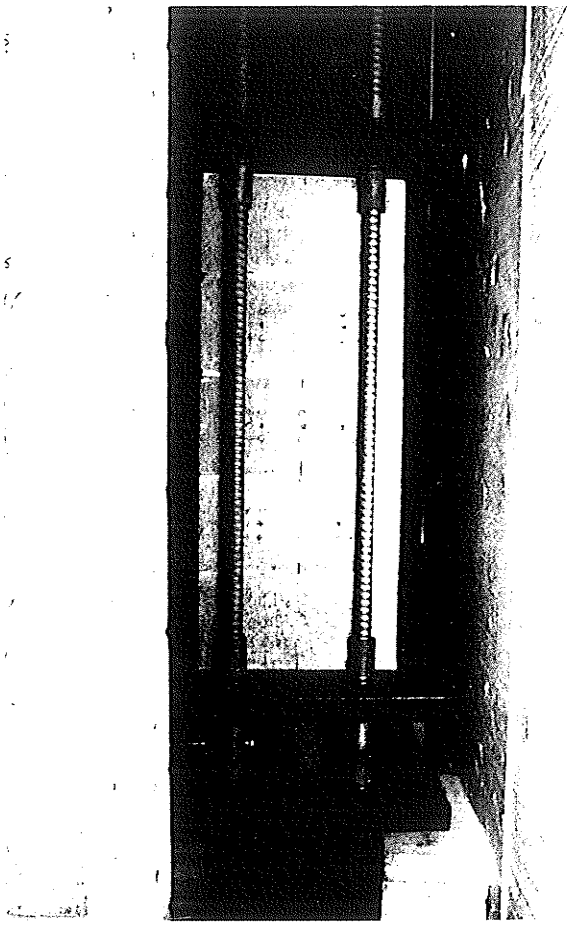

Figure 4.1. Creep frame for masonry unit

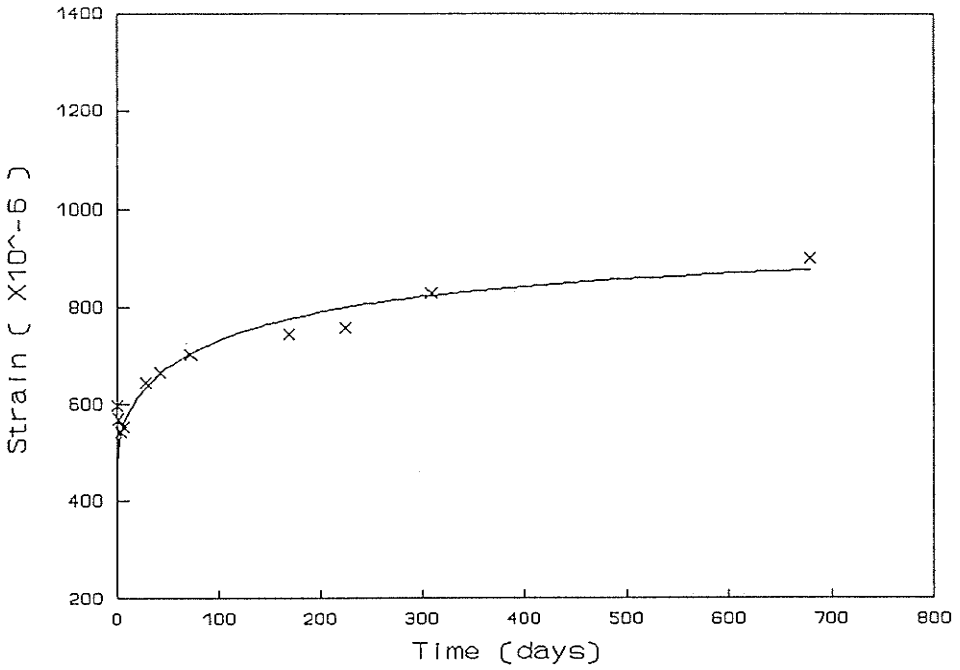

Figure 4.2. Creep strain for masonry unit Series B1

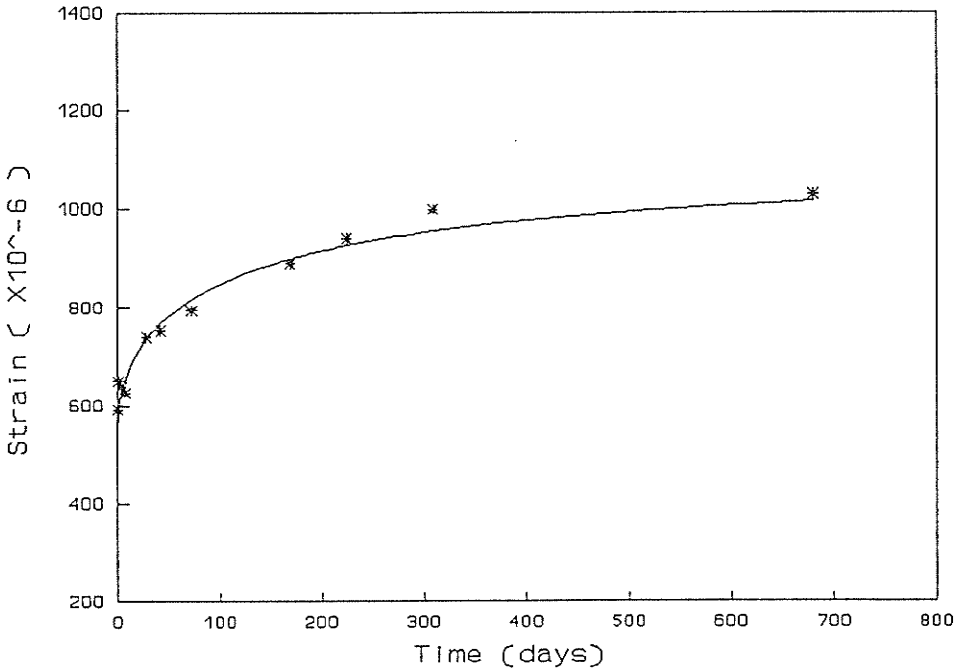

Figure 4.3. Creep strain of masonry unit Series B2

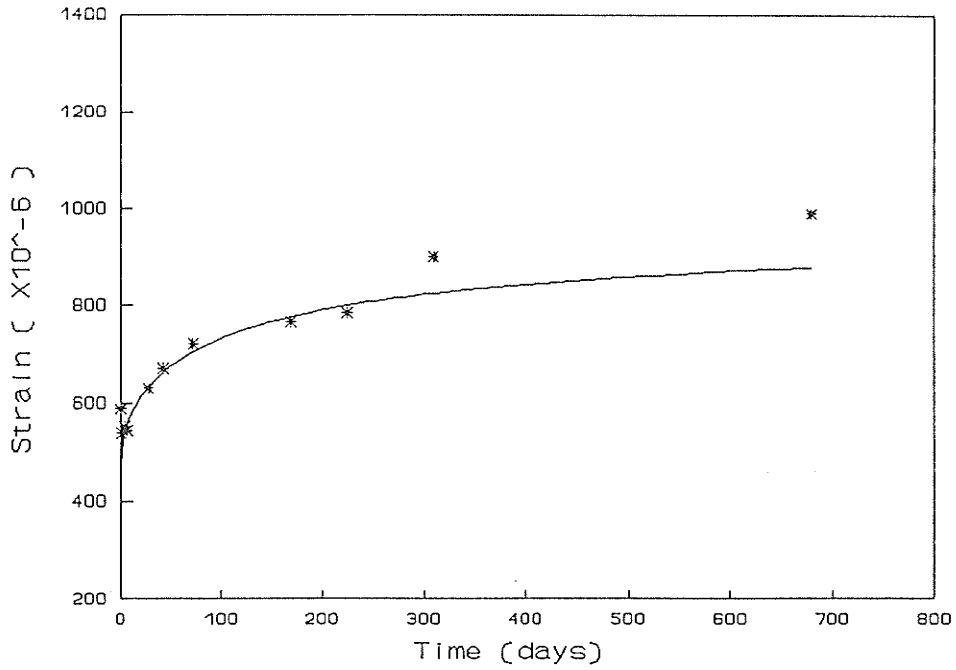

Figure 4.4. Creep strain of masonry unit Series B3

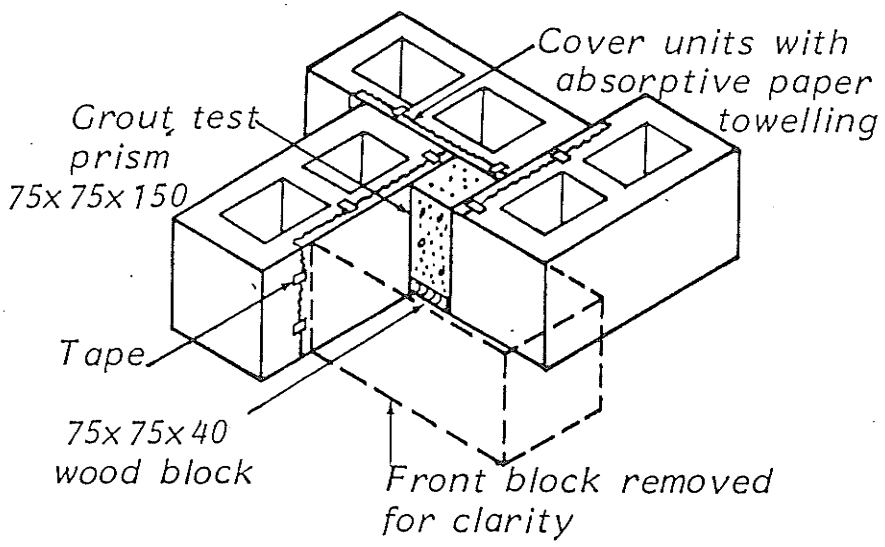

Figure 4.5. Mould for grout specimens

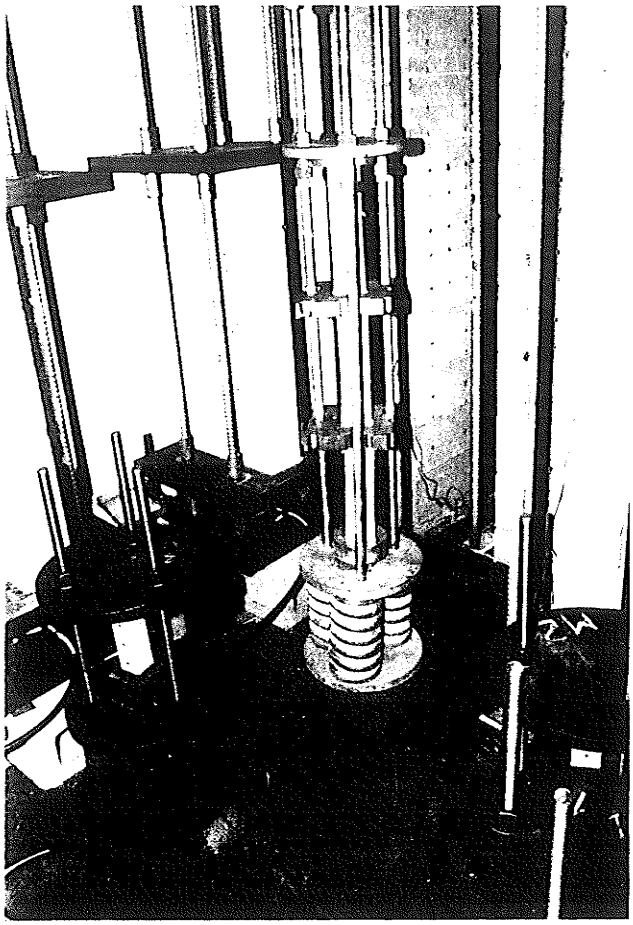

Figure 4.6. Creep frame for testing grout

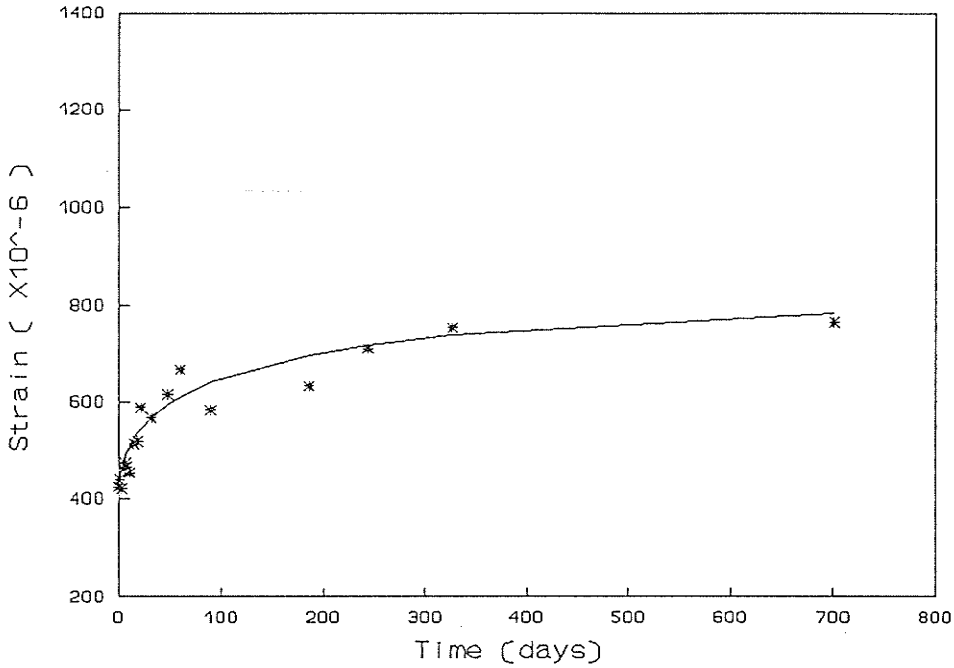

Figure 4.7. Creep strain of grout

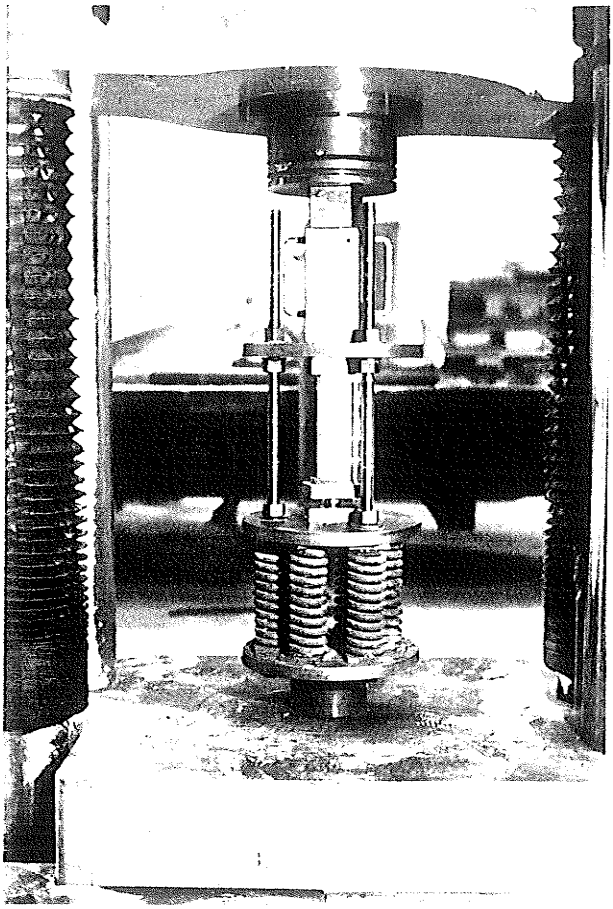

Figure 4.8. Creep frame for testing mortar

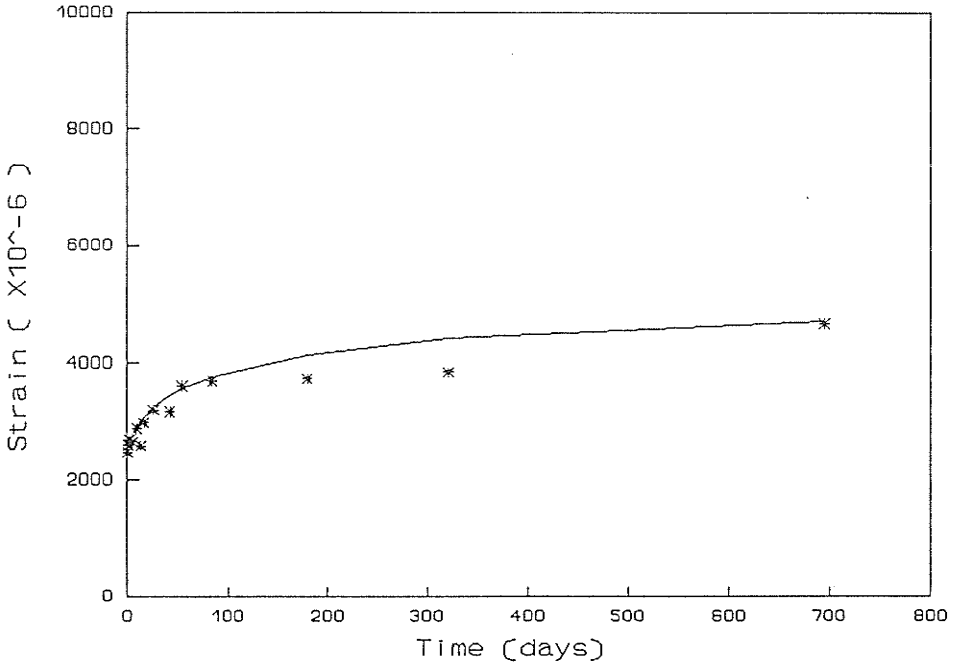

Figure 4.9. Creep strain for mortar Series M1

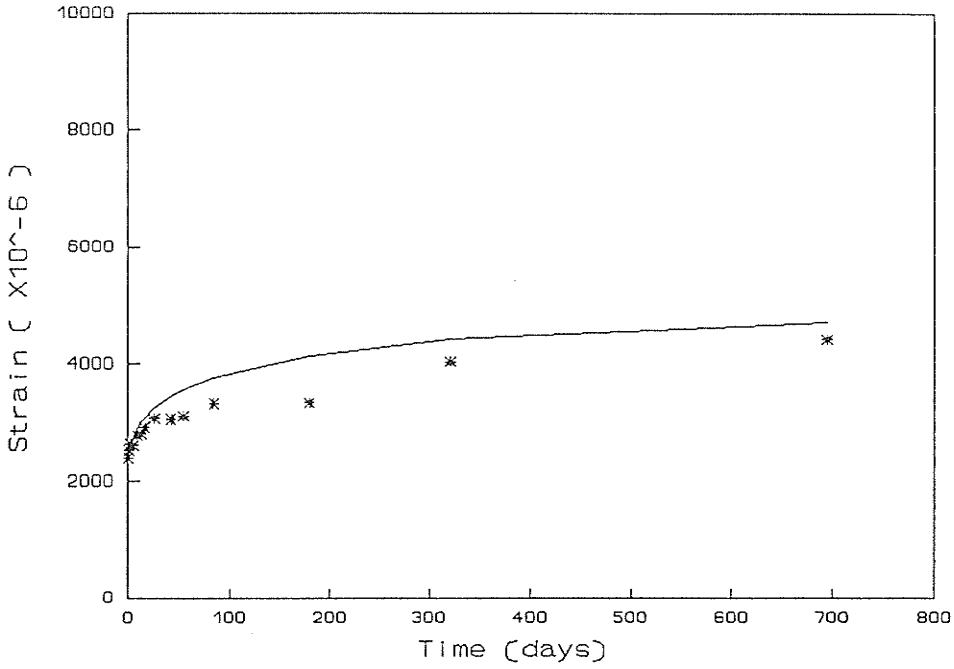

Figure 4.10. Creep strain for mortar Series M2

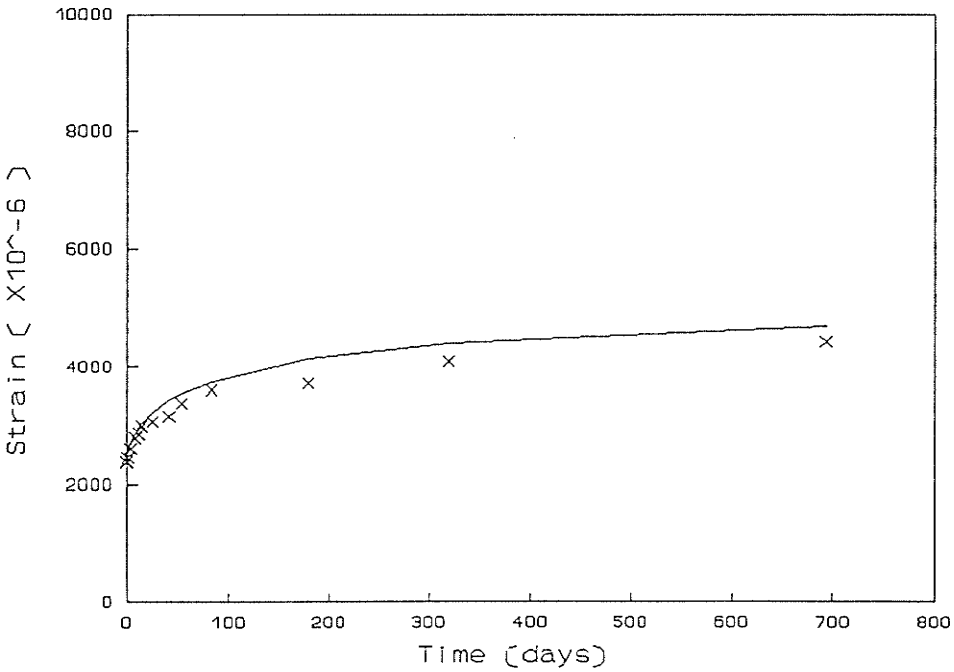

Figure 4.11. Creep strain for mortar Series M3

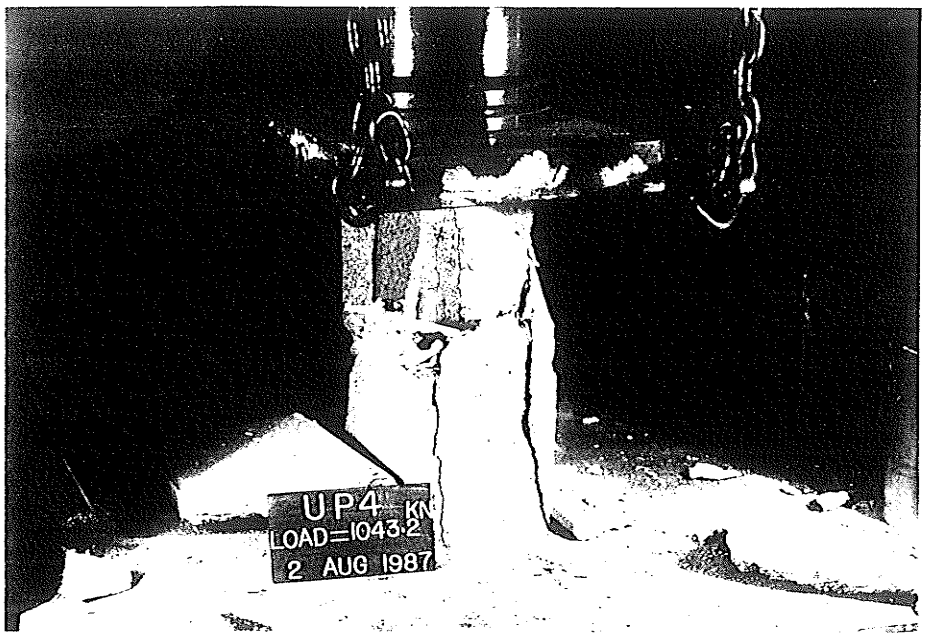

Figure 4.12. Masonry prism under testing

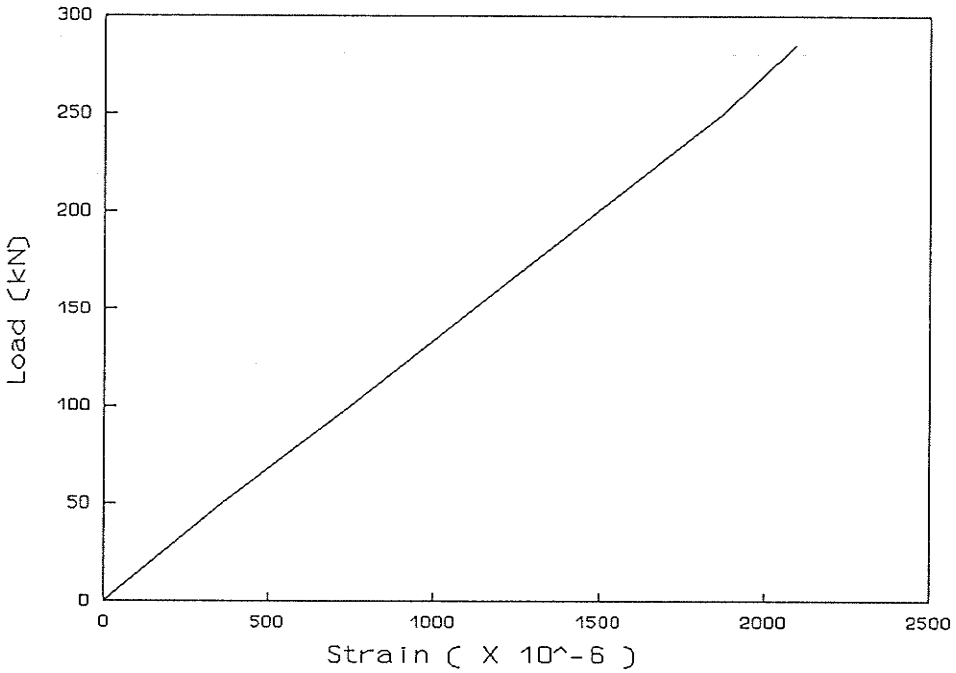

Figure 4.13. Load-strain relationship for Dywidag bar

CHAPTER V
COLUMN TEST RESULTS

5.1 Introduction

The experimental program involved testing ten pairs of reinforced concrete masonry columns. One column in each pair was subjected to sustained load for a period of time, the other column being the non-preloaded control specimen. A description of the columns tested is given in Table 3.4 of Chapter III. The responses of all specimens were monitored throughout the period of sustained load and during test to failure. Thousands of mechanical demec strain gauge readings were collected through the preloading period and from ultimate testing. A data reduction program was written and used to prepare the data for analysis.

Mechanical demec and electrical resistance strain gauge readings on all the masonry columns were input by hand to an IBM-PC. This data was collected through preloading and during ultimate testing. The computer read the testing machine load cell and electrical resistance strain gauge data directly during the ultimate testing of the masonry columns.

Using initial readings as a data base, the data reduction program processed the data into: time after preloading, concrete block column strain, Dywidag bar loads, column load, reinforcement bar loads and the percentage of column load carried by reinforcement. The program was designed to apply adjustment and correction to the demec strain gauge readings. It was also designed to warn the user of possible incorrect demec readings. Given a variation limit the program identifies the deviant strain or strains in a group of values to be averaged. Options included deletion of the value or values in question, continuing the program or aborting the program to permit editing.

The test results are presented for each phase of testing, the preloading time period and the ultimate testing of the masonry columns. The curves of the behavioral data are compared in terms of the effect of the variables included in the experimental program.

5.2 Preload Time Period

During the preload time period, strains were monitored for both the preloaded columns and their companion non-preloaded control specimens. The strain in the reinforcement bars was measured using electrical strain gauges. Mechanical strain gauges together with demec gauges were used to monitor the strain in the masonry columns and the load in the creep frame.

5.2.1 Behavior Under Sustained Load

5.2.1.1 Time-Dependent Column Strain

In addition to instantaneous elastic shortening under load, creep and drying shrinkage of masonry unit, grout and mortar contribute to further shortening. The variation of the average column strain of the pre-loaded columns is shown in Fig. 5.1 and Fig. 5.2. The column strain increased with time due to the effect of creep and shrinkage, the rate of increase being higher in the early stage when these factors have their greatest influence.

The time-dependent column deformation was significantly affected by the reinforcement percentage, among other factors. The test results given in Fig. 5.1 compare the average column strain of pre-loaded columns **CP2L**, **CP5L**, and **CP10L** with reinforcement percentages of **0.37**, **1.10**, and **1.83** respectively. The variations of the column strain for preloaded columns **CP3L**, **CP8L**, and **CP9L** with reinforcement percentages of **0.73**, **1.47**, and **1.83** respectively are shown in Fig. 5.2. These results indicate that as the reinforcement percentage increases a decreasing portion of the load

is carried by the other component materials at the initial load, consequently decreasing the time-dependent column deformation.

In an attempt to investigate the effect of reinforcement bar size, a number of columns were reinforced with different bar sizes while the reinforcement percentage was kept constant. In Fig. 5.3 the variation of column strain with time is given for pre-loaded columns **CP3L**, and **CP4L** having a reinforcement percentage of **0.73** and reinforced with **2#15** and **4#10** respectively. The test results suggest that the time-dependent column strain is influenced more by the percentage of reinforcement than by bar size. Similar comparisons are shown in Fig. 5.4, for pre-loaded columns **CP5L**, **CP6L** and **CP7L**, and in Fig. 5.5, for **CP9L** and **CP10L**.

5.2.1.2 Time-Dependent Reinforcement Strain

In reinforced masonry columns the applied load is initially distributed between the component materials according to their elastic response. However, as creep and drying shrinkage occur, a redistribution of load between the constituent materials takes place. The changes in the measured reinforcement strains in the preloaded columns are shown in Fig. 5.6 and Fig. 5.7. Predictably, the strain in the reinforcement increased throughout the preload period, the rate of increase in the time-dependent reinforcement strain being higher in the early stages where most of creep and drying shrinkage take place.

Comparison of the time-dependent reinforcement strain for pre-loaded columns with different percentages of steel, given in Fig. 5.6 and Fig. 5.7, indicates that the increase in the measured strain during the preload period was higher for the lightly reinforced columns. This is related to the initial distribution of the applied load between masonry unit, grout and reinforcement. The masonry unit and grout in the heavily reinforced column carry a small portion of the load initially, and therefore creep less than

in the case of lightly reinforced columns, and consequently less load is transferred to the reinforcement.

The bar size did not appear to influence the reinforcement strain. The variation of the reinforcement strain during the preload period for the columns with different bar sizes and having the same percentage of reinforcement is shown in Fig. 5.8 to 5.10. It was difficult to compare these curves due to the variation of the initial preload.

Fig. 5.11 to 5.15 illustrate the contribution of the reinforcement in carrying the load during the preload period. The test results indicate that the percentage of load carried by the vertical reinforcement increased during the preload period due to creep and drying shrinkage. The rate of increase was higher at the early stages where most of creep and drying shrinkage take place. The initial and final percentage of load carried by reinforcement was always higher for the heavily reinforced columns. Over the preload period the increase in this percentage was also higher for the heavily reinforced columns.

Fig. 5.16 illustrates the change in column load throughout the preload period for a typical column. The column load decreased with time due to creep and shrinkage of the column and creep of the load sustaining materials. The decrease in the column load was higher at the early stages where creep and drying shrinkage have their greatest effect. However, the column load reached a reasonably stable value after about three months. The change in column load throughout the preload period for the remaining columns is given in Appendix A.

5.2.2 Shrinkage Without Load

5.2.2.1 Time-Dependent Column Strain

Typical data from the non-preloaded columns is presented in Fig. 5.17 and Fig. 5.18. These curves show the time-dependent column strains caused by drying

shrinkage during about one year of storage at an average 22° *C* and about 50% relative humidity. All columns were initially cured under the conditions described in Section 3.2.1. The average column strain increased with time due to the effect of drying shrinkage. The rate of increase was higher at the early stages where most of the shrinkage takes place. In most cases the column strain approaches a constant level near the end of the storage period.

The data shows that the time-dependent response to long-term volume change is significantly influenced by the percentage of longitudinal reinforcement. The final time-dependent column strain caused by drying shrinkage was higher for the lightly reinforced columns. This is related to the resistance of the reinforcement to drying shrinkage of the masonry unit and grout.

The data shown in Fig. 5.19 through Fig. 5.21 gives a comparison of the time-dependent column strains due to drying shrinkage between columns reinforced with identical steel ratio but different bar sizes. Here again the data indicates that time-dependent column strain is more significantly influenced by the percentage than by the size of reinforcement.

5.2.2.2 Time-Dependent Reinforcement Strain

The time-dependent reinforcement strains for the non-preloaded columns are shown in Fig. 5.22 and Fig. 5.23. In general, the vertical reinforcement is gradually subjected to increasing compressive stress caused by drying shrinkage of masonry unit, grout and mortar. The negative or tension strain in some of the curves was probably the result of shrinkage cracks occurring at or near the location of the strain gauges.

It was difficult to see the effect of increasing the percentage of vertical reinforcement in the non-preloaded columns because of the effect of shrinkage cracking. Similarly, it is difficult to see the effect of the change in the size of the reinforcement.

However, the data presented in Fig. 5.24 and Fig. 5.25 suggests the importance of steel ratio rather than bar size in resisting drying shrinkage.

5.3 Ultimate Strength Testing

Ultimate strength tests were conducted to compare the performance of preloaded and non-preloaded columns. These tests take place over a relatively short period of time and therefore time-dependent factors such as creep and shrinkage are of little significance to the final behavior of the columns.

Upon the completion of the preload period, the preloaded and non-preloaded columns of each pair were tested successively. Strain measurements began at approximately the level of the remaining preload for the preloaded columns and at zero load for the non-preloaded columns. Details of the ultimate testing procedure are given in Section 3.3.2.

5.3.1 Average Column Strain

Variation of the column strain with respect to load during the ultimate load test for the preloaded columns is shown in Fig. 5.26 and Fig. 5.27. The data indicates the existence of an elastic behavior up to about 1200 kN. The variation of column strain was significantly affected by the percentage of the vertical reinforcement. The slope of the strain-load curve increases with increased area of steel. This illustrates the stiffening effect of the reinforcement. The change in the size of the reinforcement appear to have little effect on the strain behavior of the columns, as indicated by the results shown in Fig. 5.28 and Fig. 5.29.

Fig. 5.30 and Fig. 5.31 shows the measured load-strain relationships during the ultimate strength testing for the non-preloaded columns. These results also indicate the existence of an elastic behavior up to about 1200 kN and illustrate the stiffening effect

of increasing the percentage of vertical reinforcement. Again the test results from the non-preloaded columns shown in Fig. 5.32 and Fig. 5.33 indicate the insignificance of bar size on the load-strain relationship.

5.3.2 Reinforcement Strain

The changes in the reinforcement strains during ultimate strength testing of the preloaded columns are shown in Fig. 5.34 to Fig. 5.37. These curves confirm the near elastic column behavior up to 1200 kN. The data shows that the reinforcement strain reaches yielding before failure in all the preloaded columns. The data presented in Fig. 5.35, Fig. 5.36 and Fig. 5.37 shows the insignificant effect of bar size on the reinforcement strain of the preloaded column during testing to failure.

Fig. 5.38 to Fig. 5.42 show the variation of vertical reinforcement strain for the non-preloaded columns during testing to failure. For these columns the initial strain was taken as the unloaded strain at the start of testing rather than the strain at the end of the pre-load period. The latter, being representative of local effect, would be misleading in the interpretation of the data. The final steel strain from the preload period was included for the preloaded columns. In some cases, the reinforcement in the non-preloaded column does not reach the yielding stage before failure. This was shown clearly in the lightly reinforced columns. Similar to the preloaded columns, the reinforcement strains for the non-preloaded columns indicate elastic behavior of the columns up to about 1200 kN. They also indicate that the behavior of the columns was influenced more by the percentage of the reinforcement than by its size, as shown in Fig 5.40, Fig. 5.41 and Fig. 5.42.

5.3.3 Ultimate Strength and Mode of Failures

Ten pairs of reinforced masonry columns were tested in this research program. These columns had two major variables. These were that one column in each pair was preloaded and that the pairs of columns contained varying amounts of core reinforcement. In this section, the results of ultimate strength testing, together with the subsequent observation, are used to determine the extent to which these two factors affect column behavior. It also complements the load-strain data and helps in drawing the final conclusions.

5.3.3.1 Ultimate Strength

The test results of the ultimate load for the masonry columns are summarized in Table 5.1. These results indicate clearly that the columns ultimate strength was greatly influenced by construction variations, reinforcement area and whether or not the column was preloaded before being tested to failure. While the ultimate strength test results give no definite correlation between the preloading and the column ultimate strength, preloaded columns **CP1L**, **CP4L**,**CP7L**, **CP8L** and **CP9L** failed at an ultimate load greater than their corresponding non-preloaded columns. In the case of column pair **CP2** the preloaded column **CP2L** failed at a slightly lower ultimate load than the corresponding non-preloaded column **CP2U**. The preloaded column in this pair exhibited cracking of the top block at the end of the preloading period, as shown in Fig. 5.43, and some voids were observed at the location of failure due to poor grouting resulting from poor grout workability. These two factors together may have contributed to the lower ultimate strength of **CP2L**. Preloaded column **CP3L** failed at a lower ultimate load than the corresponding non-preloaded column and also lower than the columns in pairs **CP1** and **CP2** which contain less reinforcement. A post-failure examination of preloaded column **CP3L** revealed incomplete grouting at the location of failure, as shown in

Fig. 5.44. The grout workability was such that even with the aid of a vibrator the entire core space could not be filled with grout. Similarly, non-preloaded column **CP4U** failed at a lower load than the columns in pairs **CP1** and **CP2**, which contain less steel, due to poor grouting at the location of failure. The failure of **CP3L** and **CP4U** provide a vivid illustration of the effects of poor grout workability and/or workmanship.

The experimental results presented in Table 5.1 clearly indicate the significant effect of the amount of reinforcement on the ultimate strength of the masonry columns. Excluding **CP3L** and **CP4U**, which failed prematurely, the 100% increase in A_s between column pairs **CP1** and **CP2** and column pairs **CP3** and **CP4** resulted in an average 19.2% and 7.5% ultimate strength gain for the preloaded and non-preloaded columns respectively. Similarly, in the case of column pairs **CP3** and **CP4** and column pair **CP8**, the increase in A_s resulted in an average 5.7% and 5.5% ultimate strength gain. This indicates a positive correlation between A_s and ultimate strength.

5.3.3.2 Mode of Failure

Since it was necessary to surround the columns with plywood during the final stage of the ultimate testing to contain any flying debris, post-failure observations formed the basis on which the failure type was identified. Although the failure of the preloaded columns was more explosive than that of the non-preloaded columns, this is likely due to a partial release of strain energy stored in the load sustaining materials, since it was difficult to tighten the bolts and bring the two upper crossheads together in the final stage of testing. In the case of the non-preloaded columns, the two upper crossheads were welded together before the testing started and consequently released minimal strain energy.

In general the failure of the preloaded columns was characterized by vertical cracks on all faces with longer cracks on the face shells. These cracks were located

around the zone of failure. The failure culminated in 45° shear planes accompanied by buckling of the reinforcement bars and spalling of the block face shell, as shown in Fig. 5.45. In most cases, the failure of the preloaded columns occurred near the top, except for columns **CP5L** and **CP8L** where the failure was near the bottom of the columns, as shown in Fig. 5.46 and Fig. 5.47 respectively. Preloaded column **CP3L** failed at the middle where poor grouting was observed, as shown in Fig. 5.48.

The failure of the non-preloaded columns was less explosive and the vertical cracks shorter than those experienced by the preloaded columns. This could be attributed partly to the elimination of the strain energy released from the upper crossheads which were welded together in case of the non-preloaded columns. The non-preloaded columns with small areas of steel (200 - 400 mm^2) failed at the top of the columns due to crushing of the block and grout, as shown in Fig. 5.49, except for column **CP4U** which failed near the middle where poor grouting was observed at the same location as shown in Fig. 5.50. The columns with larger steel areas (600 - 1000 mm^2) failed at the middle. These columns exhibited long cracks and post failure buckling of steel bars similar to that of the preloaded columns as shown in Fig. 5.51. Columns **CP7U** and **CP8U** failed due to crushing of the concrete block and grout at the top and the bottom as shown in Fig. 5.52 and Fig. 5.53 respectively. These columns have a comparatively large area of steel but smaller bar size. In the case of column **CP8U**, it was also observed that the grout was segregated and the bottom block was not completely filled with grout at the location of the clean-out.

TABLE 5.1 Summary of Test Results

Column Number	Grout Strength (MPa)	Steel Yield Strength (MPa)	Ultimate Load (kN)
CP1U	37	391	1787.3
CP1L			1831.5
CP2U	37.8	396	1841.2
CP2L			1833.0
CP3U	28.5	351	1961.1
CP3L			1761.9
CP4U	36.4	355	1681.3
CP4L			2183.7
CP5U	34	365	2355.8
CP5L			2255.3
CP6U	43.5	374	2396.0
CP6L			2328.4
CP7U	33.2	356	2245.1
CP7L			2403.5
CP8U	34	351	2057.8
CP8L			2308.0
CP9U	35.8	350	2444.9
CP9L			2561.8
CP10U	36.4	356	2473.8
CP10L			2369.8

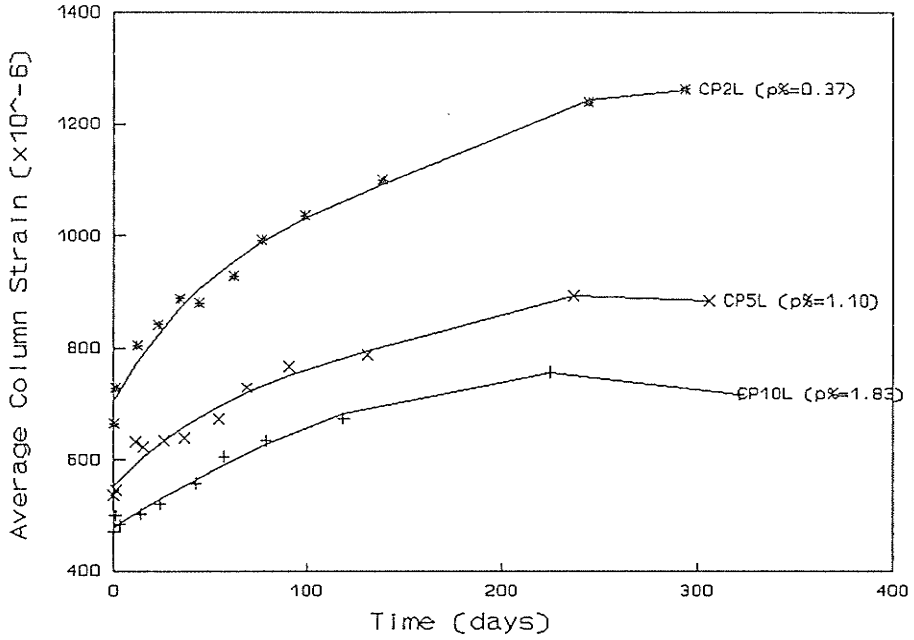

Figure 5.1. Variation of time-dependent column strain (preloaded columns CP2L, CP5L, CP10L)

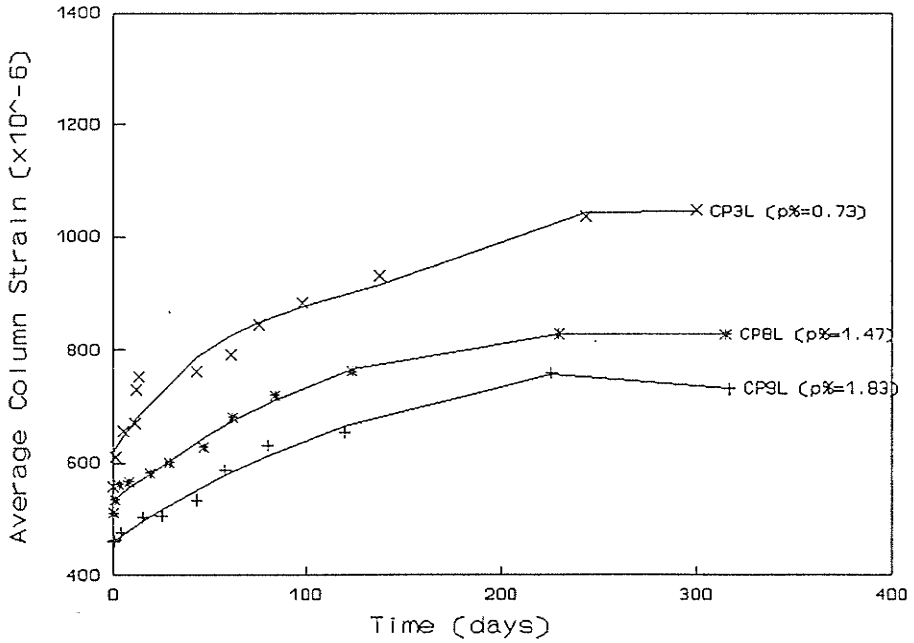

Figure 5.2. Variation of time-dependent column strain (preloaded columns CP3L, CP8L, CP9L)

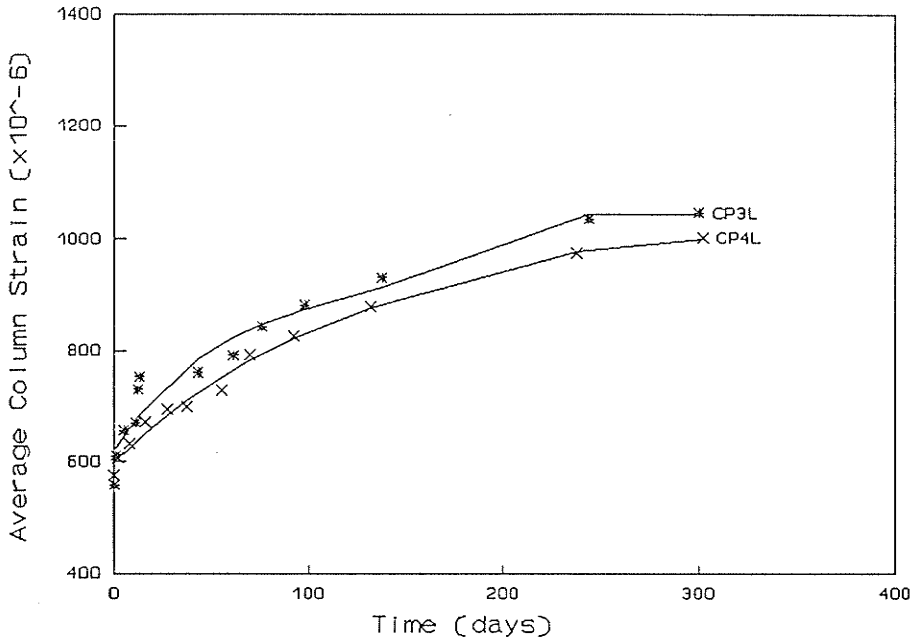

Figure 5.3. Effect of bar size on time-dependent column strain (Preloaded columns - p% =0.73)

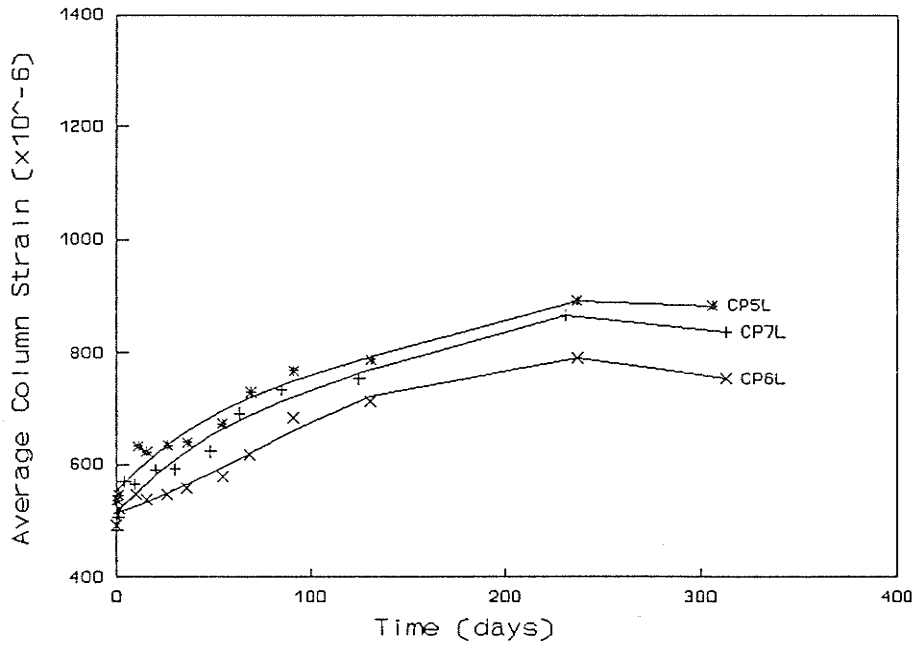

Figure 5.4. Effect of bar size on time-dependent column strain (Preloaded columns - p% =1.10)

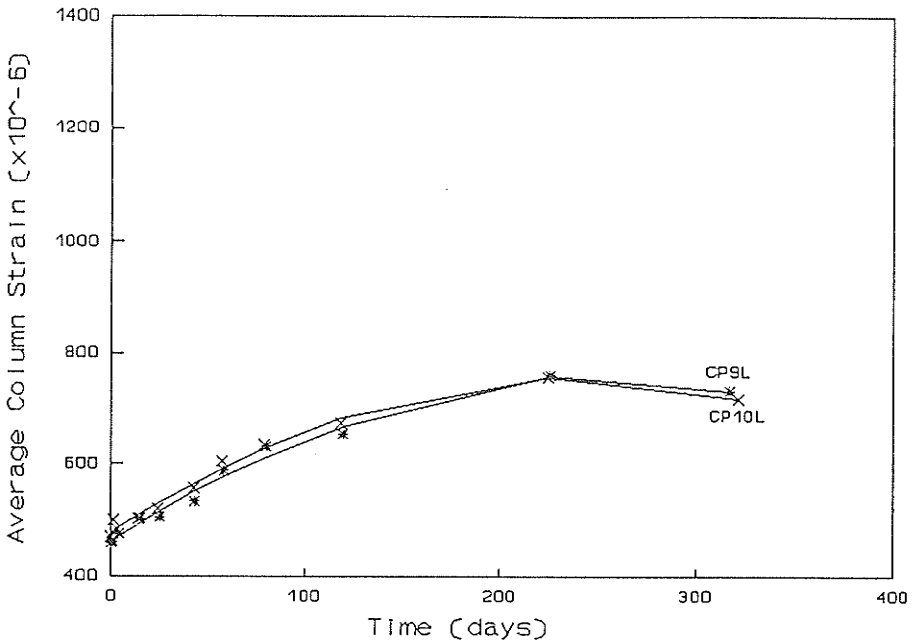

Figure 5.5. Effect of bar size on time-dependent column strain (Preloaded columns - p% =1.83)

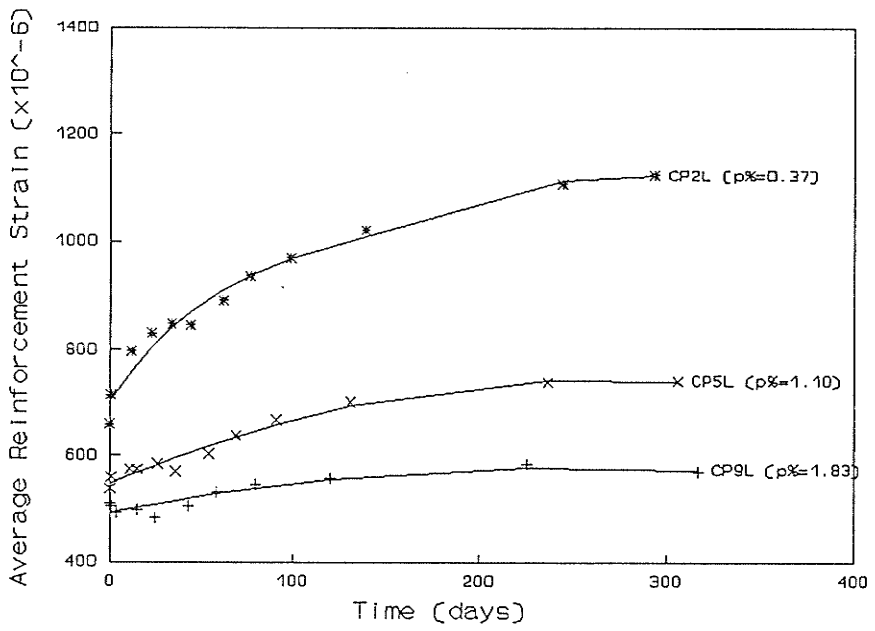

Figure 5.6. Variation of time-dependent reinforcement strain (preloaded columns CP2L, CP5L, CP9L)

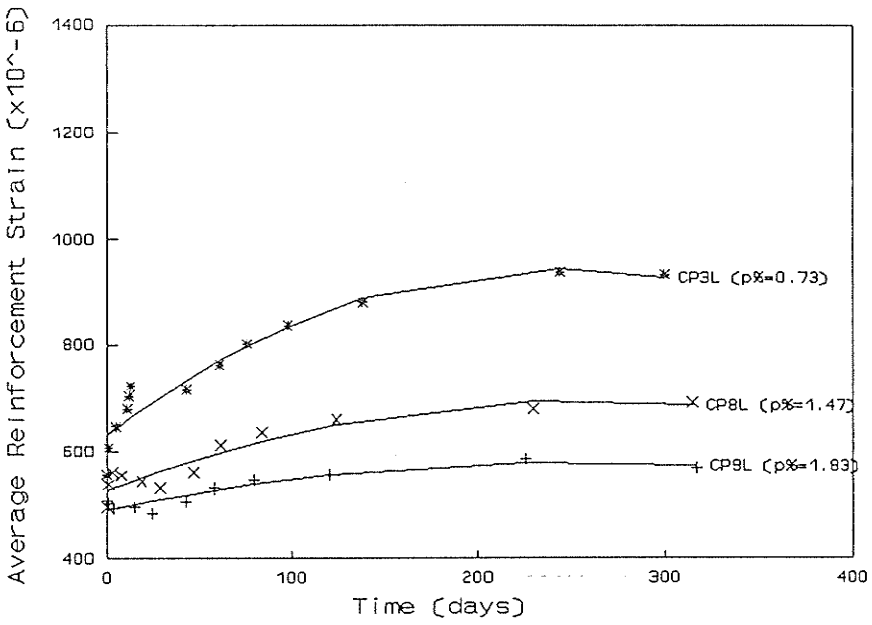

Figure 5.7. Variation of time-dependent reinforcement strain (preloaded columns CP3L, CP8L, CP9L)

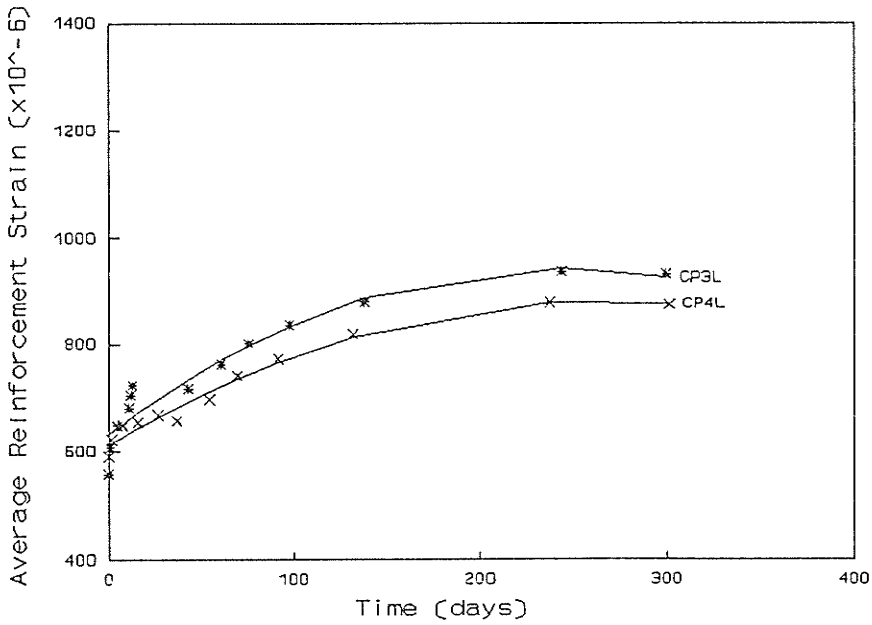

Figure 5.8. Effect of bar size on time-dependent reinforcement strain (Preloaded columns - p% =0.73)

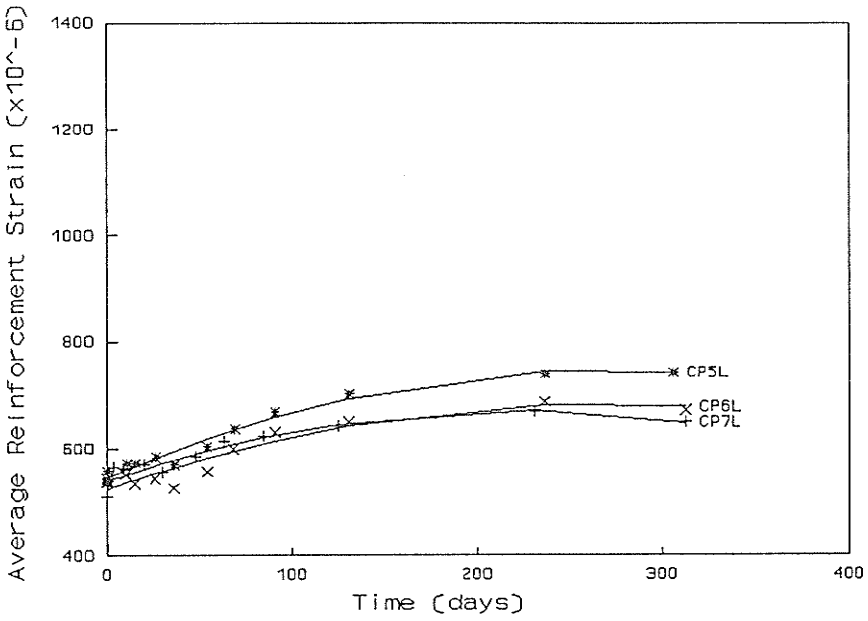

Figure 5.9. Effect of bar size on time-dependent reinforcement strain (Preloaded columns - p% =1.10)

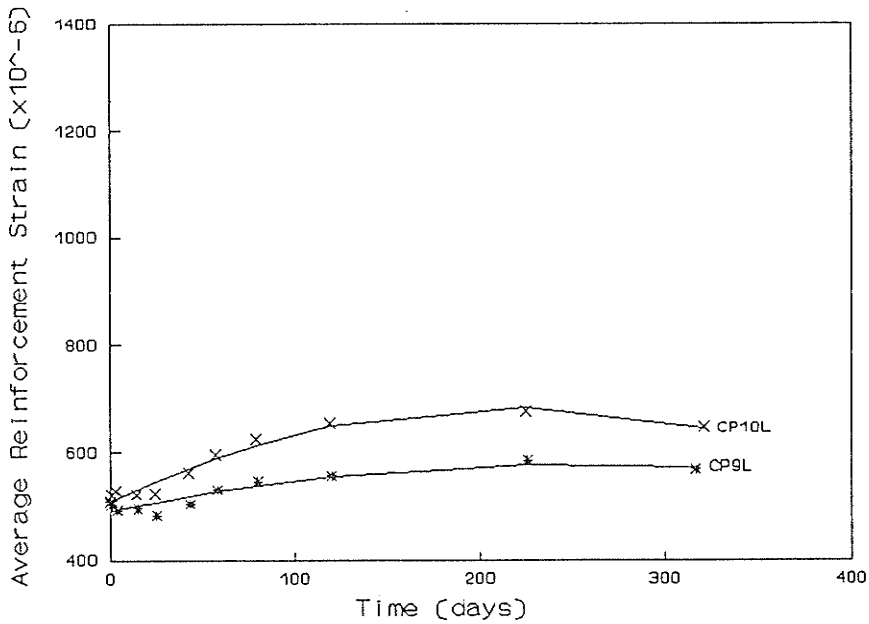

Figure 5.10. Effect of bar size on time-dependent reinforcement strain (Preloaded columns - p% =1.83)

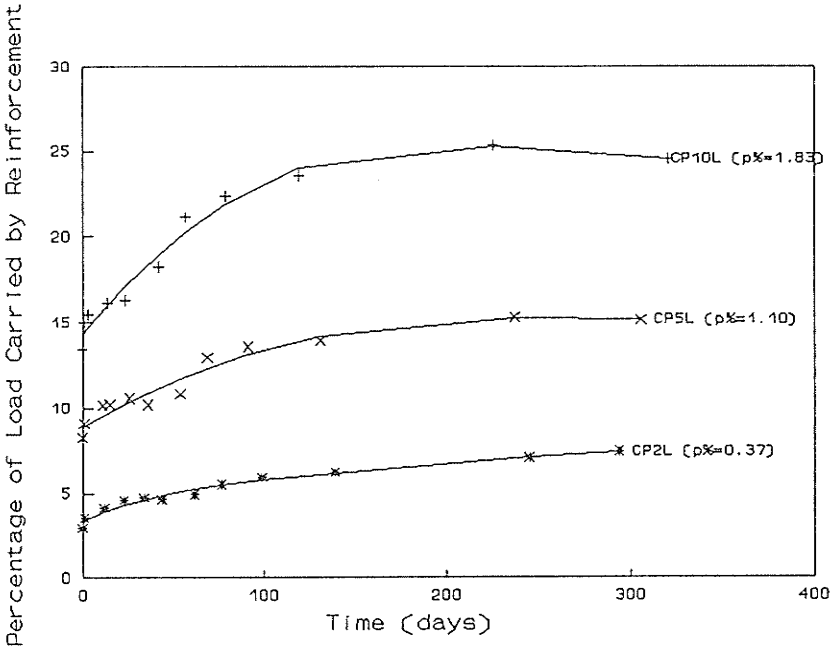

Figure 5.11. Contribution of reinforcement during preload period (preloaded columns CP2L, CP5L, CP10L)

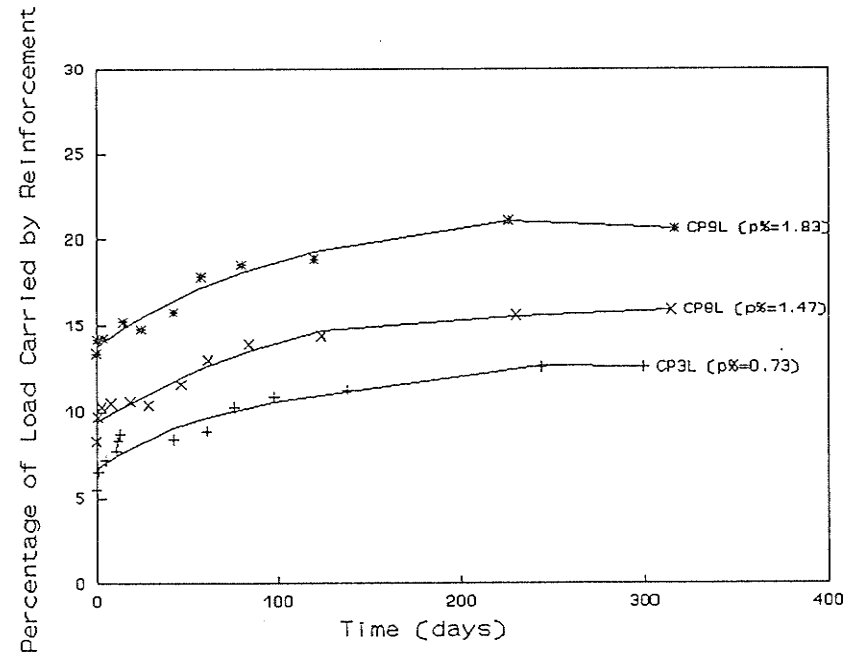

Figure 5.12. Contribution of reinforcement during preload period (preloaded columns CP3L, CP8L, CP9L)

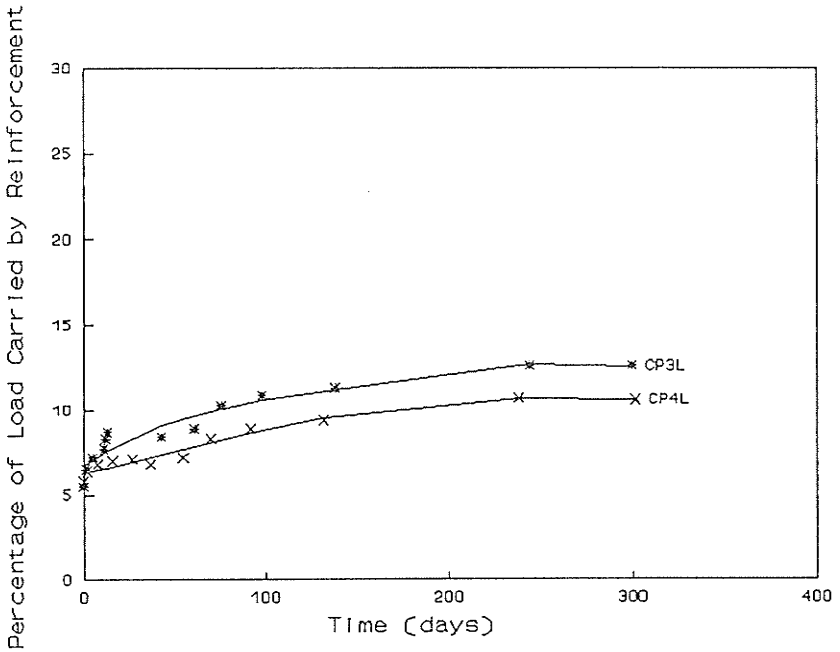

Figure 5.13. Effect of bar size on the contribution of reinforcement during preload period (p% =0.73)

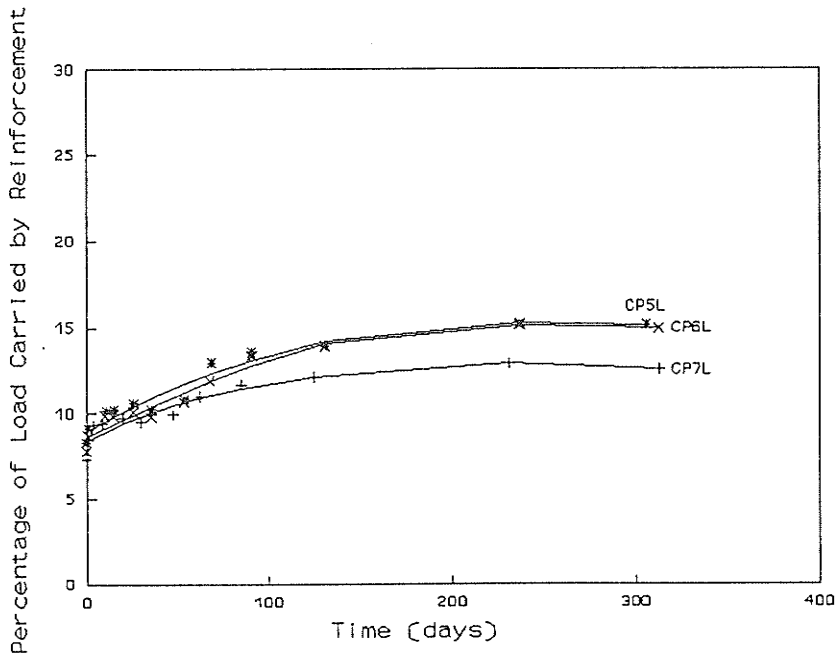

Figure 5.14. Effect of bar size on the contribution of reinforcement during preload period (p% =1.10)

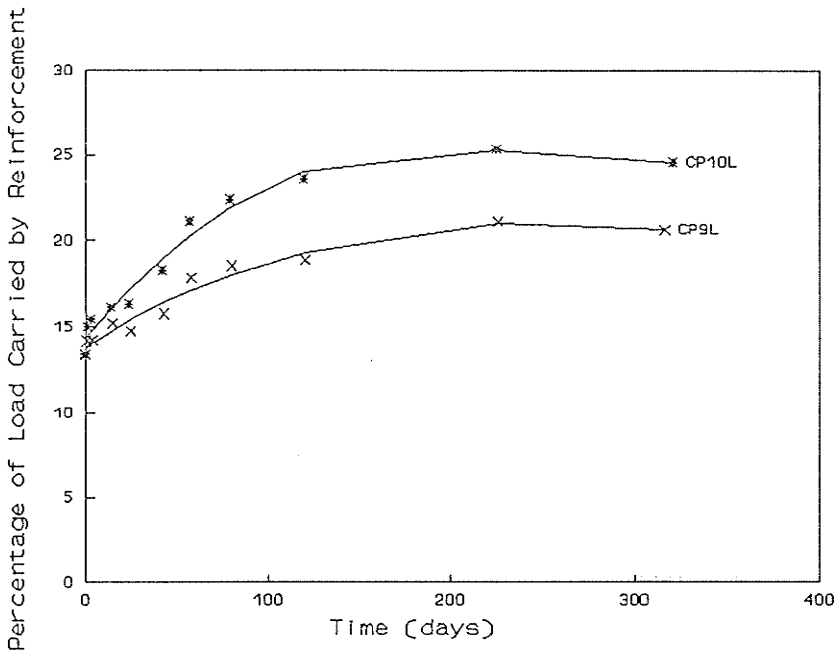

Figure 5.15. Effect of bar size on the contribution of reinforcement during preload period (p% =1.83)

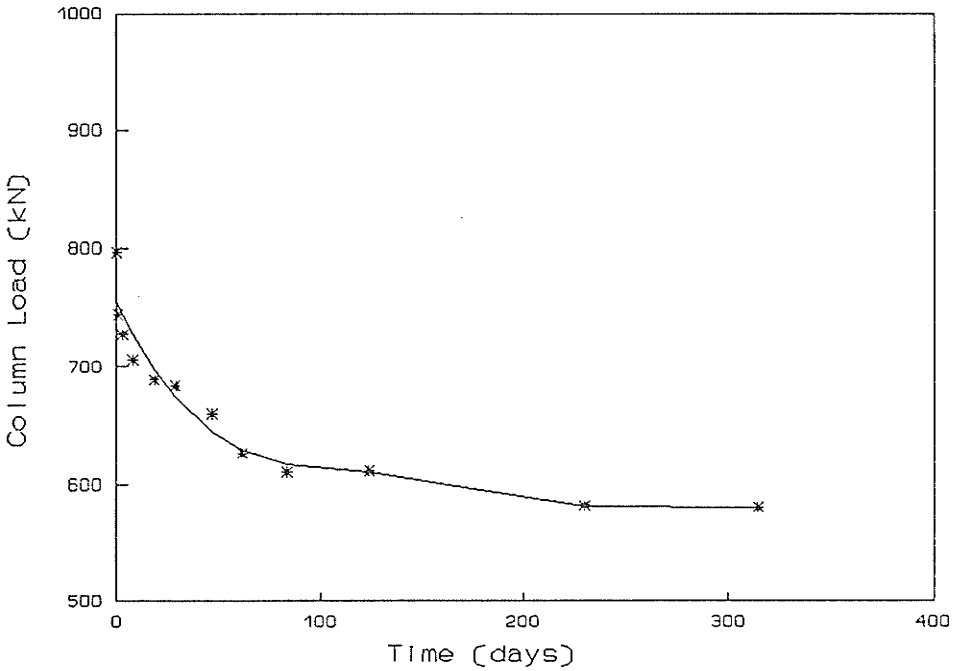

Figure 5.16. Variation of column load during preload period (Preload column CP8L)

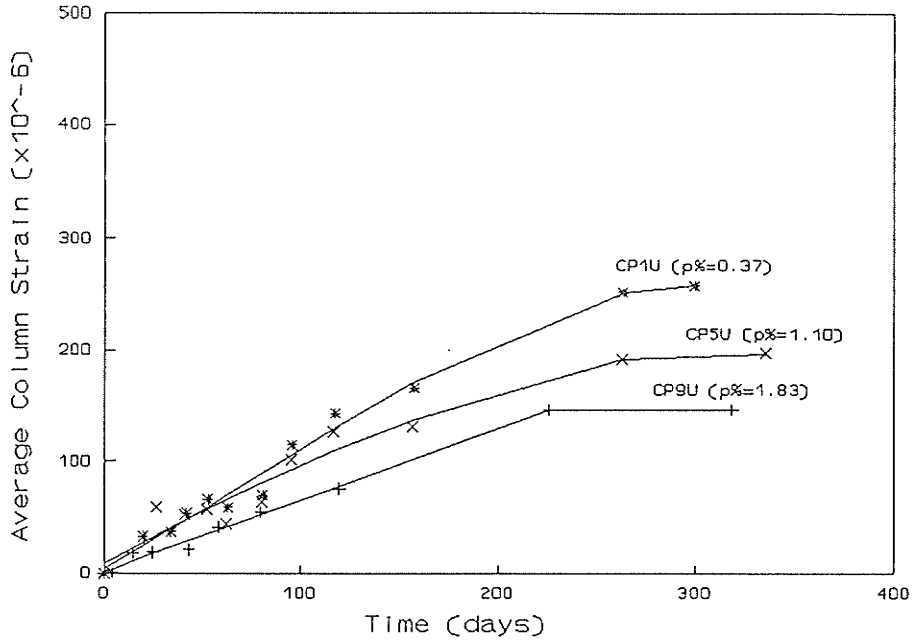

Figure 5.17. Variation of time-dependent column strain (Non-preloaded columns CP1U, CP5U, CP9U)

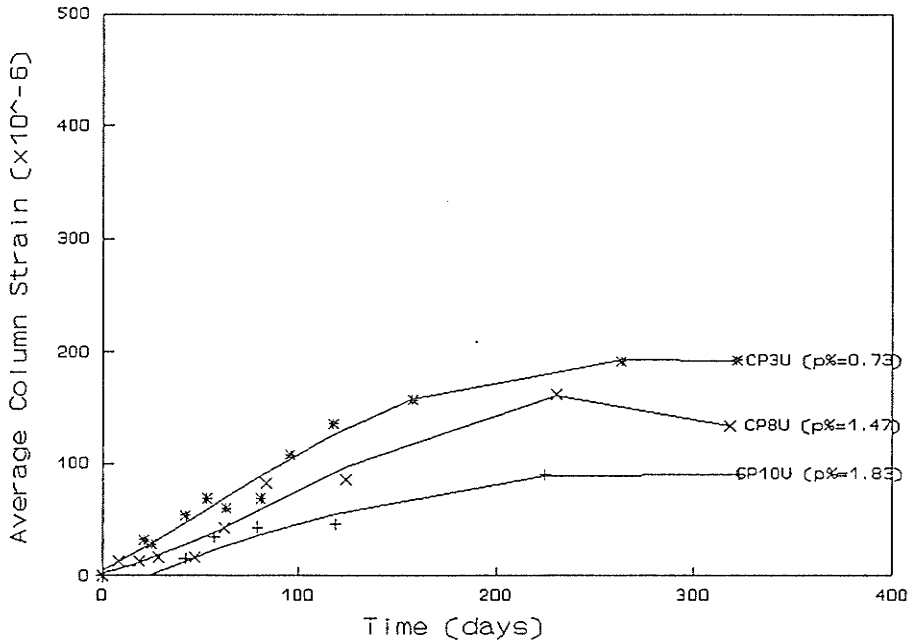

Figure 5.18. Variation of time-dependent column strain (Non-preloaded columns CP3U, CP8U, CP10U)

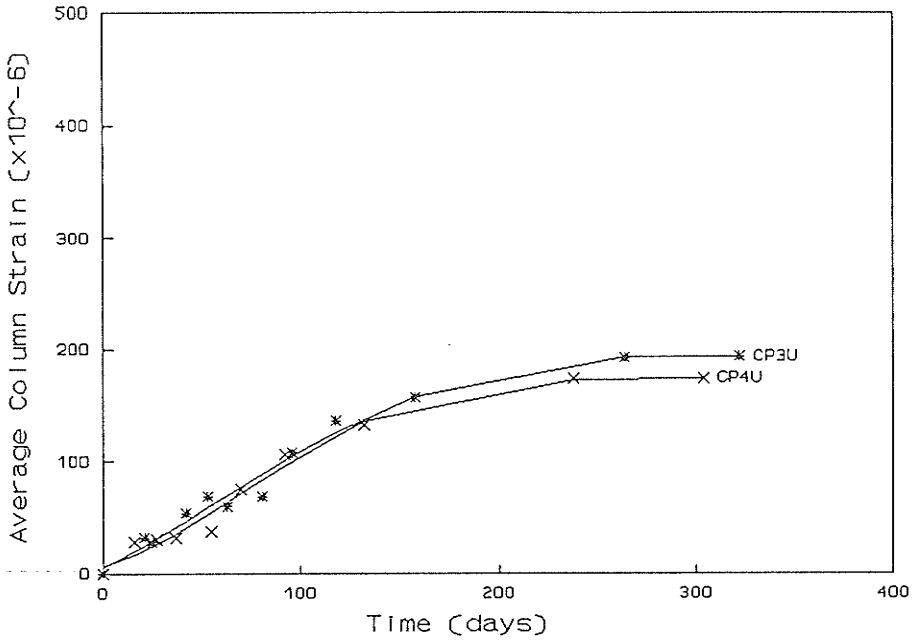

Figure 5.19. Effect of bar size on time-dependent column strain
(Non-preloaded columns - p% =0.73)

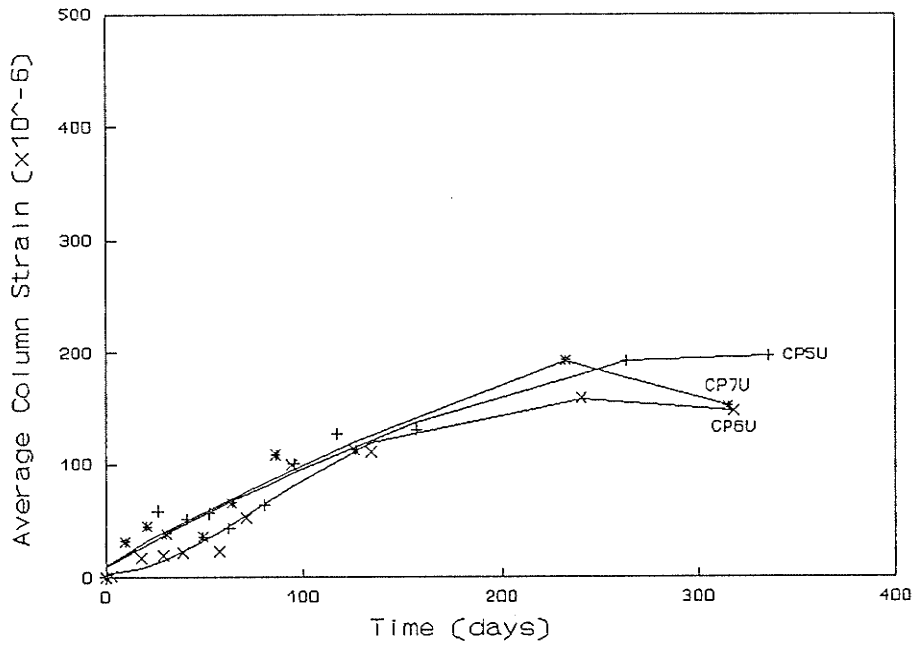

Figure 5.20. Effect of bar size on time-dependent column strain
(Non-preloaded columns - p% =1.10)

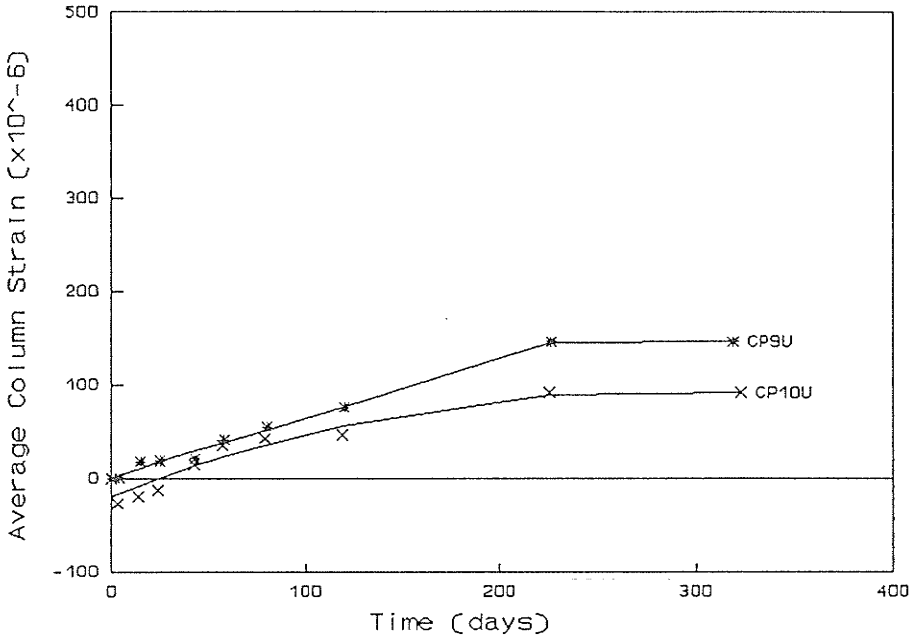

Figure 5.21. Effect of bar size on time-dependent column strain (Non-preloaded columns - P% = 1.83)

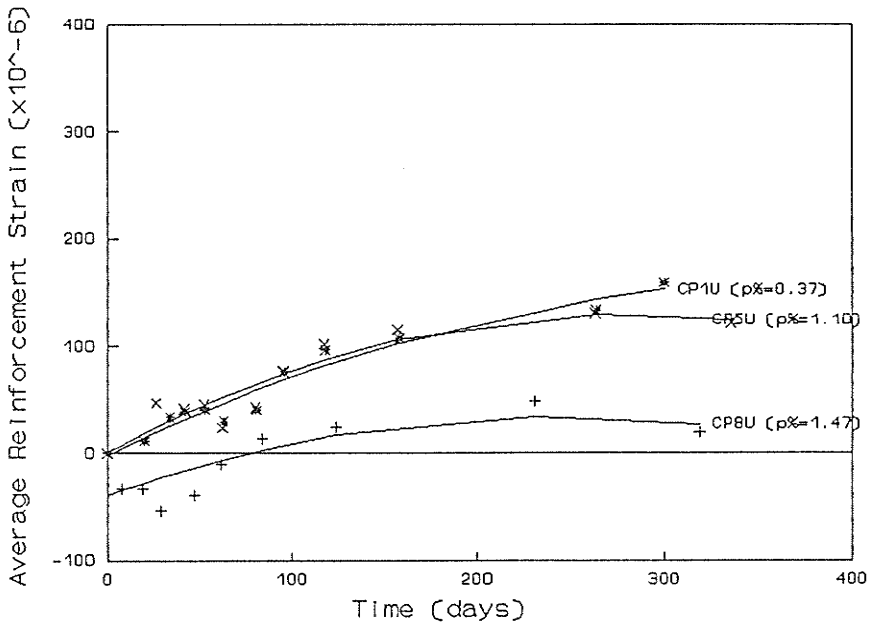

Figure 5.22. Variation of time-dependent reinforcement strain (Non-preloaded columns CP1U, CP5U, CP8U)

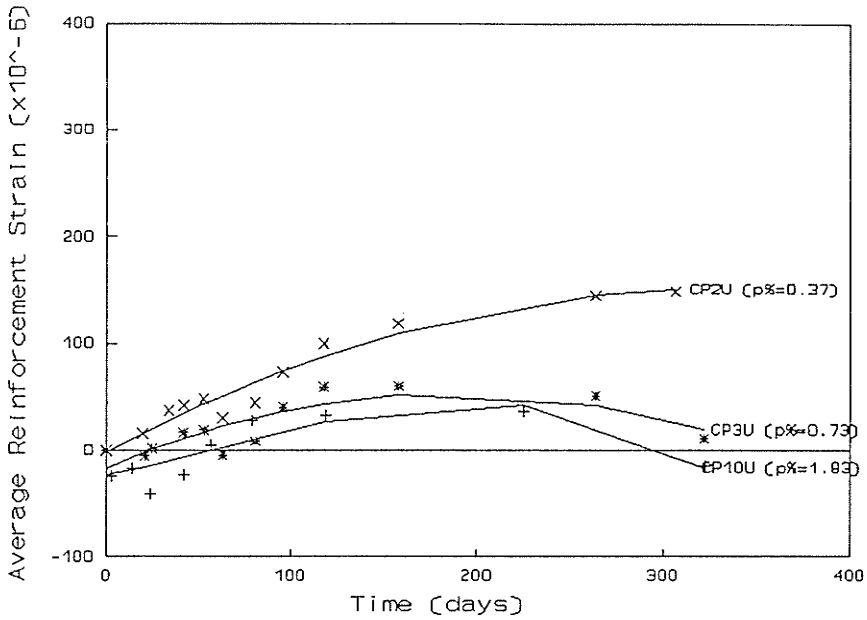

Figure 5.23. Variation of time-dependent reinforcement strain (Non-preloaded columns CP2U, CP3U, CP10U)

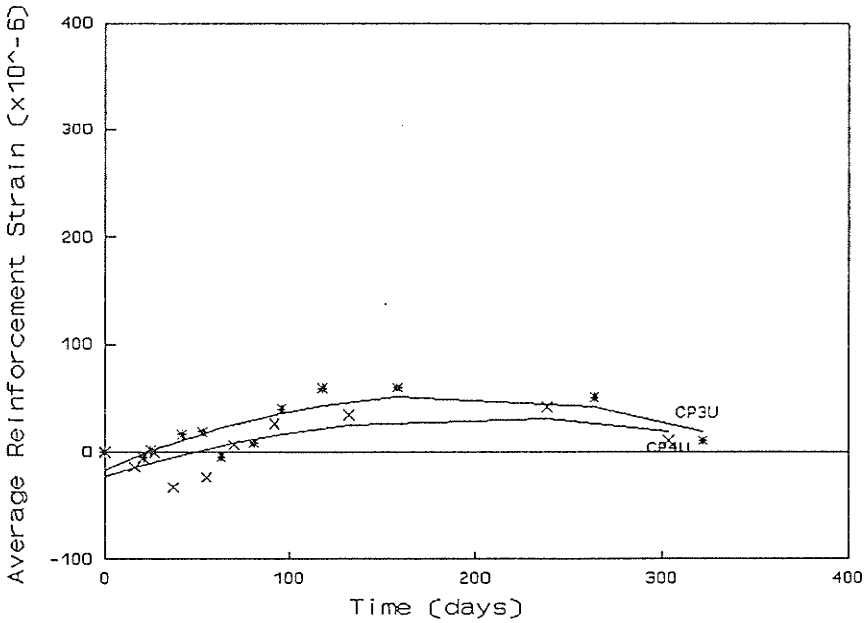

Figure 5.24. Effect of bar size on time-dependent reinforcement strain (Non-preloaded columns - p% =0.73)

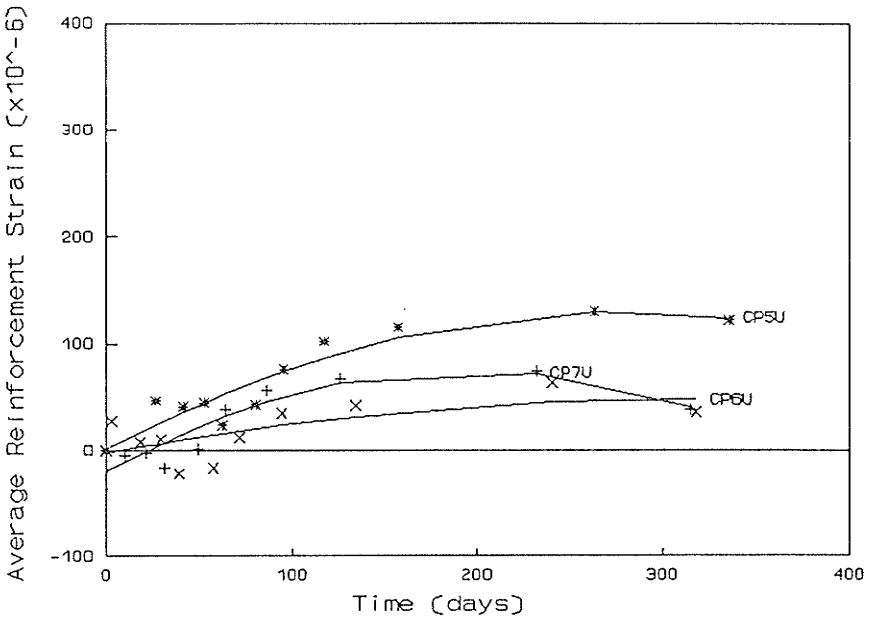

Figure 5.25. Effect of bar size on time-dependent reinforcement strain (Non-preloaded columns - p% =1.10)

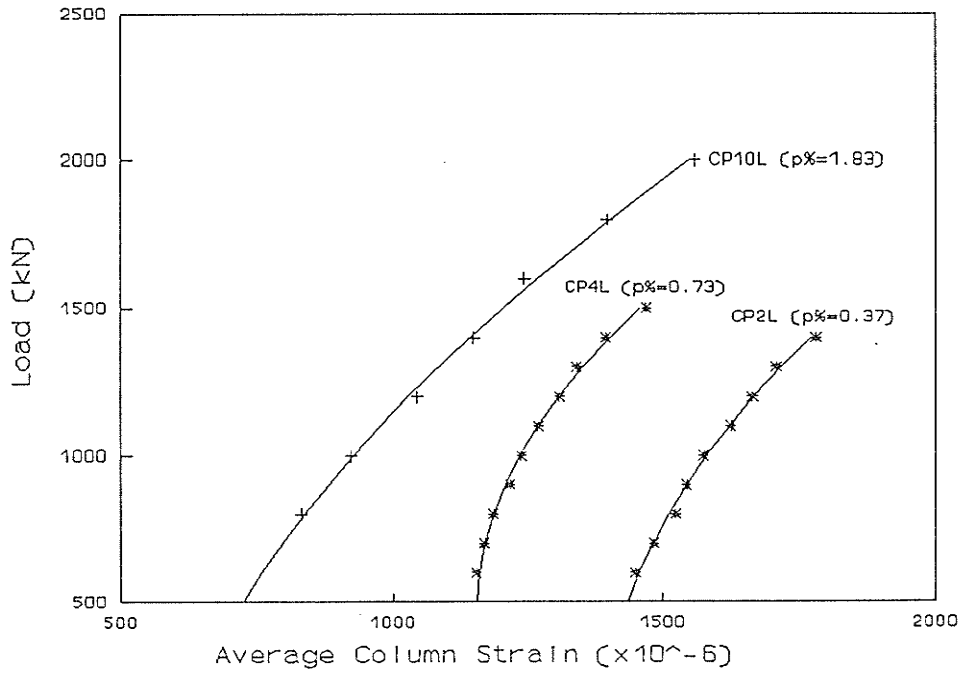

Figure 5.26. Variation of columns strain during ultimate strength testing (Preloaded columns CP2L, CP4L, CP10L)

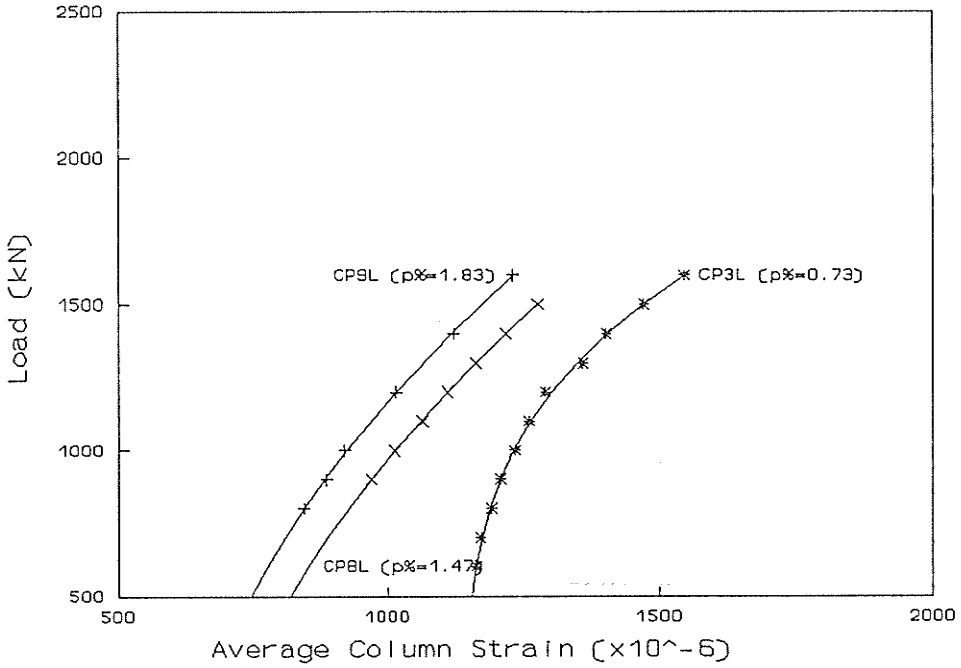

Figure 5.27. Variation of columns strain during ultimate strength testing (Preloaded columns CP3L, CP8L, CP9L)

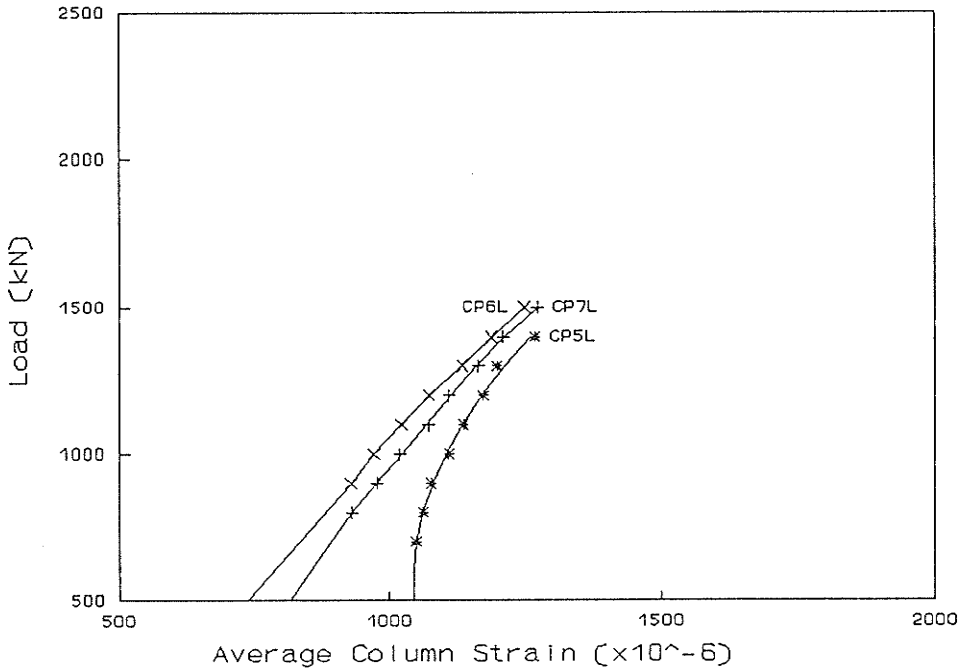

Figure 5.28. Effect of bar size on columns strain During ultimate strength testing (Preloaded columns - P% = 1.10)

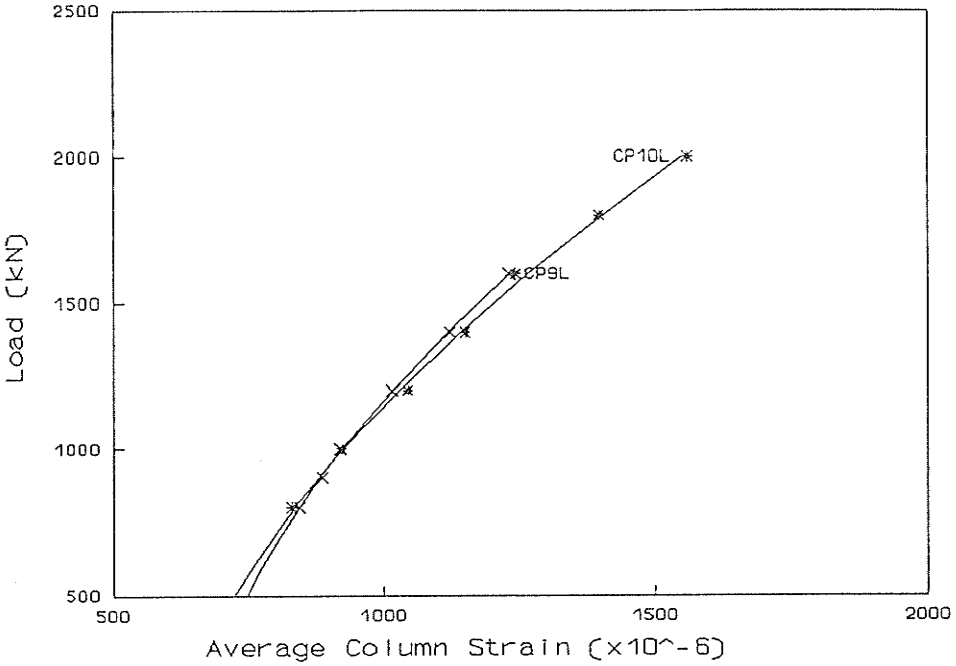

Figure 5.29. Effect of bar size on column strain during ultimate strength testing (Preloaded column - p% = 1.83)

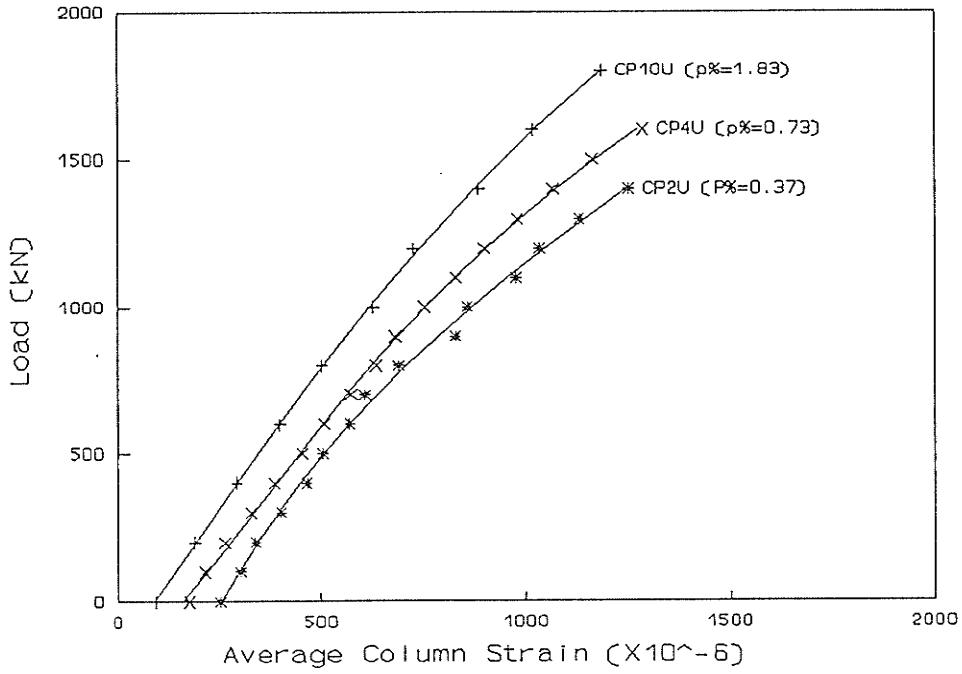

Figure 5.30. Variation of columns strain during ultimate strength testing (Non-preloaded columns CP2U, CP4U, CP10U)

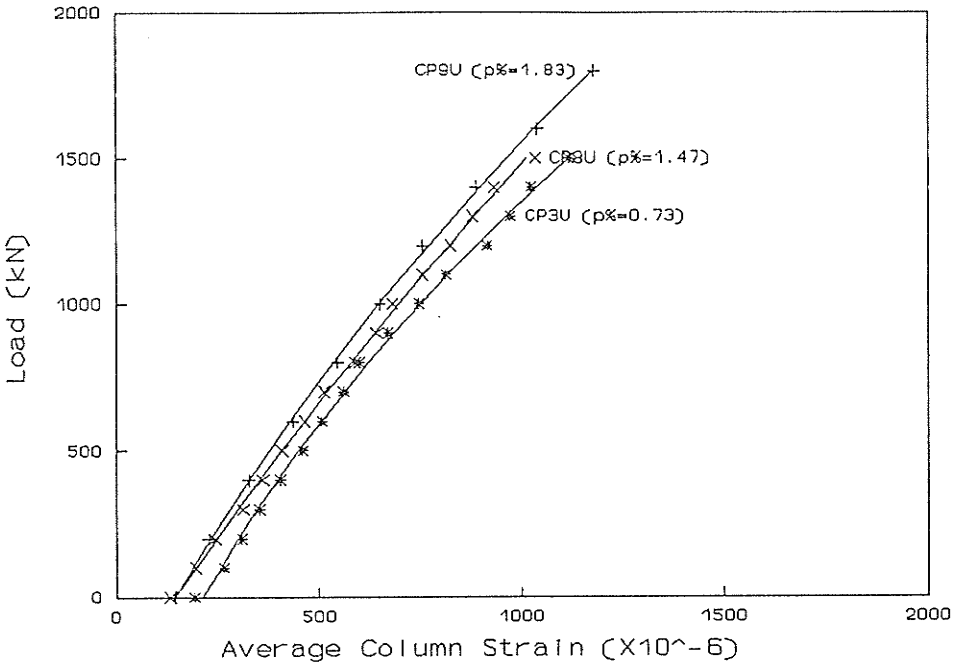

Figure 5.31. Variation of columns strain during ultimate strength testing (Non-preloaded columns CP3U, CP8U, CP9U)

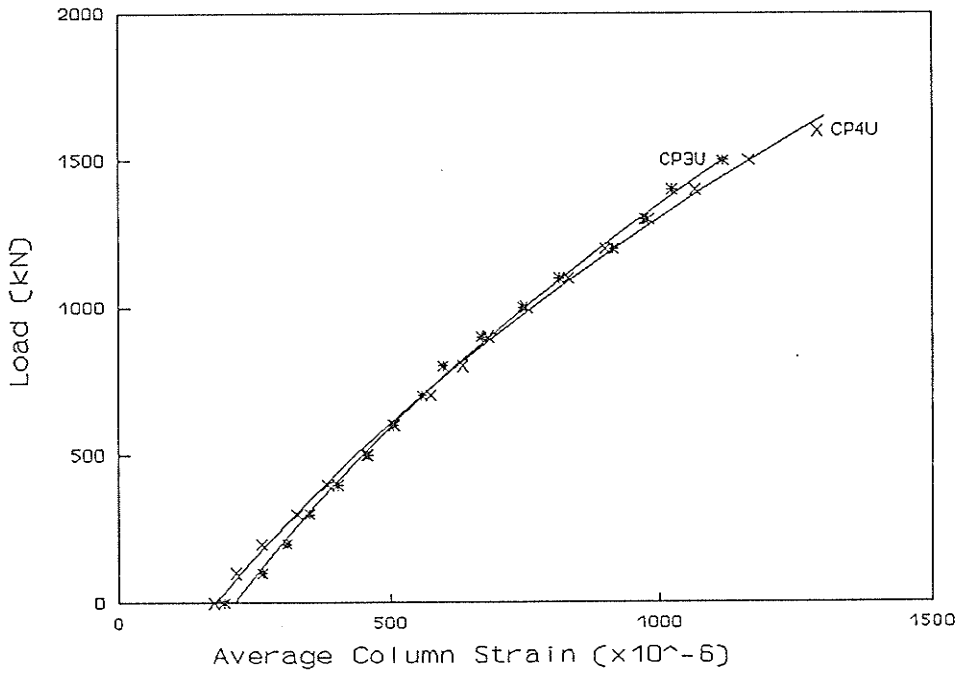

Figure 5.32. Effect of bar size on columns strain During ultimate strength testing (Non-preloaded columns - P% =0.73)

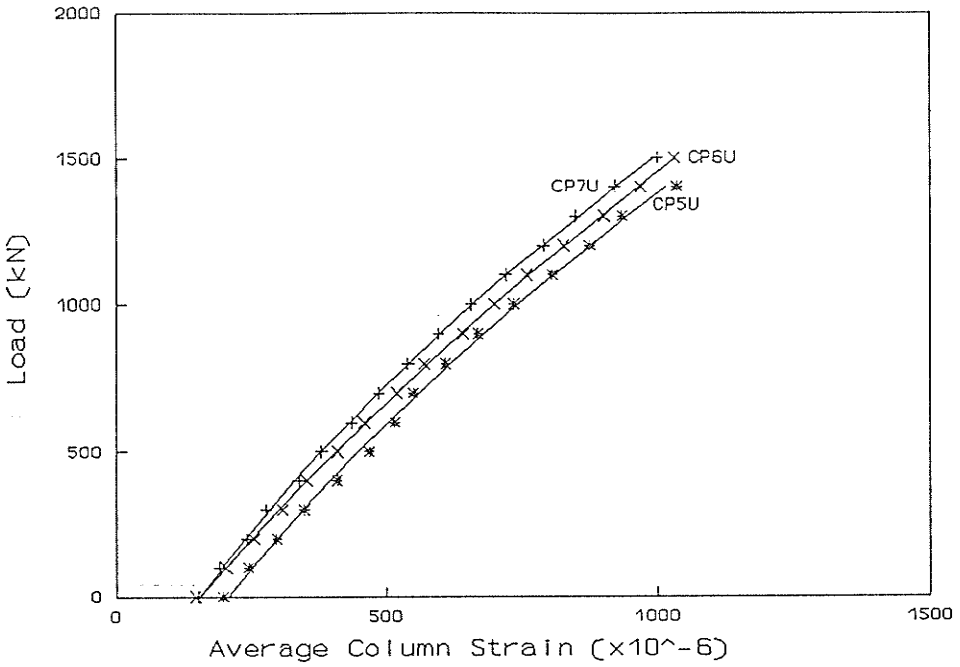

Figure 5.33. Effect of bar size on column strain during ultimate strength testing (Non-preloaded column - p% = 1.10)

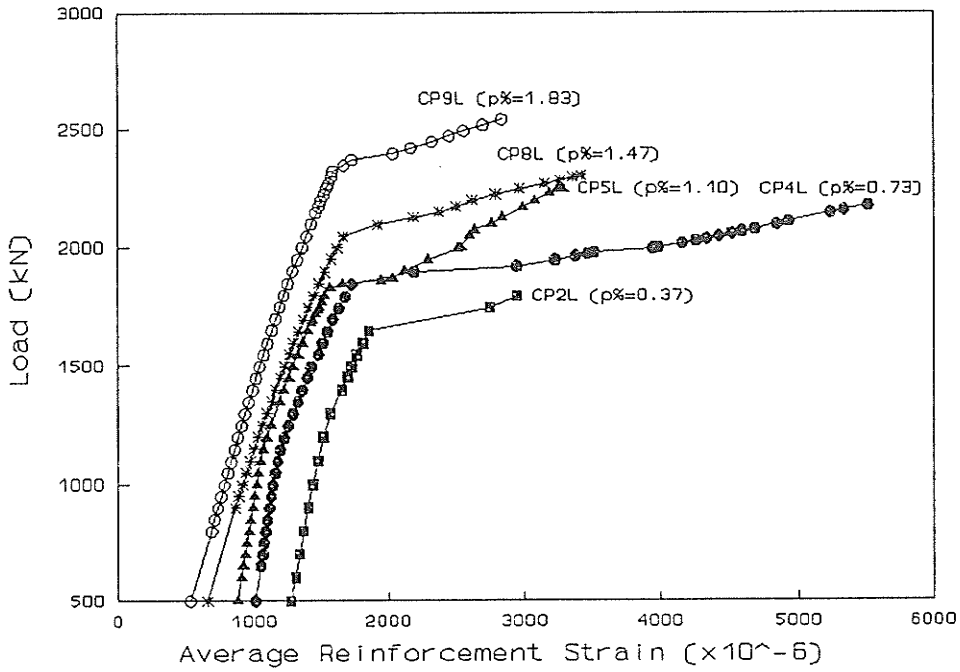

Figure 5.34. Variation of reinforcement strain during ultimate strength testing (Preloaded columns CP2L, CP4L, CP5L, CP8L and CP9L)

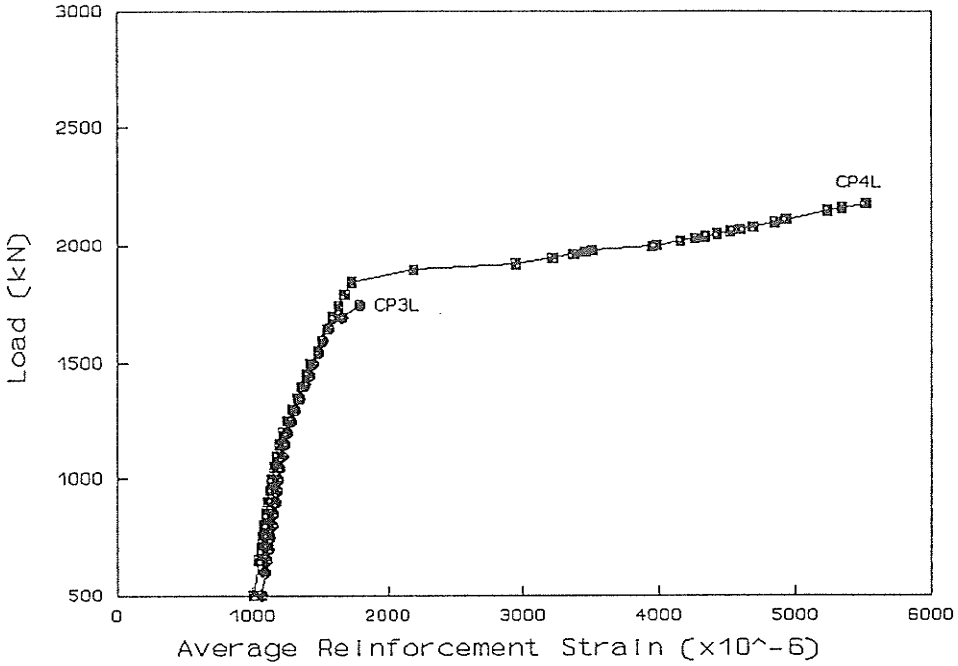

Figure 5.35. Effect of bar size on reinforcement strain during ultimate strength testing (Preloaded columns - p% = 0.73)

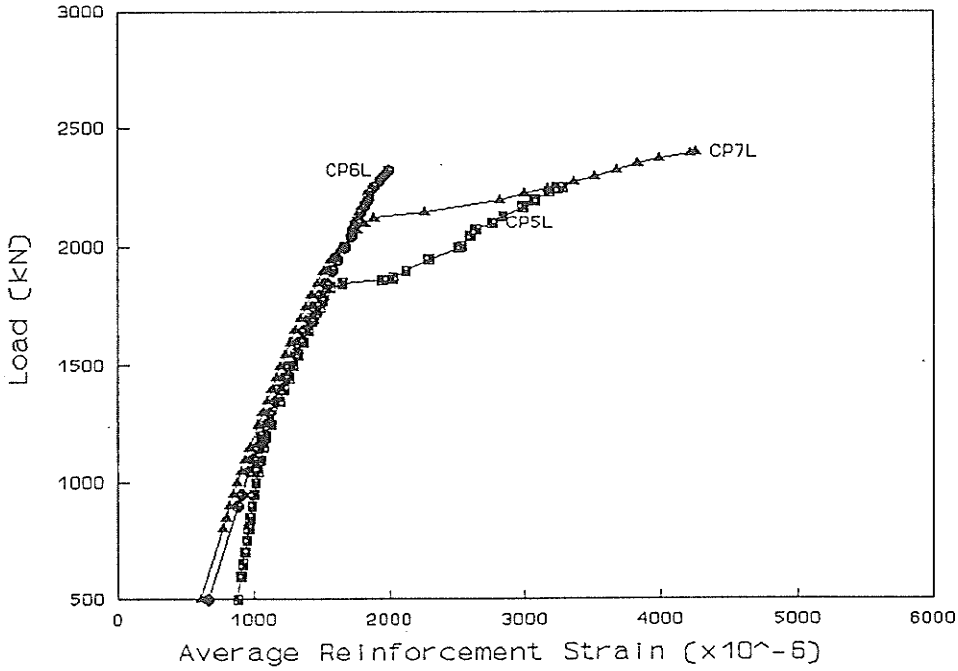

Figure 5.36. Effect of bar size on reinforcement strain during ultimate strength testing (Preloaded columns - p% = 1.10)

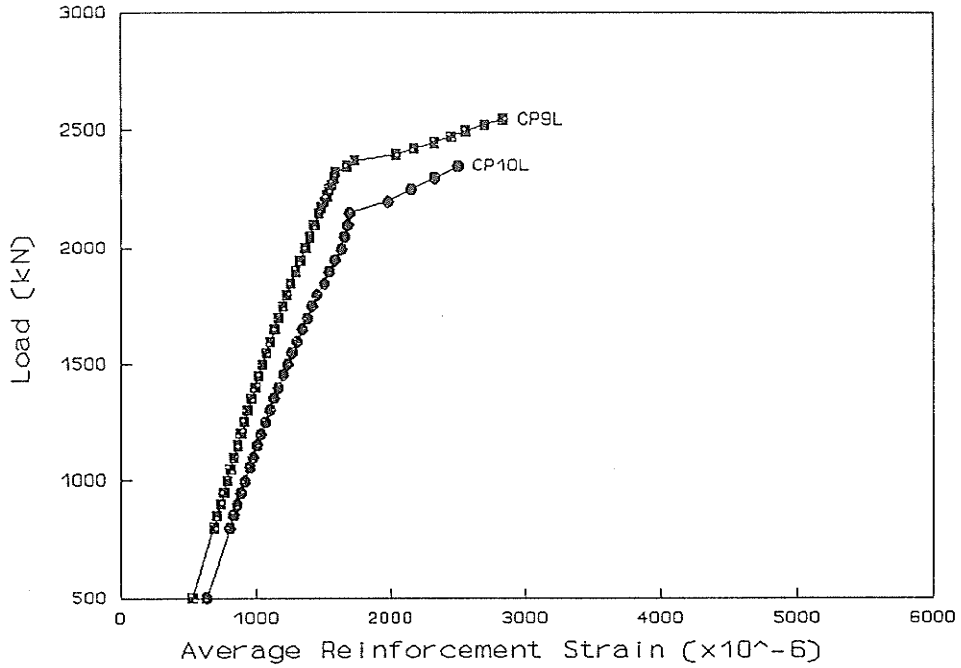

Figure 5.37. Effect of bar size on reinforcement strain during ultimate strength testing (Preloaded columns - p% = 1.83)

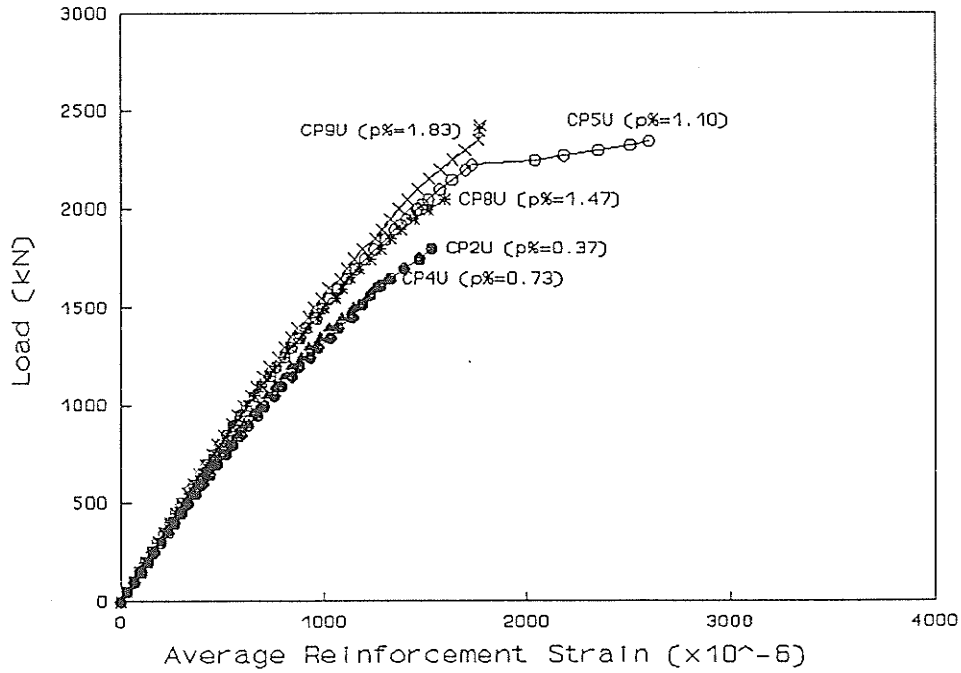

Figure 5.38. Variation of reinforcement strain during ultimate strength testing (Non-preloaded columns CP2U, CP4U, CP5U, CP8U and CP9U)

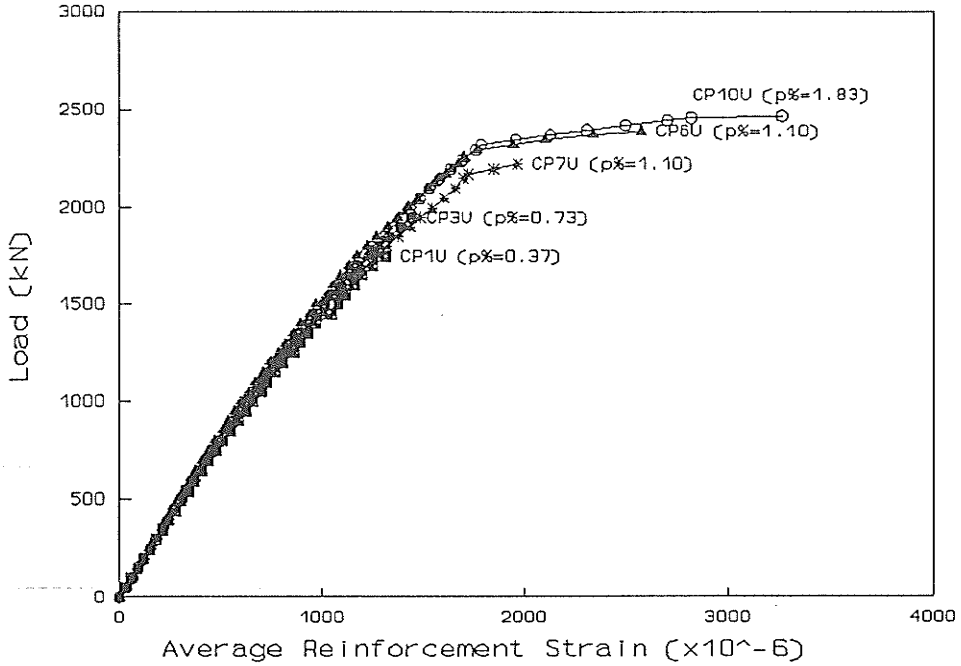

Figure 5.39. Variation of reinforcement strain during ultimate strength testing (Non-preloaded columns CP1U, CP3U, CP6U, CP7U and CP10U)

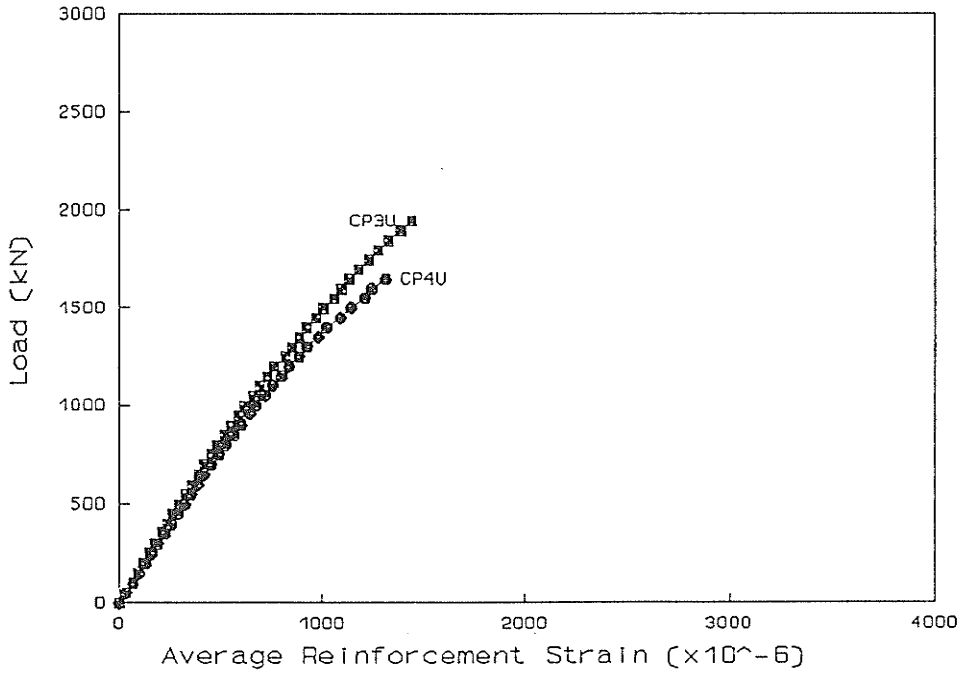

Figure 5.40. Effect of bar size on reinforcement strain during ultimate strength testing (Non-preloaded columns - p% =0.73)

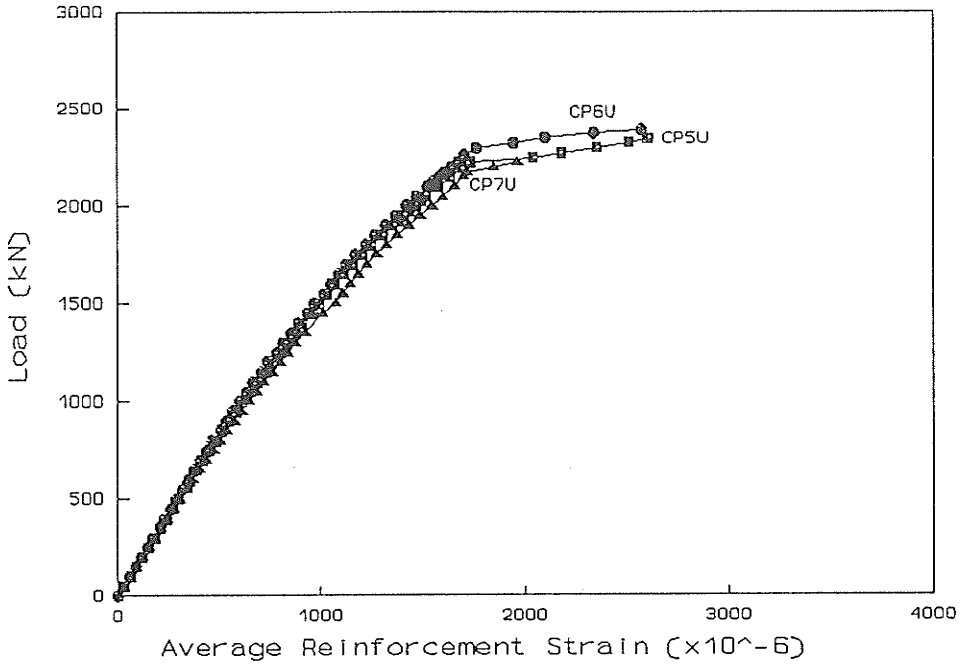

Figure 5.41. Effect of bar size on reinforcement strain during ultimate strength testing (Non-preloaded columns - p% = 1.10)

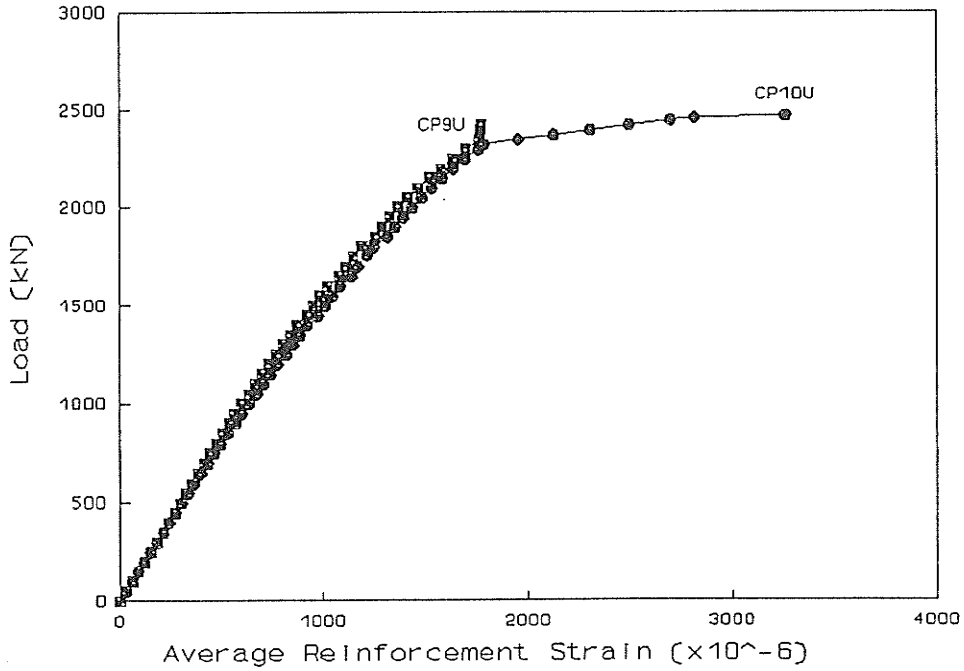

Figure 5.42. Effect of bar size on reinforcement strain during ultimate strength testing (Non-preloaded columns - p% = 1.83)

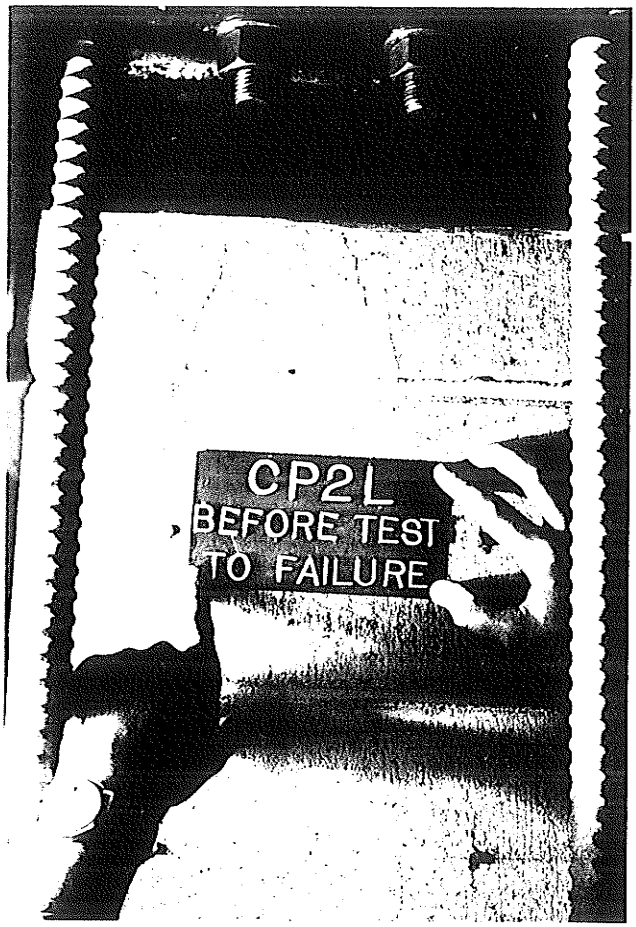

Figure 5.43. Preloaded column CP2L before testing to failure

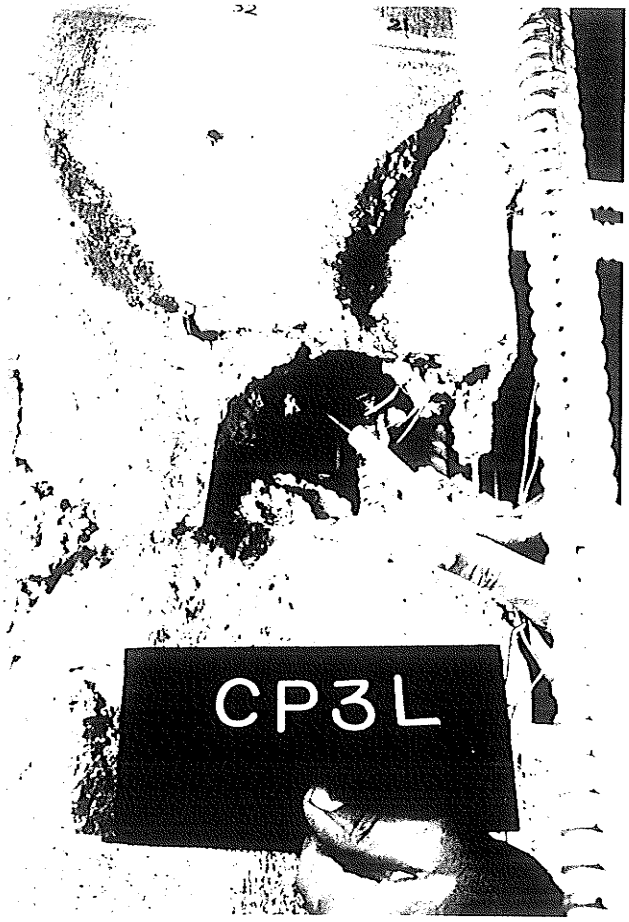

Figure 5.44. Poor grouting in preloaded column CP3L

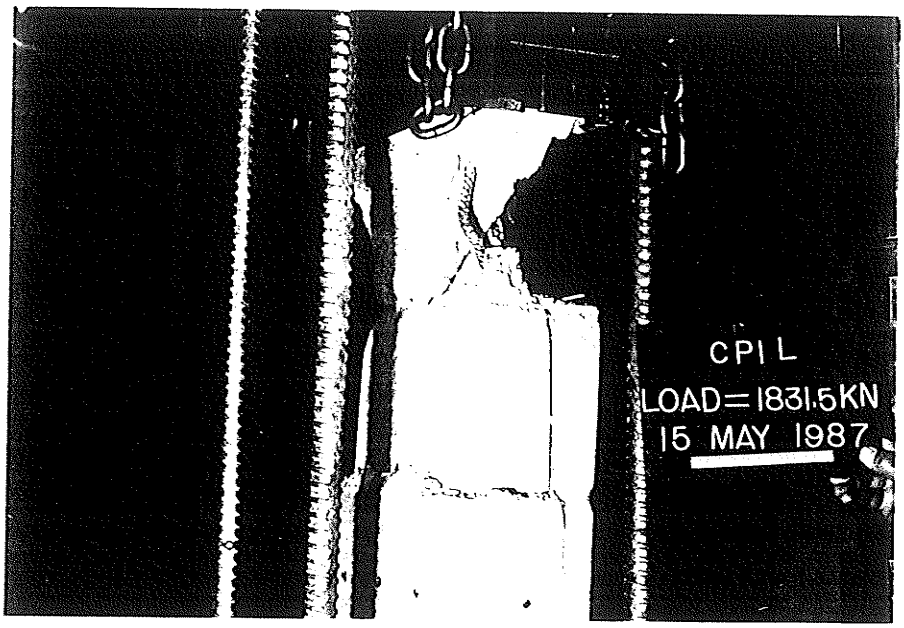

Figure 5.45. Failure of preloaded column CP1L

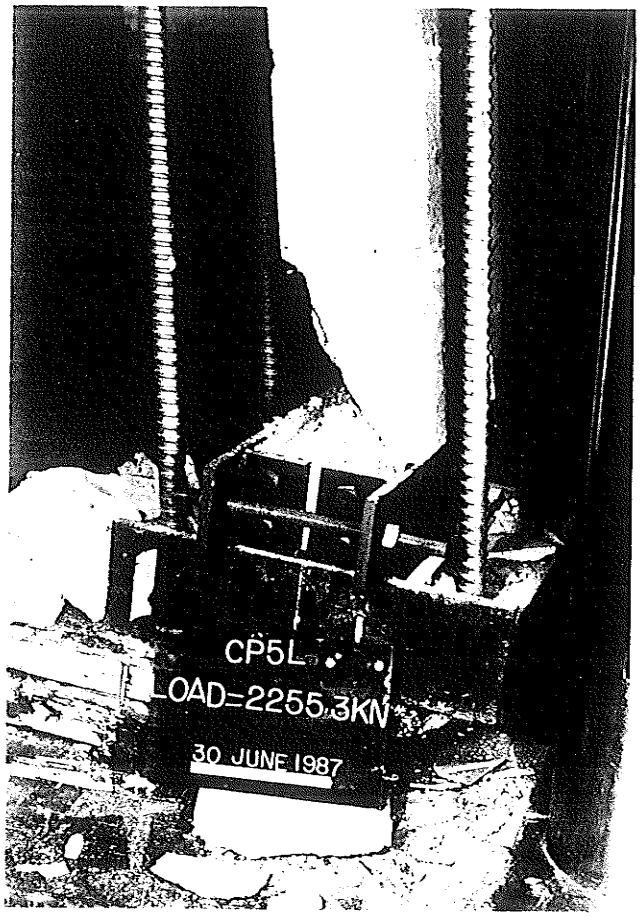

Figure 5.46. Failure of preloaded column CP5L

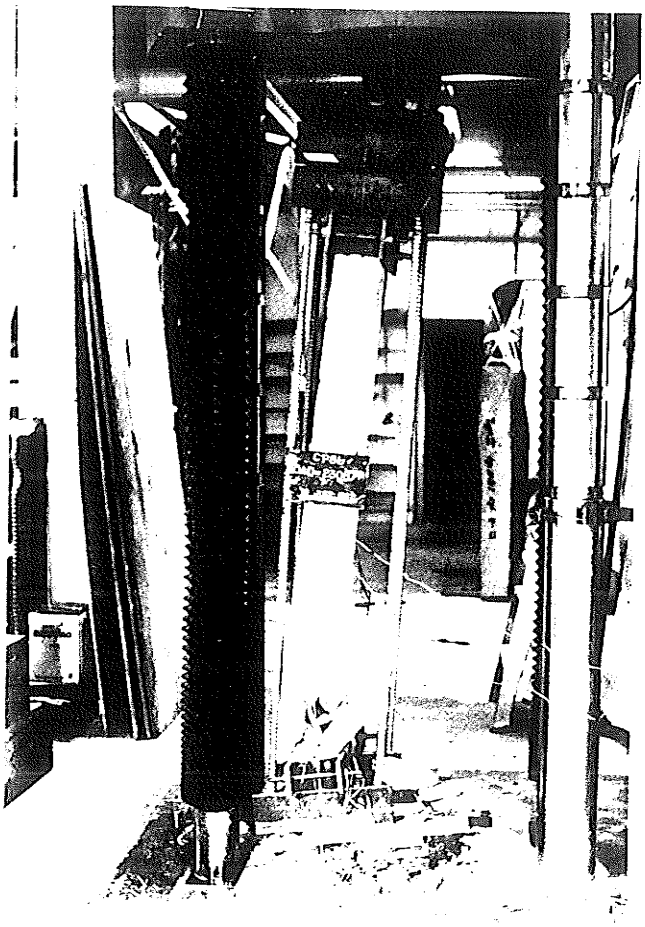

Figure 5.47. Failure of preloaded column CP8L

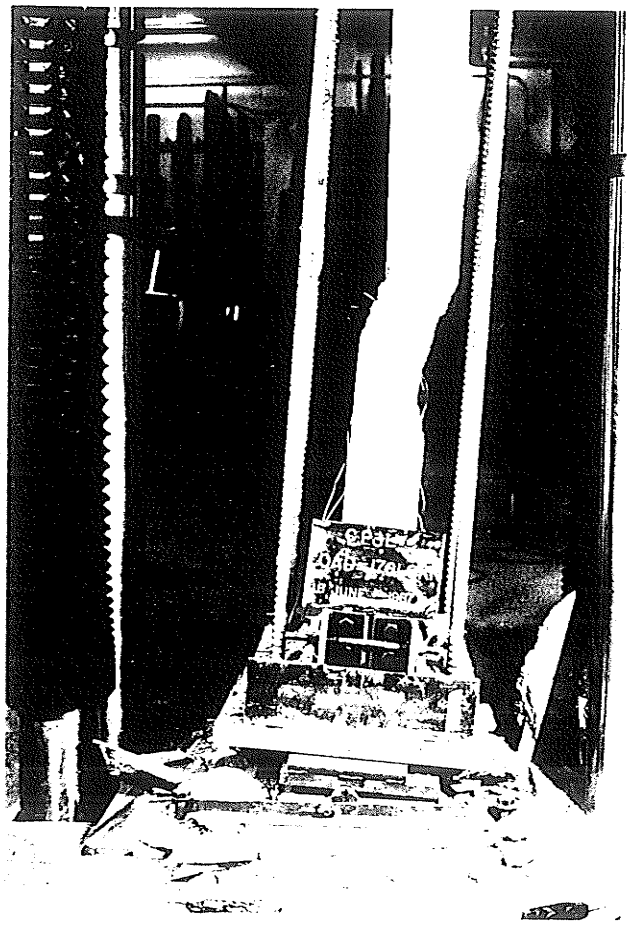

Figure 5.48. Failure of preloaded column CP3L

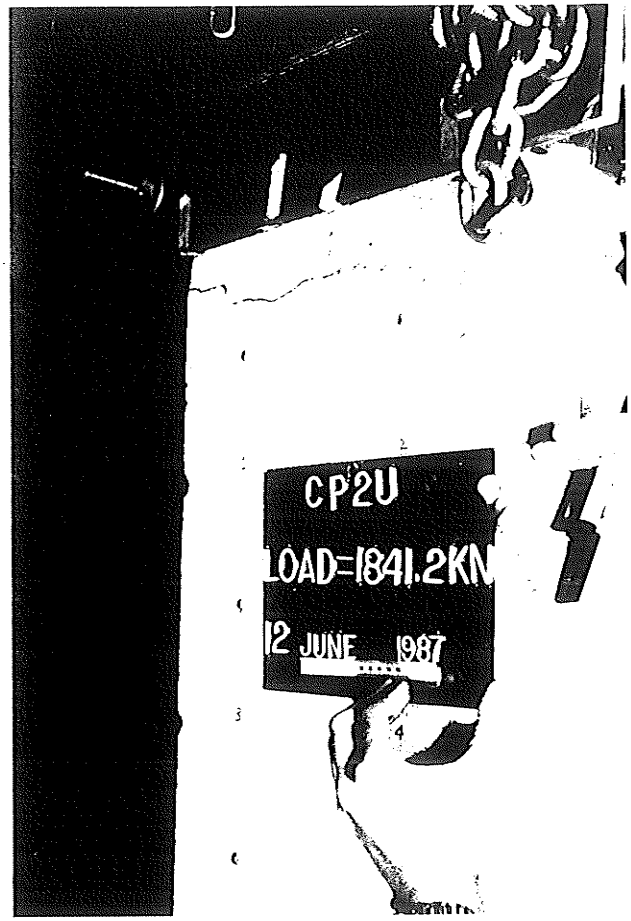

Figure 5.49. Failure of non-preloaded column CP2U

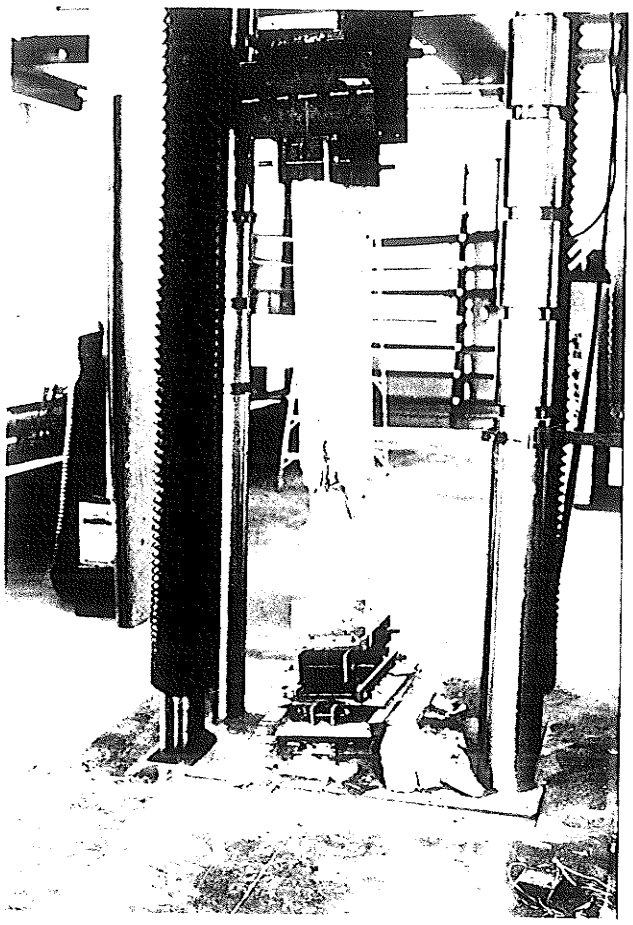

Figure 5.50. Failure of non-preloaded column CP4U

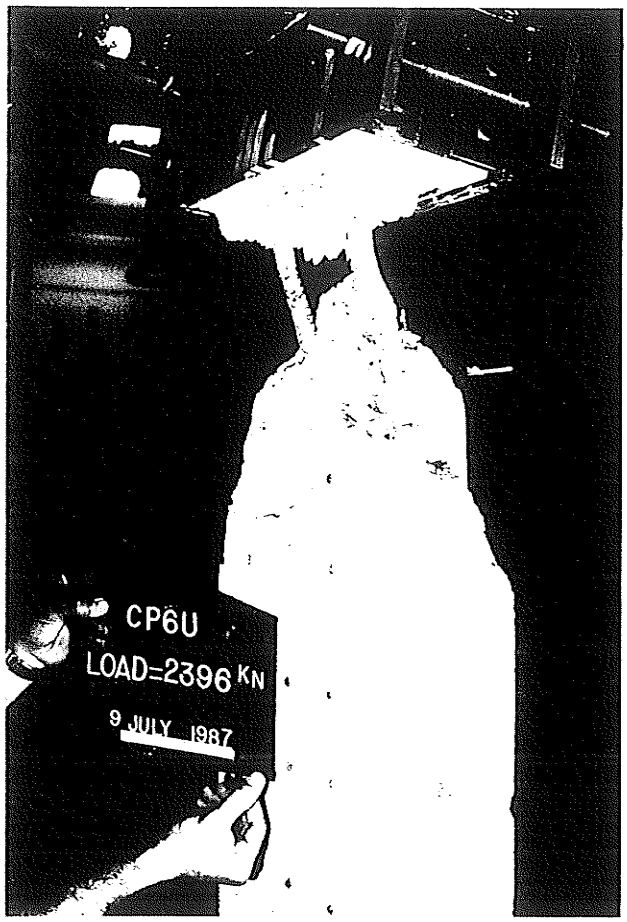

Figure 5.51. Failure of non-preloaded column CP6U

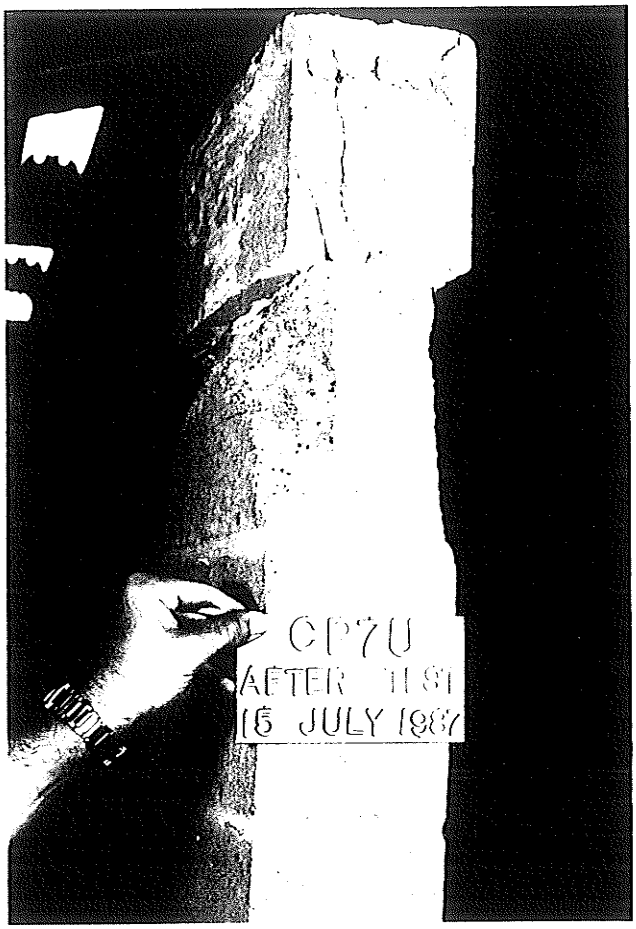

Figure 5.52. Failure of non-preloaded column CP7U

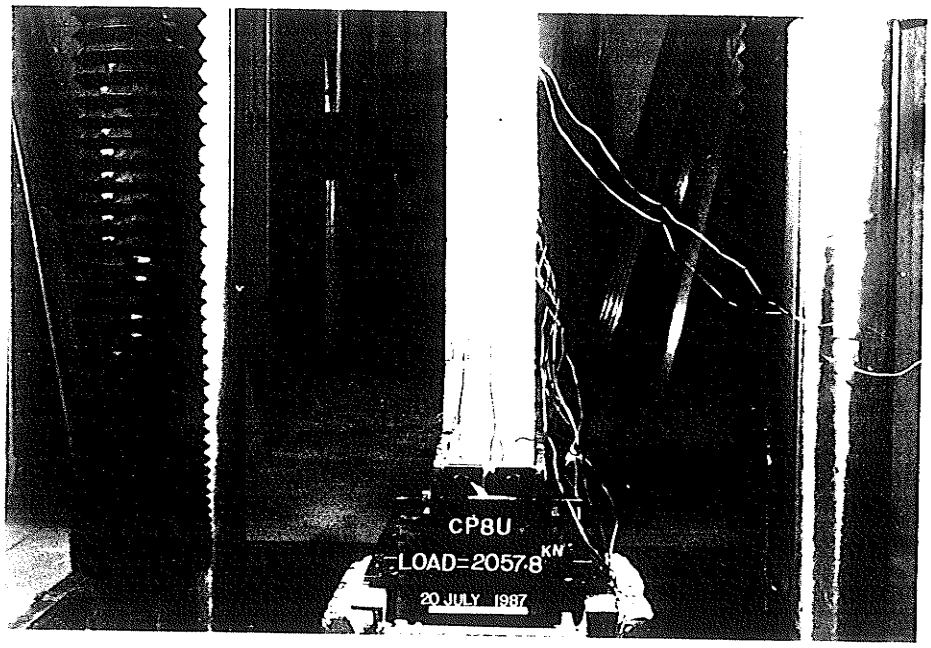

Figure 5.53. Failure of non-preloaded column CP8U

CHAPTER VI
THEORETICAL ANALYSIS

6.1 Introduction

Reinforced masonry is a multi-component structural member composed of four materials; masonry unit, mortar, grout and reinforcing steel. The structural properties of these constituent materials are quite different under both short-term and long-term loading conditions. For example, the compressive strength and modulus of elasticity of the mortar are considerably lower than the corresponding values for the masonry unit and grout. Under short-term loading, the mortar tends to deform laterally more than the unit and in combination with the bond and friction between the unit and the mortar lateral tensile and compressive stresses are developed in the unit and mortar respectively. This is especially true when the applied load approaches the ultimate strength of the mortar[22]. Under long-term loading conditions, the masonry unit, grout and mortar are subjected to creep under sustained loading and other strains due to environmental changes such as temperature and humidity.

In this chapter, the task of incorporating these different materials into a mathematical model to explain the behavior is outlined. The properties of the constituent materials chosen for the analysis are defined in this chapter. The first stage of this analysis is restricted to the behavior in one dimension and then expanded to include the deformation characteristics in a three dimensional consideration. The intention is to use the three-dimensional analysis to confirm the validity of the simpler one-dimensional model.

6.2 Material Properties

The properties of the constituent materials used in this chapter have been selected from the investigation described in previous chapters and obtained elsewhere in

engineering literature. Where required, these properties have been modified with respect to a fixed set of composition, curing, and loading conditions. These conditions are stated in Chapter III and Chapter IV.

The material relationships defined in this chapter were used in the theoretical analysis developed in this thesis. However, the analysis is not restricted by these specific relations or conditions which can be changed for future applications of the analysis.

6.2.1 Steel Reinforcement

Steel has been assumed to be an ideal elasto-plastic material. Strain hardening is not considered because of the small strains involved. Creep or relaxation of steel under sustained load is also neglected. The assumed stress-strain relationship for reinforcing steel is shown in Fig. 6.1 and can be written in the typical form

$$\sigma_{zs} = \epsilon_z E_s \qquad \leq f_y \tag{6.1}$$

where

σ_{zs} = steel stress.

ϵ_z = strain under the applied load

E_s = modulus of elasticity of steel

f_y = yield stress of steel.

6.2.2 Masonry Unit

The masonry unit is assumed to have a non-linear stress-strain relationship under short-term loading, to creep when subjected to long-term loading and to exhibit shrinkage under the change of environmental conditions. While there are a variety of stress-strain relationships for concrete available in the literature[23, 24, 25, 26], the following

relationship[25] has been selected to represent the behavior of the masonry unit under short-term loading conditions for the present analytical development. The relationship has the form

$$\sigma_{zb} = \frac{\epsilon_z E_b}{1 + \left(\epsilon_z / \epsilon_{bo} \right)^2} \tag{6.2}$$

where

σ_{zb} = masonry unit stress at any strain ϵ_z

ϵ_{bo} = masonry unit strain at maximum stress of f_{bo}

E_b = initial modulus of elasticity equal to $2f_{bo}/\epsilon_{bo}$.

The masonry unit is subjected to shrinkage over a period of time and to creep under sustained load. The approach to shrinkage and creep used in this analysis follows the general principles outlined by Balaguru and Nawy[9] and discussed in Chapter II.

The proposed expression relates the amount of strain due to shrinkage with time in the following form

$$\epsilon_{shb}(t) = \epsilon_{shub} \left(1 - e^{-0.067 t_1} \right) \tag{6.3}$$

where

$\epsilon_{shb}(t)$ = time-dependent shrinkage strain for the masonry unit.

ϵ_{shub} =ultimate shrinkage strain for masonry unit.

t_1 =age expressed as the square root of the actual time in days.

The creep model[9] relates the time-dependent creep strain under sustained load to the instantaneous strain of the masonry unit through a creep coefficient *CB*. The creep coefficient *CB* has the form

$$CB = KB \left(1 - e^{-0.08753 t_2} \right) \tag{6.4}$$

where

t_2 = time under load expressed as the square root of the actual time in days.

KB = $k_b\ k_c\ k_d\ k_e$, which are coefficients that depend on variables such as composition of masonry unit mix, relative humidity of storage, age at loading and thickness of member respectively.

The coefficients k_b, k_c, k_d, and k_e are quantities that can be obtained using graphs provided by **CEB-FIB**[10].

6.2.3 Grout

Grout is also assumed to have a non-linear stress-strain relationship under short-term loading, creeps when subjected to long-term loading and exhibits shrinkage under a change of environmental conditions. Similarly, the stress-strain relationship proposed for concrete under short-time loading is selected to represent the behavior of the grout. The relationship has the form

$$\sigma_{zg} = \frac{\epsilon_z E_g}{1 + \left(\epsilon_z / \epsilon_{go} \right)^2} \tag{6.5}$$

where

σ_{zg} = grout stress at any strain ϵ_z

ϵ_{go} = grout strain at maximum stress of f_{go}

E_g = initial modulus of elasticity equal to $2f_{go}/\epsilon_{go}$.

The grout is also subjected to shrinkage over a period of time and to creep under sustained load. Similarly the expression that relates the amount of strain due to grout shrinkage with time has the following form

$$\epsilon_{shg}(t) = \epsilon_{shug}\left(1 - e^{-0.067t_1}\right) \tag{6.6}$$

where

$\epsilon_{shg}(t)$ = time-dependent shrinkage strain for the grout,

ϵ_{shug} = ultimate shrinkage strain for the grout,

t_1 = age expressed as the square root of the actual time in days.

The creep model[9] relates the time-dependent creep strain under sustained load to the instantaneous strain of the grout through a creep coefficient *CG*. The creep coefficient *CG* has the form

$$CG = KG\left(1 - e^{-0.08753t_2}\right) \tag{6.7}$$

where

t_2 = time under load expressed as the square root of the actual time in days.

$KG = k_b\ k_c\ k_d\ k_e$, which are coefficients that depend on variables such as composition of grout mix, relative humidity of storage, age at loading and thickness of member respectively.

The coefficients k_b, k_c, k_d, and k_e are quantities that can be obtained using graphs provided by **CEB-FIB**[10].

6.2.4 Mortar

Similarly, mortar is assumed to have a non-linear stress-strain relationship under short-term loading, creeps when subjected to long-term loading and exhibits shrinkage under a change of environmental conditions. The stress-strain relationship proposed for concrete under short-time loading is selected to represent the behavior of the mortar. The relationship has the form

$$\sigma_{zm} = \frac{\epsilon_z E_m}{1 + \left(\epsilon_z / \epsilon_{mo} \right)^2} \tag{6.8}$$

where

σ_{zm} = mortar stress at any strain ϵ_z

ϵ_{mo} = mortar strain at maximum stress of f_{mo}

E_m = initial modulus of elasticity equal to $2f_{mo}/\epsilon_{go}$.

The mortar is also subjected to shrinkage over a period of time and to creep under sustained load. Similarly the expression that relates the amount of strain due to mortar shrinkage with time has the following form

$$\epsilon_{shm}(t) = \epsilon_{shum} \left(1 - e^{-0.067 t_1} \right) \tag{6.9}$$

where

$\epsilon_{shm}(t)$ = time-dependent shrinkage strain for the mortar,

ϵ_{shum} = ultimate shrinkage strain for mortar,

t_1 = age expressed as the square root of the actual time in days.

The creep model[9] relates the time-dependent creep strain under sustained load to the instantaneous strain of the mortar through a creep coefficient *CM*. The creep coefficient *CM* has the form

$$CM = KM \left(1 - e^{-0.08753 t_2} \right) \tag{6.10}$$

where

t_2 = time under load expressed as the square root of the actual time in days.

KM = k_b k_c k_d k_e, which are coefficients that depend on variables such as composition of mortar mix, relative humidity of storage, age at loading and thickness of member respectively.

The coefficients k_b, k_c, k_d, and k_e are quantities that can be obtained using graphs provided by **CEB-FIB**[10].

Two combinations of loading stages are considered in this thesis. First, short-time loading where the loading increments are produced by the application of increments of short-time strain through to failure. Second, short-time loading to a specified level, followed by a period of sustained load at this load level, followed by short-time loading to failure. In this case, the first loading increments are produced by the application of short-time strain increments up to the level of the sustained load. Strains under sustained load are calculated from the application of time increments. Subsequent loading to failure is produced by the application of short-time strain increments.

6.3 One Dimensional Analysis

In this model, the analysis is limited to the behavior in the direction of the applied load. The significant materials considered are the masonry unit, grout and the vertical

reinforcement. The mortar and joint reinforcement, being small in quantity and lying in a plane perpendicular to the load, are assumed to have little effect and are excluded from the analysis.

6.3.1 Assumptions of the analysis

The following assumptions are made for this analysis:

1. The masonry unit and grout do not take any tension.
2. A perfect bond is assumed at the interface between the masonry unit, grout and reinforcing steel.
3. A perfect bond at the mortar joint and unit interface to prevent local failure.
4. The effects of mortar and joint reinforcement are neglected.
5. Axial load is assumed with no eccentricity.

6.3.2 Method of Analysis

The analysis utilizes the use of the stress-strain relationships and the time-dependent properties of the constituent materials. The conditions of equilibrium and compatibility were applied at each stage of the analysis. The stress-strain relationships of the masonry unit and grout can be rewritten in the following form to account for the shrinkage that takes place before any loading stage is considered:

for concrete masonry units

$$\sigma_{zb} = \frac{E_b \left(\epsilon_z - \epsilon_{shb}(t) \right)}{1 + \left(\frac{\epsilon_z - \epsilon_{shb}(t)}{\epsilon_{bo}} \right)^2} \geq 0 \qquad (6.11)$$

and, for grout

$$\sigma_{zg} = \frac{E_g \left(\epsilon_z - \epsilon_{shg}(t) \right)}{1 + \left(\frac{\epsilon_z - \epsilon_{shg}(t)}{\epsilon_{go}} \right)^2} \geq 0 \qquad (6.12)$$

Under short-term loading condition, the internal axial load is computed by applying the principles of equilibrium and compatibility. At any instant of short-term loading, the following equation is used to determine the internal load P_z

$$P_z = \sigma_{zb} A_b + \sigma_{zg} A_g + \sigma_{zs} A_s \qquad (6.13)$$

Where A_b, A_g and A_s are the areas of the masonry unit, grout and vertical steel reinforcement respectively. The stresses in the masonry unit, σ_{zb}, in the grout, σ_{zg}, and in the reinforcement, σ_{zs}, are computed from equations 6.11, 6.12, and 6.1 respectively. At any stage of the short-term loading, the strain in the direction of the load is applied in increments and the internal load P_z is computed.

In the case of the long-term loading condition, the instantaneous strain in the direction of the load ϵ_{zi} is computed using an iteration method. The instantaneous strain ϵ_{zi} is used to calculate the strains in the constituent materials due to creep. For a known level of sustained load P_{zi}, the instantaneous strain ϵ_{zi} is computed by substituting the stress equations for the constituent materials, equations 6.1, 6.11 and 6.12, into equation 6.13 and assuming that the strain in the direction of the load has the value of the instantaneous strain ϵ_{zi}. The relationship used to compute the instantaneous strain ϵ_{zi} has the following form:

$$P_{zi} = \left[\epsilon_{zi} E_s A_s + \frac{E_b A_b (\epsilon_{zi} - \epsilon_{shb}(t))}{1 + \left(\frac{\epsilon_{zi} - \epsilon_{shb}(t)}{\epsilon_{bo}} \right)^2} + \frac{E_g A_g (\epsilon_{zi} - \epsilon_{shg}(t))}{1 + \left(\frac{\epsilon_{zi} - \epsilon_{shg}(t)}{\epsilon_{bo}} \right)^2} \right] \quad (6.14)$$

Where P_{zi} is the sustained load, and ϵ_{zi} is the instantaneous strain in the column under the sustained load.

Once the load is sustained, creep and further drying shrinkage strains will take place with the passage of time. The shrinkage strains and the creep coefficients at any increment of time are obtained by substituting the appropriate values in equations 6.3 and 6.4 for the masonry unit and equations 6.6 and 6.7 for the grout. Consequently, the strains (and thus the stresses) in the constituent materials will change due to those time-dependent deformations. From the compatibility of strains, the following relationships relating the time dependent deformations in the masonry column to those of the individual constituent materials can be written as follows:

for the masonry unit

$$\epsilon_{eb}(t) = \frac{\epsilon_{zi} + \epsilon_c(t) - \epsilon_{shb}(t)}{(1 + CB)} \quad (6.15)$$

where

$\epsilon_{eb}(t)$ = elastic strain of the concrete masonry unit,

$\epsilon_c(t)$ = Time-dependent strain in the masonry column due to creep;

and, for the grout

$$\epsilon_{eg}(t) = \frac{\epsilon_{zi} + \epsilon_c(t) - \epsilon_{shg}(t)}{(1 + CG)} \quad (6.16)$$

where

$\epsilon_{eg}(t)$ = elastic strain of the grout.

Redistribution of the internal stresses between the constituent materials will occur due to the time-dependent deformation. The change in the masonry unit stress ($\Delta\sigma_b(t)$) is computed as follows:

$$\Delta\sigma_{zb}(t) = E_b \left[\frac{\epsilon_{eb}(t)}{1+\left(\frac{\epsilon_{eb}(t)}{\epsilon_{bo}}\right)^2} - \frac{(\epsilon_{zi}-\epsilon_{shb}(t))}{1+\left(\frac{\epsilon_{zi}-\epsilon_{shb}(t)}{\epsilon_{bo}}\right)^2} \right] \tag{6.17}$$

and, for the grout ($\Delta\sigma_g(t)$) is

$$\Delta\sigma_{zg}(t) = E_g \left[\frac{\epsilon_{eg}(t)}{1+\left(\frac{\epsilon_{eg}(t)}{\epsilon_{go}}\right)^2} - \frac{(\epsilon_{zi}-\epsilon_{shg}(t))}{1+\left(\frac{\epsilon_{zi}-\epsilon_{shg}(t)}{\epsilon_{go}}\right)^2} \right] \tag{6.18}$$

and for the reinforcement steel ($\Delta\sigma_s(t)$) is

$$\Delta\sigma_{zs}(t) = E_s\epsilon_c(t) \tag{6.19}$$

The above equations are used to determine the stresses in the constituent materials at any increment of time in terms of the time-dependent column strain $\epsilon_c(t)$. The value of the strain $\epsilon_c(t)$ at any increment of time is calculated by substituting equations 6.17, 6.18, and 6.19 into the following equilibrium equation:

$$\Delta\sigma_{zb}A_b + \Delta\sigma_{zg}A_g + \Delta\sigma_{zs}A_s = 0 \tag{6.20}$$

Finally, if a relatively rapid loading is being considered following the sustained load period, the procedure adopted in computing the stresses in both the masonry unit

and grout is to shift the stress-strain relationships by the creep and shrinkage values which existed at the end of the sustained load periods. This means that the instantaneous strain component is calculated as for short-term loading with the creep and shrinkage strain components retain the values which existed at the end of the sustained load period. This procedure is similar to that used by Manuel et al[27] in the analysis of restrained reinforced concrete columns under sustained load.

At each stage of the analysis, the strains in both the masonry unit and the grout are compared with limiting values to determine the failure load. The failure of the column is assumed to initiate when the instantaneous component of total strain in the masonry unit and/or the grout reaches the maximum strains ϵ_{bo} and ϵ_{go} respectively. Again, this assumption is used by Manuel and MacGregor[28] in the analysis of reinforced concrete columns under sustained load. The values for the strains and its limits in both the masonry unit and grout can be written as follows:

for the masonry unit

$$\epsilon_{eb}(t) \leq \left(\epsilon_{shb}(t) + \epsilon_{cb}(t) + \epsilon_{bo}\right) \tag{6.21}$$

where

$\epsilon_{cb}(t)$ = creep strain of the concrete masonry unit equal to $CB\ \epsilon_{cb}(t)$

and, for the grout

$$\epsilon_{eg}(t) \leq \left(\epsilon_{shg}(t) + \epsilon_{cg}(t) + \epsilon_{go}\right) \tag{6.22}$$

where

$\epsilon_{cg}(t)$ = creep strain of the grout equal to $CG\ \epsilon_{cg}(t)$

A computer program to perform this analysis is listed in Appendix B. Under short-term loading, the program predicts the load-strain relationship through increments of strain. Prediction of the behavior under sustained load is achieved through increments of time. The results of the analysis are discussed in Chapter VII.

6.4 Three Dimensional Analysis

In this model, the analysis considers the behavior in the transverse directions in addition to that in the direction of the load. Under axial load, three-dimensional states of stress develop in the constituent materials. Mathematical solution of the stresses in a cross-section like the one shown in Fig. 6.2 is very complex due to the geometric configuration of the cross-section. To reduce the complexity of the problem, an idealized masonry ring shown in Fig. 6.3 is used to solve for the stresses in the transverse directions. To verify the validity of this assumption, a finite element analysis was performed on both a rectangular cross-section representing half a concrete block and an equivalent circular section, using 3-D finite element analysis (*FEAP*). The results of the program for both section were compared and are shown graphically in Figs. 6.4 to 6.6 for the stresses in the three directions (z, r, θ). Comparison of the stresses indicate that the assumption of circular section is reasonable.

6.4.1 Assumptions of the 3-D analysis

The following assumptions are made for this analysis:

1. A perfect bond is assumed at the interface between the constituent materials.
2. A perfect bond at the mortar joint and unit interface to prevent local failure.
3. The effect of joint reinforcement is neglected.
4. Axial loading is assumed with no eccentricity.
5. Stresses in the transverse direction can be predicted using an idealized masonry ring.
6. Masonry unit, grout and mortar shrink uniformly in all directions.

6.4.2 Method of Analysis

The analysis was undertaken at two cross-sections: one at the masonry unit level consisting of reinforcement, grout and masonry unit; the other at the mortar joint level consisting of reinforcement, grout and mortar. Both cross-sections are then connected by the principles of equilibrium and compatibility.

Consider an axisymmetric homogeneous element in each of the component materials. The radial equilibrium of such element leads to the following differential equation[29]:

$$\frac{d^2u}{dr^2} + \frac{1}{r}\frac{du}{dr} - \frac{u}{r^2} = 0 \qquad (6.23)$$

Where

u = radial displacement.

r = radius of the cross-section.

The solution for this differential equation is in the form[29]

$$u = Ar + \frac{B}{r} \qquad (6.24)$$

Where A and B are constants to be evaluated by imposing certain boundary conditions. These boundary conditions are discussed later in this chapter.

Expressions for the strains in the radial and tangential directions (r,θ) can be written as follows[29]:

$$\epsilon_r = A - \frac{B}{r^2} \qquad (6.25)$$

Where

$$\epsilon_\theta = A + \frac{B}{r^2} \tag{6.26}$$

ϵ_r = strain in the radial direction r.

ϵ_θ = strain in the tangential direction θ

The stress-strain relationships in the longitudinal, radial and circumferential directions (z,r,θ) are:

$$\sigma_z = \frac{E}{(1+\nu)(1-2\nu)} \left[(1-\nu)\epsilon_z + \nu(\epsilon_r+\epsilon_\theta) \right] \tag{6.27}$$

$$\sigma_r = \frac{E}{(1+\nu)(1-2\nu)} \left[(1-\nu)\epsilon_r + \nu(\epsilon_\theta+\epsilon_z) \right] \tag{6.28}$$

$$\sigma_\theta = \frac{E}{(1+\nu)(1-2\nu)} \left[(1-\nu)\epsilon_\theta + \nu(\epsilon_r+\epsilon_z) \right] \tag{6.29}$$

where σ_z, σ_r, σ_θ, ϵ_z, ϵ_r, and ϵ_θ are the stresses and strains in the principal directions (z, r, θ) respectively, ν is the Poisson's ratio and E is the elastic modulus for each of the constituent materials.

The elastic modulus for the reinforcement bars is assumed to be constant and equal to 200,000 MPa. For the masonry unit, grout and mortar the elastic modulus is assumed to change at each increment of the longitudinal strain (ϵ_z) following the stress-strain relationships of concrete for short-term loading[25] such that

$$E = \frac{E_i}{1 + \left(\frac{\epsilon_z}{\epsilon_o}\right)^2} \tag{6.30}$$

where E_i is the initial modulus of elasticity and ϵ_o is the strain corresponding to the maximum axial compressive stress.

At each cross-section, plane strain distribution is assumed in the longitudinal direction (z), with the strain in the longitudinal direction at the block level being applied incrementally. Applying the principle of strain compatibility and including the time-dependent deformations of shrinkage and creep, the strains in the three principal directions (z, r, θ) for the constituent materials at each cross-section can be written as follows:

1. Cross-section at the block:

for the masonry unit

$$\epsilon_{zb}(t) = \frac{\epsilon_{z_1} + \epsilon_{c_1}(t) - \epsilon_{shb}(t)}{(1 + CB)} \tag{6.31}$$

$$\epsilon_{rb}(t) = \left(\frac{A_1 - B_1}{r_b^2}\right)(1 + CB) - \epsilon_{shb}(t) \tag{6.32}$$

$$\epsilon_{\theta b}(t) = \left(\frac{A_1 + B_1}{r_b^2}\right)(1 + CB) - \epsilon_{shb}(t) \tag{6.33}$$

for the grout

$$\epsilon_{zg_1}(t) = \frac{\epsilon_{z_1} + \epsilon_{c_1}(t) + \epsilon_{shg}(t)}{(1 + CG)} \tag{6.34}$$

$$\epsilon_{rg_1}(t) = \left(\frac{A_2 - B_2}{r_g^2}\right)(1 + CG) - \epsilon_{shg}(t) \tag{6.35}$$

$$\epsilon_{\theta g_1}(t) = \left(\frac{A_2 + B_2}{r_g^2}\right)(1 + CG) - \epsilon_{shg}(t) \tag{6.36}$$

and for the reinforcement steel

$$\epsilon_{zs_1}(t) = \epsilon_{z_1} + \epsilon_{c_1}(t) \tag{6.37}$$

$$\epsilon_{rs_1} = \epsilon_{\theta s_1} = A_3 \tag{6.38}$$

2. Cross-section at the mortar joint:

for the mortar

$$\epsilon_{zm}(t) = \frac{\epsilon_{z_2} + \epsilon_{c_2}(t) - \epsilon_{shm}(t)}{(1 + CM)} \tag{6.39}$$

$$\epsilon_{rm}(t) = \left(\frac{A_4 - B_3}{r_m^2}\right)(1 + CM) - \epsilon_{shm}(t) \tag{6.40}$$

$$\epsilon_{\theta m}(t) = \left(\frac{A_4 + B_3}{r_m^2}\right)(1 + CM) - \epsilon_{shm}(t) \tag{6.41}$$

for the grout

$$\epsilon_{zg_2}(t) = \frac{\epsilon_{z_2} + \epsilon_{c_2}(t) - \epsilon_{shg}(t)}{(1 + CG)} \tag{6.42}$$

$$\epsilon_{rg_2}(t) = \left(\frac{A_5 - B_4}{r_g^2}\right)(1 + CG) - \epsilon_{shg}(t) \tag{6.43}$$

$$\epsilon_{\theta g_2}(t) = \left(\frac{A_5 + B_4}{r_g^2}\right)(1 + CG) - \epsilon_{shg}(t) \tag{6.44}$$

and for the reinforcement steel

$$\epsilon_{zs_2} = \epsilon_{z_2} + \epsilon_{c_2}(t) \tag{6.45}$$

$$\epsilon_{rs_2} = \epsilon_{\theta s_2} = A_6 \tag{6.46}$$

The stresses in the principal directions z, r, and θ for the constituent materials are obtained by substituting the appropriate strain into the stress-strain relationships of equations 6.27, 6.28, and 6.29. The result of the substitution is a total of 16 stress equations. These equations contain thirteen unknowns (ten constants of integration A_1 to A_6 and B_1 to B_4, the creep strains in the column in a cross-section at the block and mortar levels $\epsilon_{c_1}(t)$, and $\epsilon_{c_2}(t)$ respectively and the strain in the longitudinal direction at the mortar level ϵ_{z_2}) with the longitudinal strain at the block level ϵ_{z_1} being applied incrementally. To obtain a solution for these unknowns, proper boundary conditions of equilibrium of stresses and compatibility of strains in the three directions (z, r, θ) are applied. These conditions are discussed in the following sub-section.

6.4.3 Boundary Conditions

The following boundary conditions utilize the principles of equilibrium and compatibility in the longitudinal and radial directions at each strain increment.

1. The stresses and displacements in the radial direction are equal in both the grout and vertical reinforcement at their interface in both cross-sections, that is

$$\sigma_{rg_1} = \sigma_{rs_1} \tag{6.47}$$

$$\sigma_{rg_2} = \sigma_{rs_2} \tag{6.48}$$

$$u_{rg_1} = u_{rs_1} \tag{6.49}$$

$$u_{rg_2} = u_{rs_2} \tag{6.50}$$

2. The stresses and displacements in the radial direction are equal for both the grout and the masonry unit at their interface in the cross-sections at the block level, and for the mortar and grout at the cross-section at the mortar joint level, that is

$$\sigma_{rg_1} = \sigma_{rb} \tag{6.51}$$

$$u_{rg_1} = u_{rb} \tag{6.52}$$

$$\sigma_{rg_2} = \sigma_{rm} \tag{6.53}$$

$$u_{rg_2} = u_{rm} \tag{6.54}$$

3. The internal axial load at both cross-sections are equal, that is

$$\sigma_{zb}A_b + \sigma_{zg_1}A_g + \sigma_{zs_1}A_s = \sigma_{zm}A_m + \sigma_{zg_2}A_g + \sigma_{zs_2}A_s \qquad (6.55)$$

4. The internal radial forces are in equilibrium and the radial displacements are equal at the block-mortar interface, that is

$$\sigma_{rb}t_b + \sigma_{rm}t_m = 0 \qquad (6.56)$$

where

t_b = height of the masonry unit

t_m = mortar joint thickness

$$u_{rb} = u_{rm} \qquad (6.57)$$

A computer program based on the preceding analysis is listed in Appendix C. The program calculates the internal stresses in the component materials at each loading stage. In the case where only short-time loading is being considered, the creep strain component is taken as zero and the stresses are computed by incrementing the longitudinal strain ϵ_{z1}. Under sustained load the internal stresses are computed through increments of time. Following the sustained load period, loading to failure is considered and the stresses are calculated as for short-term loading with the creep and shrinkage retaining the values which existed at the end of the sustained load periods.

6.4.3 Failure Criteria

At each stage of the analysis, the principal stresses in the constituent materials were compared with specific limiting values to check for column failure. The values chosen for this analysis are similar to the limit state used by others[30, 31], however the analysis is not limited to these criteria and it can be modified with the advance in the

knowledge of material properties. The limiting stress states used for this analysis can be written for each of the constituent materials as follows:

for the masonry unit,

(1) the maximum principal axial compressive stress in the block (σ_{zb}) reaches the compressive strength of the block (f_{bo}) such that

$$\sigma_{zb} \leq f_{bo} \tag{6.58}$$

(2) the maximum principal tangential stress in the block ($\sigma_{\theta b}$) reaches the tensile strength in the block (f_{tb}) such that

$$\sigma_{\theta b} \leq f_{tb} \tag{6.59}$$

for the grout,

(3) the maximum axial compressive strength in the grout at the block or mortar joint, σ_{zg1} or σ_{zg2} respectively reaches the confined crushing strength of the grout. The strength of the confined grout is assumed to be govern by the same relationship proposed by Richart et al.[32] for the strength of hydrostatically confined concrete, such that

$$\sigma_{zg_1} \leq (f_{go} + 4.1 \sigma_{\theta g_1}) \tag{6.60}$$

or

$$\sigma_{zg_2} \leq (f_{go} + 4.1 \sigma_{\theta g_2}) \tag{6.61}$$

where

$\sigma_{\theta g1}$ = the tangential stress in the grout at the block.

$\sigma_{\theta g2}$ = the tangential stress in the grout at the mortar joint.

and for the mortar

(4) the maximum principal axial compressive stress in the mortar (σ_{zm}) reaches the confined crushing strength of the mortar. The strength of the confined mortar is also assumed to follow the relationship proposed by Richart et al[32]. Therefore, the confined strength of the mortar is expressed by

$$\sigma_{zm} \leq (f_{mo} + 4.1 \sigma_{\theta m}) \tag{6.62}$$

where

$\sigma_{\theta m}$ = the tangential stress in the mortar.

6.5. Conclusion

The method of analysis presented in Section 6.4. is developed to confirm the validity of the simpler one-dimension analysis presented in Section 6.3. While the one-dimensional model neglects the effect of the mortar joint, it is a simple model and does explain the mechanism by which the reinforced masonry columns resist the applied load. On the other hand, the three-dimensional model does consider the effect of the mortar joint and the effect of the deformations of the constituent materials in the lateral directions. This model is more comprehensive and requires the knowledge of some of the material properties that are difficult to obtain experimentally such as the Poisson's ratio ν. Both methods of analysis will be discussed and compared with the experimental results in Chapter VII.

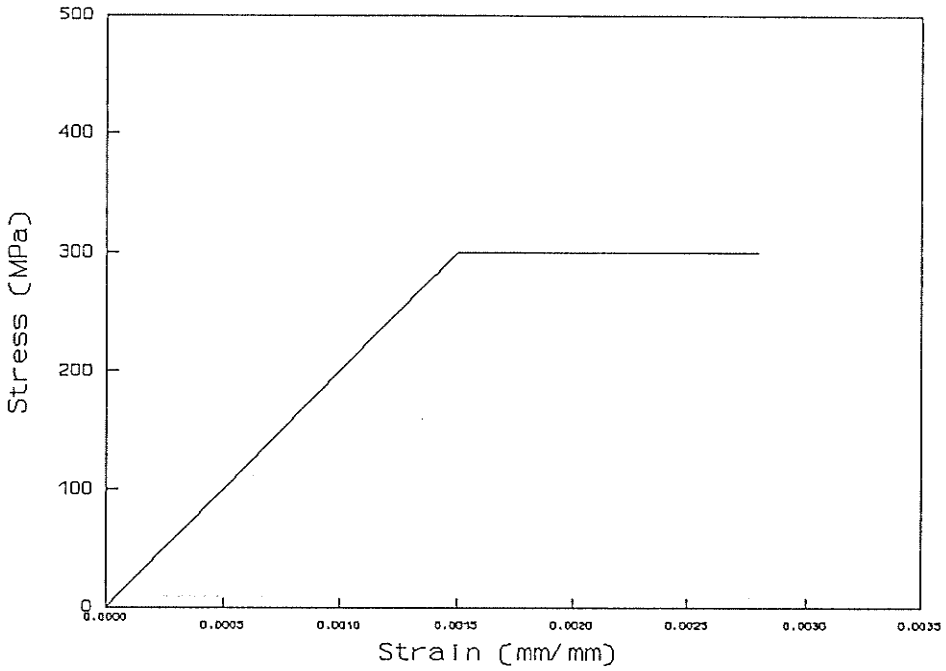

Figure 6.1 Idealized stress-strain relation for reinforcing steel

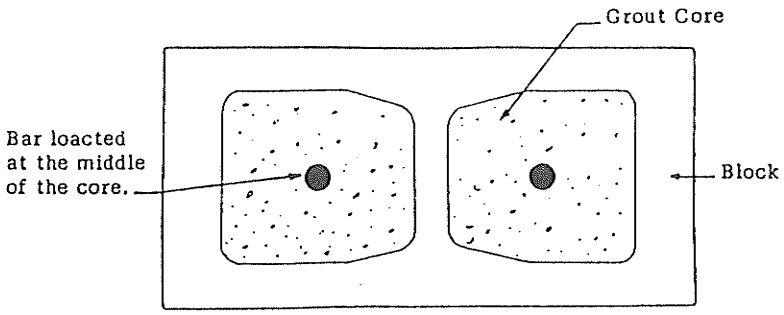

Figure 6.2 Reinforced masonry column cross-section

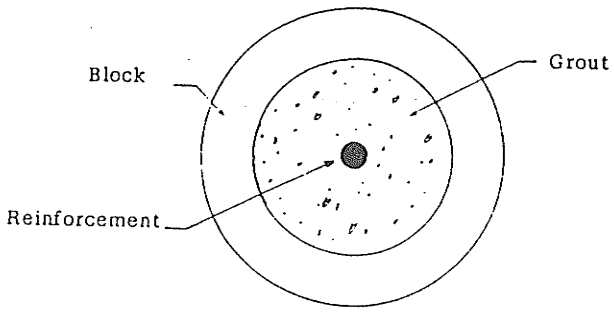

Figure 6.3 Assumed masonry ring

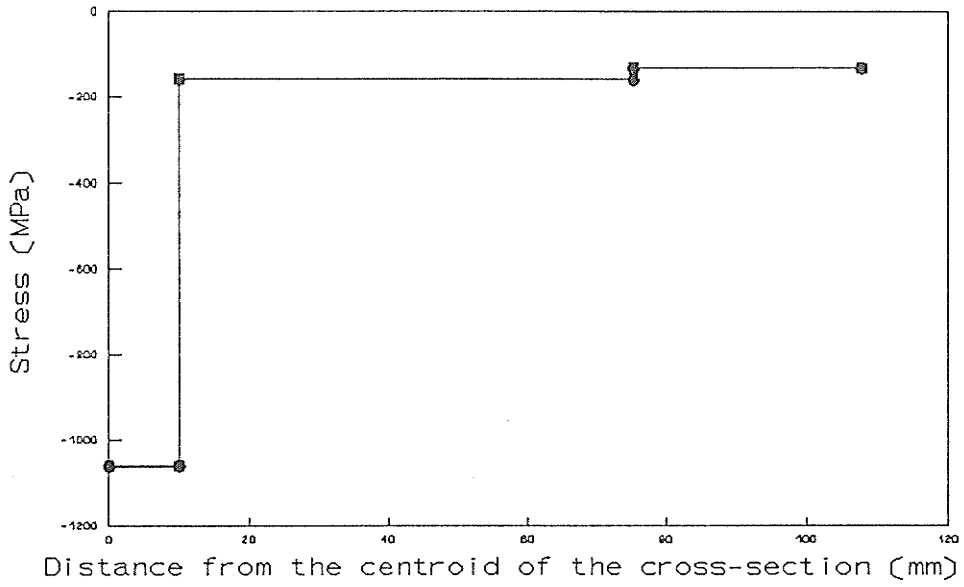

Figure 6.4 Comparison of stress in z-direction

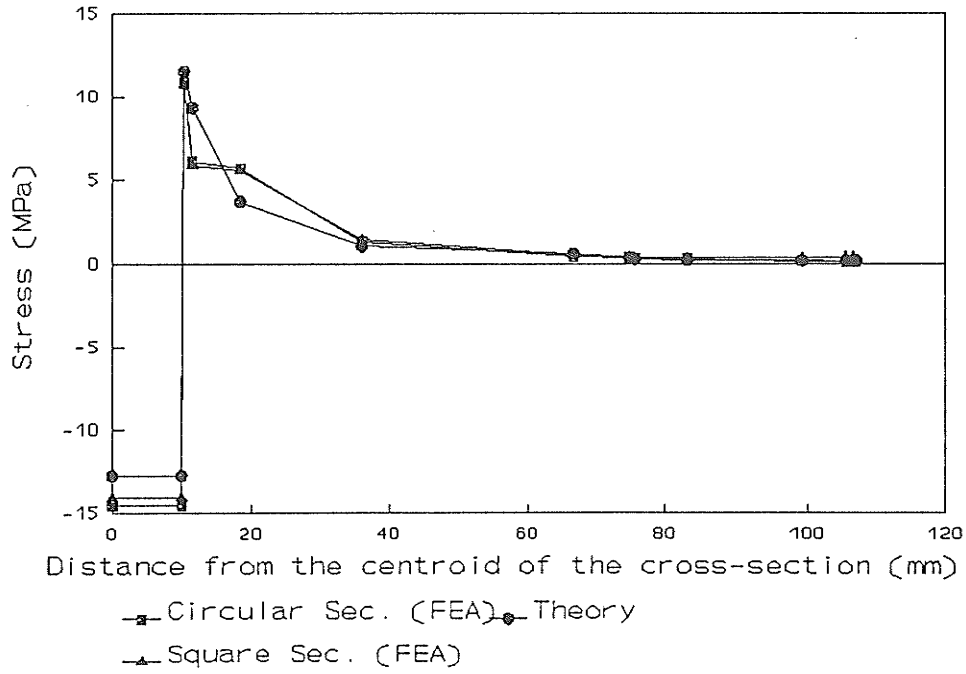

Figure 6.5 Comparison of stress in r-direction

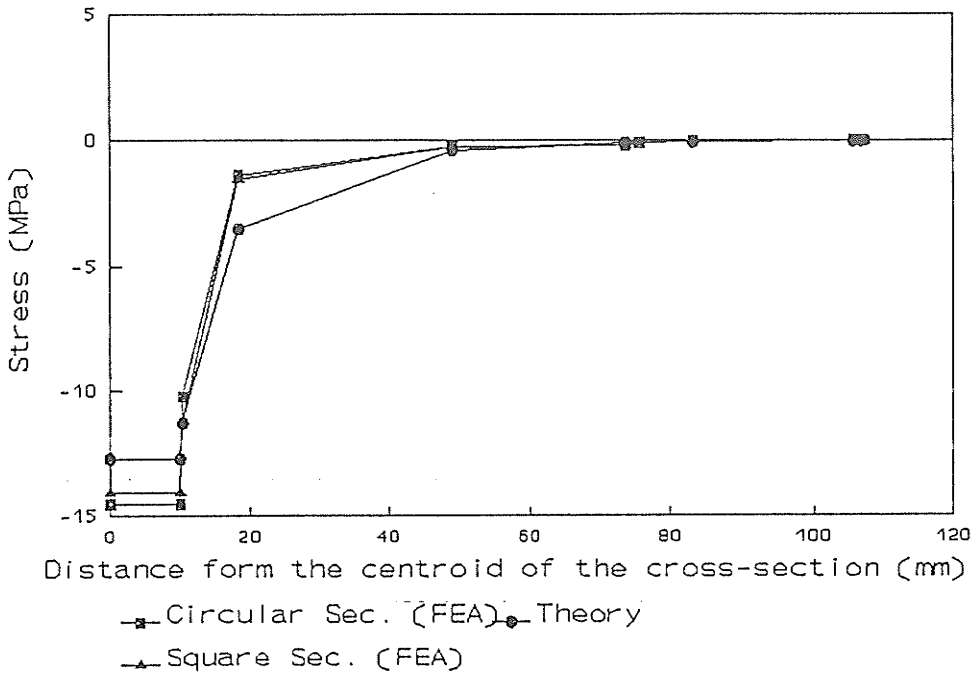

Figure 6.6 Comparison of stress in θ-direction

CHAPTER VII
APPLICATION OF THE THEORETICAL ANALYSIS TO THE EXPERIMENTAL RESULTS

7.1 Introduction

This chapter contains a comparison of experimental and analytical results in an attempt to verify the applicability of both methods of analysis described in Chapter VI. The experimental results used in this comparison are those discussed in Chapter V. Deformation characteristics are used as the basis of comparison since they influence the distribution and redistribution of stresses between the constituent materials. The ultimate strength results of the reinforced masonry columns tested in this investigation are also compared with the values predicted by both theoretical methods.

The creep and shrinkage relationships for the masonry unit, grout and mortar outlined in Chapter VI have been modified to apply to the specific conditions of the testing program conducted in this investigation. Since the ultimate shrinkage strains for the masonry unit, grout and mortar were not obtained experimentally in this investigation, the values that are used in the analysis were developed with the guidance of the engineering literature on the subject. The ultimate shrinkage strain of masonry units (manufactured in the same plant as those used in this investigation) was found to be in the range of 0.00045 (mm/mm)[33]. However, since the masonry units used in the construction of the column specimens were a few months old at the time of delivery, it was assumed that most of the drying shrinkage had occurred and a value of 0.0001 (mm/mm) was used for the ultimate shrinkage strain of the masonry unit, ϵ_{shub}. The ultimate shrinkage strain of the grout, ϵ_{shug}, is assumed to have the average value of 0.0008 (mm/mm), as recommended by *The American Concrete Institute Committee 209*[34] for moist cured concrete. In the absence of exact data on the shrinkage of mortar and since mortar tends to shrink more than normal concrete which

has relatively larger coarse aggregate, a value of .001 is assumed to represent the ultimate shrinkage strain for the mortar, ϵ_{shum}. This value represents the upper limit of shrinkage strain recommended by *ACI Committee 209* for moist cured concrete. The strain corresponding to the maximum stress in the masonry unit, ϵ_{bo}, is assumed to be .0022, based on the experimental results by Roy [4]. The strain at the maximum stress for the grout, ϵ_{go}, and for the mortar, ϵ_{mo}, is assumed to be .002 (mm/mm). This strain value was experimentally verified for concrete and other cementitious materials.

The relationships discussed in Chapter VI for creep in the masonry unit, grout and mortar depends on the constants *KB*, *KG*, and *KM* respectively. These constants in turn depend on coefficients related to the material properties and the testing conditions. These coefficients are obtained using the graphs provided by **CEB-FIB**[10].

The following values are obtained for the masonry unit:

- the composition coefficient $k_b = 1.0$
- the environmental coefficient $k_c = 2.3$ for normal air and relative humidity of 50%
- the coefficient for the hardening at the age of loading $k_d = 0.5$ for constant temperature of 20° and normal cement
- the thickness of the member coefficient $k_e = 0.85$

Based on these values the constant *KB* has the value of 0.98.

For the grout,

- $k_b = 1.20$
- $k_c = 2.3$ for normal air and relative humidity of 50%
- $k_d = 0.45$ for constant temperature of 20° and high early strength cement
- $k_e = 0.85$

Therefore the constant *KG* has the value of 1.06

And finally for the mortar,

- $k_b = 1.0$
- $k_c = 2.3$ for normal air and relative humidity of 50%
- $k_d = 0.60$ for constant temperature of 20° and high early strength cement
- $k_e = 0.85$

Therefore the constant *KM* has the value of 1.17.

7.2 Application of the One-Dimensional Analysis to the Experimental Results

The one-dimensional model is used to predict the time-dependent deformation, the load-strain relationships and the ultimate strength of the masonry columns. The predicted values are compared with the experimental results. The predicted time-dependent deformations are first compared with the experimental results, followed by the load-strain behavior during ultimate load testing for both the preloaded and non-preloaded columns and, finally, the values of the column ultimate load predicted by the model are compared with those obtained experimentally.

7.2.1 Time-Dependent Deformation

The time-dependent deformation due to creep of the constituent materials is largely dependent upon the instantaneous strain, among other factors. The instantaneous strain is affected by the level of sustained load and the value of ultimate shrinkage strain of the constituent materials. During the testing of the columns under sustained load, the level of load decreased due to shrinkage and creep of the column and creep of the load-sustaining material. The mathematical model assumed that the level of the sustained load is constant throughout the preload period. These variables may have an effect on the comparison between the experimental values and those predicted by the model.

Fig. 7.1 compares the analytical and experimental time-dependent deformations for the preloaded column **CP3L**. It shows that the experimental results are predicted reasonably well by the analytical method. The predicted time-dependent deformation for the more heavily reinforced column **CP10L** is shown in Fig. 7.2. The analytical method appears to overestimate the time-dependent deformation for the more heavily reinforced columns. Generally, the time-dependent deformations for the preloaded columns are predicted reasonably well considering the variation of the sustained load during testing. The model considered a constant level of sustained load and consequently, an average value was used in the analysis. Comparison of the predicted time-dependent deformation with the experimental results for the remaining preloaded columns is given in Appendix D.

7.2.2 Load-Strain Relationship for Preloaded Columns

The load-strain relationships for the preloaded columns **CP3L** and **CP10L** are shown in Fig. 7.3 and Fig. 7.4 respectively. The column strain during the initial loading, that is loading up to the level of the sustained load, was not recorded due to the difficulties experienced during the transfer of the preload to the column. Also, due to the use of demec strain gauges in measuring the strain and the brittle nature of the failure of the masonry columns, the column strain measurements were terminated at a relatively early stage prior to failure. All these factors complicate the comparison between the experimental and the analytical load-strain behavior of the columns. However, the general indication is that the analytical method does predict with reasonable accuracy the behavior under load. It also indicate that with better study of the material properties the accuracy of the method will improve significantly. The load-strain behavior for the remaining preloaded columns is given in Appendix E.

7.2.3 Load-Strain Behavior for the Non-Preloaded Columns

Similar to the preloaded column, to ensure safety, the strain measurement on the non-preloaded control specimen was terminated at an early stage during the testing to failure. The available load-strain measurements were compared with those predicted analytically. Fig. 7.5 and Fig. 7.6 show the load-strain behaviour for non-preloaded columns **CP2U** and **CP8U** respectively. Again both graphs show that the methods of analysis reasonably predicts the load-strain behaviour. The load-strain behaviour for the remaining columns is given in Appendix F.

7.2.4 Ultimate Strength

The predicted ultimate strength of the masonry columns is given in Table 7.1. In most cases, the ultimate load predicted by the model was lower than that recorded experimentally, and there is some evidence that the specimens used for testing the properties of the constituent materials may not have been entirely representative of the actual materials in the columns. The model predicted a slightly higher load for the preloaded columns because of creep in redistribution of stress between the constituent materials. The increase in the ultimate load capacity of the preloaded columns is expected to be higher when a more representative grout is used. However, due to the use of less workable grout in the specimens tested in this investigation, and a consequent lower shrinkage, the increase in ultimate load due to preloading was not obvious in most cases. Also some of the columns failed prematurely due to poor grouting. Normally, a considerably more workable grout is used in the construction of masonry columns.

7.3 Application of the Three-Dimensional Analysis to the Experimental Results

The three-dimensional model is used to confirm the validity of the more simple one-dimensional model. The three-dimensional model required more input data regarding the material properties. This data, such as Poisson's ratio, varies widely for the same material and is comparatively difficult to obtain experimentally. The three-dimensional model predicted the time-dependent deformation, the load-strain behaviour and the ultimate load while taking into account the mortar joint and the state of stress in the transverse directions. The predicted time-dependent deformation and the load-strain behavior during ultimate load for both the preloaded and non-preloaded columns were similar to those presented earlier for the one-dimensional model. However the values of the ultimate load capacity of the columns were different from those predicted by the one-dimensional model. The minor difference in the predicted ultimate load between both analytical models is due to the different state of stress and to the failure criteria used for these models.

The predicted column loads are compared with both the experimental load and that predicted by the one-dimensional model and given in Table 7.1. The three-dimensional model predicted a slightly lower load than the one-dimensional model. All columns failed due to the failure of the masonry unit under axial compression which conformed with the results of the one-dimensional model and also that of the experimental results. Comparison between the one and the three-dimensional models was sufficiently close to justify the use of the simpler one-dimensional model.

TABLE 7.1 Experimental and Analytical Columns Ultimate Load

Column Number	Steel Area (mm^2)	Average Sustained Load (kN)	Ultimate Load (kN)		
			Experimental	Analytical	
				One-dimensional Model	Three-dimensional Model
CP1U		---	1787.3	1886.74	1837.42
CP1L	200	686	1831.5	1897.69	1870.98
CP2U		---	1841.2	1904.20	1853.61
CP2L	200	746	1833.0	1915.68	1887.99
CP3U		---	1951.1	1756.57	1718.01
CP3L	400	698	1761.9	1765.44	1743.52
CP4U		---	1681.3	1936.18	1886.47
CP4L	400	707	2183.7	1947.73	1921.10
CP5U		---	2355.8	1958.93	1917.78
CP5L	600	683	2255.3	1969.83	1945.96
CP6U		---	2396.0	2178.34	2121.02
CP6L	600	688	2328.4	2192.54	2159.59
CP7U		---	2245.1	1935.22	1889.17
CP7L	600	719	2403.5	1945.97	1920.79
CP8U		---	2057.8	2020.30	1972.72
CP8L	800	689	2308.0	2031.45	2005.47
CP9U		---	2444.9	2125.59	2077.35
CP9L	1000	656	2561.8	2137.26	2109.57
CP10U		---	2473.8	2158.44	2108.07
CP10L	1000	645	2369.8	2170.62	2143.68

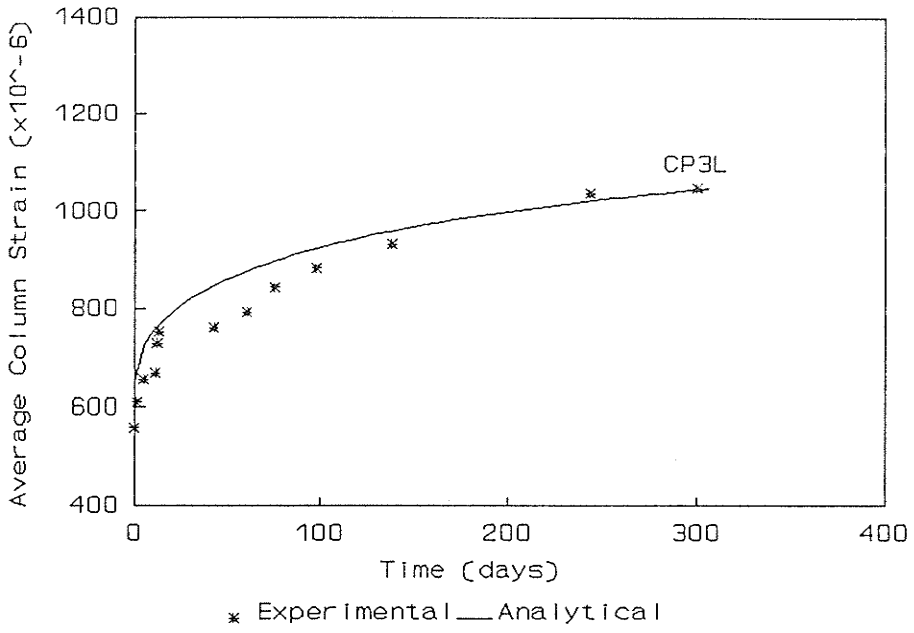

Figure 7.1 Predicted time-dependent deformation (preloaded column CP3L)

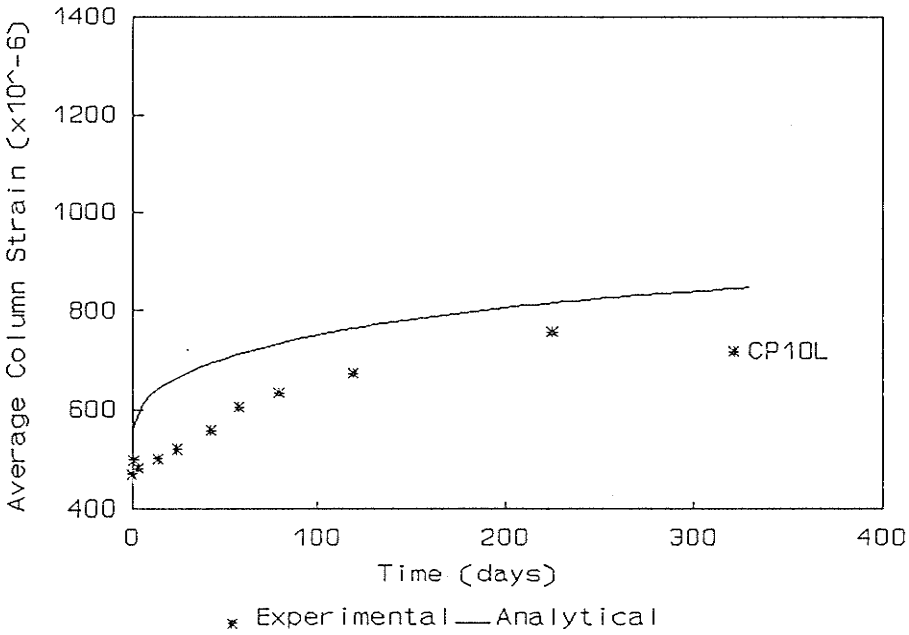

Figure 7.2 Predicted time-dependent deformation (preloaded column CP10L)

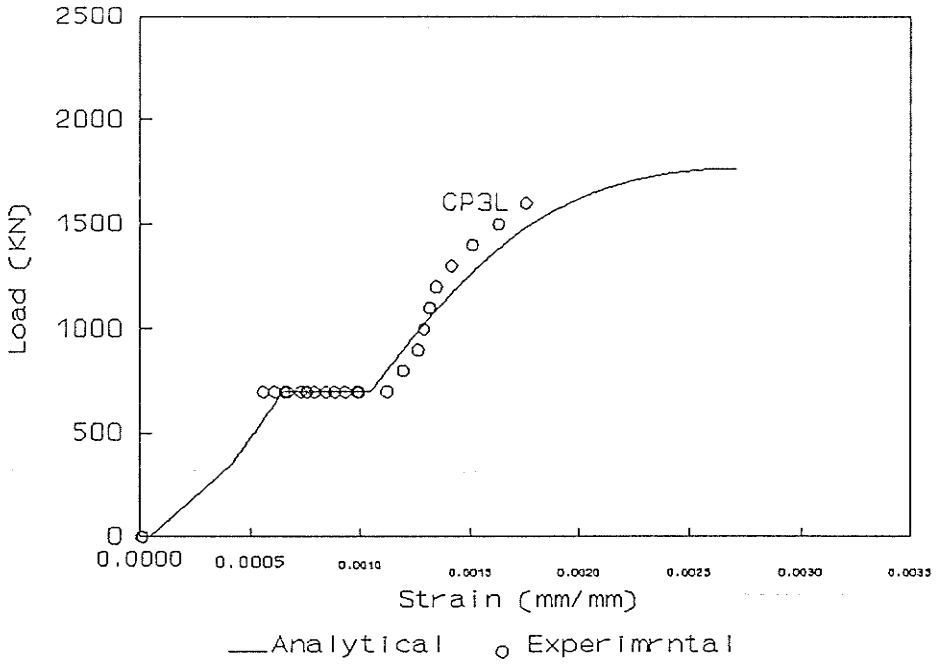

Figure 7.3 Predicted load-strain behavior
(preloaded column CP3L)

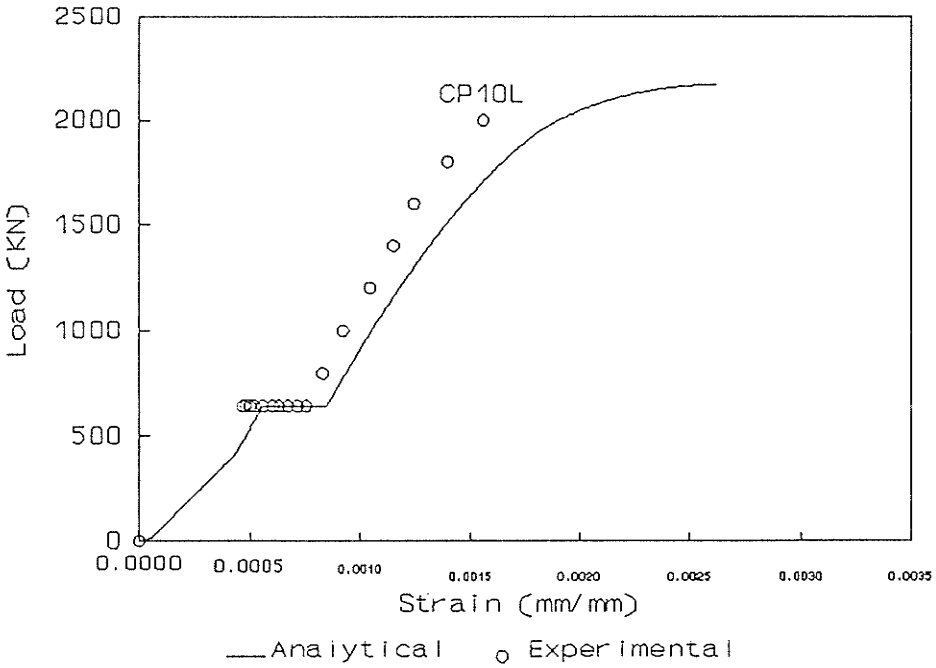

Figure 7.4 Predicted load-strain behavior
(preloaded column CP10L)

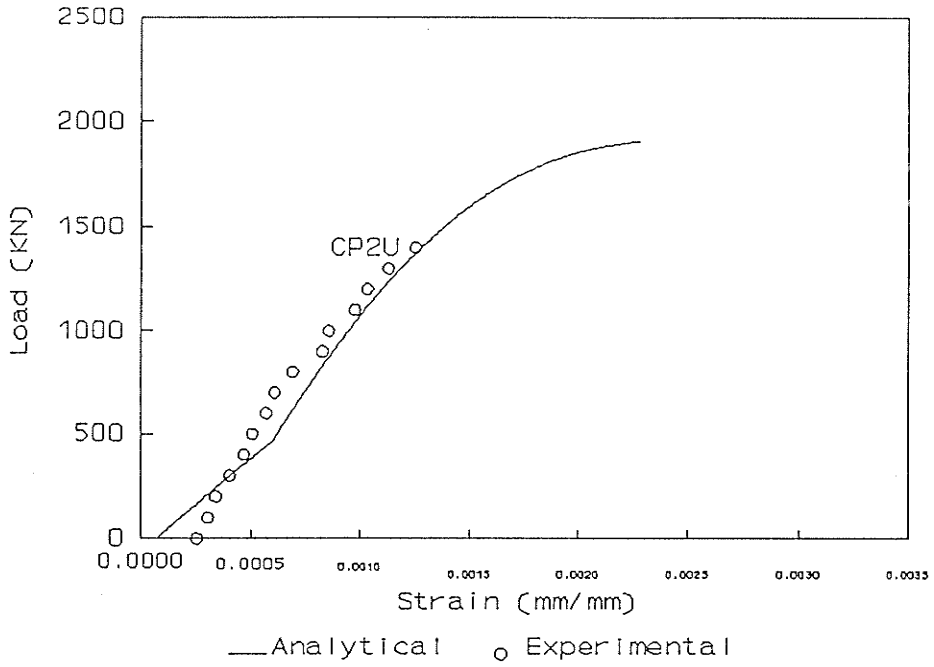

Figure 7.5 Predicted load-strain behavior
(non-preloaded column CP2U)

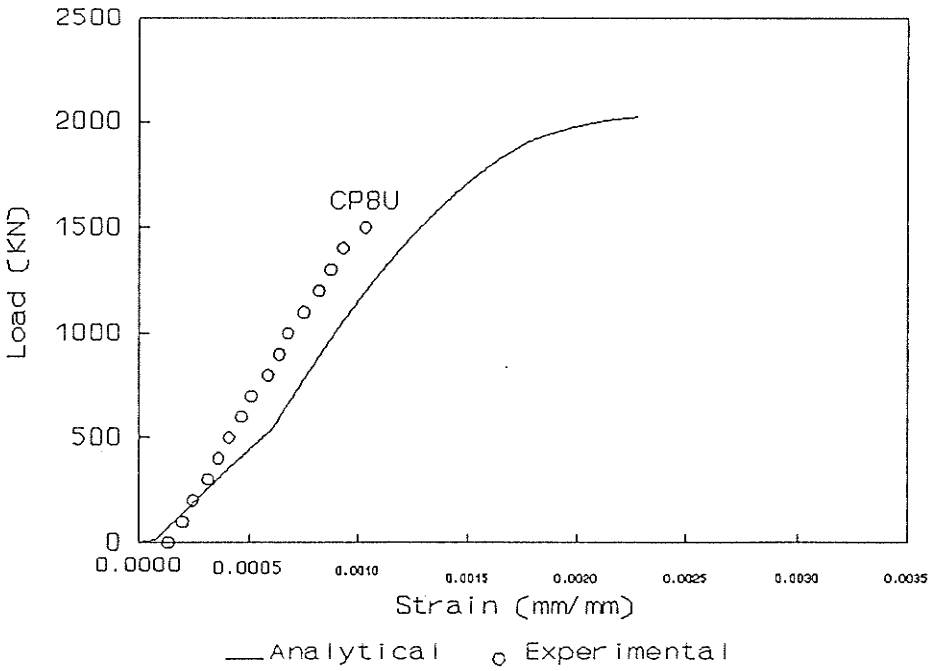

Figure 7.6 Predicted load-strain behavior
(non-preloaded column CP8U)

CHAPTER VIII
SUMMARY, CONCLUSIONS, AND RECOMMENDATIONS

8.1 Summary

Experimental and analytical studies were carried out to investigate the behaviour of reinforced masonry columns under sustained load. The experimental program consisted of testing ten pairs of 150 x 200 x 400 mm two-core reinforced masonry columns. Variables considered in the in the experimental program were the percentage and size of the vertical reinforcement and whether or not the columns were to be subjected to a sustained load before application of a load to failure. The experimental program also included creep and strength testing of the constituent materials. A one-dimensional theoretical analysis was developed to explain and predict the distribution of stresses in the constituent materials under axial load. The model also accounted for the stress redistribution between the constituent materials as a result of time-dependent deformations due to creep and shrinkage. A more comprehensive model that considered the state of stress in three-dimensions was also developed to confirm the validity of the simpler one-dimensional model.

After completing the construction and instrumentation of the columns, testing began with the preloading of one column out of each pair. The level of preload represented about 45% of the masonry prism strength. Both the preloaded and non-preloaded control specimens were stored in a relatively controlled environment for the same period of time. Column and reinforcement strains were monitored throughout the preload period. The load applied to the preloaded column was constantly monitored. After about one year, each column was then loaded to failure. The column strain was measured to a load level that was considered safe for manual reading for each individual column. The column load and reinforcement strain were monitored until failure.

The failure of the column was probably initiated by the crushing of the masonry units. However, the type of failure was identified on the basis of post failure observations. The failure of the preloaded columns was characterized by vertical cracks on all faces which were located around the failure zone. The failure culminated in 45° shear planes accompanied by buckling of the reinforcement bars and spalling of the block face shell. In most cases the failure occurred near the top of the preloaded columns. The non-preloaded columns generally experienced shorter vertical cracks than those in preloaded columns. The non-preloaded columns with lower percentage of steel failed at the top of the column due to crushing of the block and grout. The non-preloaded columns with larger steel areas failed near the middle of the column and exhibited long cracks and post failure buckling of the steel bars.

The one-dimensional analytical method was used to predict the time-dependent deformation of the preloaded column, the load-strain behaviour and the ultimate strength of both the preloaded and non-preloaded columns. The validity of the model was also checked against the more comprehensive three-dimensional model. Although, there were many variables involved in the experimental program and a lack of some experimental data related to the properties of the materials, the model was able to predict, reasonably well, the experimental results.

8.2 Conclusions

The following conclusions are derived from both the experimental and the analytical investigations

1. Creep and shrinkage of the masonry unit, grout and mortar resulted in a time-dependent deformation in addition to the instantaneous strain under load. The rate of the time-dependent deformation was highest in the early stages where the creep and shrinkage have their greatest influence.

2. The time-dependent deformation was significantly affected by the reinforcement percentage rather than the size of the steel bars when other variables were kept the same.

3. The time-dependent deformation caused a redistribution of stress between the constituent materials. Load was transferred from the cementitious materials to the steel reinforcement throughout the preload period. The rate of the load transfer was higher at the early stages where the creep and shrinkage have their greatest effect.

4. Poor grout workability resulted in incomplete grouting of some columns. This resulted in a large decrease in the ultimate strength, emphasizing the importance of quality control and workmanship.

5. The analytical models reasonably predicted the experimental results and provided reasonable estimates of the ultimate load of the columns. The models can be improved through more experimental data and more representative materials properties.

6. The theory indicates that the sustained load may favourably decrease the adverse effect of the shrinkage by reducing the load imposed on the masonry unit and therefore may increase the capacity of the masonry column. This was not very evident in the specimens tested in this investigation since the grout used was of low workability, and therefore subject to less shrinkage, than that used in normal masonry construction, and also because of the age of the column at the initial loading.

8.3 Recommendations

1. Testing of more specimens is essential to further enhance the understanding of the behavior under sustained load and to improve the analytical model.

2. Improvement in the sustained loading apparatus is important in order to have better control over the level of initial preload and to keep the load constant throughout the preload period. This will eliminate a variable preload and will allow for a more direct analysis. The control over the preload can be accomplished by the use of electrical strain gauges rather than the mechanical gauges that were used to monitor the strain in the Dywidag bars and eventually the preload values.

3. The limitation imposed by the capacity of the testing machine dictated the use of a smaller size masonry unit. The size of the units together with the less workable grout resulted in poor grouting that led to premature failure of some of the columns. Better control over the material used is essential to the success of an experimental investigation.

4. In order to better understand the behavior and to improve the analytical method, the strain in the column should be monitored up to failure to determine the complete stress-strain behavior of the column. This would have to be done using electrical resistance strain gauges.

5. The behavior of slender columns under sustained load should be investigated.

6. Further analytical studies should be carried out to include other variables and to modify the analysis through the application of new experimental data as it becomes available.

8.4 Closure

The major purpose of any research is to increase knowledge and understanding of the subject. The research reported in this thesis had as its main goal an investigation into an understanding of the fundamental response of reinforced masonry to loading. Since structural masonry elements in buildings are normally subjected to sustained load,

the research also included a consideration of the time-dependent shrinkage and creep properties of the component materials. A simpler one-dimensional analytical model has been developed to predict behaviour under axial load, and the efficacy of this model has been borne out by a three-dimensional analysis, and to some extent by an experimental investigation. More experimental work into the physical properties of the materials, and into the structural response of the masonry columns to load is required.

REFERENCES

1. Feeg, C., Longworth, J., and Warwaruk, J. "*Effects of Reinforcement Detailing for Concrete Masonry Columns.*" Structural Engineering Report No. 76, Civil Engineering Department, University of Alberta, Edmonton, Alberta, 1979.

2. Hatzinikolas, M., Longworth, J., and Warwaruk, J. "*Concrete Masonry Walls.*" Structural Engineering Report No. 70, Civil Engineering Department, University of Alberta, Edmonton, Alberta, 1978.

3. Sturgeon, G. R., Longworth, J., and Warwaruk, J. "*An Investigation of Reinforced Concrete Block Masonry Columns.*" Structural Engineering Report No. 91, Civil Engineering Department, University of Alberta, Edmonton, Alberta, 1980.

4. Roy, K. G., "*An Investigation Into The behavior and Ultimate Strength of Reinforced Masonry Columns Under Sustained Loading.*"M.Sc. Thesis, Civil Engineering Department, University of Manitoba, Winnipeg, Manitoba, 1986.

5. Troxell, G. E., Raphael, J. M., and Davis, R. E., "*Long-Time Creep and Shrinkage Tests of Plain and Reinforced Concrete.*" Proceedings, ASTM, Vol. 1958, PP. 1101-1120.

6. Holm, T. A., and Pistrang, J., "*Time-Dependent Load Transfer in Reinforced Lightweight Concrete Columns.*" Journal of the American Concrete Institute, Vol. 63, No. 11, Nov. 1966, PP. 1231-1246.

7. Peabody, D., Jr., "*Reinforced Concrete Structures.*" John Wiley and Sons, Inc., New York, 1946 pp. 186-188, 196-198.

8. Pfeifer, D. W., "*Reinforced Lightweight Concrete Columns.*" Proceedings ASCE, Journal of the Structural Division, Vol. 95, ST1, Jan. 1969, PP. 57-82.

9. Balaguru, P., and Nawy, E. G., "*Evaluation of Creep Strain and Stress Redistribution in Reinforced Concrete Columns.*" ACI Special Publication SP-76, American Concrete Institute, Detroit, 1982, PP.309-324.

10. CEB-FIP, "*International Recommendations for the Design and Construction of Concrete Structures.*" Cement and Concrete Association, London, England, 1970, PP. 80.

11. Jordaan, I. J., England, G. L., and Khalifa, M. A., "*Creep of Concrete : A Consistent Engineering Approach.*" Journal of the Structural Division, ASCE, Vol. 103, No. ST3, Proc. Paper 12771, March 1977, PP. 475-491.

12. *CSA* Standard *CSA-A179M-1976* "*Mortar and Grout for Unit Masonry.*" Published June 1976 by The Canadian Standard Association, Rexdale, Ontario, Canada.

13. *CSA* Standard *CAN3-A5-M83* "*Portland Cement.*" Published May 1983 by The Canadian Standard Association, Rexdale, Ontario, Canada.

14. Maurenbrecher, A. H. P., "*Use of the Prism Test to Determine Compressive Strength of Masonry.*" Third North American Masonry Conference, University of Colorado, Aug., 1978.

15. Maurenbrecher, A. H. P., "*Effect of Test Procedures on Compressive Strength of Masonry Prisms.*" Second Canadian Masonry Symposium, Carleton University, Ottawa, Ontario, June, 1980.

16. Glanville, J. I., and Hatzinikolas, M. A., "*Engineered Masonry Design.*" Winston House, Winnipeg, Manitoba, 1989.

17. Schneider, R. R., and Dickey, W. L., "*Reinforced Masonry Design.*" Prentice-Hall, INC., Englewood Cliffs, New Jersey, 1987.

18. 1985 Annual Book of *ASTM* Standards. "*Standard Method of sampling and Testing. Concrete Masonry Unit.*" Section 4 Construction , Volume 04.05 Chemical-Resistance Materials; Vitrified Clay, Concrete, Fibre-Cement Products; Mortar; Masonry, Designation C140-75 (re-approved 1980), PP. 116-119.

19. 1984 Annual Book of *ASTM* Standards. "*Standard Test Method for Compressive Strength of Cylindrical Concrete Specimens.*" Section 4 Construction , Volume 04.02 Concrete and Mineral Aggregates, Designation C39-83b, PP. 24-29.

20. *CSA* Standard *CAN3-S304-M84* "*Masonry Design for Building.*" Published November 1984 by The Canadian Standards Association, Rexdale, Ontario, Canada.

21. *CSA* Standard *G30.12-M1977* "*Billet-Steel Bars for Concrete Reinforcement.*" Published February 1977 by The Canadian Standards Association, Rexdale, Ontario, Canada.

22. Hilsdorf, H. K., "*Investigation Into the Failure Mechanism of Brick Masonry Loaded in Axial Compression.*" International Conference On masonry Structural System, University of Texas, Austin, 1967, PP. 34-41

23. Hognestad, E., "*A Study of Combined Bending and Axial Load in Reinforced Concrete Members.*" Bulletin No. 399, Engineering Experimental Station, University of Illinois, Urbana, November 1951, 128 PP.

24. Smith, G. M., and Young, L. E., "*Ultimate Theory in Flexure by Exponential Function.*" ACI Journal, Proceedings V. 52, No. 3, Nov. 1955, PP. 349-360

25. Desayi, P., and Krishnan, S., "*Equation for the Stress-Strain Curve of Concrete.*" ACI Journal, Proceedings V.61, No. 3, Mar. 1964, PP. 345-350

26. Wang, P. T., Shah, S. P., and Naaman, A. E., "*Stress-Strain Curves of Normal and Lightweight Concrete in Compression.*" ACI Journal, Proceedings V.75, No. 62, Nov. 1978, PP. 603-611.

27. Manuel, R. f., "*The Behavior of Restrained Reinforced Concrete Columns Under Sustained Load.*" PhD Dissertation, University of Alberta, Edmonton, Alberta, Jan. 1966, 187 PP.

28. Manuel, R. F., and MacGregor, J. G., "*Analysis of Restrained Reinforced Concrete Columns under sustained load.*" ACI Journal, Proceedings V. 64, No. 2, Jan. 1967, PP. 12-23.

29. Ugural, A. C., and Fenster, S. K., "*Advanced Strength and Applied Elasticity.*" Elsevier, New York, 1981.

30. Cheema, T. S., "*Anchorage Behavior and Prism Strength of Grouted Concrete Masonry.*" PhD Thesis, University of Texas, Austin, Texas, 1981, 537 PP.

31. Hamid, A. A., "*Behavior Characteristics of Concrete Masonry.*" PhD Thesis, McMaster University, Hamilton, Ontario, 1978.

32. Richart, F. E., Brandtzaeg, A., and Brown, R. L., "*A Study of The Failure of Concrete Under Combined Compressive Stresses.*" Bulletin No. 185, Engineering Experimental Station, University of Illinois, Urbana, November 1928, 102 PP.

33. Wright, J., "*Determining Drying Shrinkage of Concrete Block and its Application in the CSA Standard.*" B.Sc. Thesis, University of Manitoba, Winnipeg, Manitoba, 1990.

34. ACI Committee 209, "*Prediction of Creep, shrinkage and Temperature Effects in Concrete Structure,*" *Designing for the Effects of Creep, Shrinkage and Temperature in Concrete Structures*, **SP-27**, American Concrete Institute, Detroit, 1971, PP.51-93.

APPENDIX A

Variation of Column Load During Preload Period

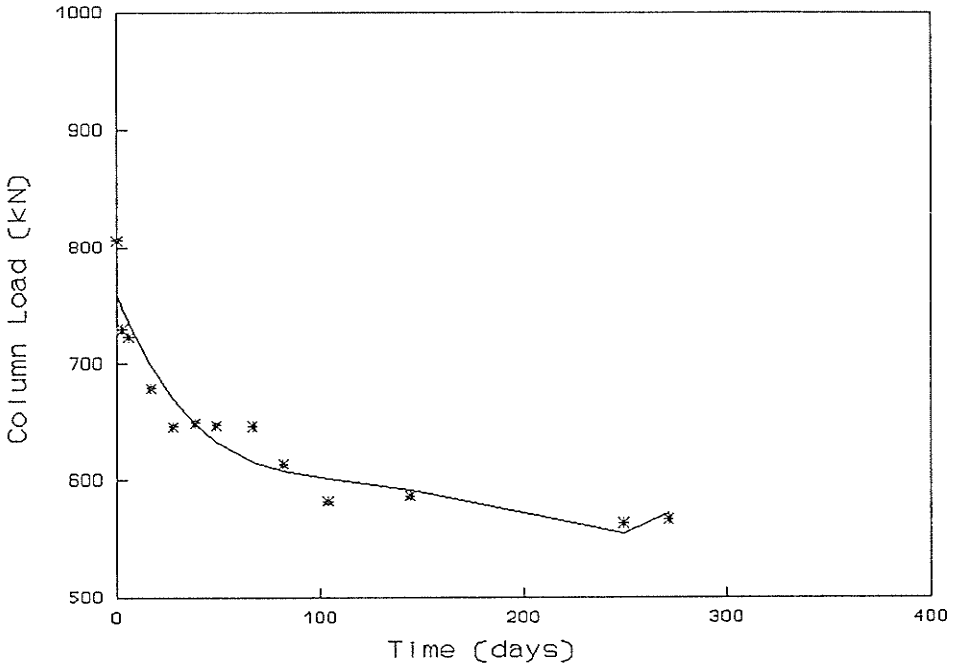

Figure A.1 Variation of column load during preload period (Preload columns CP1L)

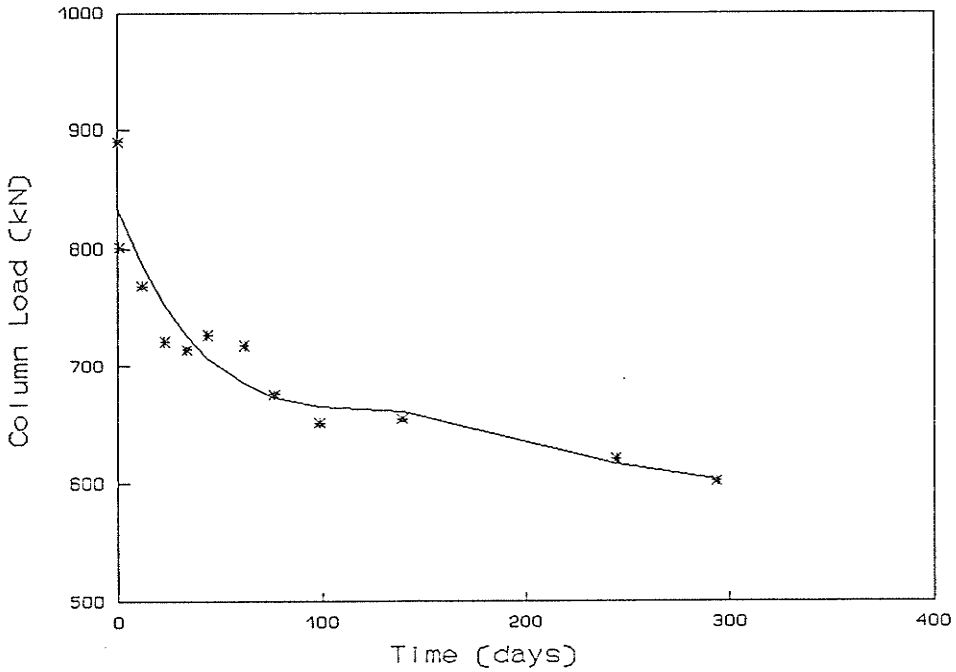

Figure A.2 Variation of column load during preload period (Preload columns CP2L)

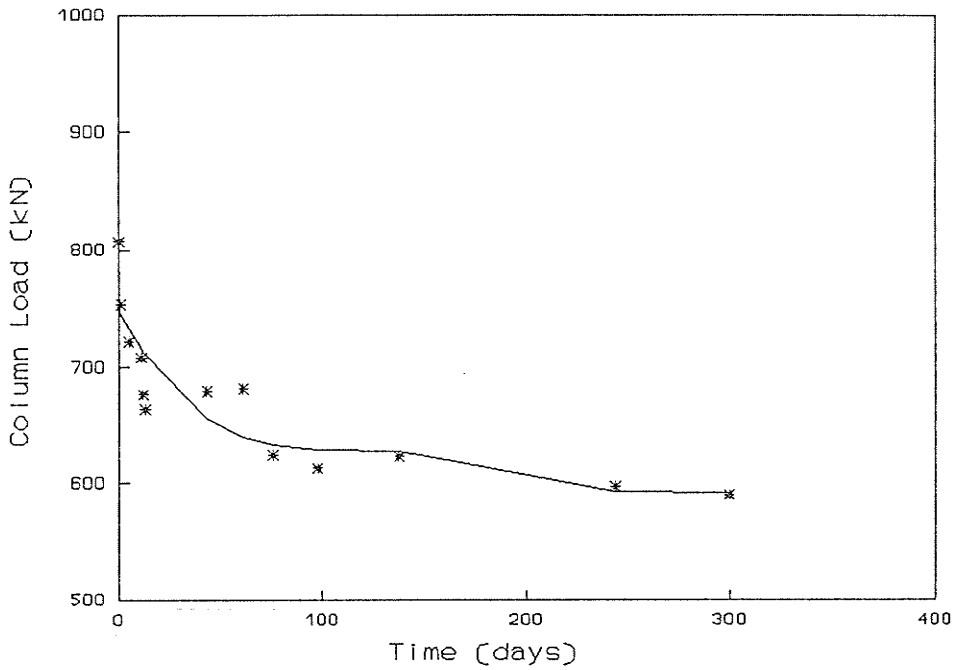

Figure A.3 Variation of column load during preload period (Preload columns CP3L)

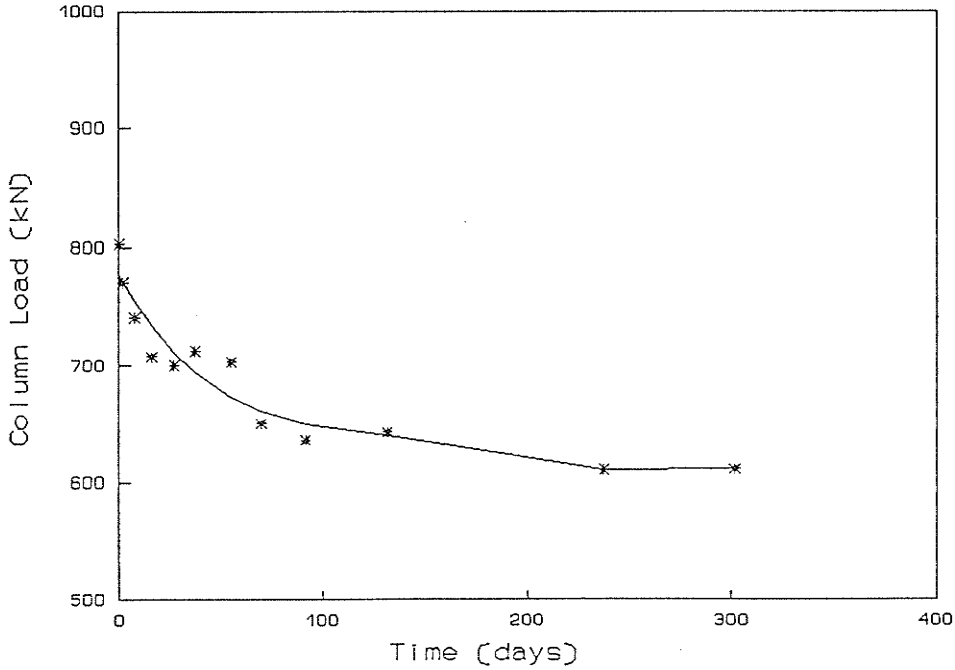

Figure A.4 Variation of column load during preload period (Preload columns CP4L)

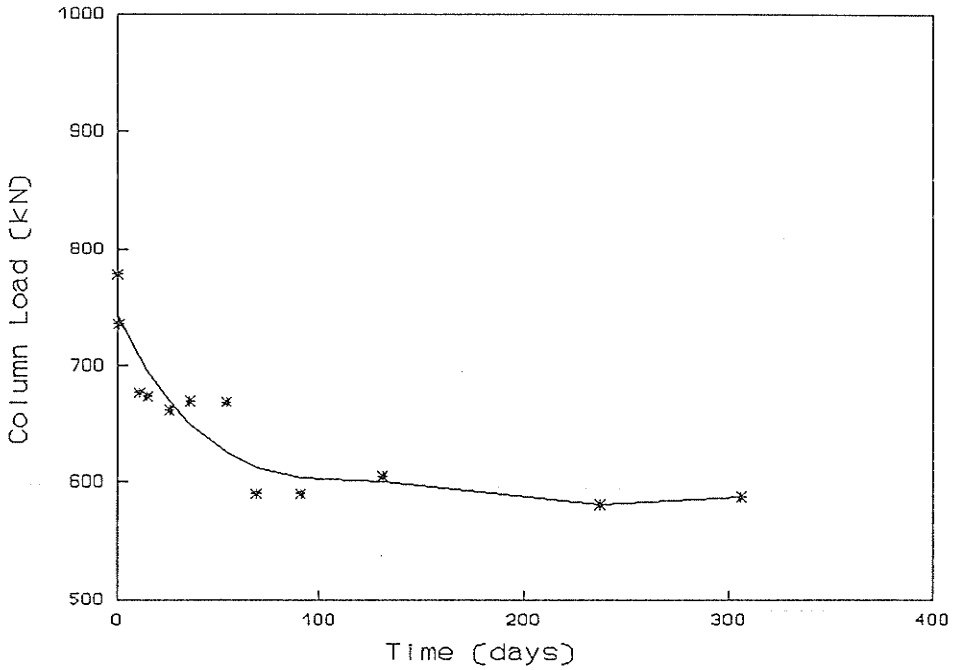

Figure A.5 Variation of column load during preload period (Preload columns CP5L)

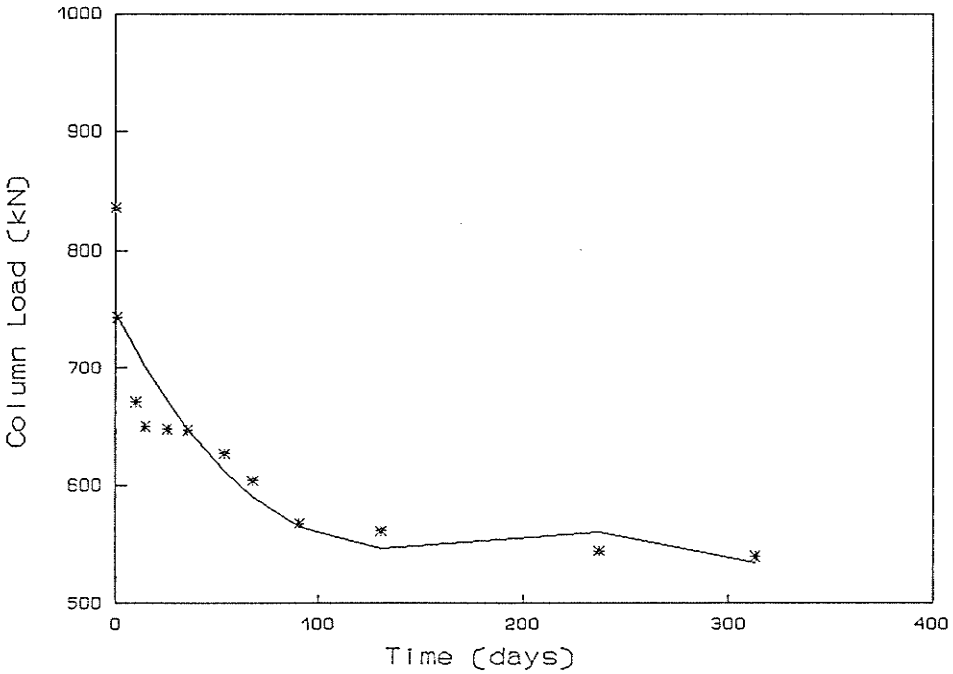

Figure A.6 Variation of column load during preload period (Preload columns CP6L)

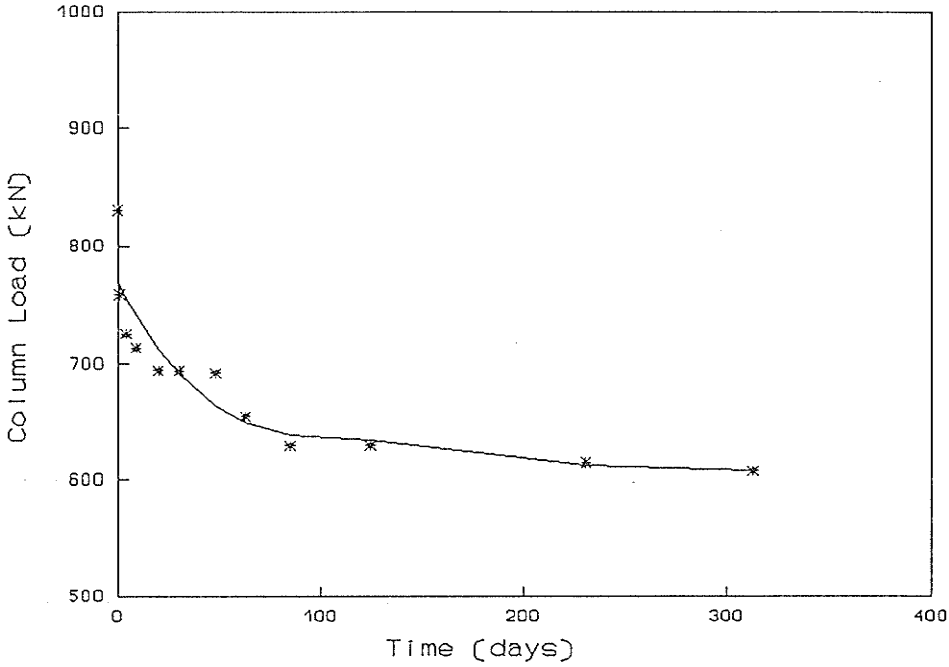

Figure A.7 Variation of column load during preload period (Preload columns CP7L)

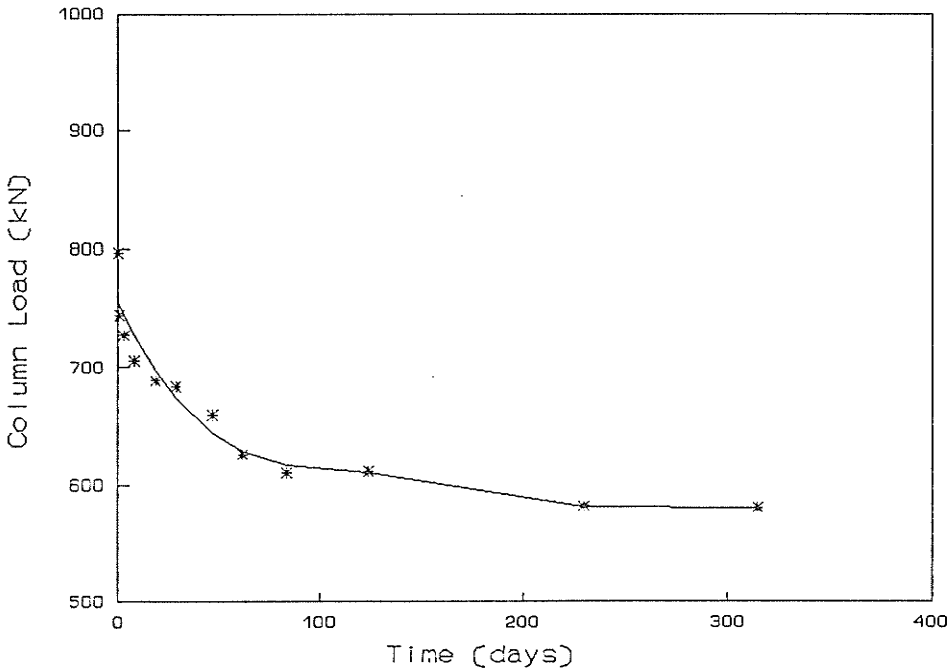

Figure A.8 Variation of column load during preload period (Preload columns CP8L)

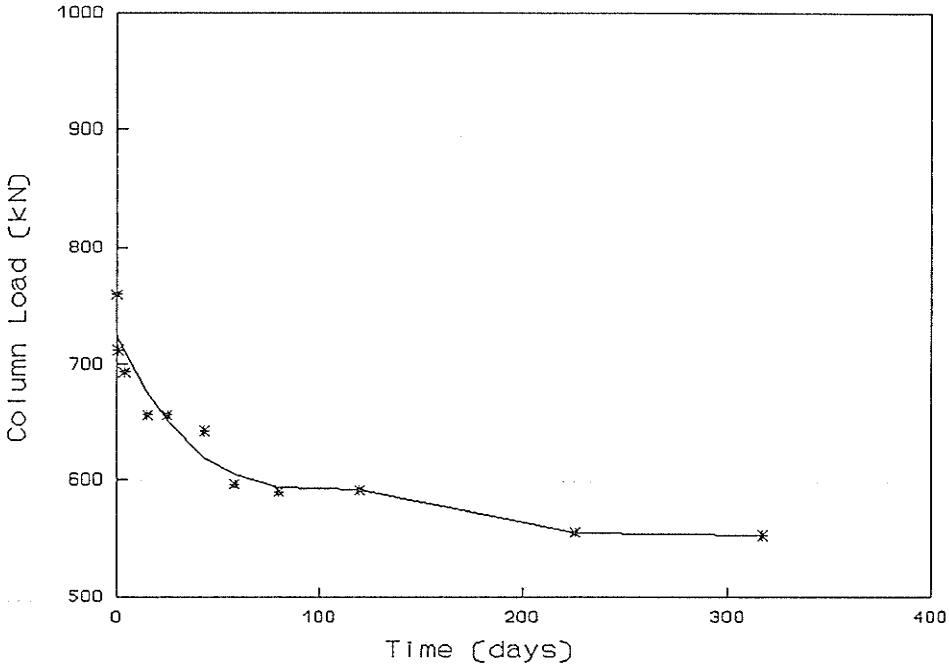

Figure A.9 Variation of column load during preload period (Preload columns CP9L)

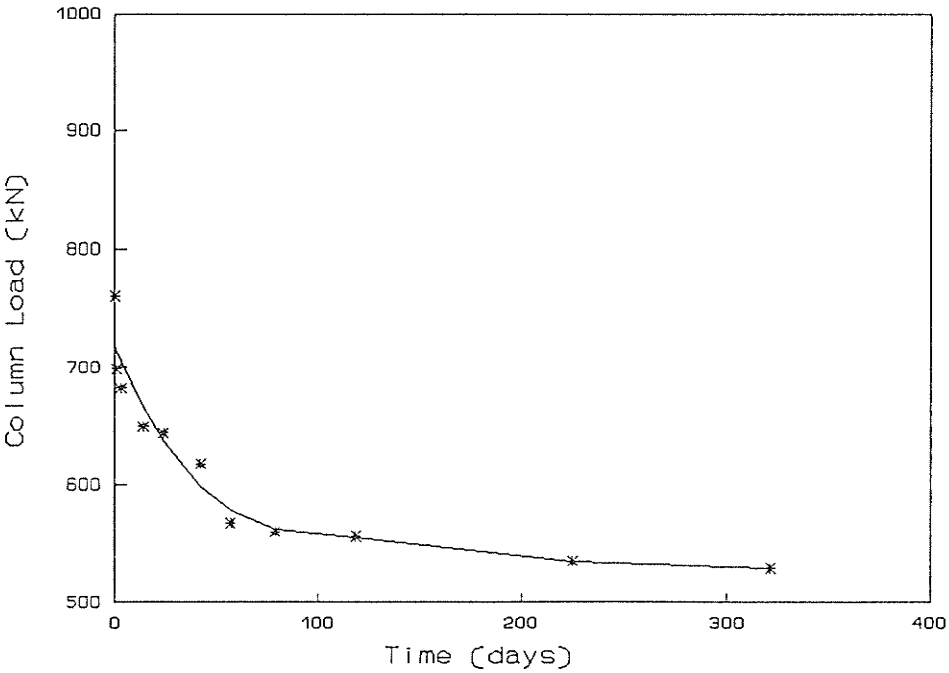

Figure A.10 Variation of column load during preload period (Preload columns CP10L)

APPENDIX B

Listing of the Programs (One-Dimensional Analysis)

```
10  ' SHRINKAGE ANALYSIS OF MASONRY COLUMN
20 CLS
30 LOCATE 1,25
40 PRINT "SHRINKAGE ANALYSIS OF MASONRY COLUMN"
50 LOCATE 5
60 INPUT "STEEL AREA    (mm^2)                          ",AST
70 INPUT "YIELD STRENGTH OF STEEL (MPa)                ",FY
80 INPUT "UNIT STRENGTH                (MPa)           ",FBO
90 INPUT "GROUT STRENGTH               (MPa)           ",FGO
100 INPUT "BLOCK MAX. STRAIN                           ",EBO
110 INPUT "GROUT MAX. STRAIN                           ",EGO
120 INPUT "BLOCK PROPERTIES COEFF. KB=kbkckdke    ",KB
130 INPUT "GROUT PROPERTIES COEFF. KG=kbkckdke    ",KG
140 INPUT "ULTIMATE SHRINKAGE STRAIN - BLOCK      ",ESBU
150 INPUT "ULTIMATE SHRINKAGE STRAIN - GROUT      ",ESGU
160 INPUT "AGE OF COLUMN AT LOADING     (days)    ",AGE
170 INPUT "RESULT FILE NAME                          ",F$
180 INPUT "IS THIS CORRECT (y/n)                     ",A$
190 IF A$="N" OR A$="n" GOTO 20
200 FILE1$="b:"+F$+".PRN"
210 OPEN FILE1$ FOR OUTPUT AS #1
220 DIM E(1000),FS(1000),FB(1000),FG(1000),P(1000),PA(1000),PS(1000),PB(1000),PG(1000)
230 AB=31700!
240 AG=22900!
250 ES=200000!
260 EB=2*FBO/EBO
270 EG=2*FGO/EGO
280 ESB=ESBU*(1-2.7183^(-.067*(AGE^.5)))
290 ESG=ESGU*(1-2.7183^(-.067*(AGE^.5)))
300 J=0
310 PA(1)=700
320 GOTO 340
330 PA(J+1)=PA(J)+10
340 J=J+1
341 K=1
342 R=.01
343 FOR I=1 TO 1000
344 E(J)=E(J)+R*((PA(J)*1000/(ES*AST))-(EB*AB*(K-ESB)/(ES*AST*(1+((K-ESB)/EBO)^2)))-(EG*AG
ES*AST*(1+((K-ESG)/EGO)^2)))-E(J))
345 IF ABS((E(J)-K)/K)*100 <=.001 GOTO 350
346 K=E(J)
347 NEXT I
348 PRINT "NO CONVERGENCE EI"
349 END
350 PRINT E(J)
351 FS(J)=E(J)*ES
360 IF FS(J)<FY GOTO 380
370 FS(J)=FY
380 FB(J)=(EB*(E(J)-ESB))/(1+((E(J)-ESB)/EBO)^2)
410 FG(J)=(EG*(E(J)-ESG))/(1+((E(J)-ESG)/EGO)^2)
440 PS(J)=(FS(J)*AST)/1000
450 PB(J)=(FB(J)*AB)/1000
460 PG(J)=(FG(J)*AG)/1000
470 P(J)=PS(J)+PB(J)+PG(J)
480 IF E(J)>(ESB+EBO) GOTO 510
490 IF E(J)>(ESG+EGO) GOTO 540
```

```
500 GOTO 330
510 KEY OFF:CLS:SCREEN 2,0
520 PRINT "BLOCK FAILS AT P(J)=   ",P(J)
530 GOTO 560
540 KEY OFF:CLS:SCREEN 2,0
550 PRINT "GROUT FAILS AT P(J)=   ",P(J)
560 I=J
570 J=0
580 J=J+1
590 WRITE #1,E(J),P(J),PS(J),PB(J),PG(J),PA(J)
600 IF J=I GOTO 620
610 GOTO 580
620 CLOSE #1
630 X=E(J)+.0005:Y=P(J)+100
640   VIEW (200,0)-(639,190):WINDOW (0,0) - (X,Y)
650 LINE (0,0) - (0,Y)
660 LINE (0,0) - (X,0)
670 X=E(1):Y=P(1)
680 LINE (0,0) - (X,Y)
690 I=0
700 I=I+1
710 X=E(I):Y=P(I)
720 LINE - (X,Y)
730 IF I=J GOTO 750
740 GOTO 700
750 X=E(1):Y=PS(1)
760 LINE (0,0) - (X,Y)
770 I=0
780 I=I+1
790 X=E(I):Y=PS(I)
800 LINE - (X,Y)
810 IF I=J GOTO 830
820 GOTO 780
830 X=E(I):Y=PB(1)
840 LINE (0,0) - (X,Y)
850 I=0
860 I=I+1
870 X=E(I):Y=PB(I)
880 LINE - (X,Y)
890 IF I=J GOTO 910
900 GOTO 860
910 X=E(1):Y=PG(1)
920 LINE (0,0) - (X,Y)
930 I=0
940 I=I+1
950 X=E(I):Y=PG(I)
960 LINE - (X,Y)
970 IF I=J GOTO 990
980 GOTO 940
990 END
```

```
10   ' SHRINKAGE AND CREEP ANALYSIS OF MASONRY COL.
20 CLS
30 LOCATE 1,25
40 PRINT "SHRINKAGE AND CREEP ANALYSIS"
50 LOCATE 5
60 INPUT "STEEL AREA                        (mm^2)      ",AST
70 INPUT "YIELD STRENGTH OF STEEL    (MPa)       ",FY
80 INPUT "UNIT STRENGTH                      (MPa)       ",FBO
90 INPUT "GROUT STRENGTH                     (MPa)       ",FGO
100 INPUT "BLOCK MAX. STRAIN                              ",EBO
110 INPUT "GROUT MAX. STRAIN                              ",EGO
120 INPUT "BLOCK PROPERTIES COEFF.KB=kbkckdke ",KB
130 INPUT "GROUT PROPERTIES COEFF.KG=kbkckdke ",KG
140 INPUT "ULTIMATE SHRINKAGE STRAIN - BLOCK   ",ESBU
150 INPUT "ULTIMATE SHRINKAGE STRAIN -GROUT    ",ESGU
160 INPUT "AGE OF COLUMN AT LOADING (days)     ",AGE
170 INPUT "SUSTAINED LOAD                  (KN)        ",PSUS
180 INPUT "PRELOAD DURATION                (days)      ",TIME
190 INPUT "RESULT FILE NAME                              ",F$
200 INPUT "IS THIS CORRECT (y/n)                        ",A$
210 IF A$="N" OR A$="n" GOTO 20
220 FILE1$="b:"+F$+".PRN"
230 OPEN FILE1$ FOR OUTPUT AS #1
235 FILE2$="A:"+F$+".PRN"
236 OPEN FILE2$ FOR OUTPUT AS #2
240 DIM E(500),FS(500),FB(500),FG(500),P(500),PS(500),PB(500),PG(500)
250 AB=31700!
260 AG=22900!
270 ES=200000!
280 EB=2*FBO/EBO
290 EG=2*FGO/EGO
300 ESB=ESBU*(1-2.7183^(-.067*(AGE^.5)))
310 ESG=ESGU*(1-2.7183^(-.067*(AGE^.5)))
320 K=1
330 R=.01
340 FOR I=1 TO 1000
350 EI=EI+R*((PSUS*1000/(ES*AST))-(EB*AB*(K-ESB)/(ES*AST*(1+((K-ESB)/EBO)^2)))-(      EG*AG*(K-
/(ES*AST*(1+((K-ESG)/EGO)^2)))-EI)
360 IF ABS((EI-K)/K)*100 <=.001 GOTO 410
370 K=EI
380 NEXT I
390 PRINT "NO CONVERGENCE EI"
400 END
410 WRITE #2,T,EI
420 J=0
430 E(1)=0
440 GOTO 460
450 E(J+1)=E(J)+(EI/100)
460 J=J+1
470 IF E(J)>EI GOTO 640
480 FS(J)=E(J)*ES
490 IF FS(J)<FY GOTO 510
500 FS(J)=FY
510 FB(J)=(EB*(E(J)-ESB))/(1+((E(J)-ESB)/EBO)^2)
520 IF FB(J)>0 GOTO 540
```

```
530 FB(J)=0
540 FG(J)=(EG*(E(J)-ESG))/(1+((E(J)-ESG)/EGO)^2)
550 IF FG(J)>0 GOTO 570
560 FG(J)=0
570 PS(J)=(FS(J)*AST)/1000
580 PB(J)=(FB(J)*AB)/1000
590 PG(J)=(FG(J)*AG)/1000
600 P(J)=PS(J)+PB(J)+PG(J)
610 IF E(J)>(ESB+EBO) GOTO 1130
620 IF E(J)>(ESG+EGO) GOTO 1160
630 GOTO 450
640 E(J)=EI
641 FS(J)=ES*E(J)
642 IF FS(J)<FY GOTO 644
643 FS(J)=FY
644 FB(J)=(EB*(E(J)-ESB))/(1+((E(J)-ESB)/EBO)^2)
645 FG(J)=(EG*(E(J)-ESG))/(1+((E(J)-ESG)/EGO)^2)
646 PS(J)=(FS(J)*AST)/1000
647 PB(J)=(FB(J)*AB)/1000
648 PG(J)=(FG(J)*AG)/1000
649 P(J)=PS(J)+PB(J)+PG(J)
650 J=J+1
651 T=T+TIME/60
660 ESBT=ESBU*(1-2.7183^(-.067*((AGE+T)^.5)))-ESB
670 ESGT=ESGU*(1-2.7183^(-.067*((AGE+T)^.5)))-ESG
680 CB=KB*(1-2.7183^(-.08753*(T^.5)))
690 CG=KG*(1-2.7183^(-.08753*(T^.5)))
700 LCC=1
710 R=.01
720 FOR I=1 TO 1000
721 EEB=(EI+LCC-ESB-ESBT)/(1+CB)
722 FEB=(EB*EEB)/(1+(EEB/EBO)^2)
723 V=(FEB*AB)/(ES*AST)
724 EEG=(EI+LCC-ESG-ESGT)/(1+CG)
725 FEG=(EG*EEG)/(1+(EEG/EGO)^2)
726 W=(FEG*AG)/(ES*AST)
730 EC=EC+R*(((PSUS*1000/(ES*AST))-EI-V-W)-EC)
740 IF ABS((EC-LCC)/LCC)*100 <=.001 GOTO 781
750 LCC=EC
760 NEXT I
770 PRINT "NO CONVERGENCE 730"
780 END
781 TDS=EI+EC
782 WRITE #2,T,TDS
790 E(J)=EI+EC
800 FS(J)=E(J)*ES
810 IF FS(J)<FY GOTO 840
820 FS(J)=FY
830 ES=FY/E(J)
840 EEB=(E(J)-ESB-ESBT)/(1+CB)
850 ECB=EEB*CB
860 EEG=(E(J)-ESG-ESGT)/(1+CG)
870 ECG=EEG*CG
880 FB(J)=(EB*EEB)/(1+(EEB/EBO)^2)
890 FG(J)=(EG*EEG)/(1+(EEG/EGO)^2)
```

```
900 PS(J)=(AST*FS(J))/1000
910 PB(J)=(AB*FB(J))/1000
920 PG(J)=(AG*FG(J))/1000
930 P(J)=PS(J)+PB(J)+PG(J)
940 IF E(J)>(ESB+EBO+ECB+ESBT) GOTO 1130
950 IF E(J)>(ESG+EGO+ECG+ESGT) GOTO 1160
951 J=J+1
960 IF T>=TIME THEN GOTO 970 ELSE GOTO 651
970 J=J-1
975 E(J)=EI+EC
980 GOTO 1010
990 E(J+1)=E(J)+.00001
1000 J=J+1
1010 FS(J)=E(J)*ES
1020 IF FS(J)<FY GOTO 1040
1030 FS(J)=FY
1040 FB(J)=EB*(E(J)-ECB-ESB-ESBT)/(1+(((E(J)-ECB-ESB-ESBT)/EBO)^2))
1050 FG(J)=EG*(E(J)-ECG-ESG-ESGT)/(1+(((E(J)-ECG-ESG-ESGT)/EGO)^2))
1060 PS(J)=(FS(J)*AST)/1000
1070 PB(J)=(FB(J)*AB)/1000
1080 PG(J)=(FG(J)*AG)/1000
1090 P(J)=PS(J)+PB(J)+PG(J)
1100 IF E(J)>(ESB+EBO+ECB+ESBT) GOTO 1130
1110 IF E(J)>(ESG+EGO+ECG+ESGT) GOTO 1160
1120 GOTO 990
1130 KEY OFF:CLS:SCREEN 2,0
1140 PRINT "BLOCK FAILS AT   P(J)=          ",P(J)
1150 GOTO 1180
1160 KEY OFF:CLS:SCREEN 2,0
1170 PRINT "GROUT FAILS AT   P(J)=          ",P(J)
1180 I=J
1190 J=0
1200 J=J+1
1210 WRITE #1,E(J),P(J),PS(J),PB(J),PG(J)
1220 IF J=I GOTO 1240
1230 GOTO 1200
1240 CLOSE #1
1260 X=E(J)+.0005:Y=P(J)+100
1270  VIEW (200,0)-(639,190):WINDOW (0,0) - (X,Y)
1280 LINE (0,0) - (0,Y)
1290 LINE (0,0) - (X,0)
1300 X=E(1):Y=P(1)
1310 LINE (0,0) - (X,Y)
1320 I=0
1330 I=I+1
1340 X=E(I):Y=P(I)
1350 LINE - (X,Y)
1360 IF I=J GOTO 1380
1370 GOTO 1330
1380 X=E(1):Y=PS(1)
1390 LINE (0,0) - (X,Y)
1400 I=0
1410 I=I+1
1420 X=E(I):Y=PS(I)
1430 LINE - (X,Y)
```

```
1440 IF I=J GOTO 1460
1450 GOTO 1410
1460 X=E(I):Y=PB(1)
1470 LINE (0,0) - (X,Y)
1480 I=0
1490 I=I+1
1500 X=E(I):Y=PB(I)
1510 LINE - (X,Y)
1520 IF I=J GOTO 1540
1530 GOTO 1490
1540 X=E(1):Y=PG(1)
1550 LINE (0,0) - (X,Y)
1560 I=0
1570 I=I+1
1580 X=E(I):Y=PG(I)
1590 LINE - (X,Y)
1600 IF I=J GOTO 1620
1610 GOTO 1570
1620 END
```

APPENDIX C

Listing of the Programs (Three-Dimensional Analysis)

```
10 !3-D NON-LINEAR ANALYSIS OF MASONRY COLUMN:SHRINKAGE
20 CLEAR
25 SET COLOR "WHITE"
26 SET BACK "BLUE"
30 PRINT "3-D NON-LINEAR ANALYSIS OF MASONRY COLUMN:SHRINKAGE"
50 INPUT PROMPT"STEEL AREA    (mm^2)                          ?": AS
60 INPUT PROMPT"YIELD STRENGTH OF STEEL (MPa)                ?": FY
80 INPUT PROMPT"MASONRY UNIT STRENGTH     (MPa)              ?": FBO
90 INPUT PROMPT"GROUT STRENGTH            (MPa)              ?": FGO
95 INPUT PROMPT"MORTAR STRENGTH           (MPa)              ?": FMO
120 INPUT PROMPT"BLOCK PROPERTIES COEFF. KB=kb*kc*kd*ke   ?": KB
130 INPUT PROMPT"GROUT PROPERTIES COEFF. KG=kb*kc*kd*ke   ?": KG
135 INPUT PROMPT"MORTAR PROPERTIES COEFF.KM=Kb*kc*Kd*Ke   ?": KM
140 INPUT PROMPT"ULTIMATE SHRINKAGE STRAIN - BLOCK          ?": ESBU
150 INPUT PROMPT"ULTIMATE SHRINKAGE STRAIN - GROUT          ?": ESGU
155 INPUT PROMPT"ULTIMATE SHRINKAGE STRAIN - MORTAR         ?": ESMU
156 INPUT PROMPT"POSSION'S RATIO - MASONRY UNIT             ?": Vb
157 INPUT PROMPT"POSSION'S RATIO - GROUT                    ?": Vg
158 INPUT PROMPT"POSSION'S RATIO - MORTAR                   ?": Vm
159 INPUT PROMPT"POSSION'S RATIO - REINFORCEMENT STEEL    ?": Vs
160 INPUT PROMPT"MASONRY UNIT ACTUAL THICKNESS (mm)         ?": Tb
161 INPUT PROMPT"MORTAR JOINT THICKNESS          (mm)       ?": Tm
165 INPUT PROMPT"AGE OF COLUMN AT LOADING     (days)        ?": AGE
170 INPUT PROMPT"RESULT FILE NAME                             ?": F$
180 INPUT PROMPT"IS THIS CORRECT (y/n)                      ?": A$
190 IF A$="N" OR A$="n" THEN 20
191 LET F$="A:" & F$ & ".PRN"
195 WHEN ERROR IN
200 OPEN #1:NAME F$ ,ACCESS OUTIN,CREATE NEW
201 USE
202 INPUT PROMPT "file already exists do you want to overwrite it?":A$
203 IF A$="Y" OR A$="y" THEN
204 OPEN #1:NAME F$
209 ERASE#1
210 ELSE
211 CLOSE #1
212 INPUT PROMPT "give another name for data output file":F$
213 LET F$="A:" & F$ & ".PRN"
214 OPEN#1:NAME F$,ACCESS OUTIN,CREATE NEW
216 END IF
219 END WHEN
220 DIM E(500),FYb(500),E1(500),FYm(500),FYg1(500),FYg2(500),P(500),PS(500),PB(500),PG(500)
221 DIM COEEQ(11,11),CONSEQ(11),SOLEQ(11),COEEQINV(11,11)
225 OPEN #2:PRINTER
226 LET P1=1
227 LET P2=1
228 LET P3=1
229 LET P4=1
230 LET AB=31700
235 LET AM=31700
240 LET AG=22900
250 LET ES=200000
251 LET EBO=.002
252 LET EGO=.002
253 LET EMO=.002
```

```
254 LET FTB=.417075*(FBO^.5)
255 LET FTG=.5561*(FGO^.5)
256 LET FTM=.581*(FMO^.5)
260 LET EB=2*FBO/EBO
270 LET EG=2*FGO/EGO
271 LET EM=2*FMO/EMO
280 LET ESB=ESBU*(1-2.7183^(-.067*(AGE^.5)))
290 LET ESG=ESGU*(1-2.7183^(-.067*(AGE^.5)))
291 LET ESM=ESMU*(1-2.7183^(-.067*(AGE^.5)))
292 LET a=((.1591549*AS)^.5)
293 LET b=((.1591549*AG)^.5)
294 LET c=((.1591549*(AB+AG))^.5)
295 LET d=b+((c-b)/2)
296 LET f=a+((b-a)/2)
297 LET I=2
298 LET L=1
300 LET J=0
310 LET E(1)=0
315 LET E1(1)=0
320 GOTO 335
330 LET E(J+1)=E(J)+.00001
331 LET E1(J+1)=SOLEQ(11)
335 LET J=J+1
336 LET EBt=EB
337 LET EGt1=EG
342 LET EGt2=EG
343 LET EMt=EM
344 IF E1(J)<=ESM THEN 360
345 LET EMt=EM/(1+((E1(J)-ESM)/EMO)^2)
350 IF EMt>EM/2 THEN 360
355 LET EMt=EM/2
360 IF E1(J)=<ESG THEN 370
365 LET EGt2=EG/(1+((E1(J)-ESG)/EGO)^2)
370 IF E(J)=<ESB THEN 381
380 LET EBt=EB/(1+((E(J)-ESB)/EBO)^2)
381 IF E(J)<ESG THEN 400
385 LET EGt1=EG/(1+((E(J)-ESG)/EGO)^2)
400 LET BK1=EBt/((1+Vb)*(1-2*Vb))
401 LET GK1=EGt1/((1+Vg)*(1-2*Vg))
402 LET GK2=EGt2/((1+Vg)*(1-2*Vg))
403 IF I>2 THEN 406
405 IF FYS1<FY THEN 411
406 LET EY=E(J-I)
407 LET I=I+1
408 LET ES=(EY*200000)/E(J)
409 GOTO 412
411 LET ES=200000
412 LET SK31=ES/((1+Vs)*(1-2*Vs))
415 IF L>1 THEN 424
420 IF FYS2<FY THEN 429
424 LET EY1=E1(J-L)
425 PRINT EY,FYS1,EY1,FYS2,J;L
426 LET L=L+1
427 LET ES=(EY1*200000)/E1(J)
428 GOTO 430
```

```
429 LET ES=200000
430 LET SK32=ES/((1+Vs)*(1-2*Vs))
431 LET MK4=EMt/((1+Vm)*(1-2*Vm))
432 CALL FILLCOEEQ
433 CALL FILLCONSEQ
434 MAT COEEQInv=Inv(COEEQ)
435 LET CHECK = DET(COEEQ)
436 IF ABS(CHECK) < 1 THEN
437 PRINT "ERROR DET=";CHECK
438 STOP
439 END IF
440 MAT SOLEQ=COEEQInv*CONSEQ
475 !STRESSES AT THE BLOCK LEVEL
476 !stresses in the block
477 LET FYb(J)=BK1*((1-Vb)*E(J)+2*Vb*SOLEQ(1)-ESB*(1+Vb))
480 LET FRbEDGE=BK1*(SOLEQ(1)-(SOLEQ(7)*(1-2*Vb)/(c^2))+Vb*E(J)-ESB*(1+Vb))
481 LET FRbMIDDLE=BK1*(SOLEQ(1)-(SOLEQ(7)*(1-2*Vb)/(d^2))+Vb*E(J)-ESB*(1+Vb))
482 LET FRbINSIDE=BK1*(SOLEQ(1)-(SOLEQ(7)*(1-2*Vb)/(b^2))+Vb*E(J)-ESB*(1+Vb))
486 LET FTbEDGE=BK1*(SOLEQ(1)+(SOLEQ(7)*(1-2*Vb)/(c^2))+Vb*E(J)-ESB*(1+Vb))
487 LET FTbMIDDLE=BK1*(SOLEQ(1)+(SOLEQ(7)*(1-2*Vb)/(d^2))+Vb*E(J)-ESB*(1+Vb))
488 LET FTbINSIDE=BK1*(SOLEQ(1)+(SOLEQ(7)*(1-2*Vb)/(b^2))+Vb*E(J)-ESB*(1+Vb))
490 !stresses in the grout at the block level
492 LET FYg1(J)=GK1*((1-Vg)*E(J)+2*Vg*SOLEQ(2)-ESG*(1+Vg))
496 LET FRg1EDGE=GK1*(SOLEQ(2)-(SOLEQ(8)*(1-2*Vg)/(b^2))+Vg*E(J)-ESG*(1+Vg))
497 LET FRg1MIDDLE=GK1*(SOLEQ(2)-(SOLEQ(8)*(1-2*Vg)/(f^2))+Vg*E(J)-ESG*(1+Vg))
498 LET FRg1INSIDE=GK1*(SOLEQ(2)-(SOLEQ(8)*(1-2*Vg)/(a^2))+Vg*E(J)-ESG*(1+Vg))
499 LET FTg1EDGE=GK1*(SOLEQ(2)+(SOLEQ(8)*(1-2*Vg)/(b^2))+Vg*E(J)-ESG*(1+Vg))
500 LET FTg1MIDDLE=GK1*(SOLEQ(2)+(SOLEQ(8)*(1-2*Vg)/(f^2))+Vg*E(J)-ESG*(1+Vg))
501 LET FTg1INSIDE=GK1*(SOLEQ(2)+(SOLEQ(8)*(1-2*Vg)/(a^2))+Vg*E(J)-ESG*(1+Vg))
502 !stresses in the vertical reinforcement at block level
503 LET FYs1=SK31*((1-Vs)*E(J)+2*Vs*SOLEQ(3))
504 LET FRs1=SK31*(SOLEQ(3)+Vs*E(J))
505 LET PS(J)=(AS*FYs1)/1000
506 LET PG(J)=(AG*FYg1(J))/1000
507 IF PG(J)>0 THEN 509
508 LET PG(J)=0
509 LET PB(J)=(AB*FYb(J))/1000
510 IF PB(J)>0 THEN 512
511 LET PB(J)=0
512 LET P(J)=PS(J)+PB(J)+PG(J)
513 !STRESSES AT THE MORTAR LEVEL
514 !stresses in the mortar
515 LET FYm(J)=MK4*((1-Vm)*SOLEQ(11)+2*Vm*SOLEQ(4)-ESM*(1+Vm))
516 LET FRmEDGE=MK4*(SOLEQ(4)-(SOLEQ(9)*(1-2*Vm)/(c^2))+Vm*SOLEQ(11)-ESM*(1+Vm))
517 LET FRmMIDDLE=MK4*(SOLEQ(4)-(SOLEQ(9)*(1-2*Vm)/(d^2))+Vm*SOLEQ(11)-ESM*(1+Vm))
518 LET FRmINSIDE=MK4*(SOLEQ(4)-(SOLEQ(9)*(1-2*Vm)/(b^2))+Vm*SOLEQ(11)-ESM*(1+Vm))
519 LET FTmEDGE=MK4*(SOLEQ(4)+(SOLEQ(9)*(1-2*Vm)/(c^2))+Vm*SOLEQ(11)-ESM*(1+Vm))
520 LET FTmMIDDLE=MK4*(SOLEQ(4)+(SOLEQ(9)*(1-2*Vm)/(d^2))+Vm*SOLEQ(11)-ESM*(1+Vm))
521 LET FTmINSIDE=MK4*(SOLEQ(4)+(SOLEQ(9)*(1-2*Vm)/(b^2))+Vm*SOLEQ(11)-ESM*(1+Vm))
522 !stresses in the grout at the mortar level
523 LET FYg2(J)=GK2*((1-Vg)*SOLEQ(11)+2*Vg*SOLEQ(5)-ESG*(1+Vg))
524 LET FRg2EDGE=GK2*(SOLEQ(5)-(SOLEQ(10)*(1-2*Vg)/(b^2))+Vg*SOLEQ(11)-ESG*(1+Vg))
525 LET FRg2MIDDLE=GK2*(SOLEQ(5)-(SOLEQ(10)*(1-2*Vg)/(f^2))+Vg*SOLEQ(11)-ESG*(1+Vg))
526 LET FRg2INSIDE=GK2*(SOLEQ(5)-(SOLEQ(10)*(1-2*Vg)/(a^2))+Vg*SOLEQ(11)-ESG*(1+Vg))
527 LET FTg2EDGE=GK2*(SOLEQ(5)+(SOLEQ(10)*(1-2*Vg)/(b^2))+Vg*SOLEQ(11)-ESG*(1+Vg))
```

```
528 LET FTg2MIDDLE=GK2*(SOLEQ(5)+(SOLEQ(10)*(1-2*Vg)/(f^2))+Vg*SOLEQ(11)-ESG*(1+Vg))
529 LET FTg2INSIDE=GK2*(SOLEQ(5)+(SOLEQ(10)*(1-2*Vg)/(a^2))+Vg*SOLEQ(11)-ESG*(1+Vg))
530 !stresses in the vertical reinforcement at mortar level
531 LET FYs2=SK32*((1-Vs)*SOLEQ(11)+2*Vs*SOLEQ(6))
532 LET FRs2=SK32*(SOLEQ(6)+Vs*SOLEQ(11))
533 IF FTbMIDDLE>0 THEN 540
534 IF FYb(J)<(FBO*((FTB+FTbMIDDLE)/FTB)) THEN 538
535 IF P1>1 THEN 538
536 PRINT #2: "BLOCK FAILS UNDER COMPRESSION TENSION AT P(J)=          ",P(J)
537 LET P1=2
538 IF -FTbMIDDLE=>FTB THEN 570
539 GOTO 541
540 IF FYb(J)=>FBO THEN 573
541 IF FTg1MIDDLE>0 THEN 548
542 IF FYg1(J)<FGO THEN 546
543 IF P2>1 THEN 546
544 PRINT #2: "GROUT AT BLOCK LEVEL FAILS UNDER AXIAL COMP. AT P(J)= ",P(J)
545 LET P2=2
546 IF -FTg1MIDDLE=>FTG THEN 576
547 GOTO 549
548 IF FYg1(J)=>(FGO+4.1*FTg1MIDDLE) THEN 579
549 IF FTg2MIDDLE>0 THEN 556
550 IF FYg2(J)<FGO THEN 554
551 IF P3>1 THEN 554
552 PRINT #2: "GROUT AT MORTAR LEVEL FAILS UNDER AXIAL COMP. AT P(J)=",P(J)
553 LET P3=2
554 IF -FTg2MIDDLE=>FTG THEN 582
555 GOTO 557
556 IF FYg2(J)=>(FGO+4.1*FTg2MIDDLE) THEN 585
557 IF FTmMIDDLE>0 THEN 568
558 IF FYm(J)<FMO THEN 566
559 IF P4>1 THEN 566
560 PRINT #2: "MORTAR FAILS UNDER AXIAL COMPRESSION AT P(J)=          ",P(J)
561 LET P4=2
566 IF -FTmMIDDLE=>FTM THEN 588
567 GOTO 569
568 IF FYm(J)=>(FMO+4.1*FTmMIDDLE) THEN 591
569 GOTO 330
570 CLEAR
571 PRINT #2: "BLOCK FAILS UNDER TENSION AT P(J)=                    ",P(J)
572 GOTO 596
573 CLEAR
574 PRINT #2: "BLOCK FAILS UNDER AXIAL COMPRESSION AT P(J)=          ",P(J)
575 GOTO 596
576 CLEAR
577 PRINT #2: "GROUT-BLOCK LEVEL FAILS UNDER TENSION AT P(J)=        ",P(J)
578 GOTO 596
579 CLEAR
580 PRINT #2: "GROUT-BLOCK LEVEL FAILS UNDER TRIAXIAL COMP. AT P(J)= ",P(J)
581 GOTO 596
582 CLEAR
583 PRINT #2: "GROUT-MORTAR LEVEL FAILS UNDER TENSION AT P(J)=       ",P(J)
584 GOTO 596
585 CLEAR
586 PRINT #2: "GROUT-MORTAR LEVEL FAILS UNDER TRIAXIAL COMP. AT P(J)=",P(J)
```

```
587 GOTO 596
588 CLEAR
589 PRINT #2: "MORTAR FAILS UNDER TENSION AT P(J)=                    ",P(J)
590 GOTO 596
591 CLEAR
592 PRINT #2: "MORTAR FAILS UNDER TRIAXIAL COMPRESSION AT P(J)=      ",P(J)
596 LET I=J
597 LET J=0
598 LET J=J+1
599 PRINT #1 : E(J);",";P(J);",";PS(J);",";PB(J);",";PG(J);","
600 IF J=I THEN 620
610 GOTO 598
620 CLOSE #1
630 LET X=E(J)+.0005
635 LET Y=P(J)+100
639 OPEN #1: SCREEN 0, .49, .51, 1
640 SET WINDOW 0,X,0,Y
641 BOX LINES 0,X,0,Y
645 SET COLOR "RED"
646 SET BACK "WHITE"
650 PLOT 0,0;0,Y
660 PLOT 0,0;X,0
670 LET X=E(1)
675 LET Y=P(1)
680 PLOT 0,0;X,Y
690 LET I=0
700 LET I=I+1
710 LET X=E(I)
715 LET Y=P(I)
720 PLOT X,Y
730 IF I=J THEN 750
740 GOTO 700
750 LET X=E(1)
755 LET Y=PS(1)
760 PLOT 0,0;X,Y
770 LET I=0
780 LET I=I+1
790 LET X=E(I)
795 LET Y=PS(I)
800 PLOT X,Y
810 IF I=J THEN 830
820 GOTO 780
830 LET X=E(I)
835 LET Y=PB(1)
840 PLOT 0,0;X,Y
850 LET I=0
860 LET I=I+1
870 LET X=E(I)
875 LET Y=PB(I)
880 PLOT X,Y
890 IF I=J THEN 910
900 GOTO 860
910 LET X=E(1)
915 LET Y=PG(1)
920 PLOT 0,0;X,Y
```

```
930 LET I=0
940 LET I=I+1
950 LET X=E(I)
955 LET Y=PG(I)
960 PLOT X,Y
961 IF I=J THEN 963
962 GOTO 940
963 CLOSE #1
964 OPEN #3: SCREEN .5, 1, .675, 1
965 SET WINDOW 0,c,-FRS1,FRs1
966 BOX LINES 0,c,-FRS1,FRs1
970 PRINT"     R-STRESSES AT BLOCK"
972 LET X=a
973 LET Y=ABS(FRs1)
974 PLOT LINES:X,Y;X,-Y
975 PLOT 0,Y;0,-Y
976 LET X=b
977 PLOT LINES:X,Y;X,-Y
978 LET X=c
979 PLOT LINES:X,Y;X,-Y
980 PLOT LINES:0,0;c,0
981 LET X=0
982 LET Y=FRs1
983 PLOT LINES:X,Y;
984 LET X=a
985 LET Y=FRg1INSIDE
987 PLOT LINES:X,Y;
988 LET X=b
989 LET Y=FRg1EDGE
990 PLOT LINES:X,Y;
991 LET X=c
992 LET Y=FRbEDGE
993 PLOT LINES:X,Y
994 CLOSE#3
995 OPEN #4: SCREEN 0, .49, 0, .49
997 SET WINDOW 0,c,-FRS2,FRs2
998 BOX LINES 0,c,-FRS2,FRs2
999 PRINT "     R-STRESS-AT MORTAR "
1000 LET Y=FRS2
1001 PLOT 0,-Y;0,Y
1002 PLOT LINES:a,Y;a,-Y
1003 PLOT LINES:b,Y;b,-Y
1004 PLOT LINES:c,Y;C,-Y
1010 PLOT 0,0;X,0
1011 LET X=0
1012 LET Y=FRs2
1013 PLOT LINES:0,0;X,Y;
1014 LET X=a
1015 LET Y=FRg2INSIDE
1016 PLOT LINES:X,Y;
1017 LET X=b
1018 LET Y=FRg2EDGE
1019 PLOT LINES:X,Y;
1020 LET X=c
1021 LET Y=FRmEDGE
```

```
1022 PLOT LINES:X,Y
1023 CLOSE#4
1025 OPEN #5: SCREEN .5, 1, .3375, .6625
1026 SET WINDOW 0,c,-FRs1,FRs1
1027 BOX LINES 0,c,-FRs1,FRs1
1028 PRINT "    TANG.STRESS AT BLOCK"
1029 LET X=c
1030 LET Y=FRs1
1032 PLOT 0,-Y;0,Y
1033 PLOT 0,0;X,0
1034 LET X=0
1035 LET Y=FRs1
1036 PLOT LINES:0,0;X,Y;
1037 LET X=a
1038 LET Y=FRs1
1039 PLOT LINES:X,Y;
1040 LET X=a
1041 LET Y=FTg1INSIDE
1042 PLOT LINES:X,Y;
1043 LET X=b
1044 LET Y=FTg1EDGE
1045 PLOT LINES:X,Y;
1046 LET X=b
1047 LET Y=FTbINSIDE
1048 PLOT LINES:X,Y;
1049 LET X=c
1050 LET Y=FTbEDGE
1051 PLOT LINES:X,Y
1052 CLOSE#5
1054 OPEN #6: SCREEN .5, 1, 0, .325
1056 SET WINDOW 0,c,-FRs2,FRs2
1057 BOX LINES 0,c,-FRs2,FRs2
1058 PRINT "    TANG-STRESS AT MORTAR"
1059 LET X=c
1060 LET Y=FRs2
1062 PLOT 0,-Y;0,Y
1063 PLOT 0,0;X,0
1064 LET X=0
1065 LET Y=FRs2
1066 PLOT LINES:0,0;X,Y;
1067 LET X=a
1068 LET Y=FRs2
1069 PLOT LINES:X,Y;
1070 LET X=a
1071 LET Y=FTg2INSIDE
1072 PLOT LINES:X,Y;
1073 LET X=b
1074 LET Y=FTg2EDGE
1075 PLOT LINES:X,Y;
1076 LET X=b
1077 LET Y=FTmINSIDE
1078 PLOT LINES:X,Y;
1079 LET X=c
1080 LET Y=FTmEDGE
1081 PLOT LINES:X,Y
```

```
1082 CLOSE#6
1086 GOTO 9800
1087 SUB FILLCOEEQ
1088 MAT COEEQ =ZER
1089 LET COEEQ (1,2)= GK1
1090 LET COEEQ (1,3)= -SK31
1091 LET COEEQ(1,8)= -GK1*(1-2*Vg)/(a^2)
1092 LET COEEQ(2,5)= GK2
1093 LET COEEQ(2,6)= -SK32
1094 LET COEEQ(2,10)= -GK2*(1-2*Vg)/(a^2)
1095 LET COEEQ(2,11)= (GK2*Vg)-(SK32*Vs)
1097 LET COEEQ(3,2)= 1
1098 LET COEEQ(3,3)= -1
1099 LET COEEQ(3,8)= 1/(a^2)
1100 LET COEEQ(4,5)= 1
1101 LET COEEQ(4,6)= -1
1102 LET COEEQ(4,10)= 1/(a^2)
1103 LET COEEQ(5,1)= -BK1
1104 LET COEEQ(5,2)= GK1
1105 LET COEEQ(5,7)= BK1*(1-2*Vb)/(b^2)
1106 LET COEEQ(5,8)= -GK1*(1-2*Vg)/(b^2)
1107 LET COEEQ(6,1)= -1
1108 LET COEEQ(6,2)= 1
1109 LET COEEQ(6,7)= -1/(b^2)
1110 LET COEEQ(6,8)= 1/(b^2)
1111 LET COEEQ(7,4)= -MK4
1112 LET COEEQ(7,5)= GK2
1113 LET COEEQ(7,9)= MK4*(1-2*Vm)/(b^2)
1114 LET COEEQ(7,10)= -GK2*(1-2*Vg)/(b^2)
1115 LET COEEQ(7,11)= (GK2*Vg)-(MK4*Vm)
1117 LET COEEQ(8,4)= -1
1118 LET COEEQ(8,5)= 1
1119 LET COEEQ(8,9)= -1/(b^2)
8000 LET COEEQ(8,10)= 1/(b^2)
8400 LET COEEQ(9,1)= 2*BK1*Vb*AB
8450 LET COEEQ(9,2)= 2*GK1*Vg*AG
8500 LET COEEQ(9,3)= 2*SK31*Vs*AS
8550 LET COEEQ(9,4)= -2*MK4*Vm*AM
8600 LET COEEQ(9,5)= -2*GK2*Vg*AG
8650 LET COEEQ(9,6)= -2*SK32*Vs*AS
8700 LET COEEQ(9,11)= -(MK4*AM*(1-Vm))-(GK2*AG*(1-Vg))-(SK32*AS*(1-Vs))
8750 LET COEEQ(10,1)= BK1*Tb
8800 LET COEEQ(10,4)= MK4*Tm
8850 LET COEEQ(10,7)= -BK1*Tb*(1-2*Vb)/(c^2)
8900 LET COEEQ(10,9)= -MK4*Tm*(1-2*Vm)/(c^2)
8950 LET COEEQ(10,11)= MK4*Tm*Vm
9000 LET COEEQ(11,1)= 1
9100 LET COEEQ(11,4)= -1
9110 LET COEEQ(11,7)= 1/(c^2)
9120 LET COEEQ(11,9)= -1/(c^2)
9130 END SUB
9140 SUB FILLCONSEQ
9150 LET CONSEQ(1)= ((SK31*Vs-GK1*Vg)*E(J))+(GK1*ESG*(1+Vg))
9200 LET CONSEQ(2)= GK2*ESG*(1+Vg)
9250 LET CONSEQ(3)= ESG
```

```
9300 LET CONSEQ(4)= ESG
9350 LET CONSEQ(5)= (E(J)*(BK1*Vb-GK1*Vg))+(GK1*ESG*(1+Vg))-(BK1*ESB*(1+Vb))
9400 LET CONSEQ(6)= ESG-ESB
9450 LET CONSEQ(7)= (GK2*ESG*(1+Vg))-(MK4*ESM*(1+Vm))
9500 LET CONSEQ(8)= ESG-ESM
9550 LET CONSEQ(9)= (BK1*AB*ESB*(1+Vb))-(MK4*AM*ESM*(1+Vm))-(E(J)*(BK1*AB*(1-Vb)+GK1*A
K31*AS*(1-Vs)))+(AG*GK1*ESG*(1+Vg))-(AG*GK2*ESG*(1+Vg))
9600 LET CONSEQ(10)= (MK4*Tm*ESM*(1+Vm))+(BK1*Tb*ESB*(1+Vb))-(BK1*Tb*Vb*E(J))
9650 LET CONSEQ(11)= ESB-ESM
9700 END SUB
9800 PAUSE 20
9900 END
```

```
10 !3-D NON-LINEAR ANALYSIS OF MASONRY COLUMN:SHRINKAGE AND CREEP
20 CLEAR
25 SET COLOR "WHITE"
26 SET BACK "BLUE"
30 PRINT "3-D NON-LINEAR ANALYSIS OF MASONRY COLUMN:SHRINKAGE AND CREEP "
50 INPUT PROMPT"STEEL AREA    (mm^2)                              ?": AS
60 INPUT PROMPT"YIELD STRENGTH OF STEEL (MPa)                   ?": FY
80 INPUT PROMPT"MASONRY UNIT STRENGTH     (MPa)                 ?": FBO
90 INPUT PROMPT"GROUT STRENGTH             (MPa)                ?": FGO
95 INPUT PROMPT"MORTAR STRENGTH            (MPa)                ?": FMO
120 INPUT PROMPT"BLOCK PROPERTIES COEFF. KB=kb*kc*kd*ke         ?": KB
130 INPUT PROMPT"GROUT PROPERTIES COEFF. KG=kb*kc*kd*ke         ?": KG
135 INPUT PROMPT"MORTAR PROPERTIES COEFF.KM=Kb*Kc*Kd*Ke         ?": KM
140 INPUT PROMPT"ULTIMATE SHRINKAGE STRAIN - BLOCK              ?": ESBU
150 INPUT PROMPT"ULTIMATE SHRINKAGE STRAIN - GROUT              ?": ESGU
155 INPUT PROMPT"ULTIMATE SHRINKAGE STRAIN - MORTAR             ?": ESMU
156 INPUT PROMPT"POSSION'S RATIO - MASONRY UNIT                 ?": Vb
157 INPUT PROMPT"POSSION'S RATIO - GROUT                        ?": Vg
158 INPUT PROMPT"POSSION'S RATIO - MORTAR                       ?": Vm
159 INPUT PROMPT"POSSION'S RATIO - REINFORCEMENT STEEL          ?": Vs
160 INPUT PROMPT"MASONRY UNIT ACTUAL THICKNESS  (mm)            ?": Tb
161 INPUT PROMPT"MORTAR JOINT THICKNESS          (mm)           ?": Tm
165 INPUT PROMPT"AGE OF COLUMN AT LOADING     (DAYS)            ?": AGE
166 INPUT PROMPT"SUSTAINED LOAD                (KN)             ?": PSUS
167 INPUT PROMPT"PRELOAD DURATION              (DAYS)           ?": DURATION
170 INPUT PROMPT"RESULT FILE NAME                               ?": F$
180 INPUT PROMPT"IS THIS CORRECT (y/n)                          ?": A$
190 IF A$="N" OR A$="n" THEN 20
191 LET F$="A:" & F$ & ".PRN"
195 WHEN ERROR IN
200 OPEN #1:NAME F$ ,ACCESS OUTIN,CREATE NEW
201 USE
202 INPUT PROMPT "file already exists do you want to overwrite it?":A$
203 IF A$="Y" OR A$="y" THEN
204 OPEN #1:NAME F$
209 ERASE#1
210 ELSE
211 CLOSE #1
212 INPUT PROMPT "give another name for data output file":F$
213 LET F$="A:" & F$ & ".PRN"
214 OPEN#1:NAME F$,ACCESS OUTIN,CREATE NEW
216 END IF
219 END WHEN
220 DIM E(600),E1(600),FYb(600),FYm(600),FYg1(600),FYg2(600),P(600),PS(600),PB(600),PG(600)
221 DIM COEEQ(11,11),CONSEQ(11),SOLEQ(11),COEEQINV(11,11)
225 OPEN #2:PRINTER
226 LET P1=1
227 LET P2=1
228 LET P3=1
229 LET P4=1
230 LET AB=31700
235 LET AM=31700
240 LET AG=22900
250 LET ES=200000
251 LET EBO=.002
```

```
252 LET EGO=.002
253 LET EMO=.002
254 LET FTB=.417075*(FBO^.5)
255 LET FTG=.5561*(FGO^.5)
256 LET FTM=.581*(FMO^.5)
260 LET EB=2*FBO/EBO
270 LET EG=2*FGO/EGO
271 LET EM=2*FMO/EMO
280 LET ESB=ESBU*(1-2.7183^(-.067*(AGE^.5)))
290 LET ESG=ESGU*(1-2.7183^(-.067*(AGE^.5)))
291 LET ESM=ESMU*(1-2.7183^(-.067*(AGE^.5)))
292 LET a=((.1591549*AS)^.5)
293 LET b=((.1591549*AG)^.5)
294 LET c=((.1591549*(AB+AG))^.5)
295 LET d=b+((c-b)/2)
296 LET f=a+((b-a)/2)
297 LET I=2
298 LET L=1
299 !STAGE 1:INITIAL LOADING
300 LET J=0
310 LET E(1)=0
315 LET E1(1)=0
320 GOTO 340
330 LET E(J+1)=E(J)+.00001
335 LET E1(J+1)=SOLEQ(11)
340 LET J=J+1
341 LET EBt=EB
342 LET EGt1=EG
343 LET EGt2=EG
344 LET EMt=EM
345 IF E1(J)<=ESM THEN 360
346 LET EMt=EM/(1+((E1(J)-ESM)/EMO)^2)
350 IF EMt>EM/2 THEN 360
355 LET EMt=EM/2
360 IF E1(J)<=ESG THEN 370
365 LET EGt2=EG/(1+((E1(J)-ESG)/EGO)^2)
370 IF E(J)<=ESB THEN 381
380 LET EBt=EB/(1+((E(J)-ESB)/EBO)^2)
381 IF E(J)<=ESG THEN 386
385 LET EGt1=EG/(1+((E(J)-ESG)/EGO)^2)
386 LET BK1=EBt/((1+Vb)*(1-2*Vb))
387 LET GK1=EGt1/((1+Vg)*(1-2*Vg))
388 LET GK2=EGt2/((1+Vg)*(1-2*Vg))
389 LET SK31=ES/((1+Vs)*(1-2*Vs))
390 LET SK32=ES/((1+Vs)*(1-2*Vs))
391 LET MK4=EMt/((1+Vm)*(1-2*Vm))
392 CALL FILLCOEEQ
393 CALL FILLCONSEQ
394 MAT COEEQInv=Inv(COEEQ)
395 LET CHECK1 = DET(COEEQ)
396 IF ABS(CHECK1) < 1 THEN
397 PRINT "ERROR DET=";CHECK1
398 STOP
399 END IF
400 MAT SOLEQ=COEEQInv*CONSEQ
```

```
405 !STRESSES AT THE BLOCK LEVEL
406 !stresses in the block
407 LET FYb(J)=BK1*((1-Vb)*E(J)+2*Vb*SOLEQ(1)-ESB*(1+Vb))
418 !stresses in the grout at the block level
419 LET FYg1(J)=GK1*((1-Vg)*E(J)+2*Vg*SOLEQ(2)-ESG*(1+Vg))
420 !stresses in the vertical reinforcement at block level
421 LET FYs1=SK31*((1-Vs)*E(J)+2*Vs*SOLEQ(3))
422 LET PS(J)=(AS*FYs1)/1000
423 LET PG(J)=(AG*FYg1(J))/1000
424 IF PG(J)>0 THEN 426
425 LET PG(J)=0
426 LET PB(J)=(AB*FYb(J))/1000
427 IF PB(J)>0 THEN 429
428 LET PB(J)=0
429 LET P(J)=PS(J)+PB(J)+PG(J)
430 !STRESSES AT THE MORTAR LEVEL
431 !stresses in the mortar
432 LET FYm(J)=MK4*((1-Vm)*SOLEQ(11)+2*Vm*SOLEQ(4)-ESM*(1+Vm))
433 !stresses in the grout at the mortar level
434 LET FYg2(J)=GK2*((1-Vg)*SOLEQ(11)+2*Vg*SOLEQ(5)-ESG*(1+Vg))
435 !stresses in the vertical reinforcement at mortar level
436 LET FYs2=SK32*((1-Vs)*SOLEQ(11)+2*Vs*SOLEQ(6))
437 PRINT EY;FYS1,EY1;FYS2,E(J);E1(J)
438 IF P(J)<(PSUS-5) THEN 330
439 IF P(J)=>PSUS THEN 444
440 LET E(J+1)=E(J)+.000001
441 LET E1(J+1)=SOLEQ(11)
442 GOTO 340
443 !STAGE 2:LOAD = SUSTAINED LOAD(PSUS)
444 LET J=J+1
445 DIM SCOEEQ(12,12),SCONSEQ(12),SSOLEQ(12),SCOEEQINV(12,12)
446 CALL SUSCOEEQ
447 CALL SUSCONSEQ
448 MAT SCOEEQINV=INV(SCOEEQ)
449 LET CHECK2 = DET(SCOEEQ)
450 IF ABS(CHECK2) < 1 THEN
451 PRINT "ERROR DET=";CHECK2
452 STOP
453 END IF
454 MAT SSOLEQ=SCOEEQINV*SCONSEQ
455 LET FYb(J)=BK1*((1-Vb)*SSOLEQ(12)+2*Vb*SSOLEQ(1)-ESB*(1+Vb))
456 LET FYg1(J)=GK1*((1-Vg)*SSOLEQ(12)+2*Vg*SSOLEQ(2)-ESG*(1+Vg))
457 LET FYs1=SK31*((1-Vs)*SSOLEQ(12)+2*Vs*SSOLEQ(3))
458 LET PS(J)=(AS*FYs1)/1000
459 LET PG(J)=(AG*FYg1(J))/1000
460 LET PB(J)=(AB*FYb(J))/1000
461 LET P(J)=PS(J)+PB(J)+PG(J)
462 LET FYm(J)=MK4*((1-Vm)*SSOLEQ(11)+2*Vm*SSOLEQ(4)-ESM*(1+Vm))
463 LET FYg2(J)=GK2*((1-Vg)*SSOLEQ(11)+2*Vg*SSOLEQ(5)-ESG*(1+Vg))
464 LET FYs2=SK32*((1-Vs)*SSOLEQ(11)+2*Vs*SSOLEQ(6))
465 LET FYbI=FYb(J)
466 LET FYG1I=FYg1(J)
467 LET FYS1I=FYs1
468 LET FYMI=FYm(J)
469 LET FYG2I=FYg2(J)
```

```
470 LET FYS2I=FYs2
471 LET EI=SSOLEQ(12)
472 LET EI1=SSOLEQ(11)
473 LET E(J)=SSOLEQ(12)
474 LET E1(J)=SSOLEQ(11)
475 LET EMt=EM/(1+((EI1-ESM)/EMO)^2)
476 IF EMt>EM/2 THEN 478
477 LET EMt=EM/2
478 LET EBt=EB/(1+((EI-ESB)/EBO)^2)
479 LET EGt1=EG/(1+((EI-ESG)/EGO)^2)
480 LET EGt2=EG/(1+((EI1-ESG)/EGO)^2)
481 LET BK1=EBt/((1+Vb)*(1-2*Vb))
482 LET GK1=EGt1/((1+Vg)*(1-2*Vg))
483 LET GK2=EGt2/((1+Vg)*(1-2*Vg))
484 LET MK4=EMt/((1+Vm)*(1-2*Vm))
485 PRINT EY;FYS1,EY1;FYS2,E(J);E1(J)
486 LET J=J+1
487 GOTO 491
489 !STAGE 3:DURING CREEP PERIOD (CREEP AND SHRINKAGE UNDER SUSTAINED LOAD)
490 LET T=T+DURATION/60
491 LET ESBT=ESBU*(1-2.7183^(-.067*((AGE+T)^.5)))-ESB
492 LET ESGT=ESGU*(1-2.7183^(-.067*((AGE+T)^.5)))-ESG
493 LET ESMT=ESMU*(1-2.7183^(-.067*((AGE+T)^.5)))-ESM
494 LET CB=KB*(1-2.7183^(-.08753*(T^.5)))
495 LET CG=KG*(1-2.7183^(-.08753*(T^.5)))
496 LET CM=KM*(1-2.7183^(-.08753*(T^.5)))
497 DIM CCOEEQ(12,12),CCONSEQ(12),CSOLEQ(12),CCOEEQINV(12,12)
498 CALL CREEPCOEEQ
499 CALL CREEPCONSEQ
500 MAT CCOEEQINV=INV(CCOEEQ)
501 LET CHECK3 = DET(CCOEEQ)
502 IF ABS(CHECK3) < 1 THEN
503 PRINT "ERROR DET=";CHECK3
504 STOP
505 END IF
506 MAT CSOLEQ=CCOEEQINV*CCONSEQ
507 LET FYb(J)=BK1*(((1-Vb)/(1+CB))*CSOLEQ(11)+((1-Vb)/(1+CB))*(EI-ESB-ESBT)+2*Vb*(1+CB)*(
2*Vb*(ESB+ESBT))
508 LET FTbMIDDLE=BK1*((1+CB)*CSOLEQ(1)+((1+CB)*(1-2*Vb)*CSOLEQ(7)/(d^2))-(ESB+ESBT)+(V
1)/(1+CB))+(Vb*(EI-ESB-ESBT)/(1+CB)))
509 LET FYg1(J)=GK1*(((1-Vg)/(1+CG))*CSOLEQ(11)+((1-Vg)/(1+CG))*(EI-ESG-ESGT)+2*Vg*(1+CG)*
-2*Vg*(ESG+ESGT))
510 LET FTg1MIDDLE=GK1*((1+CG)*CSOLEQ(2)+((1+CG)*(1-2*Vg)*CSOLEQ(8)/(f^2))-(ESG+ESGT)+(V
11)/(1+CG))+(Vg*(EI-ESG-ESGT)/(1+CG)))
511 LET FYs1=SK31*((1-Vs)*(EI+CSOLEQ(11))+2*Vs*CSOLEQ(3))
512 LET E1(J)=EI1+CSOLEQ(12)
513 LET E(J)=EI+CSOLEQ(11)
514 LET PS(J)=(AS*FYs1)/1000
515 LET PG(J)=(AG*FYg1(J))/1000
516 LET PB(J)=(AB*FYb(J))/1000
517 LET P(J)=PS(J)+PB(J)+PG(J)
518 LET FYm(J)=MK4*(((1-Vm)/(1+CM))*CSOLEQ(12)+((1-Vm)/(1+CM))*(EI1-ESM-ESMT)+2*Vm*(1+C
(4)-2*Vm*(ESM+ESMT))
519 LET FTmMIDDLE=MK4*((1+CM)*CSOLEQ(4)+((1+CM)*(1-2*Vm)*CSOLEQ(9)/(d^2))-(ESM+ESMT)+(
Q(12)/(1+CM))+(Vm*(EI1-ESM-ESMT)/(1+CM)))
```

```
520 LET FYg2(J)=GK2*(((1-Vg)/(1+CG))*CSOLEQ(12)+((1-Vg)/(1+CG))*(EI1-ESG-ESGT)+2*Vg*(1+CG)*
)-2*Vg*(ESG+ESGT))
521 LET FTg2MIDDLE=GK2*((1+CG)*CSOLEQ(5)+((1+CG)*(1-2*Vg)*CSOLEQ(10)/(f^2))-(ESG+ESGT)+(Vg
(12)/(1+CG))+(Vg*(EI1-ESG-ESGT)/(1+CG)))
523 LET FYs2=SK32*((1-Vs)*(EI1+CSOLEQ(12))+2*Vs*CSOLEQ(6))
543 IF FTbMIDDLE>0 THEN 550
544 IF FYb(J)<(FBO*((FTB+FTbMIDDLE)/FTB)) THEN 548
545 IF P1>1 THEN 548
546 PRINT #2: "BLOCK FAILS UNDER COMPRESSION TENSION AT P(J)=          ",P(J)
547 LET P1=2
548 IF -FTbMIDDLE=>FTB THEN 870
549 GOTO 551
550 IF FYb(J)=>FBO THEN 873
551 IF FTg1MIDDLE>0 THEN 558
552 IF FYg1(J)<FGO THEN 556
553 IF P2>1 THEN 556
554 PRINT #2: "GROUT AT BLOCK LEVEL FAILS UNDER AXIAL COMP. AT P(J)= ",P(J)
555 LET P2=2
556 IF -FTg1MIDDLE=>FTG THEN 876
557 GOTO 559
558 IF FYg1(J)=>(FGO+4.1*FTg1MIDDLE) THEN 879
559 IF FTg2MIDDLE>0 THEN 566
560 IF FYg2(J)<FGO THEN 564
561 IF P3>1 THEN 564
562 PRINT #2: "GROUT AT MORTAR LEVEL FAILS UNDER AXIAL COMP. AT P(J)=",P(J)
563 LET P3=2
564 IF -FTg2MIDDLE=>FTG THEN 882
565 GOTO 567
566 IF FYg2(J)=>(FGO+4.1*FTg2MIDDLE) THEN 885
567 IF FTmMIDDLE>0 THEN 574
568 IF FYm(J)<FMO THEN 572
569 IF P4>1 THEN 572
570 PRINT #2: "MORTAR FAILS UNDER AXIAL COMPRESSION AT P(J)=          ",P(J)
571 LET P4=2
572 IF -FTmMIDDLE=>FTM THEN 888
573 GOTO 575
574 IF FYm(J)=>(FMO+4.1*FTmMIDDLE) THEN 891
575 LET EEB=(EI+CSOLEQ(11)-ESB-ESBT)/(1+CB)
585 LET ECB=EEB*CB
586 LET EEG1=(EI+CSOLEQ(11)-ESG-ESGT)/(1+CG)
587 LET ECG1=EEG1*CG
588 LET EEM=(EI1+CSOLEQ(12)-ESM-ESMT)/(1+CM)
589 LET ECM=EEM*CM
590 LET EEG2=(EI1+CSOLEQ(12)-ESG-ESGT)/(1+CG)
591 LET ECG2=EEG2*CG
592 LET EMt=EM/(1+(EEM/EMO)^2)
593 IF EMt>EM/2 THEN 595
594 LET EMt=EM/2
595 LET EBt=EB/(1+(EEB/EBO)^2)
596 LET EGt1=EG/(1+(EEG1/EGO)^2)
597 LET EGt2=EG/(1+(EEG2/EGO)^2)
598 LET BK1=EBt/((1+Vb)*(1-2*Vb))
599 LET GK1=EGt1/((1+Vg)*(1-2*Vg))
600 LET GK2=EGt2/((1+Vg)*(1-2*Vg))
618 LET MK4=EMt/((1+Vm)*(1-2*Vm))
```

```
619 IF I>2 THEN 621
620 IF FYS1<FY THEN 625
621 LET EY=E(J+1-I)
622 LET I=I+1
623 LET ES=(EY*200000)/E(J)
624 GOTO 626
625 LET ES=200000
626 LET SK31=ES/((1+Vs)*(1-2*Vs))
627 IF L>1 THEN 629
628 IF FYS2<FY THEN 633
629 LET EY1=E1(J-L)
630 LET L=L+1
631 LET ES=(EY1*200000)/E1(J)
632 GOTO 634
633 LET ES=200000
634 LET SK32=ES/((1+Vs)*(1-2*Vs))
636 PRINT EY;FYS1,EY1;FYS2,E(J);E1(J)
637 IF T>=DURATION THEN 640
638 LET J=J+1
639 GOTO 490
640 !STAGE 4:FOLLOWING THE CREEP PERIOD
641 !Radial and Tangential Creep Strains in the Block
642 LET ECBRINSIDE=CB*(CSOLEQ(1)-(CSOLEQ(7)/(b^2)))
643 LET ECBRMIDDLE=CB*(CSOLEQ(1)-(CSOLEQ(7)/(d^2)))
644 LET ECBREDGE=CB*(CSOLEQ(1)-(CSOLEQ(7)/(c^2)))
645 LET ECBTINSIDE=CB*(CSOLEQ(1)+(CSOLEQ(7)/(b^2)))
646 LET ECBTMIDDLE=CB*(CSOLEQ(1)+(CSOLEQ(7)/(d^2)))
647 LET ECBTEDGE=CB*(CSOLEQ(1)+(CSOLEQ(7)/(c^2)))
648 !Radial and Tangential Creep Srains in the Grout at Block Level
649 LET ECG1RINSIDE=CG*(CSOLEQ(2)-(CSOLEQ(8)/(a^2)))
650 LET ECG1RMIDDLE=CG*(CSOLEQ(2)-(CSOLEQ(8)/(f^2)))
651 LET ECG1REDGE=CG*(CSOLEQ(2)-(CSOLEQ(8)/(b^2)))
652 LET ECG1TINSIDE=CG*(CSOLEQ(2)+(CSOLEQ(8)/(a^2)))
653 LET ECG1TMIDDLE=CG*(CSOLEQ(2)+(CSOLEQ(8)/(f^2)))
654 LET ECG1TEDGE=CG*(CSOLEQ(2)+(CSOLEQ(8)/(b^2)))
655 !Radial and Tangential Creep Strains in the Mortar
656 LET ECMRINSIDE=CM*(CSOLEQ(4)-(CSOLEQ(9)/(b^2)))
657 LET ECMRMIDDLE=CM*(CSOLEQ(4)-(CSOLEQ(9)/(d^2)))
658 LET ECMREDGE=CM*(CSOLEQ(4)-(CSOLEQ(9)/(c^2)))
659 LET ECMTINSIDE=CM*(CSOLEQ(4)+(CSOLEQ(9)/(b^2)))
660 LET ECMTMIDDLE=CM*(CSOLEQ(4)+(CSOLEQ(9)/(d^2)))
661 LET ECMTEDGE=CM*(CSOLEQ(4)+(CSOLEQ(9)/(c^2)))
662 !Radial and Tangential Creep Strains in the Grout at Mortar Level
663 LET ECG2RINSIDE=CG*(CSOLEQ(5)-(CSOLEQ(10)/(a^2)))
664 LET ECG2RMIDDLE=CG*(CSOLEQ(5)-(CSOLEQ(10)/(f^2)))
665 LET ECG2REDGE=CG*(CSOLEQ(5)-(CSOLEQ(10)/(b^2)))
666 LET ECG2TINSIDE=CG*(CSOLEQ(5)+(CSOLEQ(10)/(a^2)))
667 LET ECG2TMIDDLE=CG*(CSOLEQ(5)+(CSOLEQ(10)/(f^2)))
668 LET ECG2TEDGE=CG*(CSOLEQ(5)+(CSOLEQ(10)/(b^2)))
669 LET E(J+1)=E(J)
670 LET E1(J+1)=E1(J)
671 LET J=J+1
672 GOTO 686
673 LET E(J+1)=E(J)+.00001
```

```
674 LET J=J+1
675 LET EMt=EM/(1+((E1(J)-ECM-ESM-ESMT)/EMO)^2)
677 IF EMt>EM/2 THEN 679
678 LET EMt=EM/2
679 LET EGt2=EG/(1+((E1(J)-ECG2-ESG-ESGT)/EGO)^2)
680 LET GK2=EGt2/((1+Vg)*(1-2*Vg))
681 LET MK4=EMt/((1+Vm)*(1-2*Vm))
682 LET EBt=EB/(1+((E(J)-ECB-ESB-ESBT)/EBO)^2)
683 LET EGt1=EG/(1+((E(J)-ECG1-ESG-ESGT)/EGO)^2)
684 LET BK1=EBt/((1+Vb)*(1-2*Vb))
685 LET GK1=EGt1/((1+Vg)*(1-2*Vg))
686 IF I>2 THEN 688
687 IF FYS1<FY THEN 692
688 LET EY=E(J-I)
689 LET I=I+1
690 LET ES=(EY*200000)/E(J)
691 GOTO 693
692 LET ES=200000
693 LET SK31=ES/((1+Vs)*(1-2*Vs))
694 IF L>1 THEN 696
695 IF FYS2<FY THEN 700
696 LET EY1=E1(J-L)
697 LET L=L+1
698 LET ES=(EY1*200000)/E1(J)
699 GOTO 701
700 LET ES=200000
701 LET SK32=ES/((1+Vs)*(1-2*Vs))
702 DIM FCOEEQ(11,11),FCONSEQ(11),FCOEEQINV(11,11),FSOLEQ(11)
703 CALL FOLLOWINGCREEPCOEEQ
704 CALL FOLLOWINGCREEPCONSEQ
705 MAT FCOEEQInv=Inv(FCOEEQ)
706 LET CHECK4 = DET(FCOEEQ)
707 IF ABS(CHECK4) < 1 THEN
708 PRINT "ERROR DET=";CHECK4
709 STOP
710 END IF
711 MAT FSOLEQ=FCOEEQInv*FCONSEQ
712 LET E1(J+1)=FSOLEQ(11)
713 !STRESSES AT THE BLOCK LEVEL
714 !stresses in the block
715 LET FYb(J)=BK1*((1-Vb)*(E(J)-ECB-ESB-ESBT)+2*Vb*(FSOLEQ(1)-(ESB+ESBT))+Vb*(ECBRIN
INSIDE))
716 LET FRbEDGE=BK1*(FSOLEQ(1)-(FSOLEQ(7)*(1-2*Vb)/(c^2))+Vb*(E(J)-ECB-ESB-ESBT)-(ESB
VB)*ECBREDGE+Vb*ECBTEDGE)
717 LET FRbMIDDLE=BK1*(FSOLEQ(1)-(FSOLEQ(7)*(1-2*Vb)/(d^2))+Vb*(E(J)-ECB-ESB-ESBT)-(E
(1-Vb)*ECBRMIDDLE+Vb*ECBTMIDDLE)
718 LET FRbINSIDE=BK1*(FSOLEQ(1)-(FSOLEQ(7)*(1-2*Vb)/(b^2))+Vb*(E(J)-ECB-ESB-ESBT)-(E
1-Vb)*ECBRINSIDE+VB*ECBTINSIDE)
719 LET FTbEDGE=BK1*(FSOLEQ(1)+(FSOLEQ(7)*(1-2*Vb)/(c^2))+Vb*(E(J)-ECB-ESB-ESBT)-(ESB
Vb)*ECBTEDGE+Vb*ECBREDGE)
720 LET FTbMIDDLE=BK1*(FSOLEQ(1)+(FSOLEQ(7)*(1-2*Vb)/(d^2))+Vb*(E(J)-ECB-ESB-ESBT)-(E
(1-Vb)*ECBTMIDDLE+Vb*ECBRMIDDLE)
721 LET FTbINSIDE=BK1*(FSOLEQ(1)+(FSOLEQ(7)*(1-2*Vb)/(b^2))+Vb*(E(J)-ECB-ESB-ESBT)-(E
1-Vb)*ECBTINSIDE+Vb*ECBRINSIDE)
```

```
722 !stresses in the grout at the block level
723 LET FYg1(J)=GK1*((1-Vg)*(E(J)-ECG1-ESG-ESGT)+2*Vg*(FSOLEQ(2)-(ESG+ESGT))+Vg*(ECG1RINS
G1TINSIDE))
724 LET FRg1EDGE=GK1*(FSOLEQ(2)-(FSOLEQ(8)*(1-2*Vg)/(b^2))+Vg*(E(J)-ECG1-ESG-ESGT)-(ESG+E
1-Vg)*ECG1REDGE+Vg*ECG1TEDGE)
725 LET FRg1MIDDLE=GK1*(FSOLEQ(2)-(FSOLEQ(8)*(1-2*Vg)/(f^2))+Vg*(E(J)-ECG1-ESG-ESGT)-(ESG
+(1-Vg)*ECG1RMIDDLE+Vg*ECG1TMIDDLE)
726 LET FRg1INSIDE=GK1*(FSOLEQ(2)-(FSOLEQ(8)*(1-2*Vg)/(a^2))+Vg*(E(J)-ECG1-ESG-ESGT)-(ESG
+(1-Vg)*ECG1RINSIDE+Vg*ECG1TINSIDE)
727 LET FTg1EDGE=GK1*(FSOLEQ(2)+(FSOLEQ(8)*(1-2*Vg)/(b^2))+Vg*(E(J)-ECG1-ESG-ESGT)-(ESG+E
1-Vg)*ECG1TEDGE+Vg*ECG1REDGE)
728 LET FTg1MIDDLE=GK1*(FSOLEQ(2)+(FSOLEQ(8)*(1-2*Vg)/(f^2))+Vg*(E(J)-ECG1-ESG-ESGT)-(ESG
+(1-Vg)*ECG1TMIDDLE+Vg*ECG1RMIDDLE)
729 LET FTg1INSIDE=GK1*(FSOLEQ(2)+(FSOLEQ(8)*(1-2*Vg)/(a^2))+Vg*(E(J)-ECG1-ESG-ESGT)-(ESG
+(1-Vg)*ECG1TINSIDE+Vg*ECG1RINSIDE)
730 !stresses in the vertical reinforcement at block level
731 LET FYs1=SK31*((1-Vs)*E(J)+2*Vs*FSOLEQ(3))
732 LET FRs1=SK31*(FSOLEQ(3)+Vs*E(J))
733 LET PS(J)=(AS*FYs1)/1000
734 LET PG(J)=(AG*FYg1(J))/1000
735 LET PB(J)=(AB*FYb(J))/1000
736 LET P(J)=PS(J)+PB(J)+PG(J)
737 !STRESSES AT THE MORTAR LEVEL
738 !stresses in the mortar
739 LET FYm(J)=MK4*((1-Vm)*(FSOLEQ(11)-ECM-ESM-ESMT)+2*Vm*(FSOLEQ(4)-(ESM+ESMT))+Vm*(E
SIDE+ECMTINSIDE))
740 LET FRmEDGE=MK4*(FSOLEQ(4)-(FSOLEQ(9)*(1-2*Vm)/(c^2))+Vm*(FSOLEQ(11)-ECM-ESM-ESMT)
ESMT)+(1-Vm)*ECMREDGE+Vm*ECMTEDGE)
741 LET FRmMIDDLE=MK4*(FSOLEQ(4)-(FSOLEQ(9)*(1-2*Vm)/(d^2))+Vm*(FSOLEQ(11)-ECM-ESM-ESM
M+ESMT)+(1-Vm)*ECMRMIDDLE+Vm*ECMTMIDDLE)
742 LET FRmINSIDE=MK4*(FSOLEQ(4)-(FSOLEQ(9)*(1-2*Vm)/(b^2))+Vm*(FSOLEQ(11)-ECM-ESM-ESM
M+ESMT)+(1-Vm)*ECMRINSIDE+Vm*ECMTINSIDE)
743 LET FTmEDGE=MK4*(FSOLEQ(4)+(FSOLEQ(9)*(1-2*Vm)/(c^2))+Vm*(FSOLEQ(11)-ECM-ESM-ESMT)
ESMT)+(1-Vm)*ECMTEDGE+Vm*ECMREDGE)
744 LET FTmMIDDLE=MK4*(FSOLEQ(4)+(FSOLEQ(9)*(1-2*Vm)/(d^2))+Vm*(FSOLEQ(11)-ECM-ESM-ESM
M+ESMT)+(1-Vm)*ECMTMIDDLE+Vm*ECMRMIDDLE)
745 LET FTmINSIDE=MK4*(FSOLEQ(4)+(FSOLEQ(9)*(1-2*Vm)/(b^2))+Vm*(FSOLEQ(11)-ECM-ESM-ESM
M+ESMT)+(1-Vm)*ECMTINSIDE+Vm*ECMRINSIDE)
746 !stresses in the grout at the mortar level
747 LET FYg2(J)=GK2*((1-Vg)*(FSOLEQ(11)-ECG2-ESG-ESGT)+2*Vg*(FSOLEQ(5)-(ESG+ESGT))+Vg*(E
SIDE+ECG2TINSIDE))
748 LET FRg2EDGE=GK2*(FSOLEQ(5)-(FSOLEQ(10)*(1-2*Vg)/(b^2))+Vg*(FSOLEQ(11)-ECG2-ESG-ESGT
+ESGT)+(1-Vg)*ECG2REDGE+Vg*ECG2TEDGE)
749 LET FRg2MIDDLE=GK2*(FSOLEQ(5)-(FSOLEQ(10)*(1-2*Vg)/(f^2))+Vg*(FSOLEQ(11)-ECG2-ESG-ES
G+ESGT)+(1-Vg)*ECG2RMIDDLE+Vg*ECG2TMIDDLE)
750 LET FRg2INSIDE=GK2*(FSOLEQ(5)-(FSOLEQ(10)*(1-2*Vg)/(a^2))+Vg*(FSOLEQ(11)-ECG2-ESG-ES(
G+ESGT)+(1-Vg)*ECG2RINSIDE+Vg*ECG2TINSIDE)
751 LET FTg2EDGE=GK2*(FSOLEQ(5)+(FSOLEQ(10)*(1-2*Vg)/(b^2))+Vg*(FSOLEQ(11)-ECG2-ESG-ESGT
ESGT)+(1-Vg)*ECG2TEDGE+Vg*ECG2REDGE)
752 LET FTg2MIDDLE=GK2*(FSOLEQ(5)+(FSOLEQ(10)*(1-2*Vg)/(f^2))+Vg*(FSOLEQ(11)-ECG2-ESG-ES
G+ESGT)+(1-Vg)*ECG2TMIDDLE+Vg*ECG2RMIDDLE)
753 LET FTg2INSIDE=GK2*(FSOLEQ(5)+(FSOLEQ(10)*(1-2*Vg)/(a^2))+Vg*(FSOLEQ(11)-ECG2-ESG-ES(
G+ESGT)+(1-Vg)*ECG2TINSIDE+Vg*ECG2RINSIDE)
754 !stresses in the vertical reinforcement at mortar level
755 LET FYs2=SK32*((1-Vs)*FSOLEQ(11)+2*Vs*FSOLEQ(6))
```

```
756 LET FRs2=SK32*(FSOLEQ(6)+Vs*FSOLEQ(11))
757 PRINT EY;FYS1,EY1;FYS2,E(J);E1(J)
763 IF FTbMIDDLE>0 THEN 770
764 IF FYb(J)<(FBO*((FTB+FTbMIDDLE)/FTB)) THEN 768
765 IF P1>1 THEN 768
766 PRINT #2: "BLOCK FAILS UNDER COMPRESSION TENSION AT P(J)=          ",P(J)
767 LET P1=2
768 IF -FTbMIDDLE=>FTB THEN 870
769 GOTO 771
770 IF FYb(J)=>FBO THEN 873
771 IF FTg1MIDDLE>0 THEN 778
772 IF FYg1(J)<FGO THEN 776
773 IF P2>1 THEN 776
774 PRINT #2: "GROUT AT BLOCK LEVEL FAILS UNDER AXIAL COMP. AT P(J)= ",P(J)
775 LET P2=2
776 IF -FTg1MIDDLE=>FTG THEN 876
777 GOTO 779
778 IF FYg1(J)=>(FGO+4.1*FTg1MIDDLE) THEN 879
779 IF FTg2MIDDLE>0 THEN 786
780 IF FYg2(J)<FGO THEN 784
781 IF P3>1 THEN 784
782 PRINT #2: "GROUT AT MORTAR LEVEL FAILS UNDER AXIAL COMP. AT P(J)=",P(J)
783 LET P3=2
784 IF -FTg2MIDDLE=>FTG THEN 882
785 GOTO 787
786 IF FYg2(J)=>(FGO+4.1*FTg2MIDDLE) THEN 885
787 IF FTmMIDDLE>0 THEN 794
788 IF FYm(J)<FMO THEN 792
789 IF P4>1 THEN 792
790 PRINT #2: "MORTAR FAILS UNDER AXIAL COMPRESSION AT P(J)=          ",P(J)
791 LET P4=2
792 IF -FTmMIDDLE=>FTM THEN 888
793 GOTO 795
794 IF FYm(J)=>(FMO+4.1*FTmMIDDLE) THEN 891
795 GOTO 673
870 CLEAR
871 PRINT #2: "BLOCK FAILS UNDER TENSION AT P(J)=                    ",P(J)
872 GOTO 906
873 CLEAR
874 PRINT #2: "BLOCK FAILS UNDER AXIAL COMPRESSION AT P(J)=          ",P(J)
875 GOTO 906
876 CLEAR
877 PRINT #2: "GROUT-BLOCK LEVEL FAILS UNDER TENSION AT P(J)=        ",P(J)
878 GOTO 906
879 CLEAR
880 PRINT #2: "GROUT-BLOCK LEVEL FAILS UNDER TRIAXIAL COMP. AT P(J)= ",P(J)
881 GOTO 906
882 CLEAR
883 PRINT #2: "GROUT-MORTAR LEVEL FAILS UNDER TENSION AT P(J)=       ",P(J)
884 GOTO 906
885 CLEAR
886 PRINT #2: "GROUT-MORTAR LEVEL FAILS UNDER TRIAXIAL COMP. AT P(J)=",P(J)
887 GOTO 906
888 CLEAR
889 PRINT #2: "MORTAR FAILS UNDER TENSION AT P(J)=                   ",P(J)
```

```
890 GOTO 906
891 CLEAR
892 PRINT #2: "MORTAR FAILS UNDER TRIAXIAL COMPRESSION AT P(J)=       ",P(J)
906 LET I=J
907 LET J=0
908 LET J=J+1
909 PRINT #1 : E(J);",";P(J);",";PS(J);",";PB(J);",";PG(J);","
910 IF J=I THEN 915
914 GOTO 908
915 CLOSE #1
916 LET X=E(J)+.0005
917 LET Y=P(J)+100
918 OPEN #1: SCREEN 0, .49, .51, 1
919 SET WINDOW 0,X,0,Y
920 BOX LINES 0,X,0,Y
921 SET COLOR "RED"
922 SET BACK "WHITE"
923 PLOT 0,0;0,Y
924 PLOT 0,0;X,0
925 LET X=E(1)
926 LET Y=P(1)
927 PLOT 0,0;X,Y
928 LET I=0
929 LET I=I+1
930 LET X=E(I)
931 LET Y=P(I)
932 PLOT X,Y
934 IF I=J THEN 936
935 GOTO 929
936 LET X=E(1)
937 LET Y=PS(1)
938 PLOT 0,0;X,Y
939 LET I=0
940 LET I=I+1
941 LET X=E(I)
942 LET Y=PS(I)
943 PLOT X,Y
944 IF I=J THEN 946
945 GOTO 940
946 LET X=E(I)
947 LET Y=PB(1)
948 PLOT 0.0;X,Y
949 LET I=0
950 LET I=I+1
951 LET X=E(I)
952 LET Y=PB(I)
953 PLOT X,Y
954 IF I=J THEN 956
955 GOTO 950
956 LET X=E(1)
957 LET Y=PG(1)
958 PLOT 0,0;X,Y
959 LET I=0
960 LET I=I+1
961 LET X=E(I)
```

```
962 LET Y=PG(I)
963 PLOT X,Y
964 IF I=J THEN 966
965 GOTO 960
966 CLOSE #1
967 OPEN #3: SCREEN .5, 1, .675, 1
968 SET WINDOW 0,c,-ABS(FRs1),ABS(FRs1)
969 BOX LINES 0,c,-ABS(FRs1),ABS(FRs1)
970 PRINT"     R-STRESSES AT BLOCK"
972 LET X=a
973 LET Y=ABS(FRs1)
974 PLOT LINES:X,Y;X,-Y
975 PLOT 0,Y;0,-Y
976 LET X=b
977 PLOT LINES:X,Y;X,-Y
978 LET X=c
979 PLOT LINES:X,Y;X,-Y
980 PLOT LINES:0,0;c,0
981 LET X=0
982 LET Y=FRs1
983 PLOT LINES:X,Y;
984 LET X=a
985 LET Y=FRg1INSIDE
987 PLOT LINES:X,Y;
988 LET X=b
989 LET Y=FRg1EDGE
990 PLOT LINES:X,Y;
991 LET X=c
992 LET Y=FRbEDGE
993 PLOT LINES:X,Y
994 CLOSE#3
995 OPEN #4: SCREEN 0, .49, 0, .49
997 SET WINDOW 0,c,-ABS(FRs2),ABS(FRs2)
998 BOX LINES 0,c,-ABS(FRs2),ABS(FRs2)
999 PRINT "     R-STRESS-AT MORTAR "
1000 LET Y=ABS(FRS2)
1001 PLOT 0,-Y;0,Y
1002 PLOT LINES:a,Y;a,-Y
1003 PLOT LINES:b,Y;b,-Y
1004 PLOT LINES:c,Y;C,-Y
1010 PLOT 0,0;X,0
1011 LET X=0
1012 LET Y=FRs2
1013 PLOT LINES:0,0;X,Y;
1014 LET X=a
1015 LET Y=FRg2INSIDE
1016 PLOT LINES:X,Y;
1017 LET X=b
1018 LET Y=FRg2EDGE
1019 PLOT LINES:X,Y;
1020 LET X=c
1021 LET Y=FRmEDGE
1022 PLOT LINES:X,Y
1023 CLOSE#4
```

```
1025 OPEN #5: SCREEN .5, 1, .3375, .6625
1026 SET WINDOW 0,c,-ABS(FRs1),ABS(FRs1)
1027 BOX LINES 0,c,-ABS(FRs1),ABS(FRs1)
1028 PRINT "TANG.STRESS AT BLOCK"
1029 LET X=c
1030 LET Y=ABS(FRs1)
1032 PLOT 0,-Y;0,Y
1033 PLOT 0,0;X,0
1034 LET X=0
1035 LET Y=FRs1
1036 PLOT LINES:0,0;X,Y;
1037 LET X=a
1038 LET Y=FRs1
1039 PLOT LINES:X,Y;
1040 LET X=a
1041 LET Y=FTg1INSIDE
1042 PLOT LINES:X,Y;
1043 LET X=b
1044 LET Y=FTg1EDGE
1045 PLOT LINES:X,Y;
1046 LET X=b
1047 LET Y=FTbINSIDE
1048 PLOT LINES:X,Y;
1049 LET X=c
1050 LET Y=FTbEDGE
1051 PLOT LINES:X,Y
1052 CLOSE#5
1054 OPEN #6: SCREEN .5, 1, 0, .325
1056 SET WINDOW 0,c,-ABS(FRs2),ABS(FRs2)
1057 BOX LINES 0,c,-ABS(FRs2),ABS(FRs2)
1058 PRINT "    TANG-STRESS AT MORTAR"
1059 LET X=c
1060 LET Y=ABS(FRs2)
1062 PLOT 0,-Y;0,Y
1063 PLOT 0,0;X,0
1064 LET X=0
1065 LET Y=FRs2
1066 PLOT LINES:0,0;X,Y;
1067 LET X=a
1068 LET Y=FRs2
1069 PLOT LINES:X,Y;
1070 LET X=a
1071 LET Y=FTg2INSIDE
1072 PLOT LINES:X,Y;
1073 LET X=b
1074 LET Y=FTg2EDGE
1075 PLOT LINES:X,Y;
1076 LET X=b
1077 LET Y=FTmINSIDE
1078 PLOT LINES:X,Y;
1079 LET X=c
1080 LET Y=FTmEDGE
1081 PLOT LINES:X,Y
1082 CLOSE#6
1086 GOTO 9800
```

```
1087 SUB FILLCOEEQ
1088 MAT COEEQ =ZER
1089 LET COEEQ (1,2)= GK1
1090 LET COEEQ (1,3)= -SK31
1091 LET COEEQ(1,8)= -GK1*(1-2*Vg)/(a^2)
1092 LET COEEQ(2,5)= GK2
1093 LET COEEQ(2,6)= -SK32
1094 LET COEEQ(2,10)= -GK2*(1-2*Vg)/(a^2)
1095 LET COEEQ(2,11)= (GK2*Vg)-(SK32*Vs)
1097 LET COEEQ(3,2)= 1
1098 LET COEEQ(3,3)= -1
1099 LET COEEQ(3,8)= 1/(a^2)
1100 LET COEEQ(4,5)= 1
1101 LET COEEQ(4,6)= -1
1102 LET COEEQ(4,10)= 1/(a^2)
1103 LET COEEQ(5,1)= -BK1
1104 LET COEEQ(5,2)= GK1
1105 LET COEEQ(5,7)= BK1*(1-2*Vb)/(b^2)
1106 LET COEEQ(5,8)= -GK1*(1-2*Vg)/(b^2)
1107 LET COEEQ(6,1)= -1
1108 LET COEEQ(6,2)= 1
1109 LET COEEQ(6,7)= -1/(b^2)
1110 LET COEEQ(6,8)= 1/(b^2)
1111 LET COEEQ(7,4)= -MK4
1112 LET COEEQ(7,5)= GK2
1113 LET COEEQ(7,9)= MK4*(1-2*Vm)/(b^2)
1114 LET COEEQ(7,10)= -GK2*(1-2*Vg)/(b^2)
1115 LET COEEQ(7,11)= (GK2*Vg)-(MK4*Vm)
1117 LET COEEQ(8,4)= -1
1118 LET COEEQ(8,5)= 1
1119 LET COEEQ(8,9)= -1/(b^2)
1120 LET COEEQ(8,10)= 1/(b^2)
1121 LET COEEQ(9,1)= 2*BK1*Vb*AB
1122 LET COEEQ(9,2)= 2*GK1*Vg*AG
1123 LET COEEQ(9,3)= 2*SK31*Vs*AS
1124 LET COEEQ(9,4)= -2*MK4*Vm*AM
1125 LET COEEQ(9,5)= -2*GK2*Vg*AG
1126 LET COEEQ(9,6)= -2*SK32*Vs*AS
1127 LET COEEQ(9,11)= (-MK4*AM*(1-Vm))-(GK2*AG*(1-Vg))-(SK32*AS*(1-Vs))
1128 LET COEEQ(10,1)= BK1*Tb
1129 LET COEEQ(10,4)= MK4*Tm
1130 LET COEEQ(10,7)= -BK1*Tb*(1-2*Vb)/(c^2)
1131 LET COEEQ(10,9)= -MK4*Tm*(1-2*Vm)/(c^2)
1132 LET COEEQ(10,11)= MK4*Tm*Vm
1133 LET COEEQ(11,1)= 1
1134 LET COEEQ(11,4)= -1
1135 LET COEEQ(11,7)= 1/(c^2)
1136 LET COEEQ(11,9)= -1/(c^2)
1137 END SUB
1138 SUB FILLCONSEQ
1139 LET CONSEQ(1)= ((SK31*Vs-GK1*Vg)*E(J))+(GK1*ESG*(1+Vg))
1140 LET CONSEQ(2)= GK2*ESG*(1+Vg)
1141 LET CONSEQ(3)= ESG
1142 LET CONSEQ(4)= ESG
1143 LET CONSEQ(5)= (E(J)*(BK1*Vb-GK1*Vg))+(GK1*ESG*(1+Vg))-(BK1*ESB*(1+Vb))
```

```
1144 LET CONSEQ(6)= ESG-ESB
1145 LET CONSEQ(7)= (GK2*ESG*(1+Vg))-(MK4*ESM*(1+Vm))
1146 LET CONSEQ(8)= ESG-ESM
1147 LET CONSEQ(9)= (BK1*AB*ESB*(1+Vb))-(MK4*AM*ESM*(1+Vm))-(E(J)*(BK1*AB*(1-Vb)+GK1*AG
K31*AS*(1-Vs)))+(AG*GK1*ESG*(1+Vg))-(AG*GK2*ESG*(1+Vg))
1150 LET CONSEQ(10)= (MK4*Tm*ESM*(1+Vm))+(BK1*Tb*ESB*(1+Vb))-(BK1*Tb*Vb*E(J))
1155 LET CONSEQ(11)= ESB-ESM
1160 END SUB
1165 SUB SUSCOEEQ
1170 MAT SCOEEQ =ZER
1175 LET SCOEEQ (1,2)= GK1
1180 LET SCOEEQ (1,3)= -SK31
1185 LET SCOEEQ(1,8)= -GK1*(1-2*Vg)/(a^2)
1186 LET SCOEEQ(1,12)= Vg*GK1-Vs*SK31
1190 LET SCOEEQ(2,5)= GK2
1193 LET SCOEEQ(2,6)= -SK32
1194 LET SCOEEQ(2,10)= -GK2*(1-2*Vg)/(a^2)
1195 LET SCOEEQ(2,11)= (GK2*Vg)-(SK32*Vs)
1197 LET SCOEEQ(3,2)= 1
1198 LET SCOEEQ(3,3)= -1
1199 LET SCOEEQ(3,8)= 1/(a^2)
1200 LET SCOEEQ(4,5)= 1
1201 LET SCOEEQ(4,6)= -1
1202 LET SCOEEQ(4,10)= 1/(a^2)
1203 LET SCOEEQ(5,1)= -BK1
1204 LET SCOEEQ(5,2)= GK1
1205 LET SCOEEQ(5,7)= BK1*(1-2*Vb)/(b^2)
1206 LET SCOEEQ(5,8)= -GK1*(1-2*Vg)/(b^2)
1207 LET SCOEEQ(5,12)= GK1*Vg-BK1*Vb
1208 LET SCOEEQ(6,1)= -1
1209 LET SCOEEQ(6,2)= 1
1210 LET SCOEEQ(6,7)= -1/(b^2)
1211 LET SCOEEQ(6,8)= 1/(b^2)
1212 LET SCOEEQ(7,4)= -MK4
1213 LET SCOEEQ(7,5)= GK2
1214 LET SCOEEQ(7,9)= MK4*(1-2*Vm)/(b^2)
1215 LET SCOEEQ(7,10)= -GK2*(1-2*Vg)/(b^2)
1216 LET SCOEEQ(7,11)= (GK2*Vg)-(MK4*Vm)
1217 LET SCOEEQ(8,4)= -1
1218 LET SCOEEQ(8,5)= 1
1219 LET SCOEEQ(8,9)= -1/(b^2)
1220 LET SCOEEQ(8,10)= 1/(b^2)
1221 LET SCOEEQ(9,1)= 2*BK1*Vb*AB
1222 LET SCOEEQ(9,2)= 2*GK1*Vg*AG
1223 LET SCOEEQ(9,3)= 2*SK31*Vs*AS
1227 LET SCOEEQ(9,12)= BK1*AB*(1-VB)+GK1*AG*(1-Vg)+SK31*AS*(1-Vs)
1228 LET SCOEEQ(10,1)= BK1*Tb
1229 LET SCOEEQ(10,4)= MK4*Tm
1230 LET SCOEEQ(10,7)= -BK1*Tb*(1-2*Vb)/(c^2)
1231 LET SCOEEQ(10,9)= -MK4*Tm*(1-2*Vm)/(c^2)
1232 LET SCOEEQ(10,11)= MK4*Tm*Vm
1233 LET SCOEEQ(10,12)= BK1*Tb*Vb
1234 LET SCOEEQ(11,1)= 1
1235 LET SCOEEQ(11,4)= -1
```

```
1236 LET SCOEEQ(11,7)= 1/(c^2)
1237 LET SCOEEQ(11,9)= -1/(c^2)
1238 LET SCOEEQ(12,4)= 2*MK4*Vm*AM
1239 LET SCOEEQ(12,5)= 2*GK2*AG*Vg
1240 LET SCOEEQ(12,6)= 2*SK32*Vs*AS
1241 LET SCOEEQ(12,11)= MK4*AM*(1-Vm)+GK2*AG*(1-Vg)+SK32*AS*(1-Vs)
1245 END SUB
1248 SUB SUSCONSEQ
1249 LET SCONSEQ(1)= GK1*ESG*(1+Vg)
1250 LET SCONSEQ(2)= GK2*ESG*(1+Vg)
1251 LET SCONSEQ(3)= ESG
1252 LET SCONSEQ(4)= ESG
1253 LET SCONSEQ(5)= GK1*ESG*(1+Vg)-(BK1*ESB*(1+Vb))
1254 LET SCONSEQ(6)= ESG-ESB
1255 LET SCONSEQ(7)= (GK2*ESG*(1+Vg))-(MK4*ESM*(1+Vm))
1260 LET SCONSEQ(8)= ESG-ESM
1265 LET SCONSEQ(9)= (PSUS*1000)+(BK1*AB*ESB*(1+Vb))+(GK1*AG*(1+Vg)*ESG)
1270 LET SCONSEQ(10)= (MK4*Tm*ESM*(1+Vm))+(BK1*Tb*ESB*(1+Vb))
1275 LET SCONSEQ(11)= ESB-ESM
1276 LET SCONSEQ(12)= (PSUS*1000)+(MK4*AM*(1+Vm)*ESM)+(AG*GK2*(1+Vg)*ESG)
1280 END SUB
1285 SUB CREEPCOEEQ
1290 MAT CCOEEQ =ZER
1295 LET CCOEEQ (1,2)= GK1*(1+CG)
1300 LET CCOEEQ (1,3)= -SK31
1305 LET CCOEEQ(1,8)= -GK1*(1+CG)*(1-2*Vg)/(a^2)
1310 LET CCOEEQ(1,11)= (Vg*GK1/(1+CG))-Vs*SK31
1315 LET CCOEEQ(2,5)= GK2*(1+CG)
1320 LET CCOEEQ(2,6)= -SK32
1325 LET CCOEEQ(2,10)= -GK2*(1+CG)*(1-2*Vg)/(a^2)
1330 LET CCOEEQ(2,12)= (GK2*Vg/(1+CG))-SK32*Vs
1335 LET CCOEEQ(3,2)= 1+CG
1340 LET CCOEEQ(3,3)= -1
1345 LET CCOEEQ(3,8)= (1+CG)/(a^2)
1350 LET CCOEEQ(4,5)= 1+CG
1355 LET CCOEEQ(4,6)= -1
1360 LET CCOEEQ(4,10)= (1+CG)/(a^2)
1365 LET CCOEEQ(5,1)= -BK1*(1+CB)
1370 LET CCOEEQ(5,2)= GK1*(1+CG)
1375 LET CCOEEQ(5,7)= BK1*(1+CB)*(1-2*Vb)/(b^2)
1380 LET CCOEEQ(5,8)= -GK1*(1+CG)*(1-2*Vg)/(b^2)
1385 LET CCOEEQ(5,11)= ((GK1*Vg)/(1+CG))-((BK1*Vb)/(1+CB))
1390 LET CCOEEQ(6,1)= -(1+CB)
1395 LET CCOEEQ(6,2)= 1+CG
1400 LET CCOEEQ(6,7)= -(1+CB)/(b^2)
1405 LET CCOEEQ(6,8)= (1+CG)/(b^2)
1410 LET CCOEEQ(7,4)= -MK4*(1+CM)
1415 LET CCOEEQ(7,5)= GK2*(1+CG)
1420 LET CCOEEQ(7,9)= MK4*(1+CM)*(1-2*Vm)/(b^2)
1425 LET CCOEEQ(7,10)= -GK2*(1+CG)*(1-2*Vg)/(b^2)
1430 LET CCOEEQ(7,12)= ((GK2*Vg)/(1+CG))-((MK4*Vm)/(1+CM))
1435 LET CCOEEQ(8,4)= -(1+CM)
1440 LET CCOEEQ(8,5)= 1+CG
1445 LET CCOEEQ(8,9)= -(1+CM)/(b^2)
```

```
1450 LET CCOEEQ(8,10)= (1+CG)/(b^2)
1455 LET CCOEEQ(9,1)= 2*BK1*Vb*AB*(1+CB)
1460 LET CCOEEQ(9,2)= 2*GK1*Vg*AG*(1+CG)
1465 LET CCOEEQ(9,3)= 2*SK31*Vs*AS
1470 LET CCOEEQ(9,11)= (BK1*AB*(1-VB)/(1+CB))+(GK1*AG*(1-Vg)/(1+CG))+(SK31*AS*(1-Vs))
1475 LET CCOEEQ(10,4)= 2*AM*MK4*Vm*(1+CM)
1480 LET CCOEEQ(10,5)= 2*AG*GK2*Vg*(1+CG)
1485 LET CCOEEQ(10,6)= 2*AS*SK32*Vs
1490 LET CCOEEQ(10,12)= (MK4*AM*(1-Vm)/(1+CM))+(GK2*AG*(1-Vg)/(1+CG))+(AS*SK32*(1-Vs))
1495 LET CCOEEQ(11,1)= Tb*BK1*(1+CB)
1500 LET CCOEEQ(11,4)= Tm*MK4*(1+CM)
1505 LET CCOEEQ(11,7)= -BK1*Tb*(1+CB)*(1-2*Vb)/(c^2)
1510 LET CCOEEQ(11,9)= -MK4*Tm*(1+CM)*(1-2*Vm)/(c^2)
1515 LET CCOEEQ(11,11)= Tb*BK1*Vb/(1+CB)
1520 LET CCOEEQ(11,12)= Tm*MK4*Vm/(1+CM)
1525 LET CCOEEQ(12,1)= 1+CB
1530 LET CCOEEQ(12,4)= -(1+CM)
1535 LET CCOEEQ(12,7)= (1+CB)/(c^2)
1540 LET CCOEEQ(12,9)= -(1+CM)/(c^2)
1545 END SUB
1548 SUB CREEPCONSEQ
1549 LET CCONSEQ(1)= GK1*(ESG+ESGT)-(GK1*Vg*(EI-ESG-ESGT)/(1+CG))+(SK31*Vs*EI)
1550 LET CCONSEQ(2)= GK2*(ESG+ESGT)-(GK2*Vg*(EI1-ESG-ESGT)/(1+CG))+(SK32*Vs*EI1)
1551 LET CCONSEQ(3)= ESG+ESGT
1552 LET CCONSEQ(4)= ESG+ESGT
1553 LET CCONSEQ(5)= GK1*(ESG+ESGT)-(GK1*Vg*(EI-ESG-ESGT)/(1+CG))-(BK1*(ESB+ESBT))+(BI
ESB-ESBT)/(1+CB))
1554 LET CCONSEQ(6)= (ESG+ESGT)-(ESB+ESBT)
1555 LET CCONSEQ(7)= GK2*(ESG+ESGT)-(GK2*Vg*(EI1-ESG-ESGT)/(1+CG))-(MK4*(ESM+ESMT))+(
EI1-ESM-ESMT)/(1+CM))
1560 LET CCONSEQ(8)= (ESG+ESGT)-(ESM+ESMT)
1565 LET CCONSEQ(9)= (-AB*BK1*(1-Vb)*(EI-ESB-ESBT)/(1+CB))+(2*BK1*AB*Vb*(ESB+ESBT))+(A
AG*GK1*(1-Vg)*(EI-ESG-ESGT)/(1+CG))+(2*GK1*AG*Vg*(ESG+ESGT))+(AG*FYG1I)-(AS*SK31*(1-Vs)*E
S1I)
1570 LET CCONSEQ(10)= (-AM*MK4*(1-Vm)*(EI1-ESM-ESMT)/(1+CM))+(2*MK4*AM*Vm*(ESM+ESMT
MI)-(AG*GK2*(1-Vg)*(EI1-ESG-ESGT)/(1+CG))+(2*GK2*AG*Vg*(ESG+ESGT))+(AG*FYG2I)-(AS*SK32*(1
+(AS*FYS2I)
1575 LET CCONSEQ(11)= (Tb*BK1*(ESB+ESBT))-(Tb*BK1*Vb*(EI-ESB-ESBT)/(1+CB))+(Tm*MK4*(E
)-(Tm*MK4*Vm*(EI1-ESM-ESMT)/(1+CM))
1576 LET CCONSEQ(12)= (ESB+ESBT)-(ESM+ESMT)
1580 END SUB
1581 SUB FOLLOWINGCREEPCOEEQ
1582 MAT FCOEEQ =ZER
1583 LET FCOEEQ (1,2)= GK1
1584 LET FCOEEQ (1,3)= -SK31
1585 LET FCOEEQ(1,8)= -GK1*(1-2*Vg)/(a^2)
1586 LET FCOEEQ(2,5)= GK2
1587 LET FCOEEQ(2,6)= -SK32
1589 LET FCOEEQ(2,10)= -GK2*(1-2*Vg)/(a^2)
1590 LET FCOEEQ(2,11)= (GK2*Vg)-(SK32*Vs)
1591 LET FCOEEQ(3,2)= 1
1592 LET FCOEEQ(3,3)= -1
1593 LET FCOEEQ(3,8)= 1/(a^2)
1594 LET FCOEEQ(4,5)= 1
```

```
1595 LET FCOEEQ(4,6)= -1
1596 LET FCOEEQ(4,10)= 1/(a^2)
1597 LET FCOEEQ(5,1)= -BK1
1599 LET FCOEEQ(5,2)= GK1
1600 LET FCOEEQ(5,7)= BK1*(1-2*Vb)/(b^2)
1601 LET FCOEEQ(5,8)= -GK1*(1-2*Vg)/(b^2)
1602 LET FCOEEQ(6,1)= -1
1603 LET FCOEEQ(6,2)= 1
1604 LET FCOEEQ(6,7)= -1/(b^2)
1605 LET FCOEEQ(6,8)= 1/(b^2)
1606 LET FCOEEQ(7,4)= -MK4
1607 LET FCOEEQ(7,5)= GK2
1608 LET FCOEEQ(7,9)= MK4*(1-2*Vm)/(b^2)
1609 LET FCOEEQ(7,10)= -GK2*(1-2*Vg)/(b^2)
1610 LET FCOEEQ(7,11)= (GK2*Vg)-(MK4*Vm)
1611 LET FCOEEQ(8,4)= -1
1612 LET FCOEEQ(8,5)= 1
1613 LET FCOEEQ(8,9)= -1/(b^2)
1614 LET FCOEEQ(8,10)= 1/(b^2)
1615 LET FCOEEQ(9,1)= 2*BK1*Vb*AB
1616 LET FCOEEQ(9,2)= 2*GK1*Vg*AG
1617 LET FCOEEQ(9,3)= 2*SK31*Vs*AS
1618 LET FCOEEQ(9,4)= -2*MK4*Vm*AM
1619 LET FCOEEQ(9,5)= -2*GK2*Vg*AG
1620 LET FCOEEQ(9,6)= -2*SK32*Vs*AS
1621 LET FCOEEQ(9,11)= (-MK4*AM*(1-Vm))-(GK2*AG*(1-Vg))-(SK32*AS*(1-Vs))
1622 LET FCOEEQ(10,1)= BK1*Tb
1623 LET FCOEEQ(10,4)= MK4*Tm
1624 LET FCOEEQ(10,7)= -BK1*Tb*(1-2*Vb)/(c^2)
1625 LET FCOEEQ(10,9)= -MK4*Tm*(1-2*Vm)/(c^2)
1626 LET FCOEEQ(10,11)= MK4*Tm*Vm
1627 LET FCOEEQ(11,1)= 1
1628 LET FCOEEQ(11,4)= -1
1629 LET FCOEEQ(11,7)= 1/(c^2)
1630 LET FCOEEQ(11,9)= -1/(c^2)
1631 END SUB
1632 SUB FOLLOWINGCREEPCONSEQ
1633 LET FCONSEQ(1)= (SK31*Vs*E(J))+GK1*((ESG+ESGT)-(1-Vg)*ECG1RINSIDE-Vg*(E(J)-ECG1-ES
-(GK1*Vg*ECG1TINSIDE)
1640 LET FCONSEQ(2)= GK2*((ESG+ESGT)-(1-Vg)*ECG2RINSIDE-Vg*ECG2TINSIDE-Vg*(-ECG2-ESG
1641 LET FCONSEQ(3)= ESG+ESGT-ECG1RINSIDE
1642 LET FCONSEQ(4)= ESG+ESGT-ECG2RINSIDE
1643 LET FCONSEQ(5)= GK1*(ESG+ESGT-(1-Vg)*ECG1REDGE-Vg*ECG1TEDGE-Vg*(E(J)-ECG1-ESG-
K1*(-(ESB+ESBT)+(1-Vb)*ECBRINSIDE+Vb*ECBTINSIDE+Vb*(E(J)-ECB-ESB-ESBT))
1644 LET FCONSEQ(6)= ESG+ESGT-ECG1REDGE-(ESB+ESBT)+ECBRINSIDE
1645 LET FCONSEQ(7)= GK2*(ESG+ESGT-(1-Vg)*ECG2REDGE-Vg*ECG2TEDGE-Vg*(-ECG2-ESG-ESG
(-(ESM+ESMT)+Vm*(-ECM-ESM-ESMT)+(1-Vm)*ECMRINSIDE+Vm*ECMTINSIDE)
1646 LET FCONSEQ(8)= ESG+ESGT-ECG2REDGE-(ESM+ESMT)+ECMRINSIDE
1647 LET FCONSEQ(9)= BK1*AB*(-(1-Vb)*(E(J)-ECB-ESB-ESBT)+2*Vb*(ESB+ESBT)-Vb*(ECBRINSI
INSIDE))+AG*GK1*(-(1-Vg)*(E(J)-ECG1-ESG-ESGT)+2*Vg*(ESG+ESGT)-Vg*(ECG1RINSIDE+ECG1TINSI
SK31*(-(1-Vs)*E(J))+MK4*AM*((1-Vm)*(-ECM-ESM-ESMT)-2*Vm*(ESM+ESMT)+Vm*(ECMRINSIDE+ECM
))+GK2*AG*((1-Vg)*(-ECG2-ESG-ESGT)-2*Vg*(ESG+ESGT)+Vg*(ECG2RINSIDE+ECG2TINSIDE))
1650 LET FCONSEQ(10)= BK1*Tb*(ESB+ESBT-Vb*(E(J)-ECB-ESB-ESBT)-(1-Vb)*ECBREDGE-Vb*EC
+MK4*Tm*(ESM+ESMT-Vm*(-ECM-ESM-ESMT)-(1-Vm)*ECMREDGE-Vm*ECMTEDGE)
1655 LET FCONSEQ(11)= ESB+ESBT-ECBREDGE-(ESM+ESMT)+ECMREDGE
```

```
1660 END SUB
9800 PAUSE 20
9900 END
```

APPENDIX D

Predicted Time-Dependent Deformation

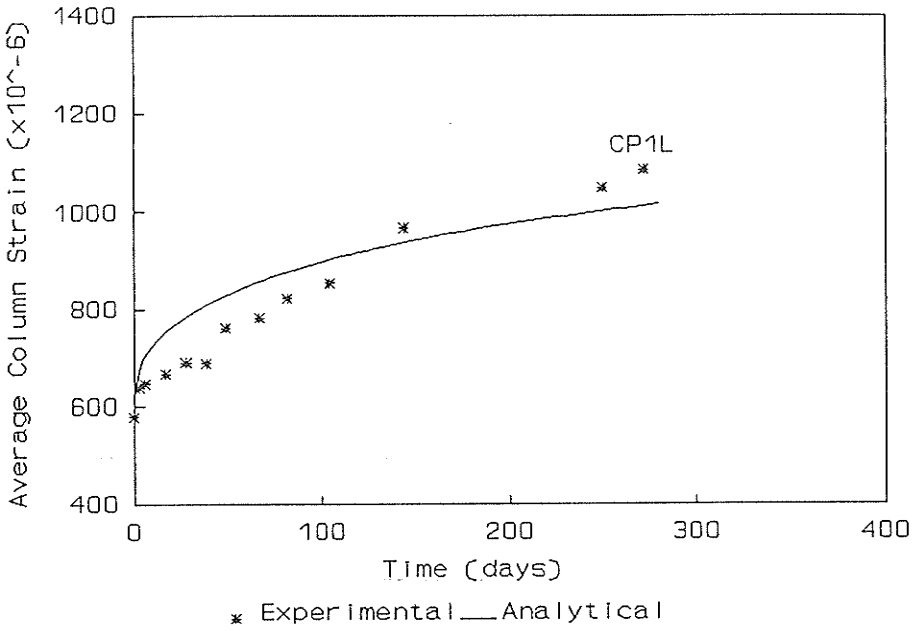

Figure D.1 Predicted time-dependent deformation (preloaded column CP1L)

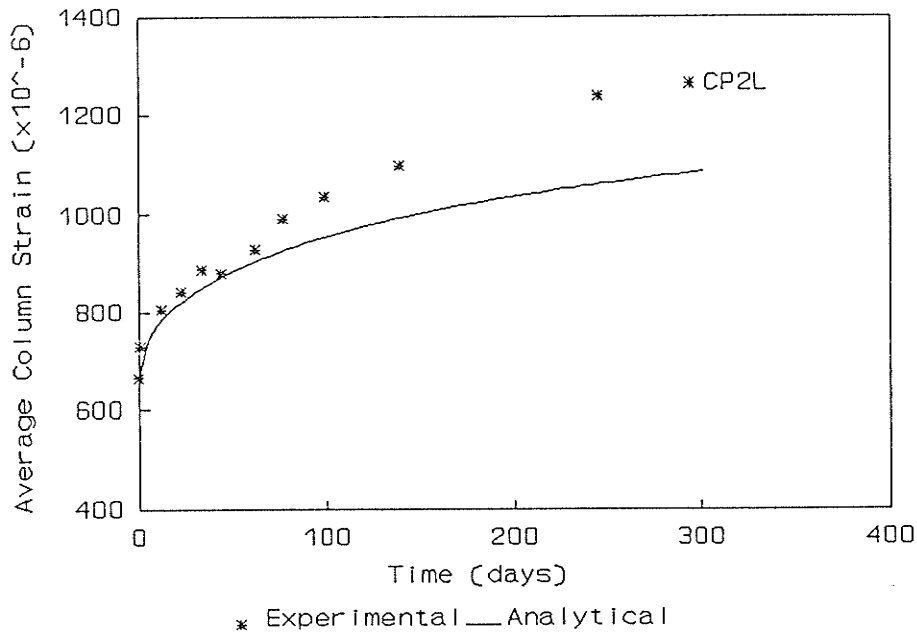

Figure D.2 Predicted time-dependent deformation (preloaded column CP2L)

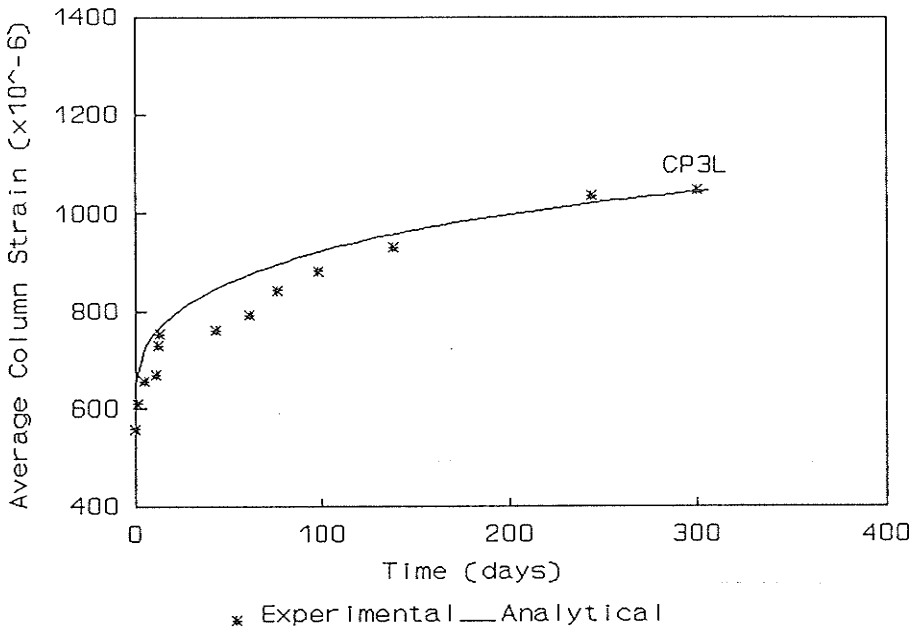

Figure D.3 Predicted time-dependent deformation (preloaded column CP3L)

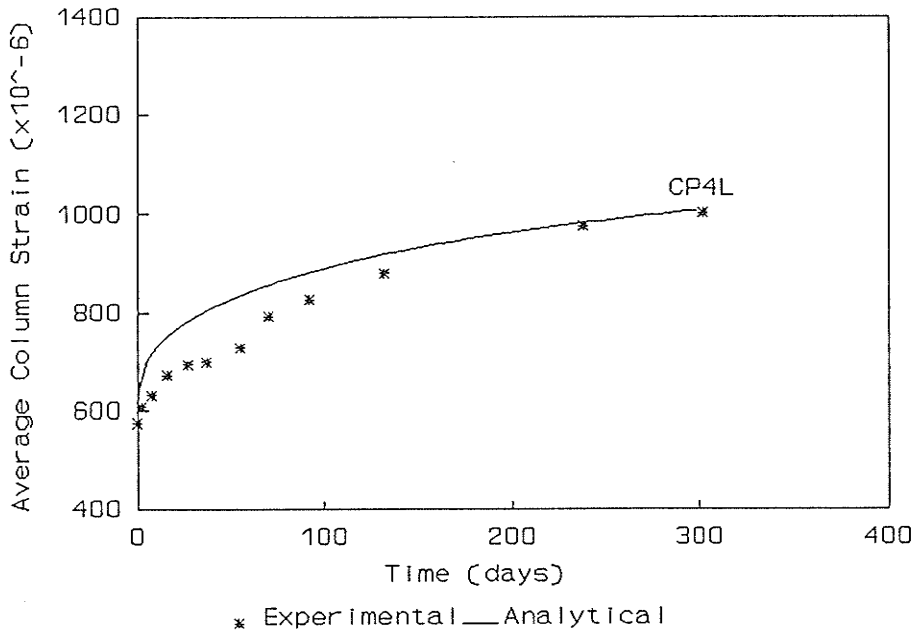

Figure D.4 Predicted time-dependent deformation (preloaded column CP4L)

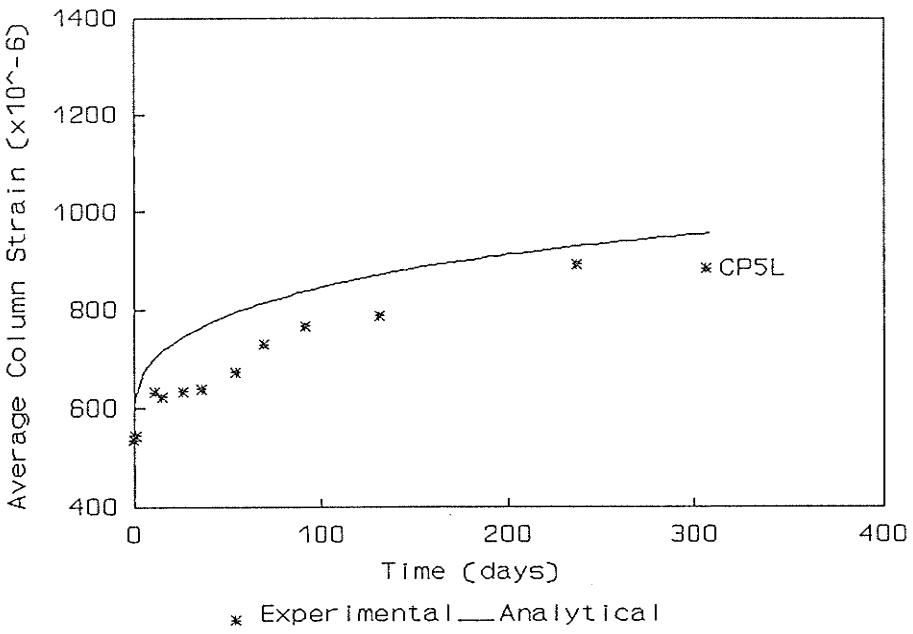

Figure D.5 Predicted time-dependent deformation (preloaded column CP5L)

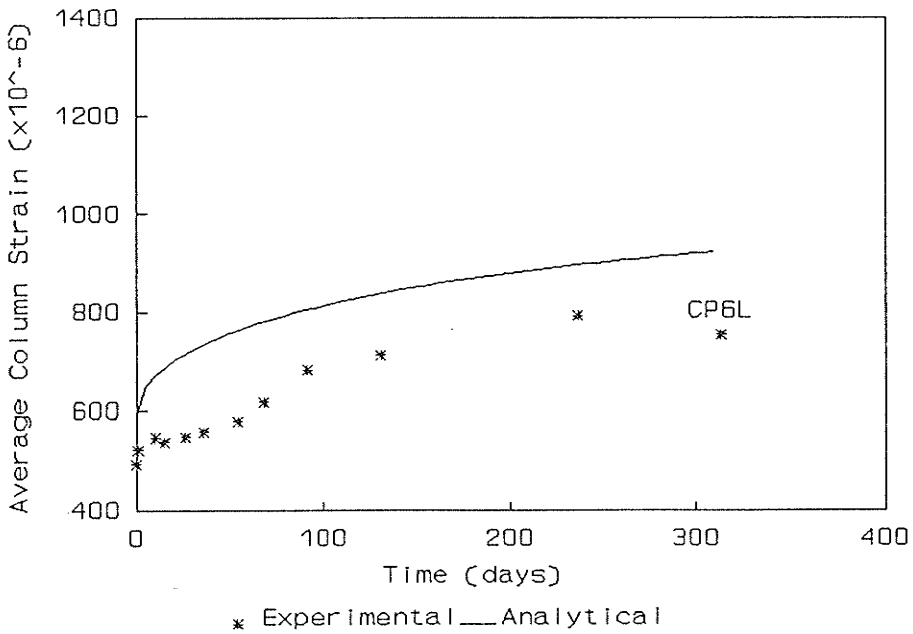

Figure D.6 Predicted time-dependent deformation (preloaded column CP6L)

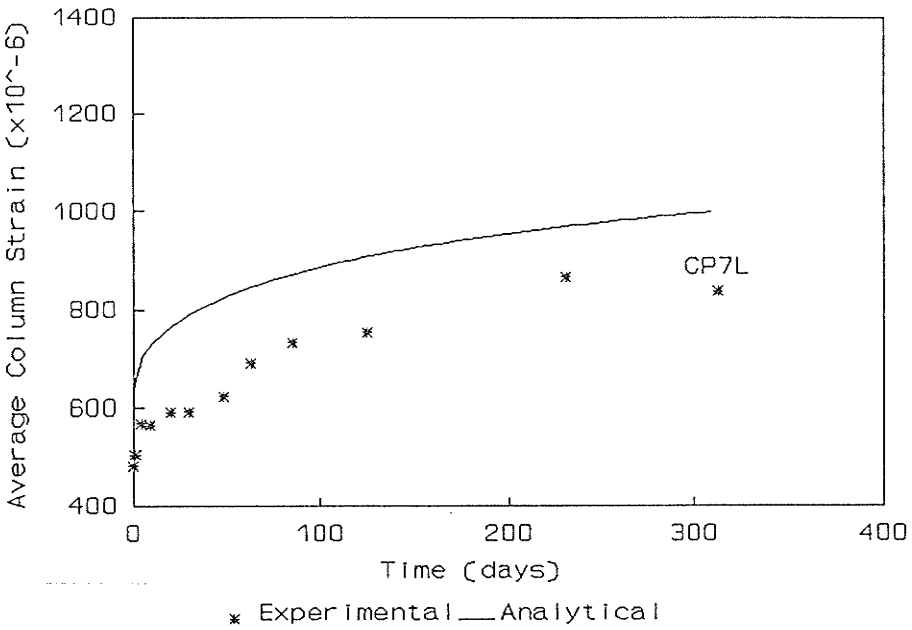

Figure D.7 Predicted time-dependent deformation (preloaded column CP7L)

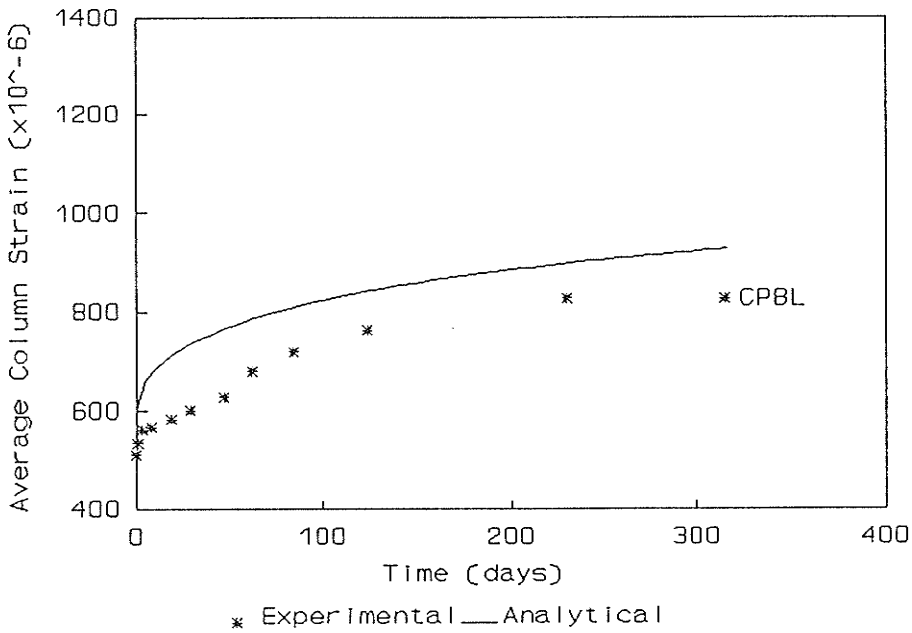

Figure D.8 Predicted time-dependent deformation (preloaded column CP8L)

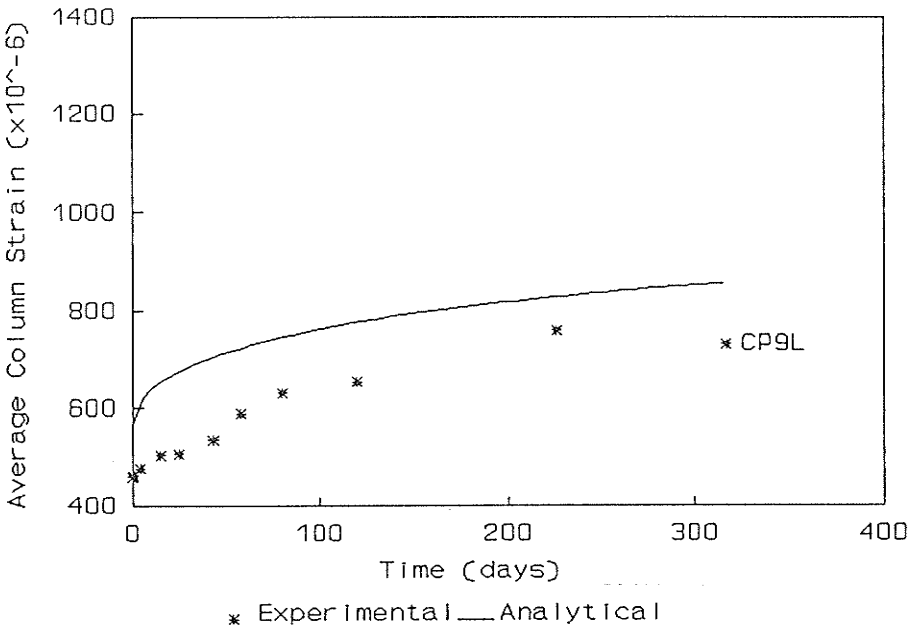

Figure D.9 Predicted time-dependent deformation (preloaded column CP9L)

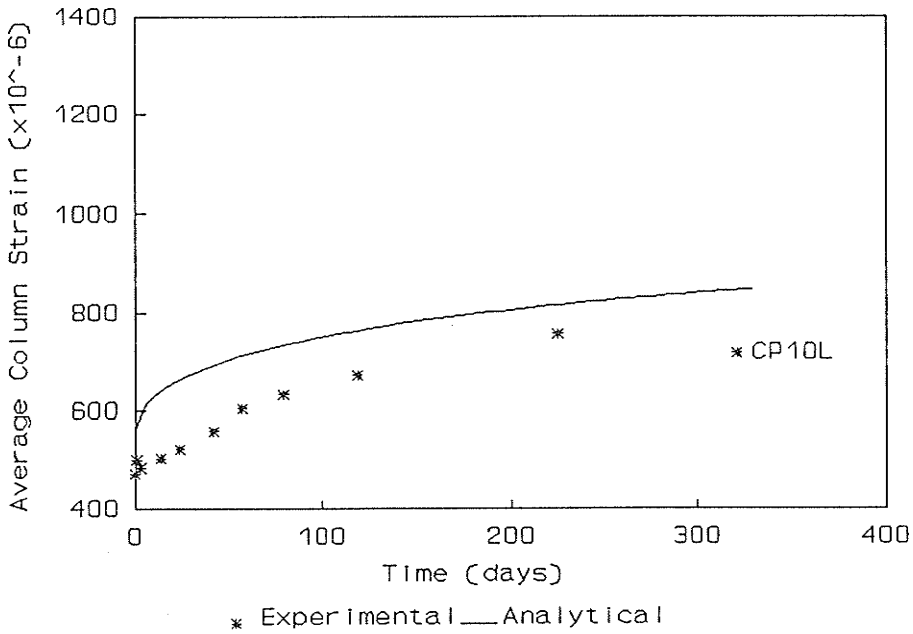

Figure D.10 Predicted time-dependent deformation (preloaded column CP10L)

APPENDIX E

Predicted Load-Strain Behavior (Preloaded Columns)

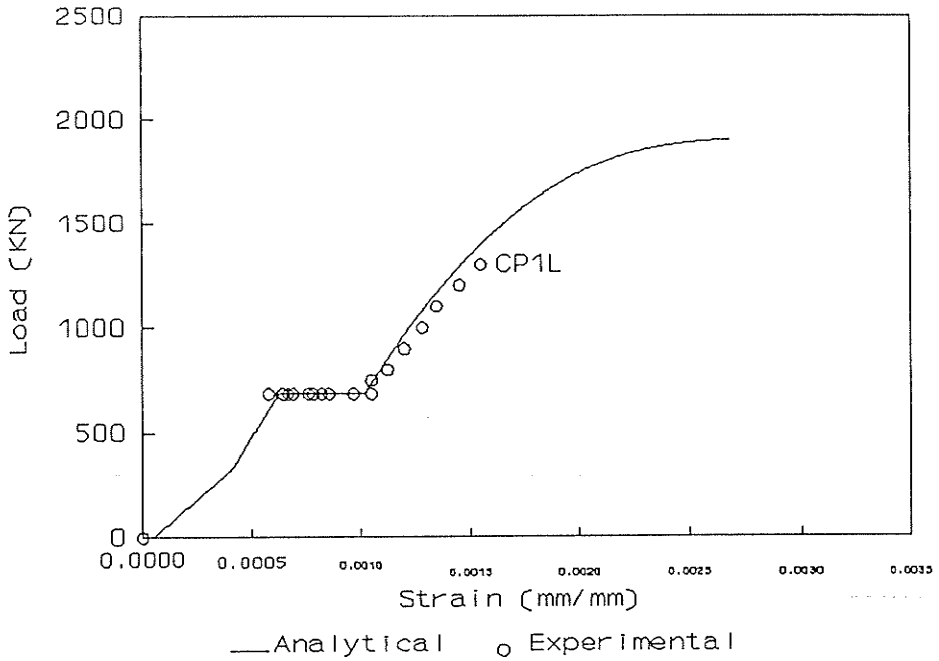

Figure E.1 Predicted load-strain behavior
(preloaded column CP1L)

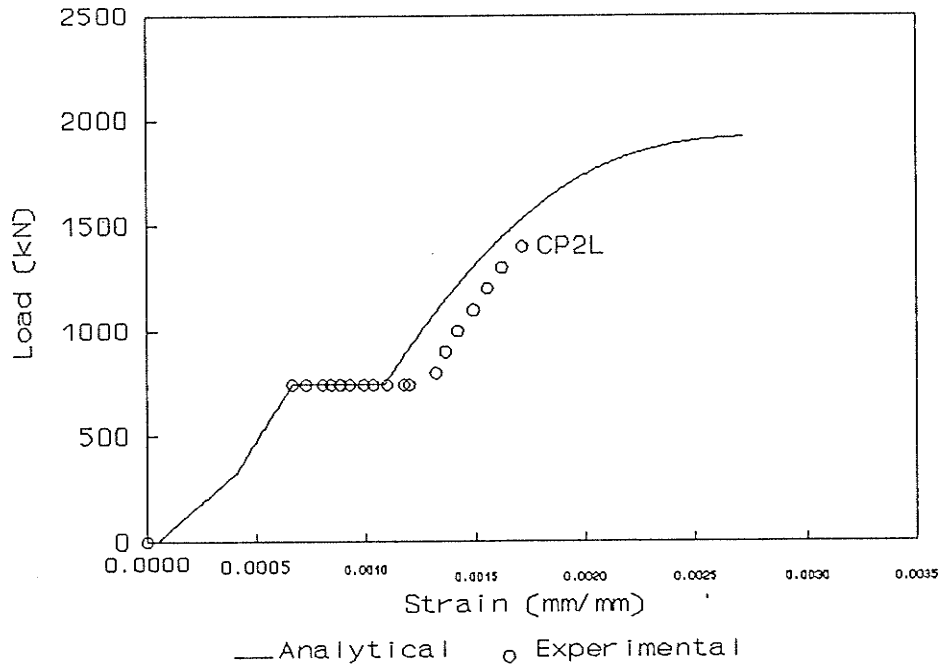

Figure E.2 Predicted load-strain behavior
(preloaded column CP2L)

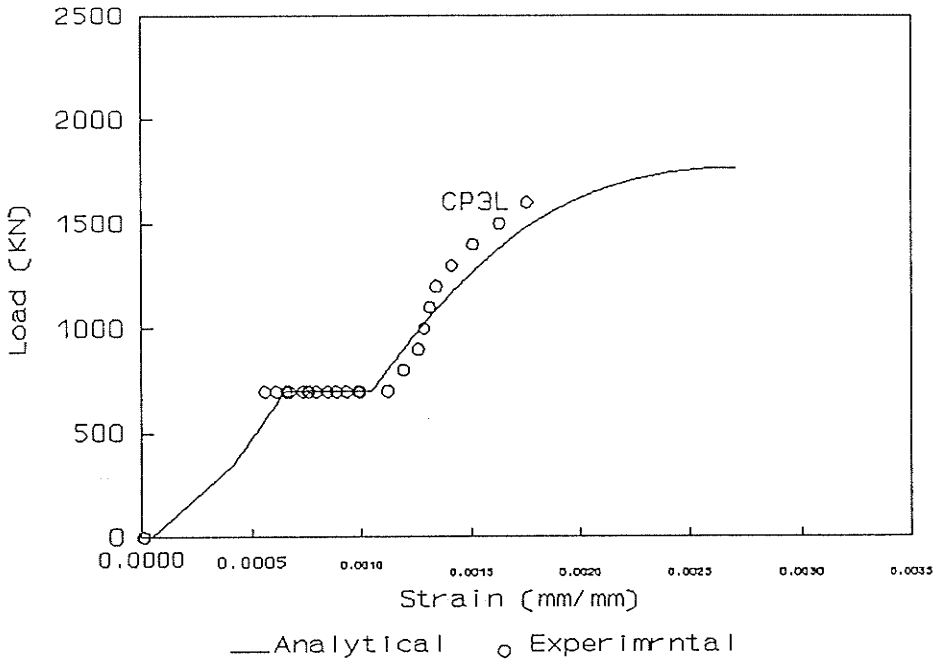

Figure E.3 Predicted load-strain behavior
(preloaded column CP3L)

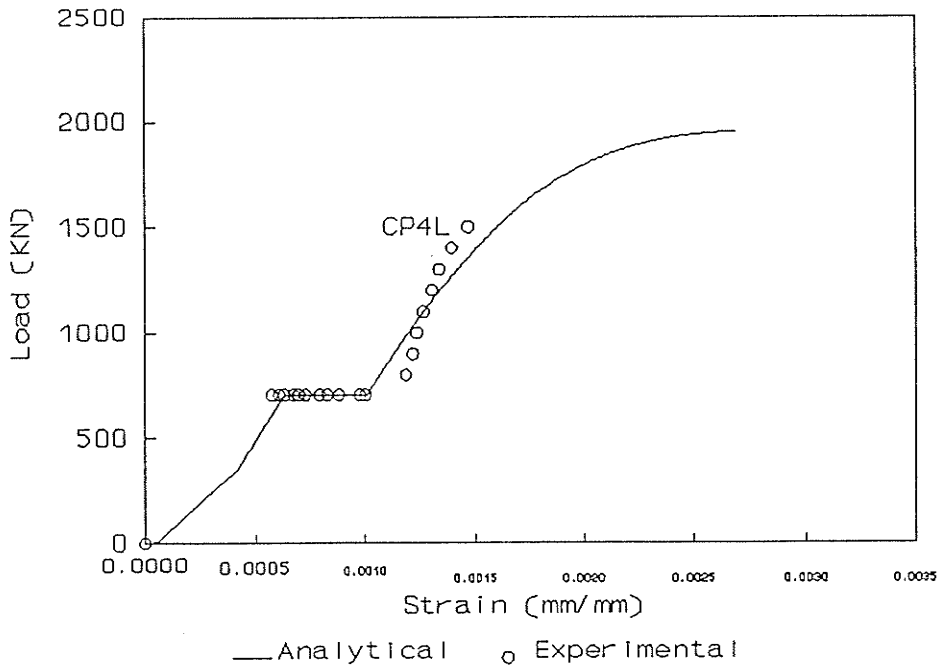

Figure E.4 Predicted load-strain behavior
(preloaded column CP4L)

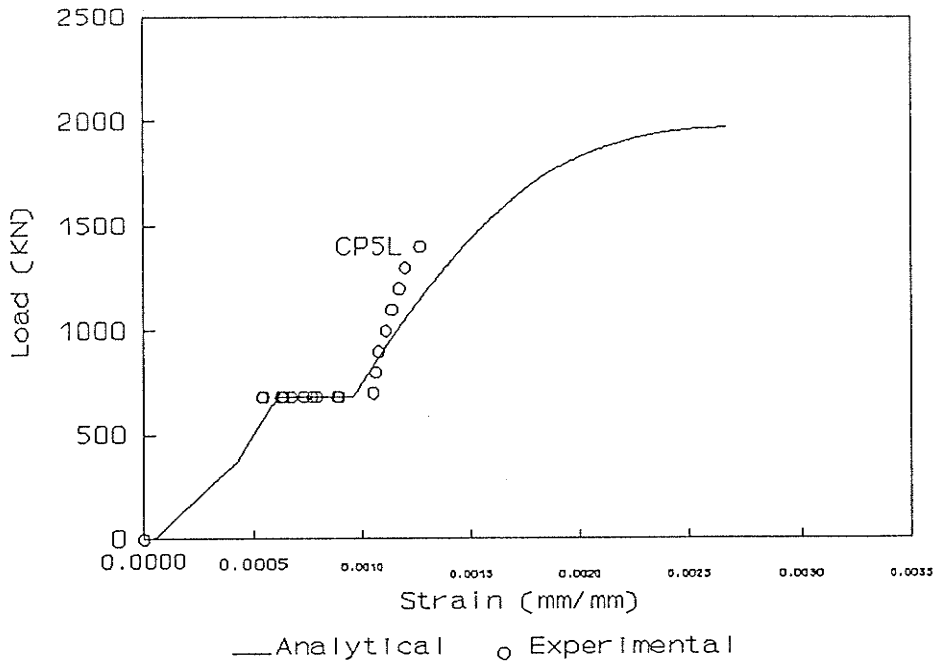

Figure E.5 Predicted load-strain behavior
(preloaded column CP5L)

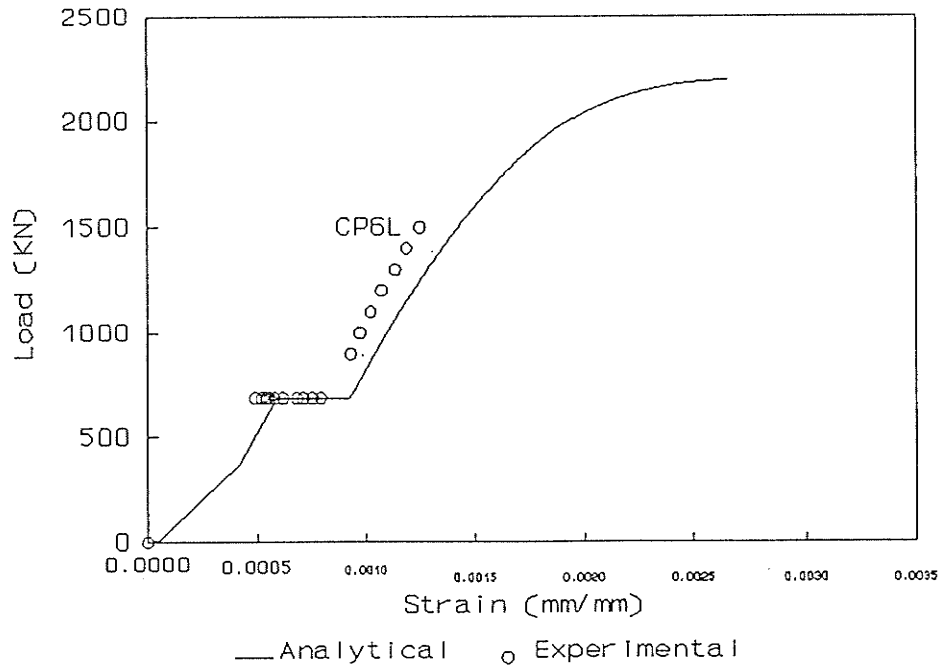

Figure E.6 Predicted load-strain behavior
(preloaded column CP6L)

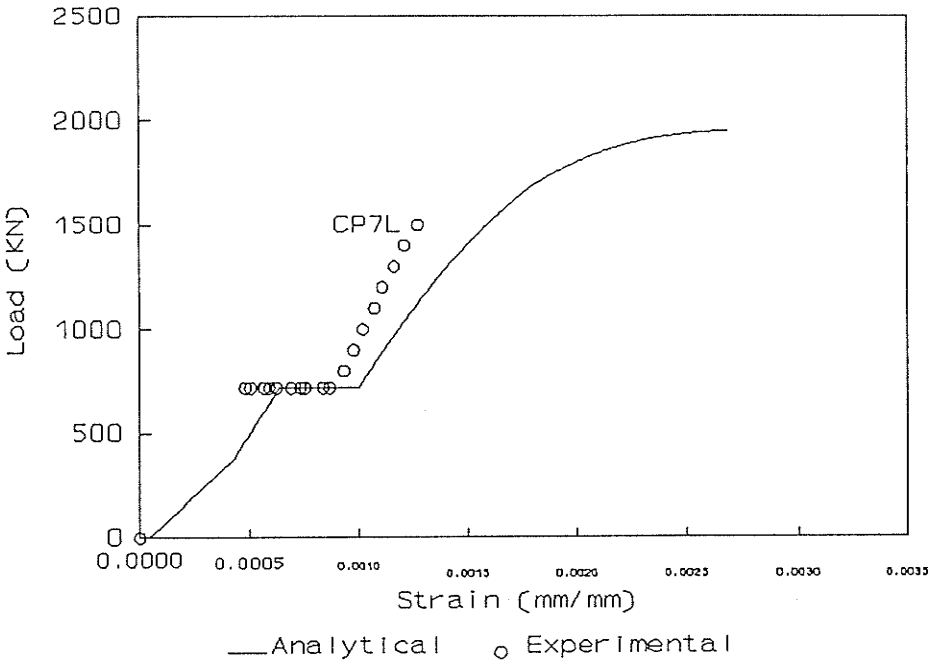

Figure E.7 Predicted load-strain behavior
(preloaded column CP7L)

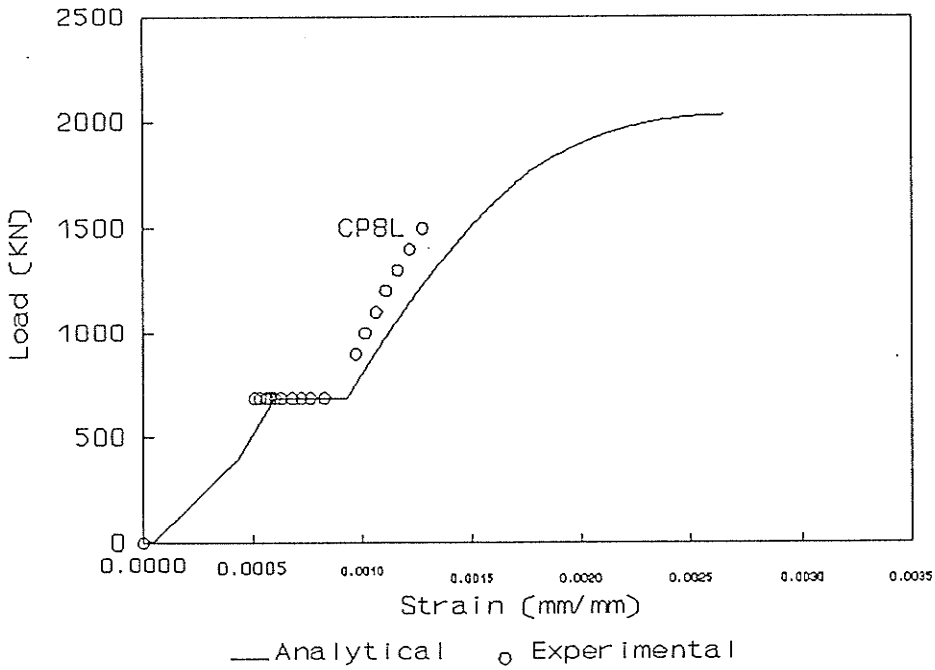

Figure E.8 Predicted load-strain behavior
(preloaded column CP8L)

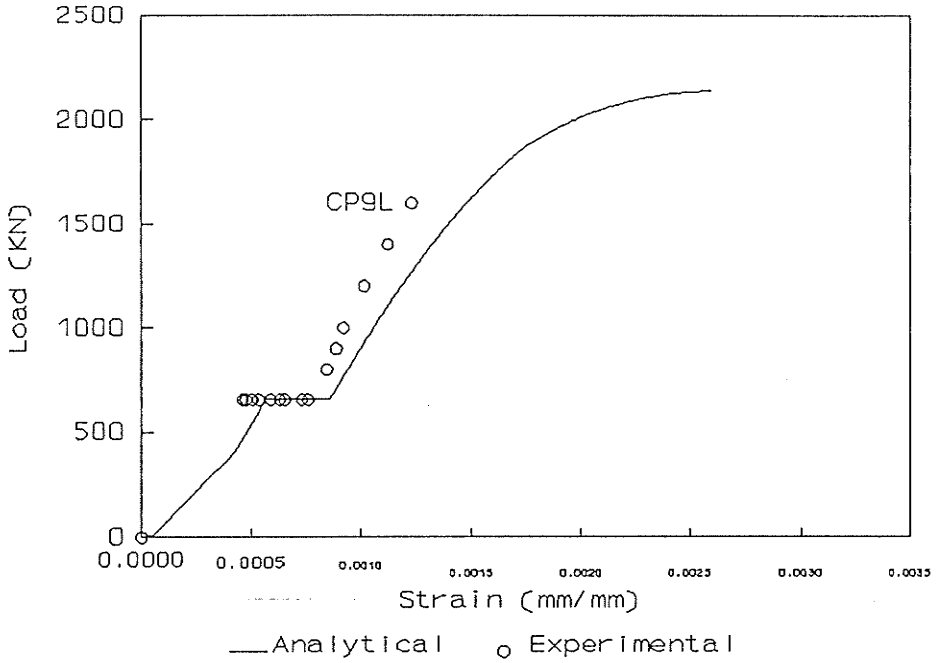

Figure E.9 Predicted load-strain behavior
(preloaded column CP9L)

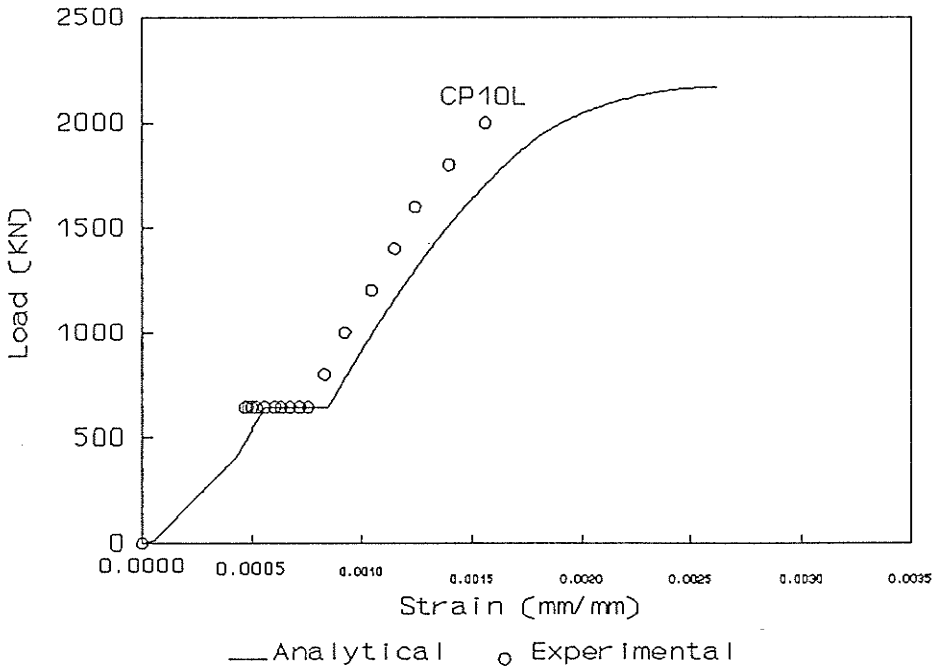

Figure E.10 Predicted load-strain behavior
(preloaded column CP10L)

APPENDIX F

Predicted Load-Strain Behavior (Non-Preloaded Columns)

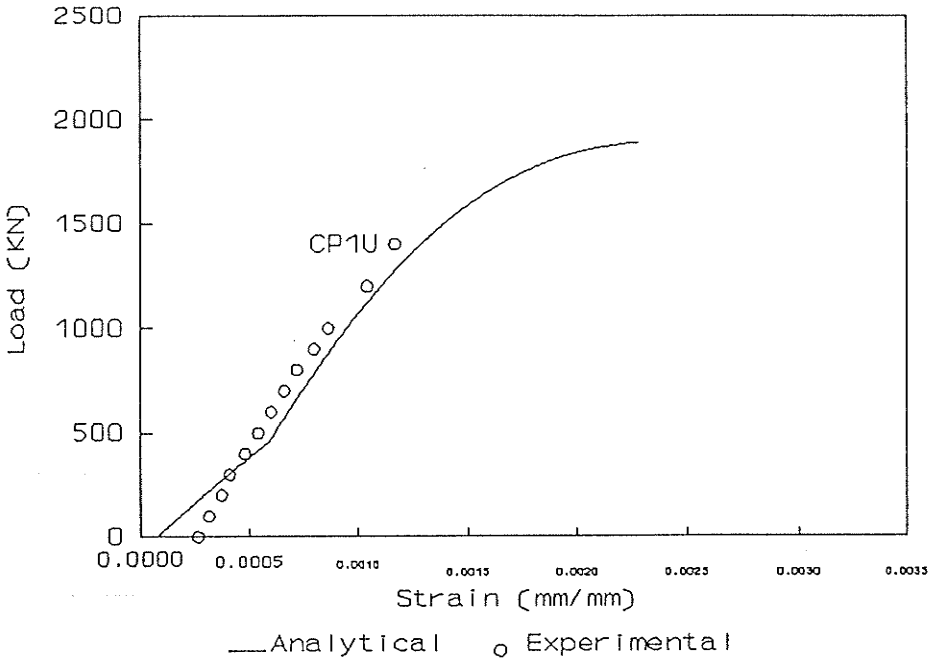

Figure F.1 Predicted load-strain behavior
(non-preloaded column CP1U)

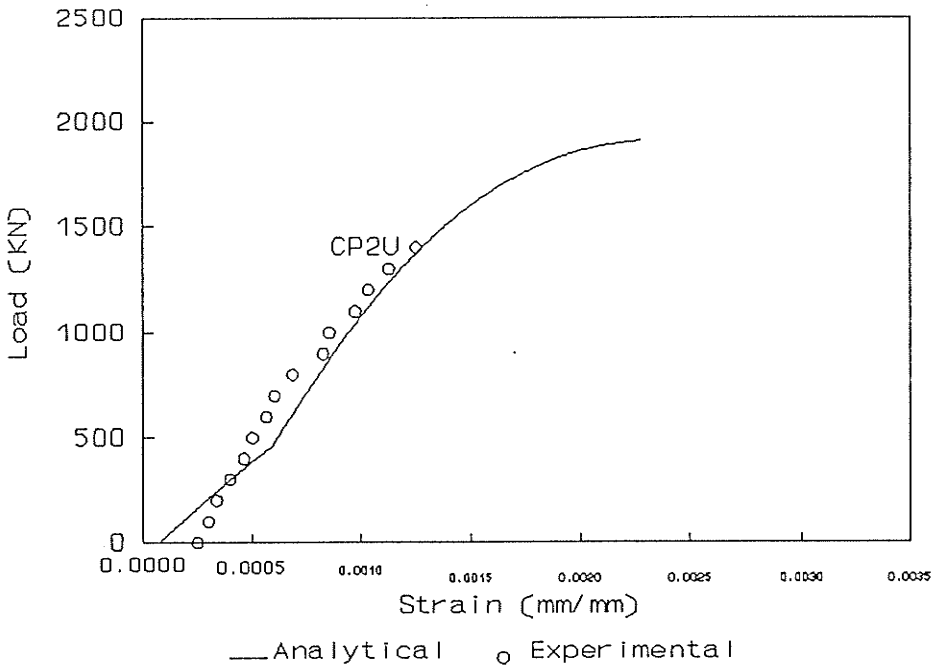

Figure F.2 Predicted load-strain behavior
(non-preloaded column CP2U)

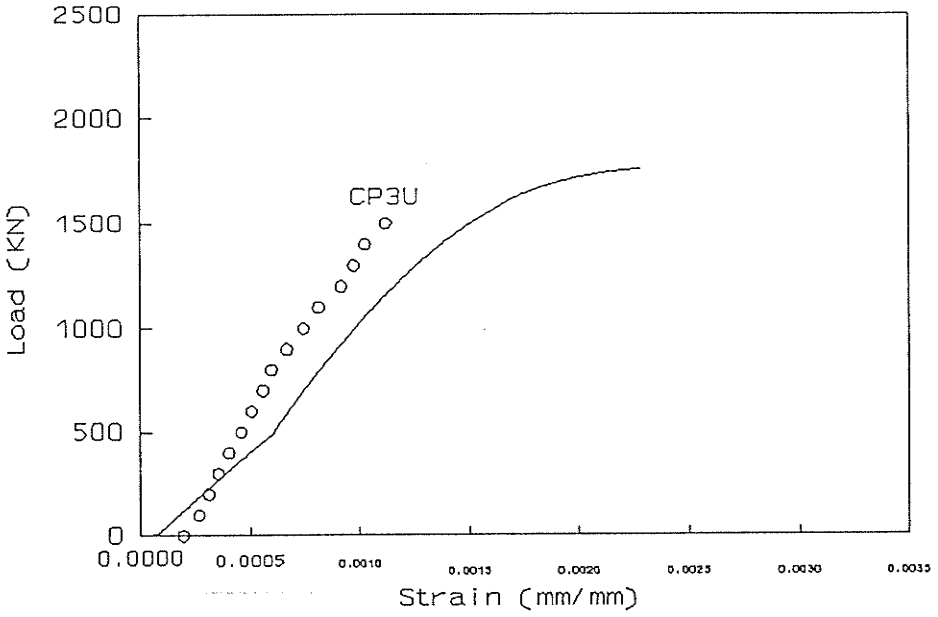

Figure F.3 Predicted load-strain behavior
(non-preloaded column CP3U)

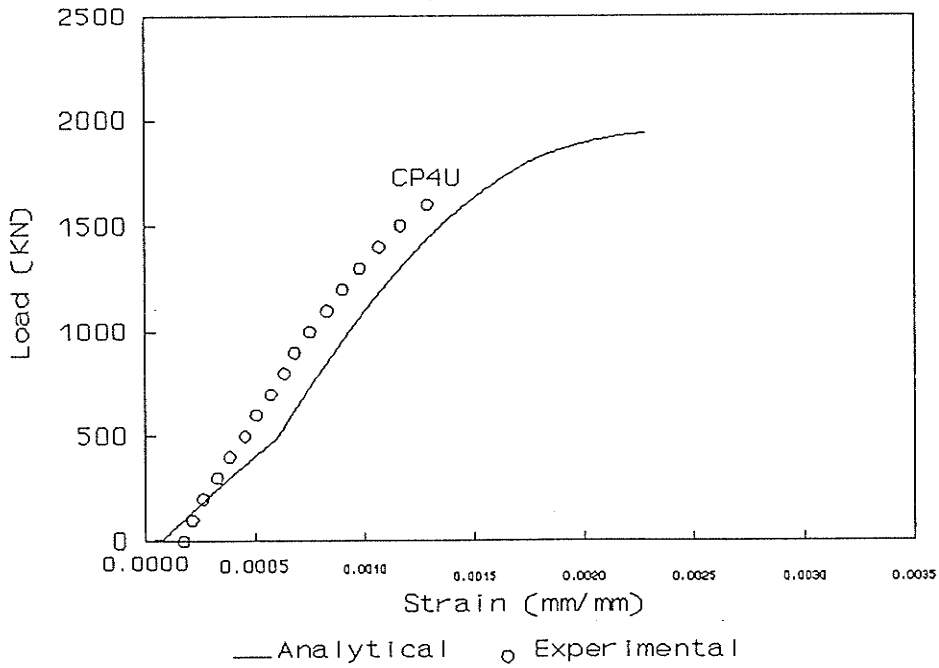

Figure F.4 Predicted load-strain behavior
(non-preloaded column CP4U)

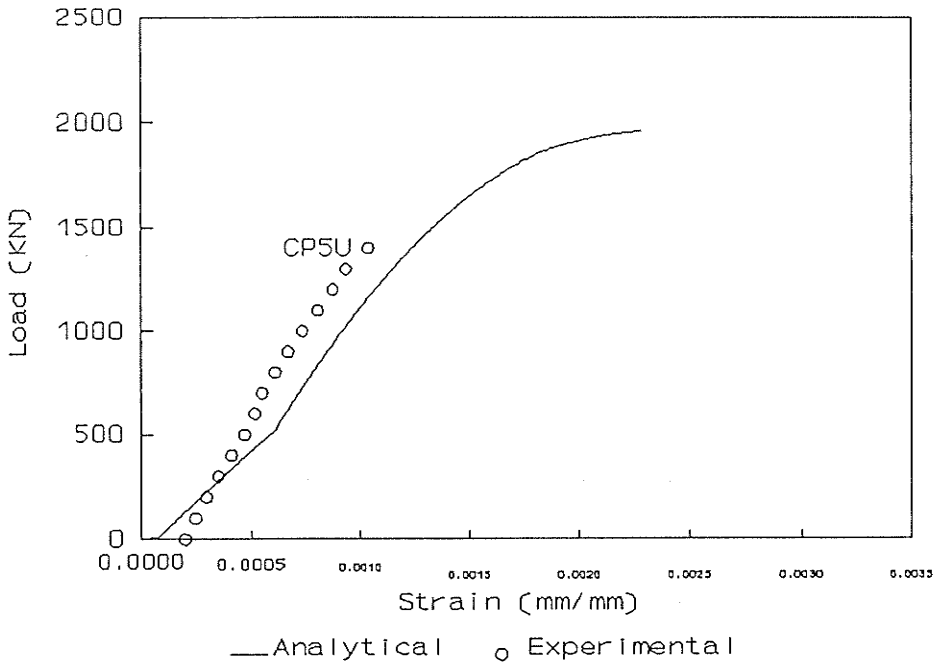

Figure F.5 Predicted load-strain behavior
(non-preloaded column CP5U)

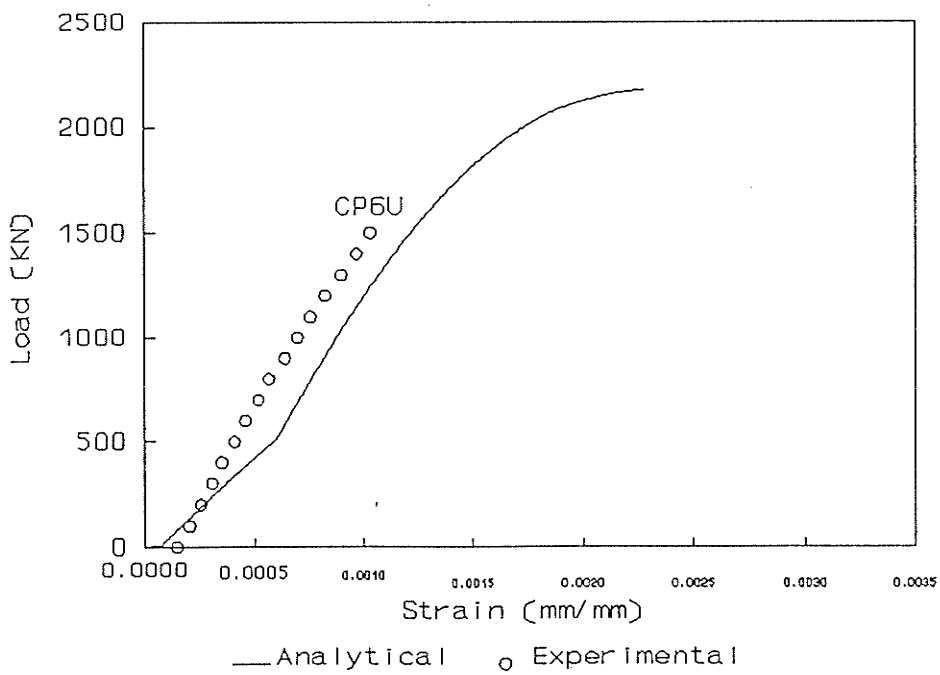

Figure F.6 Predicted load-strain behavior
(non-preloaded column CP6U)

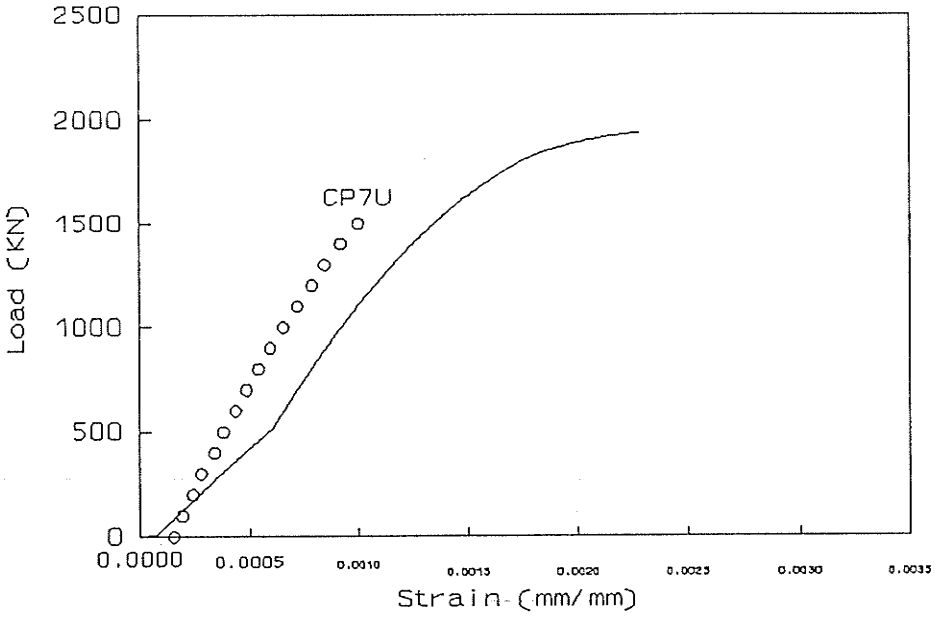

Figure F.7 Predicted load-strain behavior
(non-preloaded column CP7U)

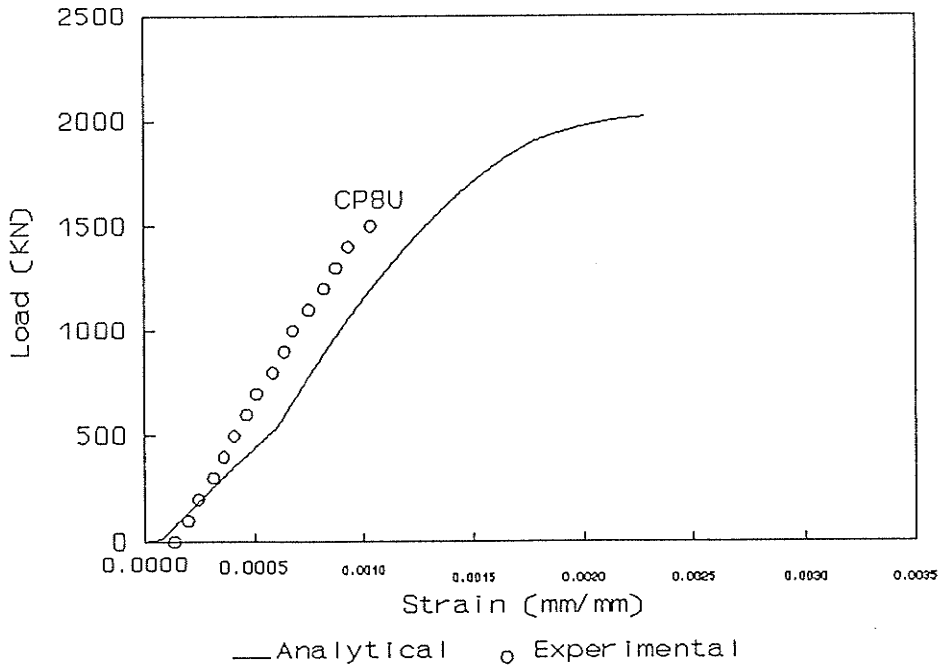

Figure F.8 Predicted load-strain behavior
(non-preloaded column CP8U)

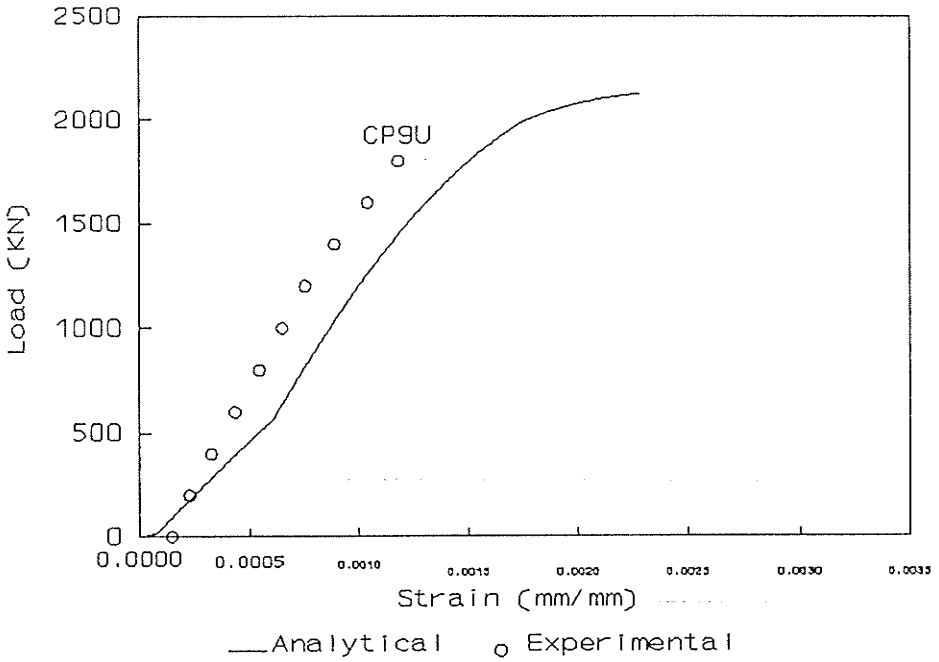

Figure F.9 Predicted load-strain behavior
(non-preloaded column CP9U)

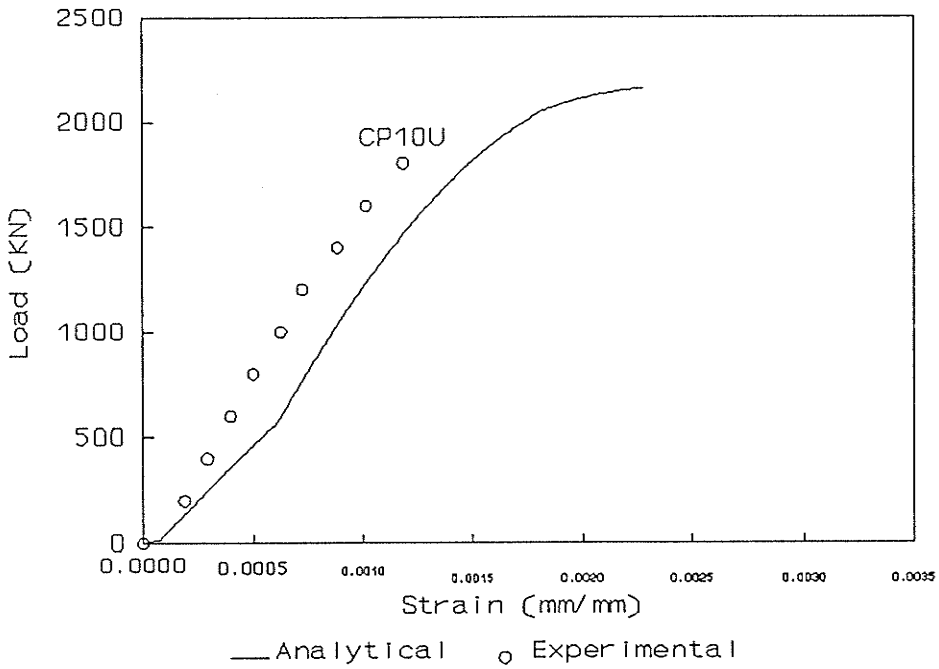

Figure F.10 Predicted load-strain behavior
(non-preloaded column CP10U)